

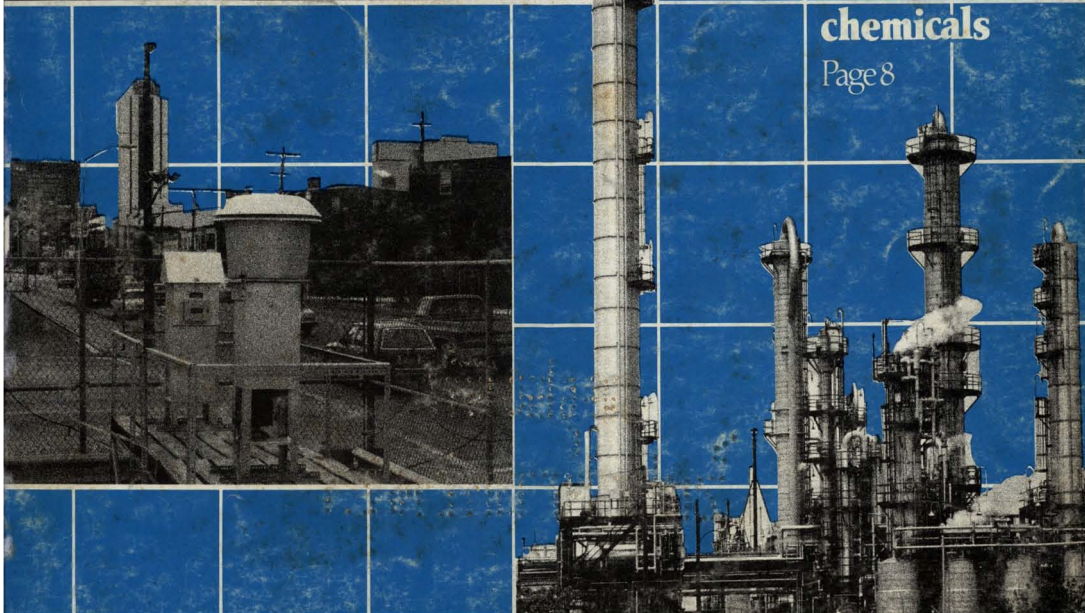
JANUARY 1986
ENVIRONMENTAL SCIENCE & TECHNOLOGY

ES&T



**Airborne
toxic
chemicals**

Page 8



ENVIRONMENTAL SCIENCE & TECHNOLOGY

ES&T



**The premiere
research
publication in the
environmental
field.**

Environmental science continues to be one of the fastest growing fields. And ES&T has grown right along with it!

ES&T continues to give you the practical, hard facts you need on this science . . . covering research, techniques, feasibility, products and services.

Essential reading for environmental scientists both in the business and academic world . . . ES&T has increased its emphasis on peer-reviewed research dealing with water, air, and waste

chemistry in addition to adding critical reviews of important environmental science issues—all relevant to understanding the management of our natural environment.

Also included are discussions on environmental analyses, governmental regulations, current environmental lab activities, and much more!

**For rate information, and to
subscribe, call toll free:
(800) 424-6747**

Editor: Russell F. Christman
Associate Editor: John H. Seinfeld
Associate Editor: Philip C. Singer

ADVISORY BOARD

Marcia C. Dodge, Steven J. Eisenreich, William H. Glaze, Roy M. Harrison, Michael R. Hoffmann, Donald Mackay, Jarvis L. Moyers, Kathleen C. Taylor, Walter J. Weber, Jr., Richard G. Zepp

WASHINGTON EDITORIAL STAFF

Managing Editor: Stanton S. Miller
Associate Editor: Julian Josephson

MANUSCRIPT REVIEWING

Manager: Janice L. Fleming
Associate Editor: Monica Creamer
Associate Editor: Yvonne D. Curry
Editorial Assistant: Diane Scott

MANUSCRIPT EDITING

Assistant Manager: Mary E. Scanlan
Assistant Editor: Ruth A. Linville

GRAPHICS AND PRODUCTION

Production Manager: Leroy L. Corcoran
Art Director: Alan Kahan
Designer: Julie Katz
Production Editor: Kate Kelly

BOOKS AND JOURNALS DIVISION

Director: D. H. Michael Bowen
Head, Journals Department: Charles R. Bertsch
Head, Production Department: Elmer M. Pusey
Head, Research and Development Department: Lorrin R. Garson

ADVERTISING MANAGEMENT

Centcom, Ltd.

Please send research manuscripts to Manuscript Reviewing, feature manuscripts to Managing Editor. For editorial policy and author's guide, see the January 1986 issue, page 30, or write Janice L. Fleming, Manuscript Reviewing Office, *ES&T*. A sample copyright transfer form, which may be copied, appears on the inside back cover of the January 1985 issue.

Environmental Science & Technology, *ES&T* (ISSN 0013-936X), is published monthly by the American Chemical Society at 1155 16th Street, N.W., Washington, D.C. 20036. Second-class postage paid at Washington, D.C., and at additional mailing offices. POSTMASTER: Send address changes to *Environmental Science & Technology*, Membership & Subscription Services, P.O. Box 3337, Columbus, Ohio 43210.

SUBSCRIPTION PRICES 1985: Members, \$26 per year; nonmembers (for personal use), \$35 per year; institutions, \$149 per year. Foreign postage, \$8 additional for Canada and Mexico, \$14 additional for Europe including air service, and \$23 additional for all other countries including air service. Single issues, \$13 for current year; \$13.75 for prior years. Back volumes, \$161 each. For foreign rates add \$1.50 for single issues and \$10.00 for back volumes. Rates above do not apply to nonmember subscribers in Japan, who must enter subscription orders with Maruzen Company Ltd., 3-10 Nihon bashi 2 chome, Chuo-ku, Tokyo 103, Japan. Tel: (03) 272-7211.

COPYRIGHT PERMISSION: An individual may make a single reprographic copy of an article in this publication for personal use. Reprographic copying beyond that permitted by Section 107 or 108 of the U.S. Copyright Law is allowed, provided that the appropriate per-copy fee is paid through the Copyright Clearance Center, Inc., 27 Congress St., Salem, Mass. 01970. For reprint permission, write Copyright Administrator, Books & Journals Division, ACS, 1155 16th St., N.W., Washington, D.C. 20036.

REGISTERED NAMES AND TRADEMARKS, etc., used in this publication, even without specific indication thereof, are not to be considered unprotected by law.

SUBSCRIPTION SERVICE: Orders for new subscriptions, single issues, back volumes, and microfiche and microform editions should be sent with payment to Office of the Treasurer, Financial Operations, ACS, 1155 16th St., N.W., Washington, D.C. 20036. Phone orders may be placed, using Visa, MasterCard, or American Express, by calling toll free (800) 424-6747 from anywhere in the continental U.S. Changes of address, subscription renewals, claims for missing issues, and inquiries concerning records and accounts should be directed to Manager, Membership and Subscription Services, ACS, P.O. Box 3337, Columbus, Ohio 43210. Changes of address should allow six weeks and be accompanied by old and new addresses and a recent mailing label. Claims for missing issues will not be allowed if loss was due to insufficient notice of change of address, if claim is dated more than 90 days after the issue date for North American subscribers or more than one year for foreign subscribers, or if the reason given is "missing from files."

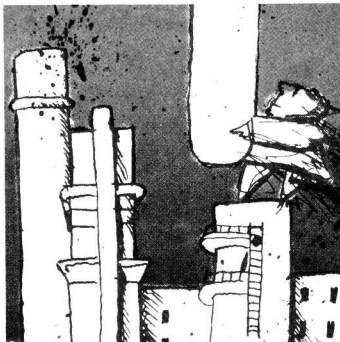
The American Chemical Society assumes no responsibility for statements and opinions advanced by contributors to the publication. Views expressed in editorials are those of the author and do not necessarily represent an official position of the society.

ES&T

CONTENTS

Volume 20, Number 1, January 1986

FEATURES



8 **Airborne toxic elements and organic substances.** A New Jersey project studied opportunities for exposure to airborne toxic substances in various source and population settings. Paul J. Lioy, Rutgers Medical School, Piscataway, N.J.; and Joan M. Daisey, New York Medical Center, Tuxedo, N.Y.

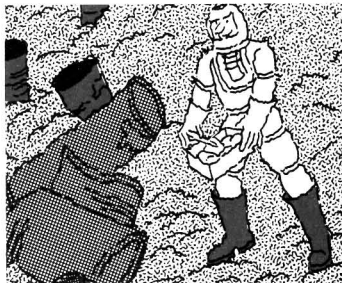


16 **Waste monitoring.** Technology is speeding up data acquisition and the translation of data into useful information for hazardous waste monitoring. Bruce P. Almich, EPA, Research Triangle Park, N.C.; William L. Budde, EPA, Cincinnati, Ohio; and W. Randall Shobe, EPA, Washington, D.C.

REGULATORY FOCUS

22 **EPA drinking-water proposals.** Richard Dowd addresses acceptable technology, required measurements, and estimated costs for compliance with proposed regulations for volatile organic compounds.

VIEWS



23 **Implementing Superfund.** The financing, contracts, and activities involved in cleaning up abandoned hazardous waste sites are discussed.

DEPARTMENTS

- 3 Editorial
 - 5 Currents
 - 29 Advisory Board
 - 30 Editorial policy
 - 30 Instructions to authors
 - 32 Peer review policy
 - 33 Consulting services
 - 34 Classified
- IBC Copyright release form

UPCOMING

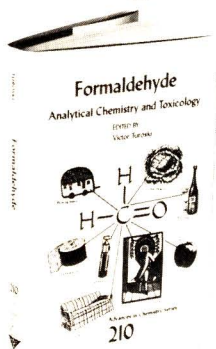
Estimating risk to human health from trichloroethylene in drinking water
Biological monitoring of exposure to metals

ESTHAG 20(1) 1-104 (1986)
ISSN 0013 936X

Credits: p. 6, Steve Delaney; p. 25, Brum & Anderson; p. 26, Julian Josephson; p. 29, Bob Kalmbach, University of Michigan Information Service; p. 29, Julie Katz

Formaldehyde

Analytical Chemistry and Toxicology



Victor Turoski, Editor
James River Corporation

Ends the dispute over the controversial chemical, formaldehyde. Airls differing opinions on its toxicity, concluding that used at "normal levels" CH_2O is not a human carcinogen. Provides valuable current knowledge on the analysis of formaldehyde at trace levels, on its toxicity, and on the risk assessment of the relative safety of this small organic chemical.

CONTENTS

Industrial Hygiene Sampling and Analytical Methods • Ion Chromatography with Pulsed Amperometric Detection • Analysis of Formaldehyde in Industrial Labs • Method Development for Determining Trace Levels in Polluted Waters • Quantitative Analysis of Condensates in Vapor State • Evolution of Testing Methodology for Atmospheric Formaldehyde in Home Environment • Predicting Release of Formaldehyde from Cellulosic Textiles • Release from Pressed Wood Products • Current Status of Measurement Techniques and Concentrations in Residences • Emission from Combustion Sources and Solid Formaldehyde-Resin-Containing Products • Field Evaluations of Sampling and Analytical Methods • Measurements in Canadian Homes Using Passive Dosimeters • Generation of Standard Gaseous Formaldehyde in Test Atmospheres • Toxicology • History and Status in Cosmetics Industry • FDA's Perspective • Exposure to Formaldehyde • Review of Epidemiologic Evidence Regarding Cancer and Exposure • Formaldehyde in Dialysis Patients • Formaldehyde and Cancer • Estimating Human Cancer Risk • Evaluation of Potential Carcinogenic Hazard • Formaldehyde Risk Analysis • Refining the Risk Assessment

Based on a symposium sponsored by the Division of Environmental Chemistry of the American Chemical Society

Advances in Chemistry Series No. 210
408 pages (1985) Clothbound
LC 85-11205 ISBN 0-8412-0903-0
US & Canada \$89.95 Export \$107.95

Order from:
American Chemical Society
Distribution Dept. 86
1155 Sixteenth St., N.W.
Washington, DC 20036
or CALL TOLL FREE 800-424-6747
and use your credit card!

RESEARCH

35

Implications of a gradient in acid and ion deposition across the northern Great Lakes states. Gary E. Glass* and Orië L. Loucks

Rainfall pH ranges from 5.3 in Minnesota to 4.3 in Michigan, which is comparable to that found at sites in northern New York and southern Scandinavia.

44

Application of mass-transfer theory to the kinetics of a fast gas-liquid reaction: Chlorine hydrolysis. E. Marco Aieta and Paul V. Roberts*

The short wetted-wall column is evaluated as a tool for quantifying the rate of a fast liquid-phase reaction—the hydrolysis of chlorine.

50

Kinetics of the reactions between molecular chlorine and chlorite in aqueous solution. E. Marco Aieta and Paul V. Roberts*

Reaction kinetics is studied experimentally by measuring the enhancement of chlorine transfer from the gas phase.

55

Effects of nonreversibility, particle concentration, and ionic strength on heavy-metal sorption. Dominic M. Di Toro,* John D. Mahony, Paul R. Kirchner, Ann L. O'Byrne, Louis R. Pasquale, and Dora C. Piccirilli

A particle interaction model is proposed that conforms with experimentally determined partition coefficient-particle concentration relationships.

62

Vertical transport processes of an acid-iron waste in a MERL stratified mesocosm. Mary Frances Fox,* Dana R. Kester, and Carlton D. Hunt

The vertical transport of Fe particles formed after an acid-Fe waste mixes with seawater and the effect of the waste on seawater trace metal composition are examined in a stratified tank.

69

Aromatic hydrocarbons in the New York Bight polychaetes: Ultraviolet fluorescence analysis and gas chromatography/gas chromatography-mass spectrometry analyses. John W. Farrington,* Stuart G. Wakeham, Joaquim B. Livramento, Bruce W. Tripp, and John M. Teal

Aromatic hydrocarbon data are presented to illustrate the utility of the hierarchical approach to the UV fluorescence screening method.

72

Products and quantum yields for photolysis of chloroaromatics in water. David Dulin, Howard Drossman, and Theodore Mill*

Photolysis of chloroaromatics is as efficient in water as it is in hexane, but the products are phenols or benzofuran rather than reduced aromatics.

78

A comparative study of combustion in kerosene heaters. Trudy Lionel, Richard J. Martin, and Nancy J. Brown*

Two kinds of experiments determine and compare the combustion characteristics of radiant, convective, and multi-stage kerosene heaters.

86

Photochemical transformation of pyrene and benzo[a]pyrene vapor-deposited on eight coal stack ashes. Robert A. Yokley, Arlene A. Garrison, E. L. Wehry,* and Gleb Mamantov

Coal stack ashes from diverse sources differ substantially in their ability to stabilize adsorbed pyrene or benzo[a]pyrene with respect to photochemical transformation.

91

Contribution of gulf area sulfur to the North American sulfur budget. Menachem Luria,* Charles C. Van Valin, Dennis L. Wellman, and Rudolf F. Poeschel

A simple model estimates the sulfur flux transported northward from the gulf area based on measurements taken from instruments on board an aircraft.

96

Sequential dehalogenation of chlorinated ethenes. Gladys Barrio-Lage,* Frances Z. Parsons, Raja S. Nassar, and Pedro A. Lorenzo

The kinetics of the biotransformation of chlorinated ethenes to vinyl chloride in environmental microcosms is described.

104

Perfluorocarbon measurement using an automated dual-trap analyzer. Ted W. D'Ottavio,* Robert W. Goodrich, and Russell N. Dietz

A new, semi-real-time analyzer simultaneously measures the concentrations of several perfluorocarbons in air.

* To whom correspondence should be addressed.

This issue contains no papers for which there is supplementary material in microform.

Toxic chemicals in surface waters

Toxic chemicals from direct and indirect industrial wastewater discharges and land runoff are often found in surface waters that are used as sources of public water supply. The problem caused by their presence is beginning to receive some of the attention it has long deserved. I am concerned, however, about the narrow focus of much of the activity and about the implications of our failure to address the problem comprehensively.

Health effects research is very costly and time consuming. Do we know enough about wastewater discharges and human exposure to set research priorities intelligently? We debate the significance of trace concentrations of toxic chemicals in water supply sources with little or no reference to the validity of sampling strategies underlying these values. How can sound sampling strategies be developed in the absence of reliable data on the quantity, nature, and periodicity of toxic chemical discharges? We have become mesmerized with computerized data management systems and mathematical modeling, while we fail to take the steps necessary to ensure the completeness and reliability of the data we manipulate.

A review of NPDES (the National Pollutants Discharge Elimination System) permits quickly discloses our fragmentary knowledge about synthetic organic chemicals in wastewater discharges. Our ambient water quality standards for toxic chemicals cover little more than toxic metals and pesticides. What does it mean to say that a permit holder is meeting permit limitations and ambient standards when both are so incomplete? Our continued certification of public water supply sources from surface water in the face of such incomplete information is nothing less than irresponsible. Underlying the problem is our failure to gain accurate disclosure by industrial dischargers of toxic chemicals manufactured, stored, and used in manufacturing and maintenance operations.

The ineffectiveness of reporting on discharges to wastewater can be illustrated by a North Carolina regulatory agency disclosure in 1982 of the extensive use of biocides in the manufacture of socks by textile mills. These highly toxic triorganotin compounds were identified only through the use of state-initiated bioassay

screening techniques. This experience and the recognition of the need to deal more effectively with toxic chemicals in water supply sources have led the state agency to begin a program requiring disclosure of available data on toxic chemicals from all industrial discharges to waters classified for use as water supply sources.

The data are often incomplete, however, and to help fill the information gap, the agency is incorporating mandatory metal and gas chromatography-mass spectrometry scans in new and reissued NPDES permits. Water supply classifications are also being modified to afford greater control over discharges and land runoff. The new classification applicable to waters that receive industrial wastewater discharges will require full disclosure of toxic chemicals, development of spill and failure plans, and more extensive monitoring.

Concern over the protection of proprietary information made available to regulatory agencies through full disclosure can be met through appropriate legal safeguards. The problem of how to deal with the hoped-for volumes of new data on toxics may be momentarily perplexing, but its very existence and our need to respond should provide the impetus to move forward in this vital area.

It is my position that we are misleading the public we ought to protect by failing to require full disclosure of chemical use and wastewater composition to regulatory agencies. That is the key to meaningful regulatory permits, sound monitoring systems, and sensible research priorities.



David H. Howells is retired from the U.S. Public Health Service and is professor emeritus at North Carolina State University and the University of North Carolina at Chapel Hill. He has just completed a six-year term on the North Carolina Environmental Commission, where he encouraged program development in the area of toxic chemicals in surface waters.

Choosing a graduate school?

Need to know who's doing research critical to yours?

*New edition
just published!*

The ACS Directory of Graduate Research 1985

All the information you need on chemical research and researchers at universities in the U.S. and Canada . . . in a single source.

Includes listings for chemistry, chemical engineering, biochemistry, pharmaceutical/medicinal chemistry, clinical chemistry, and polymer science.

Lists universities with names and biographical information for all faculty members, their areas of specialization, titles of all papers published within last two years, and individual telephone numbers.

Provides a statistical summary of academic chemical research—with information by department on numbers of full- and part-time faculty, postdoctoral appointments, graduate students, and M.S. and Ph.D. degrees granted.

1260 pages (1985) Clothbound
Price:

US & Canada \$46.00
Export \$55.00

**Now available
two ways—
print or on-line**

Interested in the on-line version? Write to the American Chemical Society, Office of Professional Training, 1155 16th Street, N.W., Washington, DC 20036, or call (202) 872-4599 for details.

CONTAINS A WEALTH OF FACTS ON

- 713 academic departments
- 11,215 faculty members
- 58,760 publication citations

No academic institution or chemically oriented business can afford to be without the ACS Directory of Graduate Research 1985! Order today by calling toll free (800) 424-6747 or using the coupon below.

Please send me _____ copy(ies) of the ACS Directory of Graduate Research 1985.

- Payment enclosed (make checks payable to American Chemical Society).
 Purchase order enclosed. P.O. # _____

Charge my MasterCard/VISA American Express Access Barclaycard
 Diners Club/Carte Blanche.

Account # _____

Expires _____ Interbank # (MC and ACCESS) _____

Name of cardholder _____ Phone # _____

Signature _____

Ship books to:

Name _____

Address _____

City, State, Zip _____

• ORDERS FROM INDIVIDUALS MUST BE PREPAID. Prepaid and credit card orders receive free postage and handling. Please allow 4-6 weeks for delivery.

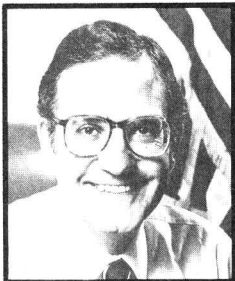
Mail this order form with your payment or purchase order to:
American Chemical Society, Distribution Office Dept. 705,
1155 Sixteenth St., N.W., Washington, DC 20036

ES&T CURRENTS

INTERNATIONAL

The world debt crisis will be responsible for sharp curtailments in environmental protection work in Latin America and other developing areas. According to the World Commission on Environment and Development (Geneva, Switzerland), which held a meeting last November in São Paulo, Brazil, on this and other crises, developing countries are under strong pressure to extract resources and raise export production as quickly as possible. They need to obtain hard currency to pay their debts to banks in developed countries. Commission spokesmen say that antipollution measures, preservation of tropical forests, and similar endeavors are subordinated by the urgency of meeting overseas debts.

FEDERAL



Mitchell: Introduced groundwater bill

Sen. George Mitchell (D-Maine) has introduced the Groundwater Protection Act of 1985, which aims at countering health risks posed by groundwater contamination. His bill would require individual states to establish standards for groundwater contaminants and undertake necessary control programs. The federal government would conduct research, provide grant assistance, and oversee state programs. Sen. Mitchell took action because "despite clear and growing evidence of serious problems, no comprehensive federal statute protects groundwater and no legislative proposal to do so is before Congress."

EPA's air pollution inspection program was inadequate for 40% of the plants inspected during fiscal

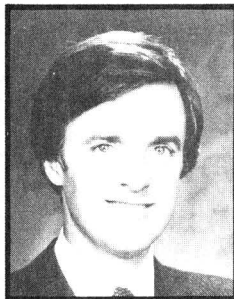
year 1984, according to a report issued in late November by the General Accounting Office. According to the report, state and local inspectors who were supposed to work under EPA guidelines inspected 95% of nearly 30,000 facilities assigned to them under terms of the Clean Air Act. But more than 40% of the inspections were not thorough enough to ensure that facilities were in compliance with emissions standards. The report charged that EPA inspectors responsible for checking facilities for air pollution violations did an even worse job; they inspected only 27% of the more than 2000 sources they should have checked.

EPA has received a suggestion for "a novel procedure to oversee chemicals newly placed on the market." The Toxic Substances Dialogue Group, consisting of representatives of industry, state agencies, and public interest organizations, proposed that EPA adopt an interim inventory for listing new chemicals under the Toxic Substances Control Act (TSCA). In this way, EPA would receive advance review of changes in the manufacture, use, or disposal of chemicals that may raise concern about potential risks. At present, TSCA requires a premanufacture notification before a new chemical is made; normally, the chemical is listed on a final inventory after EPA reviews the proposed chemical. The group met in November under the auspices of the Conservation Foundation (Washington, D.C.).

Twenty-two percent of the motor vehicles surveyed by EPA showed evidence of tampering with at least one component of their emissions control systems, according to a report the agency issued in November. Such tampering reduces a vehicle's ability to abate hydrocarbon and carbon monoxide emissions. Of 4426 cars and light trucks surveyed, 14% were fueled with leaded fuel, even though they required unleaded fuel. Emission controls malfunctioned in 4% of the vehicles, and for 29%, it could not be determined whether the vehicles' emission systems had been altered. EPA spokesmen say that emission systems inspection and

maintenance programs are helping to combat the problem.

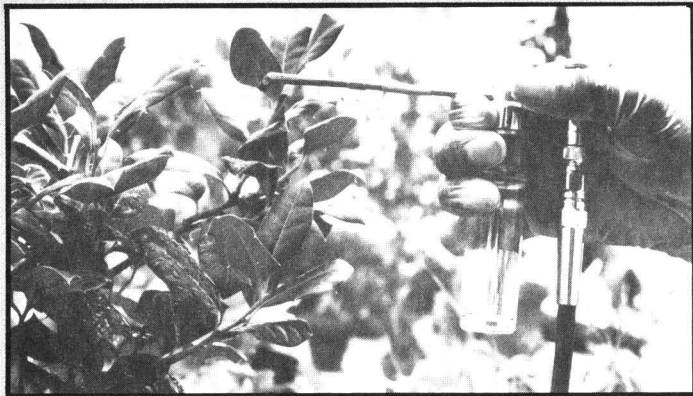
STATES



Kerrey: Groundwater effort welcomed

The Nebraska Groundwater Foundation (Lincoln, Neb.) has been formed to educate the public about groundwater topics. The foundation convened its first meeting in Lincoln in November and was addressed by Gov. Robert Kerrey, several state senators, and local scientists. Susan Seacrest, the organization's founder, said that the organization, which is apolitical, has public education as its only goal. The foundation receives no state or federal funds but is making efforts to obtain private grant money. Membership dues now support the organization, which is also receiving nonfinancial help from the Nebraska Department of Environmental Control. The foundation has started a publication, *The Aquifer*.

Farmers in Maryland will receive help with reducing the amount of pollution reaching Chesapeake Bay. Agents and specialists from the University of Maryland's Cooperative Extension Service (College Park, Md.) are developing programs to explain to farmers the relationship between agriculture and the bay's environmental health. They will help farmers test soil to determine the nutrient needs of crops, and they will encourage the use of manure as an alternative to chemical fertilizers. Specialists at the cooperative service believe that farmers will be willing to restrict use of chemical fertilizers if it can be shown that alternatives are cost effective and provide enough crop nutrients.



Florida has the toughest pesticide rules

Florida is the nation's toughest pesticide regulator, says Doyle Conner, Florida's commissioner of agriculture. He signed an agreement with the state Department of Environmental Regulation (DER) and the Department of Health and Rehabilitative Services (HRS) to coordinate responsibilities with pesticide users, applicators, and researchers. The state's Department of Agriculture will govern user registration, laboratory research, and pesticide levels in food. DER will be concerned with pesticides contaminating air and water, and HRS will certify pest control operators and mosquito control applicators. Conner says that with the agreement, "there will be no voids in the pesticide regulatory program."

New York State Environmental Conservation Commissioner Henry Williams says that liming acidic waters is a useful temporary protection and restoration technique. "But it cannot be considered an appropriate long-term solution to the acid rain problem," Williams told a conference in Albany, N.Y., last October. "What is needed is an effective, consistent national program to reduce emissions of sulfur and nitrogen oxides," he added. Williams said that liming ponds "does nothing for acidified headwater streams, nor does it restore natural ecosystems that have been damaged. It is not the answer for forest damage, nor is liming the ultimate fix for acid deposition."

State and local governments must take more responsibility than EPA has for controlling nonpoint sources of water pollution, EPA Administrator Lee Thomas told the Water Pollution Control Federation's annual conference in Kansas City, Mo., in October. He said that state

and local governments have authority over land use, "an authority that the U.S. government lacks." To help solve problems of nonpoint source pollution, EPA and the Department of Agriculture are working to assemble data on where this pollution is a problem and to conduct cleanup demonstration projects, Thomas said. He cited Oregon, Vermont, and Wisconsin for pioneering efforts to control nonpoint source pollution.

SCIENCE

Acid deposition presents great risks to northern lake states, according to a paper by Gary Glass of EPA's Environmental Research Laboratory (Duluth, Minn.) published in this issue of *ES&T*. Acid precipitation increases from west to east along a cross section of eight sites in Minnesota, Wisconsin, and Michigan.

Three years of data indicate that there is a 10-fold increase in acidity across these sites, a 56% increase in wet deposition of nitrate ion, and a 40% increase in wet deposition of sulfate. A gradient is said to exist for the concentration of man-made emissions and reaction products from west to east.

Chronic exposure to wholly vaporized unleaded gasoline may lead to increased kidney tumors in male rats and liver tumors in female mice, according to the Health Effects Institute (Cambridge, Mass.). The institute notes that human exposure is likely widespread—70% of the gasoline now pumped is self-service. Before human health risks from gasoline can be assessed, the institute suggests that researchers ask how the vapors administered to rodents compare with those typically experienced by humans, to what degree effects on rodents and humans are comparable,

what the nature and magnitude of human exposure are, and how epidemiological studies should be interpreted.

TECHNOLOGY

Pollution from oily steel and non-ferrous metal mill scales can be abated by oil-and-metal recovery, says Leonard Duval, president of Colerapa Industries (Aurora, Ohio). The metal cannot be recovered unless the oil is removed. Duval says that a proprietary hydrocarbon solvent removes the oil, which can then be separated from the solvent and re-used or burned. The solvent is also recoverable. Once the oil has been removed, the cleaned iron (or non-ferrous metal) oxides can be processed for the recovery of metal. Duval expects that many years of testing this process will result in a 1000-t/d plant.

Soil contaminated with polychlorinated biphenyls (PCBs) could be rendered innocuous in situ vitrification. Craig Timmerman of Battelle Laboratories (Richland, Wash.) says the process involves placing electrodes in the ground in PCB-contaminated soil. Electric current passing between the electrodes heats the soil to temperatures as high as 2200 °C, effectively destroying the PCBs. The soil itself melts and then cools to a rock-hard solid. Timmerman says this approach renders contaminants inert and reduces problems associated with digging, loading, transporting, and burning contaminated soil.

A partial solution to the problem of acid rain may be found in the use of sulfate-eating bacteria that live in the world's oceans. Craig Taylor and Holger Jannasch of Woods Hole Oceanographic Institution (Woods Hole, Mass.) have taken samples of these bacteria and cultured populations that consume hydrogen sulfide and sulfur dioxide. The scientists believe that after the bacteria eat the acid gases, they could be fed to shellfish. Taylor and Jannasch are seeking support for an economic feasibility study for this approach to acid gas abatement; they hope that the manufacture of shellfish food by means of their technique will become a profitable venture.

Certain kinds of sewage sludge can be used to fertilize field-grown coniferous trees, according to an EPA report issued in September. But care must be taken to ensure that tree

growth is not impaired and that weed growth is not promoted through overapplication of the sludge. Scientists from the Ohio Agricultural Research and Development Center (Wooster, Ohio) found that an application of up to 22 metric tons/ha provided necessary nutrients without causing toxicity. Amounts of sludge equal to or exceeding 45 metric tons/ha greatly inhibit conifer growth. Black locusts and yellow poplars were the only hardwoods found to benefit from sludge application.

BUSINESS

A voluntary, private-sector program for the evaluation of drinking-water additives is the objective of a contract awarded by EPA to the National Sanitation Foundation (Ann Arbor, Mich.). The program is expected to provide health-related information to state governments, manufacturers, water utilities, and consumers. Direct additives (chemicals added to water to improve its quality for public consumption) and indirect additives (contaminants such as paints and metals) will be evaluated in the study.

Bioreclamation is a cost-effective way of treating contaminated soil and groundwater, says Gaylen Brubaker of Aquifer Remediation Systems, a subsidiary of FMC (Philadelphia, Pa.). The first step is to assess a site and determine the technical feasibility of treatment. The next step is to identify the appropriate program to reduce contamination. The third step is the actual remediation through installing the equipment and then treatment and monitoring. Brubaker says that bioreclamation involving in situ treatment was used at 14 sites nationwide during 1985.

Parsons, a large engineering firm in Pasadena, Calif., will conduct a water conservation and planning program for the Imperial Irrigation District of California. This project is the first instance in the United States of a private corporation's playing a major role in a public agency's water conservation program. Parsons will provide the engineering services necessary for the reduction of use of more than 300,000 acre-ft/y of water in the Imperial Valley and will transfer some of that water to other users in southern California. The firm estimates that the project will last 12-14 years and could cost up to \$600 million (1985 dollars), depending on the size of the program and the district's goals.



A hazardous waste site is sealed with clay and textiles

One of the nation's first projects for the closure of a hazardous waste site is being carried out near Missouri City, Mo., under the regulations of the Resource Conservation and Recovery Act (RCRA). The \$4.3-million effort is being undertaken by American Environmental Construction (Bloomington, Ill.) under a contract with Browning-Ferris Industries. Soil from the site will be moved and compacted to predetermined densities; it must meet RCRA-mandated permeability requirements for site liners. Up to 57 acres of the site is lined with 1.2-million yd² of geotextile materials that will seal it off from surrounding soils. The area will be capped with clay and synthetic impermeable materials to protect the surrounding areas against erosion. The closed site will be monitored for at least 30 years as required by RCRA.

Analytec (Corrales, N.M.) and Anarad (Santa Barbara, Calif.) will provide a continuous emissions monitoring system to Central Illinois Light Company. The system uses microprocessor-based nondispersive infrared analyzers for carbon monoxide and dioxide and ultraviolet absorption analyzers for NO_x, SO₂, hydrogen sulfide, and oxygen. Analytec spokesmen say that many of the sampling and particle filtration problems encountered with other samplers have been solved. Emissions from a 400-MW power plant that burns high-sulfur coal and uses a precipitator and wet scrubber will be measured. The system was developed by Kilkelly Environmental Associates under a contract with the Electric Power Research Institute.

One of the largest environmental engineering firms in the United States will result from the merger of

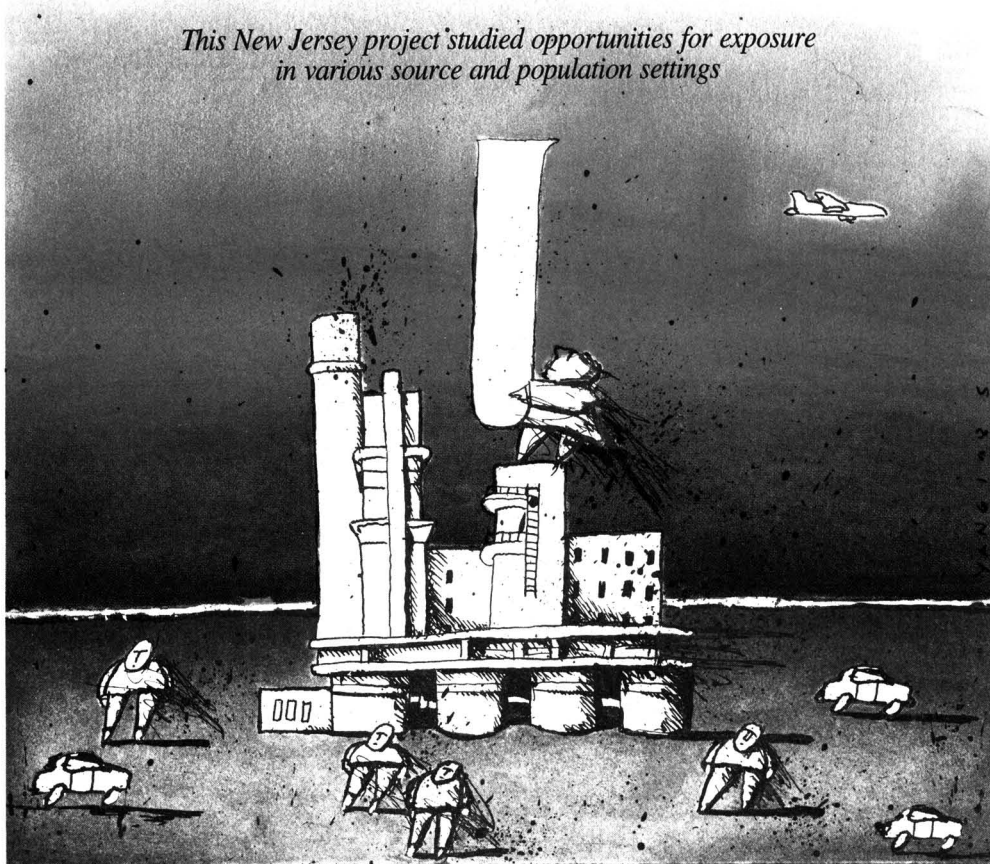
Environmental Research and Technology (ERT, Concord, Mass.) and Resource Engineering (Houston, Tex.). ERT representatives explain that the merger enhances the company's ability to do research on air quality and acid rain and to solve problems related to toxic wastes. The new firm has greatly increased the number of professional staff that work on hazardous waste problems for clients.

Chevron U.S.A. has been assessed a \$6-million fine by Judge Harry Lee Hudspeth of the U.S. District Court for the Western District of Texas, as a result of a lawsuit brought by EPA. Agency spokesmen say that the penalty, assessed Sept. 30, is the largest civil penalty imposed in EPA's history. Chevron was accused of violating state SO₂ emission standards almost 1000 times over a period of 522 days between October 1977 and March 1979. The violations stemmed from what EPA charged was the improper burning of hydrogen sulfide, which is converted to SO₂. Judge Hudspeth said that Chevron did not avail itself of opportunities to respond to problems caused by the burning of hydrogen sulfide before the violations were uncovered.

The production of chlorofluorocarbons 11 and 12 increased in 1984 from 647,100 metric tons to 694,500 metric tons, according to the Chemical Manufacturers Association (CMA, Washington, D.C.). These production levels are slightly below those of 1977, a peak year. Chlorofluorocarbons have been implicated in the degradation of the stratospheric ozone layer, which filters out harmful ultraviolet radiation from the sun. CMA's figures cover 21 companies in western countries.

Airborne toxic elements and organic substances

*This New Jersey project studied opportunities for exposure
in various source and population settings*



Paul J. Liroy
Department of Environmental
and Community Medicine
Rutgers Medical School
Piscataway, N.J. 08854

Joan M. Daisey
New York University
Medical Center
Institute of Environmental Medicine
Tuxedo, N.Y. 10987

Populations that live near industrial centers are at risk of exposure to airborne toxic substances. The Airborne

Toxic Elements and Organic Substances (ATEOS) project was designed to simultaneously measure atmospheric levels of more than 50 toxic and carcinogenic chemicals within three urban population centers and one rural area. The study was conducted during the summers of 1981 and 1982 and the winters of 1982 and 1983. The extensive analyses already conducted on these data have included examinations of seasonal variations, pollution episodes, interurban differences, and source apportionment (1-17). This article discusses some of the general conclusions and suggests useful directions

in designing studies of human exposure and possibly toxic air pollution epidemiology.

The urban sites were in Newark, Elizabeth, and Camden, N.J. Each was representative of a different kind of population-industrial-commercial interface. The rural site, in Ringwood, N.J., was considered a northeastern regional background location.

The toxic or carcinogenic pollutants sampled and the rationale for their selection have been described by Liroy et al. (5). Species measured were either components of inhalable particulate matter (IPM, particles primarily < 15

μm in diameter), trace elements, SO_4^{2-} , extractable organic matter (EOM), polycyclic aromatic hydrocarbons (PAHs), alkylating agents, or one of 26 measured volatile organic compounds (VOCs).

Extractable organic matter was determined by sequential Soxhlet extraction with increasingly polar solvents to remove three organic fractions: nonpolar, semipolar, and polar organics (4, 18). The nonpolar fraction was analyzed for PAHs (7, 13). Seasonal composites of each organic extract from each site were prepared and tested for mutagenic activity with four or five strains of *Salmonella typhimurium* (\pm S9) using the Ames plate incorporation test (11, 19, 20). Trace elements also were measured to assist in identification of sources of IPM or VOCs. The winter and summer were chosen for sampling because they are affected by different meteorological conditions and because the influence of space heating can be easily identified.

Health effects perspective

To assess health risks from exposures to outdoor air pollutants, health scientists must consider the nature and concentration of each pollutant. Other factors to study include time variations in concentrations of pollutants and the number of persons affected. For example, long-term cumulative exposures to carcinogens are generally believed to be of more significance than single peak exposures. For certain other genotoxic effects, such as birth defects, peak exposures are more significant. For short-term respiratory effects, peak concentrations and episodes are important for pollutants such as ozone and sulfuric acid.

For IPM both long-term and short-term exposures can be important. IPM is a complex mixture of many chemical components that can come from different sources. The emphasis in the past in particulate matter sampling has been on measuring the annual average and peak concentrations of total suspended particulates (TSP). The TSP standard is expected to change to PM_{10} , which represents a sampling criterion for collection of particulates primarily $\leq 10 \mu\text{m}$ in diameter, and is more representative of materials that can deposit in the tracheobronchial and gas exchange regions of the lung to cause health effects.

However, the chemical composition of airborne particles must also be determined to assess human health risks more accurately (21, 22). The health risks from particulate matter exposure in cities with the same average or peak concentrations of IPM will vary because of compositional differences.

Both seasonal and interurban differences in the chemical composition and mutagenic activity of IPM are apparent from the ATEOS studies.

Many activities can create toxic air pollutants, but the magnitude of source emissions and proximity of humans to the sources will affect exposures to various compounds. Source effects at each ATEOS site ranged from the local to regional scale. These were not just related to the density of the typical or obvious large sources, such as chemical plants, industrial processes, and ubiquitous area point sources (e.g., automobiles, space heating). Small local sources were found to have significant effects at a site and at times could dominate human exposures to outdoor emissions of specific pollutants (7, 8, 10, 14, 15, 17).

Compositional differences

The intersite differences in the concentrations of IPM and EOM are shown in Figure 1. Newark had the greatest average concentrations for both, although the overall mean IPM concentration did not exceed the previously projected annual standard of $60 \mu\text{g}/\text{m}^3$ (23). This standard was never proposed, and PM_{10} cannot be assessed in the ATEOS analysis (24). The Elizabeth and Camden sites had similar average concentration patterns, for both winter and summer, and Ringwood had much lower concentrations.

Average concentrations of IPM were virtually the same in Newark for the summer of 1981 and winter of 1982— $46 \mu\text{g}/\text{m}^3$ (3). During the summer, however, EOM constituted only 22% of the IPM, and crustal components such as resuspended soil constituted 43% (5). In the winter, the particulate organic fraction increased to 36% of the IPM; crustal components were estimated to be only 32%. Similar patterns were observed in Elizabeth and Camden (15). These results show compositional differences that can occur.

The distribution of the extractable organics among the individual fractions also showed differences between sites and seasons (Figure 2). The average distribution of the three fractions was similar at Newark and Elizabeth for both winters. In Camden and Ringwood, the polar organic fraction was a higher percentage of total organic matter.

In contrast to the winters, the two summers showed compositional differences at all sites. For example, the semipolar fraction increased to $> 10\%$ (14% at the urban sites) of extractable organics during the summer of 1982. This increase was related to the intensity of an eight-day-long major photochemical pollution episode. During this

ATEOS study sites

Ringwood (northern New Jersey, 45 km north of Newark). The study site was in a large clearing surrounded by a wooded area in Ringwood State Park, N.J. It is not located near any major local source or roadways. It is approximately 1 km from a low-density housing development.

Camden (southwestern New Jersey, 110 km southwest of Newark). The sampling site was on the roof of a trailer in a residential and commercial district. The center of Philadelphia is 6–7 km to the west–northwest, and downtown Camden is to the northeast. Refineries and other industrial facilities are located along the Delaware River, to the west. To the immediate east are major traffic arteries and residential communities.

Elizabeth (northcentral New Jersey, 7 km south of Newark). The study site was on the rooftop (two stories above the street) of a building north of the central business area. Refineries and chemical facilities are 1–3 km to the south–southeast. Major traffic routes are 1–3 km to the east. Newark Airport is to the east–northeast.

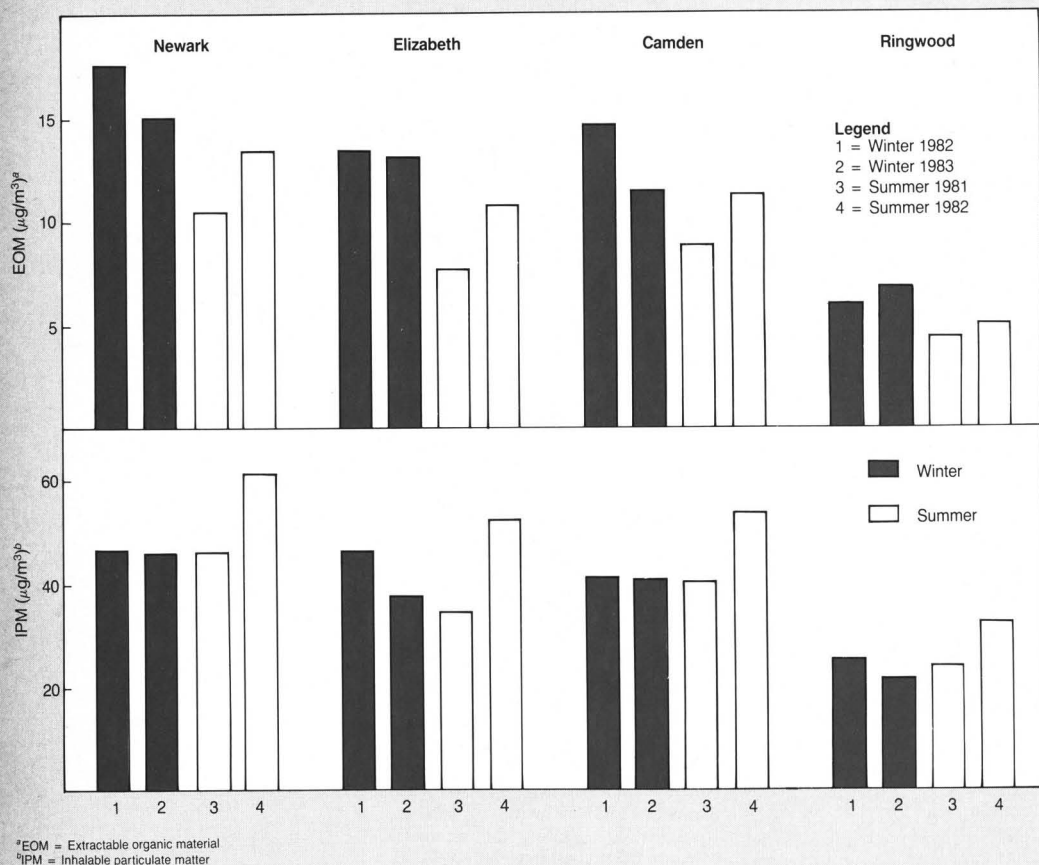
Newark (northcentral New Jersey, 30 km west–southwest of New York City). The study site was on a rooftop (two stories above the street) in the Ironbound district, which has established residential areas and industrial facilities (small and large) within and on the district perimeter. The Newark central business district is 2–3 km to the northwest. Newark Airport, the city of Elizabeth, and major refineries and other chemical facilities are to the south. Major traffic arteries surround the area.

time the moderately polar fraction averaged $\geq 2 \mu\text{g}/\text{m}^3$ for seven days. During other periods throughout the rest of that summer one-day peaks $> 2 \mu\text{g}/\text{m}^3$ were recorded for shorter episodes.

The greatest seasonal differences in composition were for the increases in nonpolar organics during the winter at all urban sites. This reflected seasonal changes in the influence of local space heating and motor vehicle traffic.

The PAHs have been examined by Harkov et al. (8) and Greenberg et al. (13). During the summer PAH concentrations in urban areas were two to three times greater than those at the rural site. Summertime concentrations were $< 1 \mu\text{g}/\text{m}^3$ because of lower fuel combustion and greater photochemical degradation. At all sites, the wintertime PAH concentrations were usually four

FIGURE 1
Geometric mean at ATEOS sites



to six times higher than the summer values. The volatile or reactive PAHs showed an even greater increase.

Researchers have inferred that motor vehicles and space heating are the major contributors to airborne PAHs in New Jersey (25). Emissions data have suggested that the primary heating source influencing statewide PAH levels in the winter is wood burning. In the ATEOS study Greenberg et al. also noted a wintertime correlation between the zinc from smelter emissions and PAH concentrations in Newark and Elizabeth (13).

Seasonal and intersite differences were observed for atmospheric concentrations and distributions of mutagenic activity, as determined by the Ames bioassay (19, 20). The magnitude of the mutagenic activity, revertants per cubic meter, for the four sites decreased in the following way: Newark > Elizabeth \geq Camden > Ringwood. Although the average urban concentrations of EOM and IPM were about two

times greater than those measured at the rural site, the average urban-to-rural ratio for one measure of mutagenic activity (TA98, -S9) was about four to one (13).

All sites had higher mutagenic activity per cubic meter in the wintertime than in the summer. This increase, however, was not proportional to changes in IPM or EOM. At Newark and Camden, the average values of inhalable particles were the same for the summer of 1981 and the winter of 1982; concentrations of EOM were 70% higher in winter in Newark and 30% higher in winter in Camden. For both sites, the wintertime mutagenic activity of the aerosol (TA98, -S9) was three to four times higher than in the summer of 1981. A similar pattern has been observed in New York City (26). Recent studies by Butler and co-workers have demonstrated that between-site variations in concentrations of EOM and of airborne particulate matter do not necessarily reflect similar

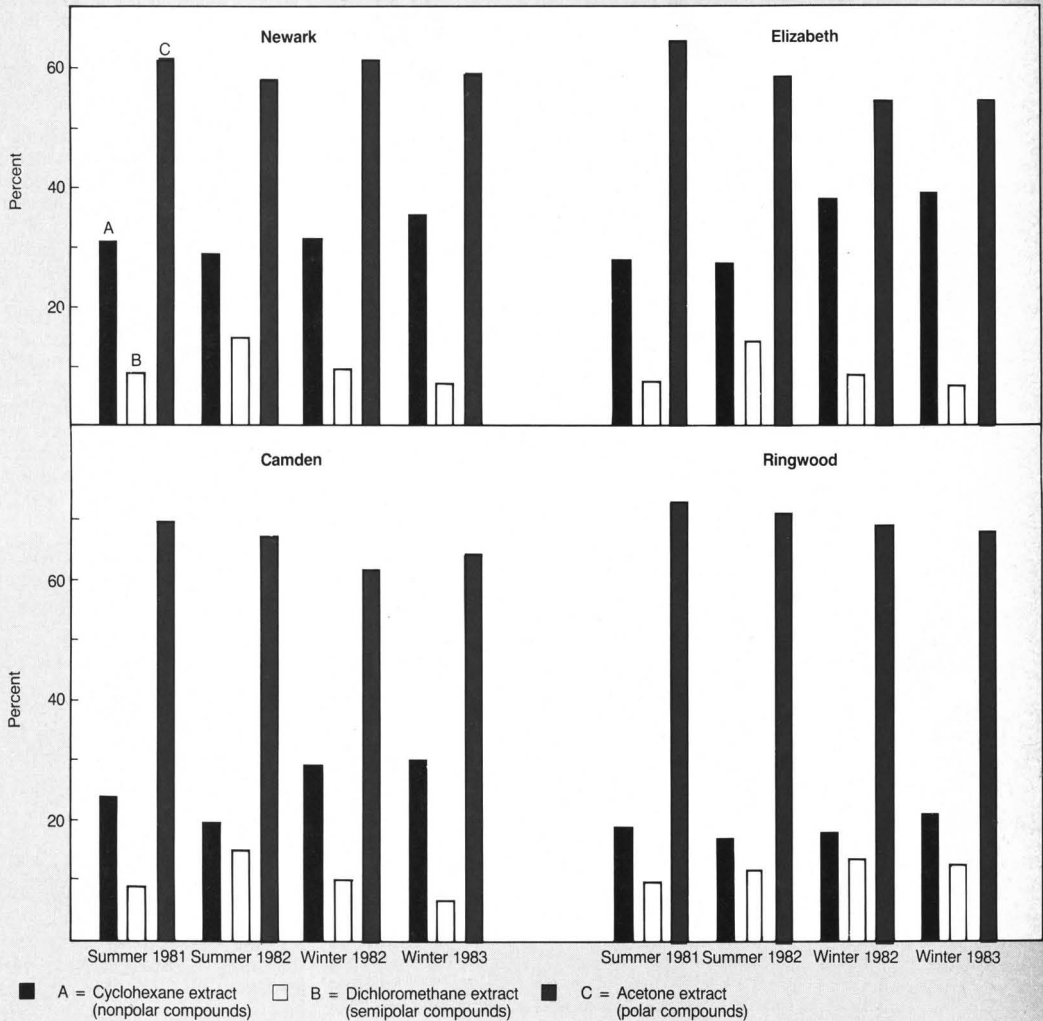
differences in the biological activity of the aerosols (22).

Air pollutant sources

Variations in the concentration, composition, and mutagenicity of the aerosol reflect microscale and mesoscale source effects at these sites. Estimates of the contributions of various sources to IPM were provided by receptor modeling studies (14, 15). Sulfate, its associated cations, and some polar organic matter accounted for approximately half of the IPM and had the same total mass concentrations at all three urban sites ($\sim 25 \mu\text{g}/\text{m}^3$).

The receptor modeling studies for IPM (Figure 3) at the Newark site showed that IPM was affected by a variety of industrial sources such as chemical plants, smelters, and paint-spraying operations (14, 15). In addition, the major sources—automobiles, oil burning, soil, and secondary particles (predominantly SO_4^{2-}) that affect most cities in the eastern U.S. contrib-

FIGURE 2
Distribution of EOM fractions



uted to the IPM.

Within 3 km of the Newark site, a number of sources—including small industrial and smelting operations, paint-spraying and paint pigment operations, and occasionally a zinc smelter—could affect the neighborhood. In one instance, the 24-h average zinc oxide contribution was $32.3 \mu\text{g}/\text{m}^3$, a maximum. In Elizabeth and Camden, the typical major urban source categories contributed almost all of the IPM. In Camden minor contributions were derived from incineration emissions transported from Philadelphia.

At each site the mean levels of extractable organics were higher in winter than in summer. In Newark the winter

values were 37% higher, in Camden 29% higher, in Elizabeth 43% higher, and in Ringwood 31% higher (Figure 1). During the winter areawide emissions from residential and commercial space heating, as well as greater traffic density, accounted for the urban increases in EOM. Housing density and the prevalence of burning oil or other fuels for heating in a given community would be the most important factor in defining intersite differences.

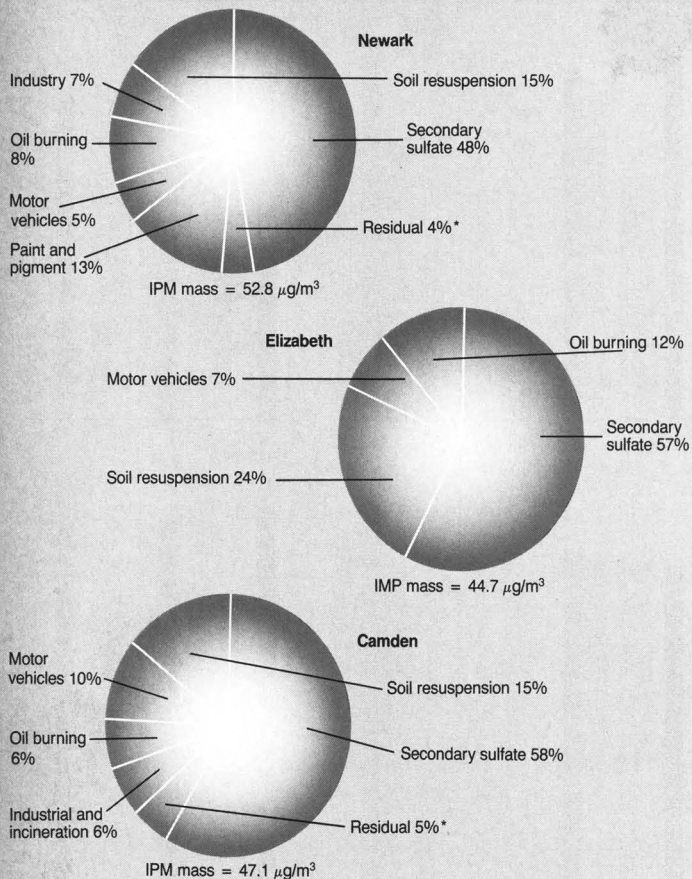
Areawide sources of IPM, such as motor vehicles and soil resuspension, had similar average effects at the three urban sites. Contributions differ for heavier or lighter traffic and the distribution of areas with uncovered soil.

Similarly, contributions of emissions from space heating differ depending on meteorology and the fuels used. For example, receptor modeling studies indicate that oil burning contributed $5.3 \mu\text{g}/\text{m}^3$ to IPM at the Elizabeth site but only $2.8 \mu\text{g}/\text{m}^3$ in Camden.

Air pollution episodes

Air pollution episodes, such as those in Donora, Pa., in 1948, in London in 1952, and in New York City in 1966, have been shown to contribute to excess mortality and morbidity (27). In the past, the concentration and nature of the specific contaminants were largely unknown, although later estimates indicated some combination of

FIGURE 3
Source contributions to IPM at urban sites



*Insignificant

Source: Reference 15

very high levels of particulate matter, soot, and SO_2 . Air pollution episodes have decreased in intensity but still occur in the U.S. More recently, summertime episodes of photochemical air pollution have been of primary concern. Recent studies by Lippmann et al. (28) and Liroy et al. (29) have shown that these can affect the pulmonary function of active children. During the ATEOS study summer and winter air pollution episodes occurred.

During the summer of 1981, peak concentrations of SO_4^{2-} ($>25 \mu\text{g}/\text{m}^3$) were equivalent at all sites. Daily values ranged from $2 \mu\text{g}/\text{m}^3$ to $30 \mu\text{g}/\text{m}^3$. In the winter, the range of values at all sites was smaller, and the peak daily levels were usually $\leq 20 \mu\text{g}/\text{m}^3$. On the worst day of the 1983 winter pollution

episode, the 24-h average SO_4^{2-} value was $26.3 \mu\text{g}/\text{m}^3$ in Newark. The mean sulfate concentrations were equivalent for all four sites in the summer and for all urban sites in the winter.

In both the summer and the winter SO_4^{2-} accounted for approximately 25% of the mass. Unfortunately, no SO_4^{2-} speciation was available for these samples. Other work suggests that during the summer higher H_2SO_4 exposures would occur in the more rural areas of this region, such as Ringwood, even though SO_4^{2-} levels could be equivalent in all locations (30, 31).

Summertime pollution episodes also influenced the composition of the organic fraction of the urban aerosol. During these periods of photochemical smog, increased concentrations of ex-

tractable organic matter were observed at all four sites in 1981 and 1982 (4, 32). In general, the concentrations of polar organics increased to a greater extent than did concentrations of non-polar organics, indicating the formation of secondary (polar) particulate organic matter via photochemical reactions and gas-to-particle conversions.

In a study of the EOM during the summer of 1981, it was reported that three processes were associated with the accumulation of this material (4). The first was a contribution of local primary polar and nonpolar emissions that can accumulate irrespective of meteorological conditions. The second was a regional secondary or polar organics contribution produced during the period of photochemical smog ($\sim 2 \mu\text{g}/\text{m}^3$). The third was a local excess associated with the polar fraction found during periods of photochemical smog. The local excess in polar organics was probably produced by the oxidation of VOCs emitted by local sources. Only

Source types near the Newark, N.J., ATEOS site

Within 1.5 km

- Auto and truck body painting and repair shops
- Chemical manufacturers
- Foundries
- Metal fabricators (tool and die, etc.)
- Metal processing (smelting and refiners)
- Metal reconditioning and finishing (alloying, painting, etc.)
- Paint spray and paint pigment manufacturers
- Space heating
- Motor vehicle traffic
- Waste paper facilities
- Welding

1.5–3.0 km

- Two zinc smelters
- Five plating operations
- Two casting foundries
- Metal refiners
- Two welding facilities
- Two other smelters
- Newark commercial business district
- Motor vehicle traffic
- Space heating

More than 3 km

- Chemical plants
- Petrochemical facilities
- Refineries
- Newark Airport
- Motor vehicles
- Space heating
- Central business districts of other communities

Newark was found to be significantly affected by all three, and the third process produced a mean excess of $6.3 \mu\text{g}/\text{m}^3$. This excess was again ascribed to the complex array of small and large point sources surrounding the Newark site. This industrialized sector of Newark appears to illustrate an environment in which population exposures to locally accumulated polar organics are possible in the summer.

The February 1983 pollution episode yielded some important between-site differences that also illustrate the need to focus on industry-population interfaces as potential locations for study of acute human exposures to air pollution. During this period, a peak IPM concentration of $201 \mu\text{g}/\text{m}^3$ was observed at Newark. The measurements of IPM in Elizabeth and Camden on this day were $104 \mu\text{g}/\text{m}^3$ and $77 \mu\text{g}/\text{m}^3$. Statistically significant IPM differences between Newark and the other three sites were observed on the preceding and following days. Similar results were observed for EOM, with the highest concentrations in Newark, followed by Elizabeth, Camden, and Ringwood. The extractable organics ranged from $50 \mu\text{g}/\text{m}^3$ to $70 \mu\text{g}/\text{m}^3$ on the worst days. These were among the highest levels ever recorded by our laboratory in domestic or foreign studies.

Hazardous VOCs

Fewer studies have been conducted on VOCs than on airborne particulate matter. Daily variations in the concentrations of 26 compounds were monitored at the three urban sites during the summer of 1981 and the winter of 1982 (7, 16).

The sources, geographical distributions, and dynamics of the VOCs differ substantially from those of airborne particulate matter. The sources of these compounds, particularly for the chlorinated hydrocarbons (16), were more local than the sources of much of the IPM. This was apparent from the between-site differences for the average and peak concentrations of some compounds. It should be noted that VOC concentrations are generally 10–100 times higher than those of individual particulate organic compounds.

The aromatic compounds—benzene; toluene; *o*-, *m*-, and *p*-xylenes; ethylbenzene; and styrene—generally had the highest concentrations and greatest frequency of occurrence of the 26 compounds measured. Of the chlorinated VOCs, vinylidene chloride, methylene chloride, trichloroethylene, perchloroethylene, and chlorobenzene had the highest concentrations. Generally, the highest mean VOC and the peak VOC concentrations were found in Newark, again followed in decreasing concentra-

tion by Elizabeth and then Camden. Peak concentrations of individual VOCs, however, occurred on different days at different sites. Toluene, for example, had a peak concentration of 137 ppb at the Newark site. On the same day, concentrations of toluene at both the Elizabeth and Camden sites were <5 ppb.

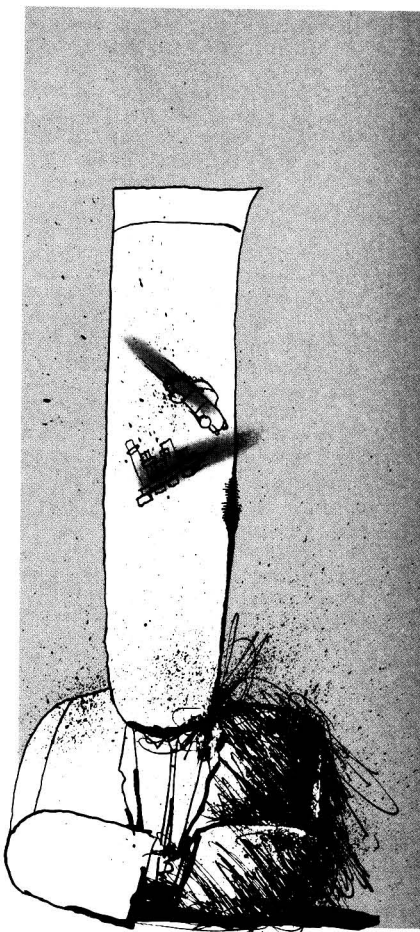
The accumulation of VOCs during air pollution episodes also was investigated. For periods of photochemical smog, methylene chloride, trichloroethylene, perchloroethylene, benzene, toluene, and *o*-, *m*-, and *p*-xylenes increased between two- and tenfold in Newark and Elizabeth. Only benzene increased in Camden. In the winter the situation was somewhat different; Newark had the maximum values for seven of these compounds. The only exception was benzene, which was higher in Elizabeth.

In the winter of 1982, excursions—that is, increases in the chemical concentration of pollutants in the air—were associated with local nocturnal stagnation (16). As a consequence, the presence of local sources around the sampling sites strongly affected VOC concentrations. Degreasing operations, chemical plants, refineries, paint shops, dry cleaners, gasoline stations, tanners, and other commercial operations were located near one or more of these urban sites (15).

For both seasons the aromatic hydrocarbons (benzene, toluene, and the xylenes) were identified primarily with evaporative and tailpipe emissions from automobiles or evaporative emissions from gasoline stations (7, 16). In the winter, however, oil burning appeared to be a second major source of benzene in Elizabeth. Factor analyses completed by Daisey et al. (33) have shown that benzene and toluene were associated with four or five factors, suggesting multiple sources for these compounds.

Point sources with emission rates of <50 t/y can make significant contributions to air pollution. For instance, the daily levels of toluene ranged from <1 ppb to 137 ppb. The toluene was emitted from automobiles and from auto body repair and paint shops. This is supported by the frequency and concentrations of the 24-h average peaks in toluene observed for both seasons in Newark. The seasonal pattern of toluene was consistent with the presence of auto body painting emissions sources. Doors to these buildings are usually open in the summer and closed in the winter, producing higher summertime values. Excursions of this magnitude were not seen at the other two sites.

The chlorinated compounds also had site-specific variations, although Harkov et al. (7, 16) showed that these



were poorly coupled with other pollutants measured in the ATEOS project. On some days, especially during the winter, the chlorinated compounds became the major component of the VOCs.

Summary and conclusions

On an average and daily basis, the Newark site had the highest concentrations of individual contaminants, even though the Elizabeth site was only 7 km away. Elizabeth was affected by the same area sources as Newark and by major petrochemical and refinery point sources. The Camden site was affected by the same kinds of area sources, the Philadelphia urban plume, and southwestern New Jersey-Philadelphia industrial plumes. The pollutant concentrations in Camden, however, usually were lower than those observed in Elizabeth or Newark.

The Newark site had a special feature—it could be affected by the large number of smaller sources in the area as well as large point sources and the stationary and mobile area sources.

This was demonstrated for both seasons and was acutely apparent in excursions due to episodes. The average contributions from individual point sources were not generally estimable. On individual days, however, the peak contributions were seen from the Zn smelter, the VOC sources, the industrial operations, and the area sources.

The population living in this section of Newark was surrounded by a number of sources that could affect them on any given day. Depending on the location of the source and the human receptor, these intermittent exposures could be much higher along any particular street. Because the area has a relatively stable population, long-term exposures to these pollutants would be expected. Peak exposures to outdoor VOCs can also be expected in such mixed industrial and residential areas, both from penetration indoors and from participation in outdoor activities (resulting in higher lung ventilation rates) in areas near a source. The ATEOS study has shown that under certain circumstances the concentrations may increase by two orders of magnitude. Such local peak exposures to VOCs offer the potential of causing genotoxic effects, such as birth defects and miscarriages. The extent to which such exposures occur and the potential population risk are unknown, but further investigation may be warranted.

The area studied in Newark is not unusual. It is typical of older industrialized population centers in major urban areas of the midwestern and eastern U.S. Locations such as these should be considered as targets of opportunity for future studies to quantify the risk of populations to outdoor emissions of toxic air pollutants.

Because the sources affecting each ATEOS site differ in nature and relative concentration, the concentrations of the IPM in the ambient atmosphere do not necessarily reflect the potential for damage to the health of the population in a particular location. Two cities or sections in a city with essentially the same average IPM may not have the same chemical composition or biological activity. In designing future epidemiological studies, therefore, consideration must be given to the chemical composition and biological activity of the atmospheres to which specific populations or subpopulations are exposed and to the relationship of these atmospheres to specific health effects.

Systematic and population-specific studies such as ATEOS can generate data that provide a better picture of exposures to outdoor and, if measured, indoor pollutants for various areas within the U.S. If such studies are coupled with personal monitoring (34)

and include biological markers of exposure and measurement of health effects, the risks associated with human exposure to high concentrations of outdoor and indoor pollutants can be assessed.

Acknowledgment

The ATEOS project was sponsored by the New Jersey Department of Environmental Protection's Office of Science and Research and the Division of Environmental Quality. We acknowledge work of our collaborators, Maria Morandi, University of Texas; Ronald Harkov, Judith Louis, and Leslie McGeorge of the New Jersey Department of Environmental Protection; Arthur Greenberg, Barbara Kebbekus, and Joseph Bozzelli, New Jersey Institute of Technology; Thomas Atherholt, Institute of Medical Research; and Nathan Reiss of Rutgers University. We would like to give special thanks to Theo. Kneip, New York University Medical Center.

Before publication this article was reviewed for suitability as an *ES&T* feature by Robert Harris, University of North Carolina, Chapel Hill, N.C.; and George Hidy, Desert Research Institute, Reno, Nev.

References

- (1) Lioy, P. J. et al. "Annual Report, Year 02, November 1981 to October 1982 of Project ATEOS"; Office of Cancer and Toxic Substances Research, Department of Environmental Protection: Trenton, N.J., 1982.
- (2) Lioy, P. J. et al. "Midyear Report on the New Jersey Airborne Toxic Element and Organic Substances (ATEOS) Project"; Office of Cancer and Toxic Substances Research, Department of Environmental Protection: Trenton, N.J., June 1983.
- (3) Lioy, P. J. et al. "New Jersey Airborne Toxic Element and Organic Substances (ATEOS) Project Report"; Office of Cancer and Toxic Substances Research, Department of Environmental Protection: Trenton, N.J., 1984; Vols. I and II.
- (4) Daisey, J. M. et al. *Atmos. Environ.* **1984**, *18*, 1411-19.
- (5) Lioy, P. J. et al. *J. Air Pollut. Control Assoc.* **1983**, *33*, 649-57.
- (6) Lioy, P. J. et al. *Atmos. Environ.* **1983**, *17*, 2321-30.
- (7) Harkov, R. et al. *J. Air Pollut. Control Assoc.* **1983**, *33*, 1177-83.
- (8) Harkov, R. et al. *Environ. Sci. Technol.* **1984**, *18*, 287-91.
- (9) Lioy, P. J.; Kneip, T. J.; Daisey, J. M. *J. Geophys. Res.* **1984**, *89*, 1355-59.
- (10) Lioy, P. J. et al. *Atmos. Environ.* **1985**, *19*, 429-36.
- (11) Atherholt, T. B. et al. *Environ. Int.*, 1985.
- (12) Lioy, P. J. et al. *J. Air Pollut. Control Assoc.* **1985**, *35*, 653-57.
- (13) Greenberg, A. et al. *Atmos. Environ.* **1985**, *19*, 1325-39.
- (14) Morandi, M. T.; Daisey, J. M.; Lioy, P. J. Paper 83-14.2. In "Proceedings of the 76th Annual Meeting of the Air Pollution Control Association"; Air Pollution Control Association: Pittsburgh, Pa., 1983.
- (15) Morandi, M. T. Ph.D. Dissertation, New York University, 1985.
- (16) Harkov, R.; Fisher, R. Paper 82-1.1. In "Proceedings of the 75th Annual Meeting of the Air Pollution Control Association"; Air Pollution Control Association: Pittsburgh, Pa., 1982.
- (17) Harkov, R. et al. *Sci. Total Environ.* **1984**, *38*, 259-74.
- (18) Daisey, J. M. et al. *Aero. Sci. Technol.*, in press.
- (19) Ames, B. N.; McCann, J.; Yamaski, E. *Mutat. Res.* **1974**, *31*, 347-64.

- (20) Maron, D. M.; Ames, B. N. *Mutat. Res.* **1983**, *113*, 173-215.
- (21) National Academy of Sciences. "Airborne Particles"; University Park Press: Baltimore, Md., 1979.
- (22) Butler, J. P. et al. In "Short-Term Bioassay in the Evaluation of Complex Environmental Mixtures"; Waters, D. D. et al., Eds.; Plenum: New York, N.Y., 1985; Vol. IV, pp. 233-46.
- (23) Pace, T. In "Proceedings of the Technical Basis for a Size Specific Particulate Standard, Parts I and II, Specialty Conference"; Air Pollution Control Association: Pittsburgh, Pa., 1980; pp. 26-39.
- (24) *Fed. Regist.* **1984**, *49*, 10408.
- (25) Harkov, R.; Greenberg, A. *J. Air Pollut. Control Assoc.* **1985**, *35*, 239-43.
- (26) Daisey, J. et al. *Environ. Sci. Technol.* **1980**, *14*, 1487-90.
- (27) "Air Quality Criteria for Particulate Matter and Sulfur Oxides," EPA-600/8-82-029c; EPA: Research Triangle Park, N.C., 1982; Vol. III.
- (28) Lippmann, M. et al. *Adv. Mod. Environ. Toxicol.* **1983**, *5*, 423-46.
- (29) Lioy, P. J.; Vollmuth, T. A.; Lippmann, M. *J. Air Pollut. Control Assoc.* **1985**, *35*, 1068-71.
- (30) Lioy, P. J. et al. *Atmos. Environ.* **1980**, *14*, 1391-1407.
- (31) Morandi, M. T. et al. *Atmos. Environ.* **1983**, *17*, 843-48.
- (32) Daisey, J. M. et al. Paper 84-80.1. In "Proceedings of the 77th Annual Meeting of the Air Pollution Control Association"; Air Pollution Control Association: Pittsburgh, Pa., 1984.
- (33) Daisey, J. M. et al. Presented at the APCA Specialty Conference on Receptor Methods for Source Apportionment, Real World Issues and Applications; Williamsburg, Va., March, 1985.
- (34) Pellizzari, E. D. et al. "Total Exposure Assessment Methodology (TEAM) Study: First Season—Northern New Jersey." Interim Report RTI/2392/03-03s; Research Triangle Institute: Research Triangle Park, N.C., 1984.



Paul J. Lioy (l.) is an associate professor and director of Exposure Measurement and Assessment, Department of Environmental and Community Medicine, Rutgers Medical School, Piscataway, N.J. He was involved with ATEOS while at New York University Medical Center, where he was associate director of the Laboratory of Aerosol and Inhalation Research.

Joan M. Daisey (r.) is an associate professor and associate director of the Environmental Studies Laboratory at the Institute of Environmental Medicine, New York University. She is the chair of the Peer Review Panel on the EPA Air Cancer Project. Her research interests include the nature, sources, reactions, and biological and health effects of toxic and carcinogenic airborne organic pollutants.

NEW AND SELECTED TITLES IN

Pesticide Chemistry

FROM THE AMERICAN CHEMICAL SOCIETY

Treatment and Disposal of Pesticide Wastes

Raymond F. Krueger and James N. Seiber, Eds.

Outlines the problems of pesticide waste disposal with special emphasis on developing better disposal strategies. Examines the chemical, biological and physical methods of disposal, the basic principles underlying each of these methods, and the analytical and modeling approaches applicable to waste disposal conditions. Also looks at the EPA regulatory viewpoint on safe disposal. Includes some novel approaches that have potential for wide scale use in the future.

ACS Symposium Series No. 259
373 pages (1984) Clothbound
US & Canada \$64.95

Export \$77.95

Bioregulators: Chemistry and Uses

Robert L. Ory and Falk R. Rittig, Eds.

Reports the latest research on the "miracle compounds" of agriculture—bioregulators. Covers the chemistry of these compounds and their applications and uses in improving crop yields and/or quality of various crops. Discusses synthetic bioregulators and their effects on major cereals, oil seeds, legumes, citrus, tree fruits, nuts, and more. Looks at bioregulator applications for resistance to insects, fungi, and microbial toxins; temperature extremes; and environmental stress. Also covers research on natural bioregulators present in certain crops.

ACS Symposium Series No. 257
296 pages (1984) Clothbound
US & Canada \$44.95

Export \$53.95

Pesticide Synthesis Through Rational Approaches

Philip S. Magee, Gustave K. Kohn, and Julius J. Menn, Eds.

Investigates the different methods used to design and synthesize new agricultural chemicals. Discusses successful strategies using a biorational rather than empirical approach to design and discover new pesticide chemicals. Looks at the next generation of pesticides as well as tools and techniques that will optimize their biological activity. Includes sections on

guided and serendipitous discovery, biochemical and physical design-assisted synthesis, and computer-assisted synthesis and QSAR.

ACS Symposium Series No. 255
351 pages (1984) Clothbound
US & Canada \$54.95

Export \$65.95

Dermal Exposure Related to Pesticide Use

Discussion of Risk Assessment

Richard C. Honeycutt, Gunter Zweig, and Nancy Ragsdale, Eds.

Confronts the issue of a serious chemical risk—pesticide exposure. Reports data vital for assessing and regulating farm worker safety. Looks at dermal absorption, field studies of exposure methodology, exposure assessment and protection, predicting exposure levels, and interpretation of data.

ACS Symposium Series No. 273
544 pages (1985) Clothbound
US & Canada \$79.95

Export \$95.95

Advances in Pesticide Formulation Technology

Herbert B. Scher, Ed.

Assesses new developments in pesticide formulations research. Looks at the most active areas of research and new products concepts. Examines the physical chemical principles of pesticide formulation science as well as the pesticide chemical structure-biological activity relationship.

ACS Symposium Series No. 254
264 pages (1984) Clothbound
US & Canada \$44.95

Export \$53.95

The Chemistry of Allelopathy Biochemical Interactions Among Plants

Alonzo C. Thompson, Ed.

Reports on the rapidly growing field of allelopathy, stressing the biological and chemical techniques. Assesses the allelopathic effect in weeds, crops, and aquatic plants, and studies the chemistry of allelopathic agents and the synthesis of cooperative efforts of biologists and chemists in solving the problems related to this topic and in using this natural phenomena to control weeds.

ACS Symposium Series No. 268
471 pages (1984) Clothbound
US & Canada \$79.95

Export \$95.95

Bioregulators for Pest Control

Paul A. Hedin, Ed.

Looks at new concepts and trends in pesticide chemistry and unifies approaches to the control of plants, insects, and diseases. Highlights the mechanisms of herbicides, fungicides, and endogenous plant hormones. Covers advances in bioregulators, both natural and synthetic. Will add much to the elucidation and adoption of novel chemical compounds for the control of pests.

ACS Symposium Series No. 276
570 pages (1985) Clothbound
US & Canada \$89.95

Export \$107.95

The Agrochemicals Handbook

Provides comprehensive data and information on a wide variety of products. Lists trade, chemical and approved names as well as manufacturers of active components of agricultural products. Covers toxic effects, chemical and physical properties, precautionary measures, and degradation metabolism of active components. Includes herbicides, fungicides, insecticides, nematocides, acaricides, rodenticides, and more. Special feature! Regular updates with announcements and introduction by agrochemical manufacturers of new active ingredients, new pesticidal formulations, and new uses of existing products. (Supplements will be shipped as soon as they are available.)

Published by the Royal Society of Chemistry
1,000 pages. Pillar-post binder. (1983)
US & Canada \$248.00 (includes Supplements 1-5)
Replacement Supplements \$20.00 each

Order from:
American Chemical Society
Distribution Office Dept 124
1155 Sixteenth Street, NW
Washington, DC 20036



To charge your books by phone, call toll free (800) 424-6747 and use your VISA, MasterCard, or American Express.

Waste monitoring

Technology is speeding up data acquisition and the translation of data into useful environmental information

Bruce P. Almich

*Environmental Protection Agency
Research Triangle Park, N. C. 27711*

William L. Budde

*Environmental Protection Agency
Cincinnati, Ohio 45268*

W. Randall Shobe

*Environmental Protection Agency
Washington, D. C. 20460*

Environmental management has a strong technical data component. A major problem is the conversion of raw data into the information needed for decision making. Nowhere is this problem more apparent than in hazardous waste management.

Former EPA Administrator William Ruckelshaus acknowledged that the agency was unable to move as quickly as the public would have liked in dealing with the problem of hazardous waste control (1). Reasons for this delay include issues of priority among thousands of known waste sites, concerns over the effectiveness of various cleanup strategies, and very high cleanup cost estimates. At the heart of many of these issues are the chemical analytical data used in setting priorities, planning cleanup strategies, and making cost estimates. For example, the presence of 2,3,7,8-tetrachlorodibenzo-*p*-dioxin (TCDD) at parts-per-million levels in a waste disposal area presents a more serious problem than does the presence of volatile solvents such as hexane and toluene.

Each year, hundreds of chemicals that are considered hazardous are routinely sought and, if present, are measured in tens of thousands of samples from waste sites. The validation, assessment, and use of all the data from these measurements are important components of decision making. The way in which these data have been acquired, stored, and used in recent years

may be a significant factor in hazardous waste management in years to come.

Traditional monitoring

Since its creation, EPA has been concerned with the collection, storage, retrieval, and analysis of environmental data. This activity, which is usually called monitoring, has been conducted by EPA staff and by contractors. Monitoring also is conducted under the permits and compliance programs that require industries, states, and municipalities to provide environmental measurement data to the agency. Monitoring encompasses the identification and measurement of concentrations of analytes in all environmental media, physical measurements, and biological tests.

It is required by most of the legislation administered by EPA.

Because of legislative mandates and administration policy, the environmental data used for decision making originate in a large number of laboratories nationwide. All these data must be assessed, validated where possible, organized, stored, and made readily accessible to decision makers.

Before the mid-1970s, EPA's monitoring programs consisted mostly of sampling and analysis that included a relatively small number of chemical and biological tests and physical measurements. The limited number of measurement methods, analytes, and organizational units involved during those years allowed a simple approach to data



collection and storage. Although EPA did, at the time, initiate a few projects aimed at automating laboratory data collection, the bulk of the automated data processing (ADP) effort was concentrated on the development and maintenance of large-scale computerized data repositories.

The vast amount of monitoring data was copied by hand from laboratory notebooks to reporting forms. These forms subsequently were sent to managers responsible for environmental programs. A portion of the monitoring data was sent from laboratories to ADP units where the data were prepared for transmission to the data repositories. Data in machine-readable form could be transmitted for only a few programs, such as the program by which states furnish air quality monitoring data to the national computerized air data base (SAROAD).

During those years, environmental data handling presented many opportunities for errors and long transmission delays as the data were copied and passed in handwritten form from one group to the next. Chances for errors in data entry and processing were increased because many of the organizations responsible for handling the data had little to do with the field sampling and laboratory analytical operations. Moreover, procedures for collecting and storing quality assurance data had not been adopted. Few tools were available to evaluate the quality of the stored

information and doubts were expressed about the reliability of many measurements.

The environmental monitoring requirements imposed on EPA have increased greatly since the mid-1970s. New legislation dictated an increase in the number of measured analytes, sampling sites, and kinds of media from which samples are taken. New data reporting procedures were required by a mandatory quality assurance order in 1979 (2). The typical environmental sample is now analyzed for hundreds of target analytes and nontarget constituents; a variety of quality assurance measurements must accompany the analytical results.

Advances in instrumentation

Together with EPA's increased data needs, there has been a virtual explosion in the capability of laboratory analytical instruments to generate raw, intermediate, and finished data. All modern instruments are equipped with at least a microprocessor capable of controlling the instrument and displaying results in digital form. The most versatile and powerful instruments, such as gas chromatography-mass spectrometry (GC/MS) systems and emission spectrometers, may be purchased with powerful minicomputers, large-capacity disk drives, multiple work stations, fast printers, industry standard magnetic tape drives, and multiuser, multitasking software (soft-

ware capable of doing several tasks simultaneously). These systems can produce vast quantities of data in a very short time.

Some systems have software that can produce the desired final results. More often, however, additional external calculations are required to convert raw and partially processed or intermediate data into usable information in final form. Although the number of target analytes has increased along with quality control requirements and cost per sample, the cost for the analysis of each analyte is far lower than it was in the mid-1970s because of advancements in instrument technology.

Automated data processing

The ADP resources of the agency have long been used to assist in the storage and evaluation of environmental monitoring data. But since the mid-1970s, uneven progress has been made in adapting these systems to meet ever-greater data processing demands.

Larger, faster, and far more capable computer hardware has been installed at the EPA's National Computer Center (NCC, Research Triangle Park, N.C.). Telecommunication networks have been implemented and advanced software tools have been developed. But major problems in information definition and handling have not yet received adequate attention. These include the standardization of monitoring data elements and the efficient, error-free transmission of data from the computerized laboratory instruments to the NCC systems in which data are stored and assessments are made.

Electronic transmission

In 1983, the idea for an improved system for handling and processing monitoring data was suggested (3). The proposal was based on the standardizing of data elements and on capturing information in machine-readable form at the earliest possible point in the acquisition process for input into agency data systems. These data would then be transmitted by electronic or magnetic means and machine-read into appropriate integrated computer data bases. EPA developed a plan to begin a series of experiments to test the feasibility of this approach.

One goal of the project was to demonstrate the rapid and accurate movement of finished analytical and quality control data and related information from laboratory computers to the NCC. Another objective was to demonstrate the rapid, error-free automated evaluation of quantitative and administrative data. (Some qualitative evaluations, such as whether a compound has been identified correctly, are difficult to au-

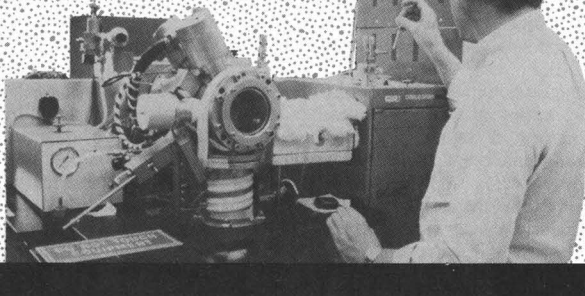
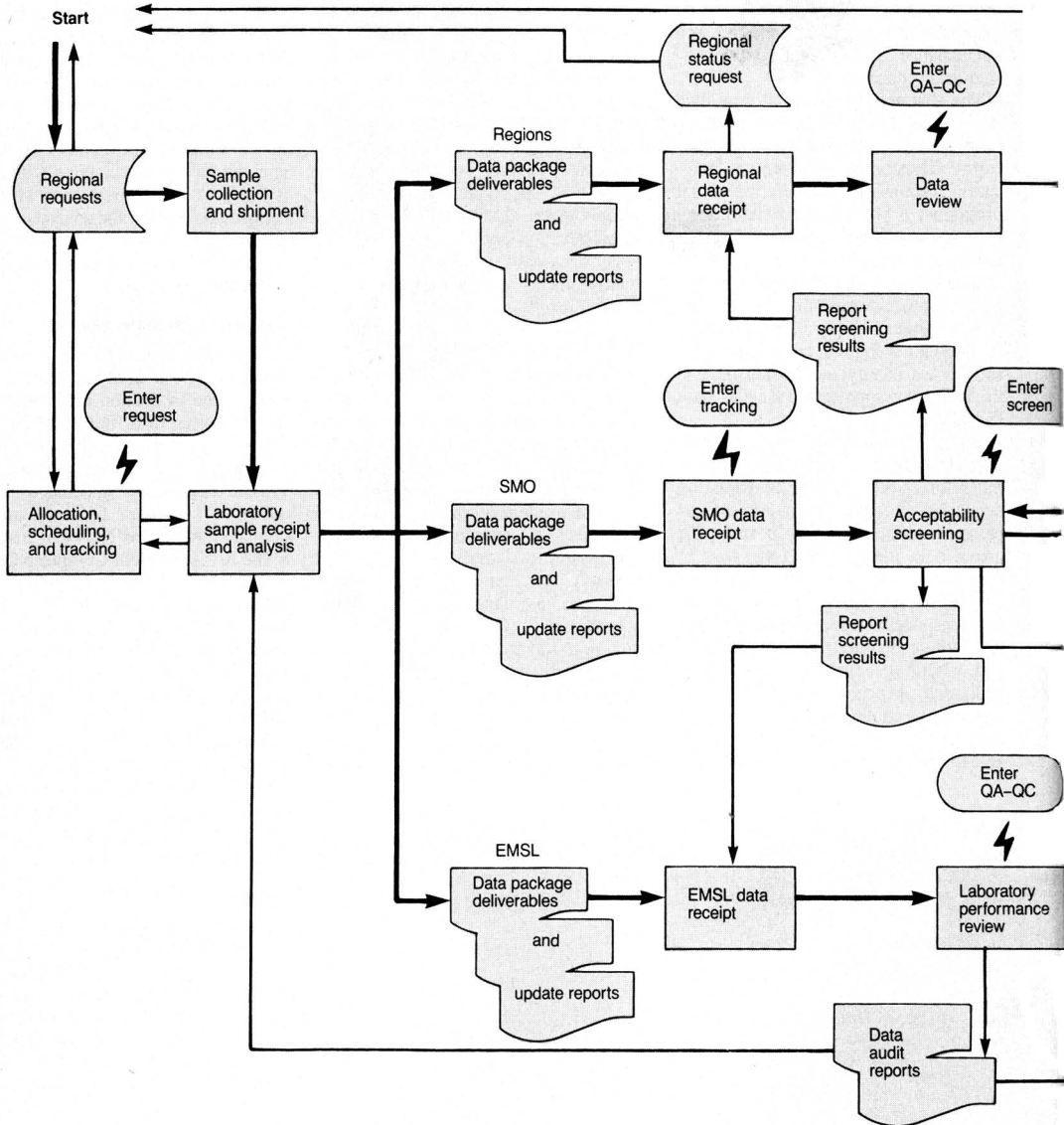


FIGURE 1
Current data flow and access for CLP



*Superfund remedial field investigation teams contract
 *National program office and regional division program office

tomate and will be handled manually for the present.) The Superfund contract laboratory program (CLP) was considered the most likely candidate to evaluate the system, since it was by far the largest and most diversified monitoring program in the agency and one of critical national importance.

Contract laboratory program

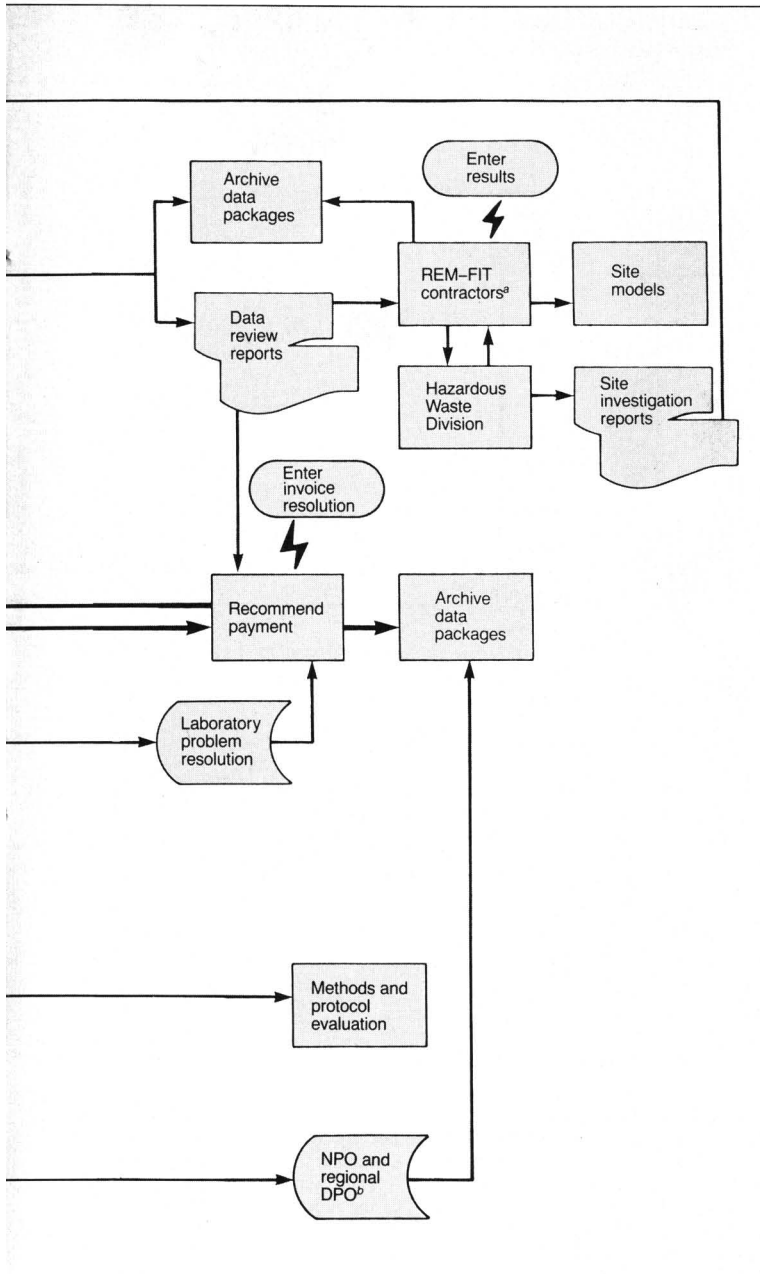
The Comprehensive Environmental Response, Compensation, and Liability Act of 1980 established Superfund to

investigate and clean up abandoned hazardous waste disposal sites. EPA's Office of Emergency and Remedial Response administers this program. The agency established a large contract laboratory program to perform the thousands of chemical analyses required each year.

In 1980, the CLP consisted of 13 laboratories that analyzed about 1600 samples. By 1985, an estimated 50 laboratories were analyzing samples at a rate in excess of 40,000/y. Some important

features of the CLP are its use of uniform sample collection, preservation, shipment, and storage procedures. Standardized, state-of-the-art analytical methods are enhanced by a strong and uniform quality assurance program.

The reporting of results, however, remains a paper-intensive manual system that uses traditional reporting forms and is not supported by contemporary ADP. Current requirements for the delivery of data from the CLP result in EPA's receiving a 2 1/4-in.-



thick stack of paper (three copies of a 3/4-in.-thick stack) for each sample analyzed. The result will be a stack of paper one and one-half miles high to be examined by the agency this year alone. The potential for error in transcription, transmission, and review is enormous. The conversion of all these data into useful information to support sound environmental management is a formidable task.

Figure 1 is a flow chart of inputs, processes, and outputs in the handling

of CLP data. Regional offices, the Sample Management Office (SMO), and the Environmental Monitoring Systems Laboratory (EMSL, Las Vegas, Nev.) receive identical copies of the laboratory reports and work on different portions of the data assessment task. Each oval symbol in Figure 1 denotes a keyboard data entry into one or more computer systems. Each rectangular symbol represents a process, and each printer symbol stands for the generation of additional paper reports of

reduced or reorganized data. Reporting in triplicate allows the processing to proceed concurrently, although some duplication is inevitable and coordination and communication among reviewing groups are required.

Standard transmission format

The orderly movement of information through electronic or magnetic media requires the use of a detailed, standardized format. If each data contributor were to use any format that is convenient, a large number of different input control and validation programs would be needed at the NCC to receive all the data from different sources. The cost of developing and maintaining all of these programs would soon more than outweigh the benefits gained through electronic data transmission.

The so-called free-form or text transmission approach is unacceptable for similar reasons. This would have required elaborate, intelligent software to interpret the various data elements and store them properly. In such a complex data reporting system, text interpretation is probably well beyond the current state of the art in data processing. Through a standard transmission format approach, it is possible to minimize the impact on the operations of the central data base management system and achieve the desired standardization of the monitoring data elements.

A standard was developed and proposed that could accommodate any qualitative or quantitative environmental measurement in any environmental medium and for any method of analysis (4). It can accommodate the required analytical quality control data and is flexible so that it can be adapted to meet future needs. This flexibility is made possible either by the addition of new kinds of records and data or by table entries that may be changed at any time to meet individual program needs. The standard is designed to avoid the transmission of redundant data, that is, results that may be obtained by simple mathematical processing of other data elements in the standard. The standard is also transmission-media-independent; it can be used in connection with magnetic tape, high-speed telecommunications, floppy disks, and other transmission systems.

The current standard contains a number of general classes of information. A variable number of specific data elements correspond to each class, and only a few examples are given for each class. Each data element is reported in a specific format in a specific field of a standard 80-byte record. Records are combined into files that are compatible with commonly used telecommunications protocols and magnetic media.

Some of the data elements are self-explanatory, such as the dates and times of key analytical events. Others, such as matrix codes, are related to an externally maintained table that may be revised and updated without affecting the transmission format. As a rule, the use of externally maintained lists adds great flexibility and power to the proposed standard.

Instrument software

Typical instrument software does not produce finished results for the purposes of environmental monitoring; this deficiency needed to be remedied to eliminate potential sources of error. Software that would allow keyboard entry of some data elements and generate a standardized transmission format was required.

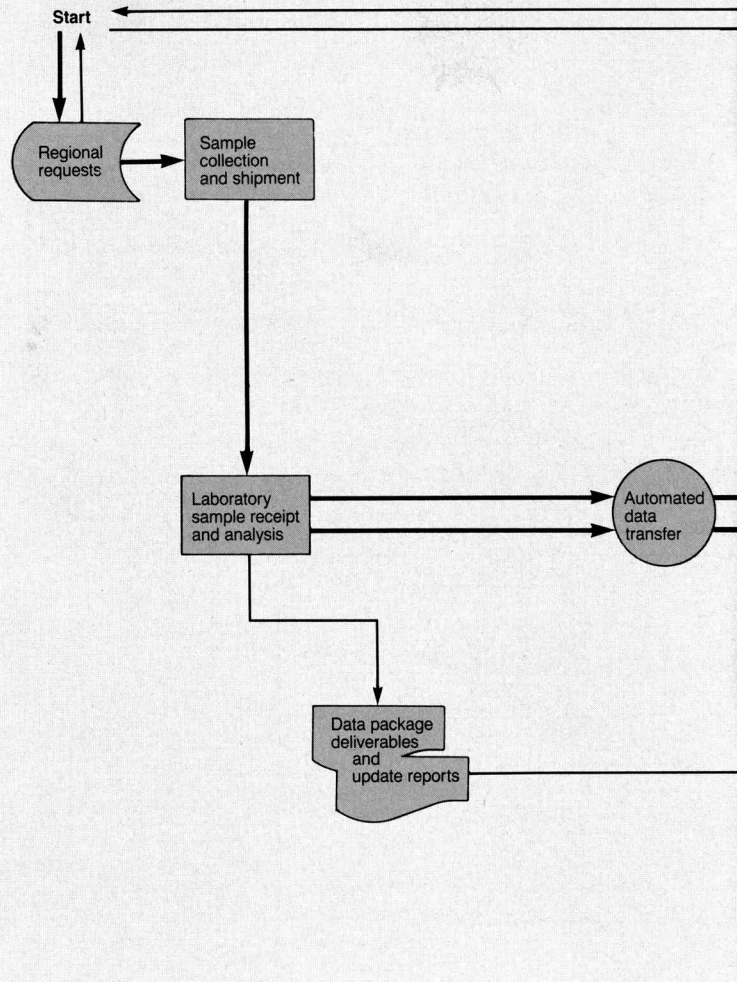
Demonstration software was developed for two commercial GC/MS data systems that are used extensively in the Superfund CLP. All EPA-sponsored software is in the public domain and will be maintained by EPA until it is tested and validated. Although the programs are constructed so that they are as independent as possible from those

Electronically transmitted monitoring data

The proposed standard format for the electronic transmission of analytical measurements for environmental monitoring programs contains the following classes of information:

- Dates and times of key events—extraction, analysis, reporting.
- Analysis requester codes—project and shipping data, administrative information, reports.
- Identification codes—sample, laboratory, instrument model, contracts.
- Analysis codes—method, analytes, quality control, matrices.
- Limits—quality control, sample-dependent and independent detection.
- Results—names, Chemical Abstracts Service registry numbers, units of measure, concentrations, amounts.
- Experimental conditions—wavelengths, chromatography columns, temperatures, flow rates, voltages, pressures.
- Calibration data—response factors, concentrations.
- Laboratory performance checks—reference compounds, instrument tests.
- Dilution factors—volumes, weights, sample sizes, injection volumes.
- Raw data—areas, peak heights, retention times.

FIGURE 2
Proposed data flow and access for CLP



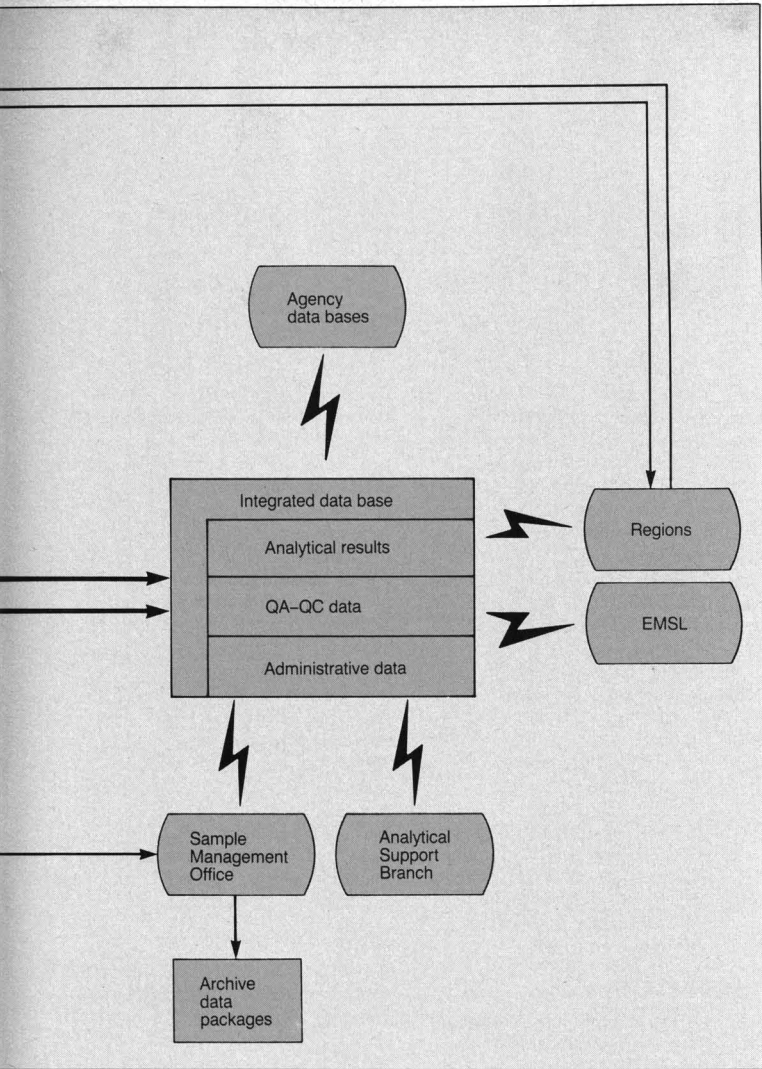
offered by vendors, the system makes use of existing vendor-supplied software whenever possible. Absolutely no proprietary software from any vendor is modified. Interface programs are written to read data elements from proprietary instrument data files into the EPA demonstration software files.

The use of EPA-sponsored software extensions requires that data be entered by keyboard only once by the person most knowledgeable about its accuracy. Most data are not entered by keyboard because they are generated by the analytical instrument and stored in disk files. These data are never printed and then reentered from a keyboard. Manual transcription of results is entirely eliminated, and the software minimizes operator interaction and redundant operations. A test of this software, using a vendor-supplied GC/MS system, was

completed in a number of laboratories last spring. Testing and development continued for the balance of last year.

The computer programs were written in the most widely available dialect of FORTRAN to make them compatible with most vendor-supplied instrument systems. Most input and output are in FORTRAN and use a minimum of vendor-specific operations. File manipulation is carried out separately for each different operating system.

Source codes are supplied to any vendor interested in adopting this system. If such a delivery system is adopted, laboratories will have a choice of using EPA-sponsored demonstration software or software developed by a vendor, by an independent software development firm, or by the laboratory itself. The main requirements would be the generation of data files in the exact transmis-



sion format and the inclusion of all data elements required by the laboratory's contract with EPA (4).

Centralized data base

The remaining step in the process of modernizing and improving EPA's monitoring-data handling is the construction of an integrated data base at NCC. Figure 2 shows the system proposed for development during this fiscal year. After the laboratory received samples and data from their analysis, the data would be transferred either by magnetic or electronic media.

The integrated data base consists of administrative information, analytical results, and quality assurance data. Users of these data will have access to them through remote work stations and high-speed, error-free telecommunication equipment that is currently being

installed at EPA facilities.

The round symbol in Figure 2 denotes an initial method of transmission that uses industry-standard nine-track magnetic tape. As high-speed, error-free telecommunications become more widely available, this data transfer method will be the procedure of choice.

A good start has been made toward substantially improving the efficiency with which EPA handles environmental monitoring data. The result is expected to be faster and more accurate data assessment and conversion of data into useful environmental information. This information will be used to address the difficult decisions involved in hazardous waste cleanup.

Acknowledgment

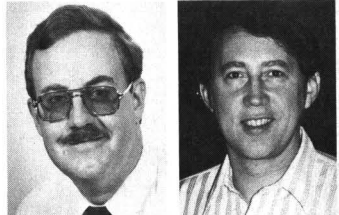
The authors thank William Benoit, Robert Booth, and Frances Fallon of EPA, Cincin-

nati, Ohio; Willis Greenstreet and M. David Cline of EPA, Research Triangle Park, N.C.; Stan Kovell and Tom Dunne of EPA, Washington, D.C.; and Ross Robeson and John Moore of EPA, Las Vegas, Nev. Figures 1 and 2 were constructed with assistance from Don Trees of Viar and Company (Alexandria, Va.).

Before publication, this article was reviewed for suitability as an *ES&T* feature by Lawrence Keith, Radian Corporation, Austin, Tex. 78766.

References

- (1) Ruckelshaus, W. D. "Establishing the National Hazardous Waste Control Programs: Goals and Realities," address to the American Public Works Association International Solid Waste Congress, Philadelphia, Pa., Sept. 17, 1984. EPA Office of Public Affairs: Washington, D.C., 1984.
- (2) *Fed. Regist.* **1983**, *48*, 45061.
- (3) Borman, S. A. *Anal. Chem.* **1983**, *55*, 943-48 A.
- (4) Almich, B. P.; Fallon, F.; Budde, W. L. "Proposed Standard Format for Electronic Transmission of Analytical Chemical Measurements for Environmental Monitoring Programs," EPA internal report; EPA: Cincinnati, Ohio, 1985; available from authors.



Bruce P. Almich (l.) is the manager of EPA telecommunications in the agency's Office of Data Processing. He is concerned with ADP modernization as well as the implementation of information and statistical quality control standards for environmental monitoring programs.

William L. Budde (r.) is chief of the advanced instrumentation section at EPA's Environmental Monitoring and Support Laboratory (Cincinnati, Ohio). He is concerned with methods development in gas chromatography-mass spectrometry and laboratory automation.



W. Randall Shobe is currently scientific automatic data processing coordinator in EPA's Office of Research and Development. His interests include the introduction and application of advanced technology to solving problems of environmental management.

EPA drinking-water proposals: Round two



Richard M. Dowd

Last month's "Regulatory Focus" (*ES&T*, December 1985, p. 1156) outlined the new drinking-water regulations proposed by EPA Nov. 13, 1985 (*Fed. Regist.* 1985, 50, 46880). These rules included the establishment of Recommended Maximum Contaminant Levels (RMCLs)—nonenforceable goals for 43 substances; the proposal of Maximum Contaminant Levels (MCLs)—enforceable standards for eight volatile organic compounds (VOCs); and RMCLs for an additional 51 VOCs.

The regulations' preamble notes that the Safe Drinking Water Act requires that MCLs be set as close to RMCLs as feasible. The feasibility analysis must consider the technical and economic availability of analytical methods, the lowest contaminant concentration obtained by the best treatment techniques generally available, and the cost of treatment.

For the eight VOCs, EPA has proposed MCLs and has specified which techniques are considered feasible for reducing contamination below these levels.

Technology and cost

The two major technologies specified are packed-tower aeration (PTA) and granular activated carbon (GAC) adsorption. According to EPA, PTA can remove 90–99% of the organics, and GAC can remove more than 99% of the volatiles. These removal percentages would lower some concentrations to below the limit (for regulatory purposes) of quantitation that is possible through normal laboratory methods. Although

these reductions can place contaminant levels below standard laboratory detection limits, EPA has decided to propose MCLs rather than invoke mandatory adoption of these technologies. The *Federal Register* notice requests public comment on this approach.

EPA estimates that for small water supply systems it will cost between 56¢ and \$1.01/1000 gal to remove VOCs using PTA and between 57¢ and \$1.50/1000 gal using GAC. For larger systems, the estimates range from 5¢ to 18¢ per 1000 gal. The agency notes that although these costs are relatively large for small systems, its analysis is based on worst-case assumptions of high contaminant levels. Costs could be less if contaminant levels are lower. EPA further estimates that capital costs required for the estimated 1300 public water supply systems to comply with its ruling will come to \$208 million nationwide, with an annual operating cost of \$21 million.

Measurements needed

One of the more notable features of these proposed regulations is the agency's reliance on analytical chemistry and on the practical quantitation limit (PQL) in setting MCLs. PQLs are based on the results of detailed performance evaluation studies of several laboratories. The studies established those analytical levels that are between five and ten times the minimum detection limit results achievable by generally available laboratory methods. Acceptance of this range appears to ensure that more than 80% of the laboratories involved could detect values at $\pm 40\%$ of the actual values.

For seven of the eight regulated VOCs, the detection levels are set at 5 $\mu\text{g/L}$, based on these laboratory evaluation studies. The results showed, however, that only two-thirds of the laboratories studied were able to produce results within 20% of that figure for six of the VOCs.

This finding becomes important because as part of its rule EPA proposes

to establish a laboratory certification program to set minimum quality assurance and quality control criteria for analytical laboratories that perform compliance measurements. These minimum criteria would require detection within 40% of the true value for all concentrations below 10 mg/L and within 20% for all concentrations above 100 mg/L.

The one exception to the 5- $\mu\text{g/L}$ PQL is that for vinyl chloride. Because vinyl chloride is difficult to analyze, EPA proposes an apparent anomaly—that the vinyl chloride MCL-PQL be set at 1 $\mu\text{g/L}$ and be measured less frequently and by fewer laboratories.

In determining PQLs, EPA has determined that several existing analytical methods are acceptable: methods 502.1, 503.1, and 524.1; all gas chromatography techniques; and gas chromatography-mass spectrometry, which is the method of choice.

Extent of the proposal

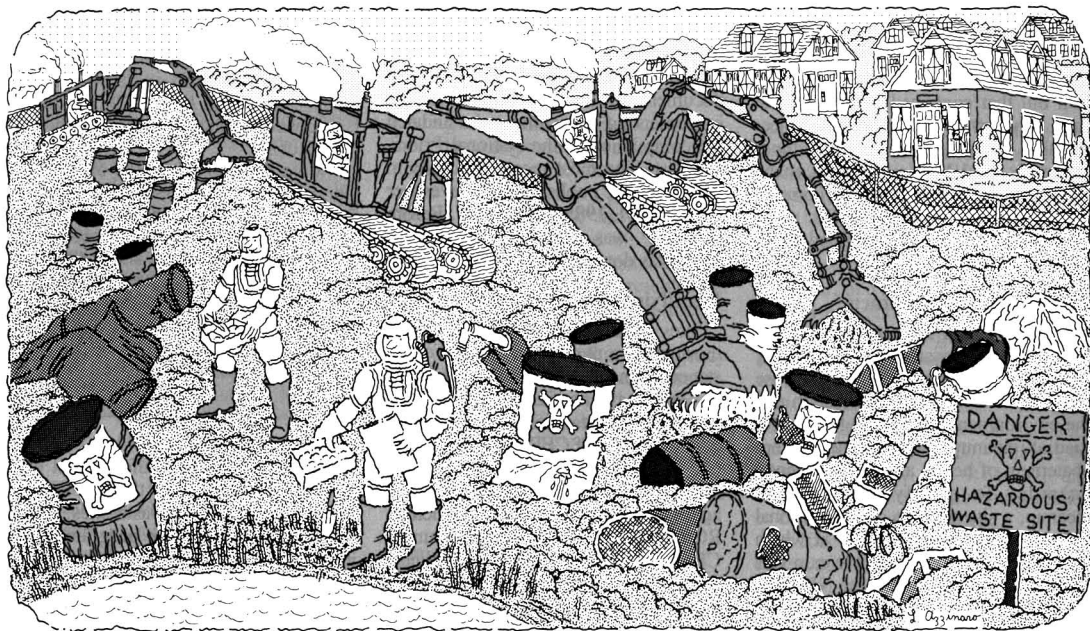
This rule also proposes a compliance monitoring method for 50 VOCs in addition to the eight that are regulated. About 45,000 public groundwater and 15,000 surface water systems must undertake monitoring over the next four to five years. Each system must be checked for contaminants at least once during this four-year period; operators of the largest systems must do so within the first year. If VOCs are detected, the system must be rechecked quarterly. The cost of this sampling is estimated at \$9 million initially, with repeat sampling estimated at \$17 million annually.

The combination of these monitoring requirements and the proposed laboratory certification program may affect standards and practices throughout the U.S. for laboratories performing analyses associated not only with drinking water but with any measurements concerning groundwater contamination.

Richard M. Dowd, Ph.D., is a Washington, D.C., consultant to Environmental Research & Technology, Inc.

Implementing Superfund

Although beset by funding uncertainties, the business of cleaning up abandoned hazardous waste sites is active and should grow when the law is reauthorized



Waste sites abound in the United States. One important aspect of abandoned, uncontrolled hazardous waste sites is their dissimilarity; another is their physical and chemical complexity. So plans and procedures for cleanup under the Comprehensive Environmental Response, Compensation and Liability Act of 1980 (CERCLA or Superfund) must be custom tailored to the physical characteristics of each site and the chemicals it contains.

Superfund differs from the Resource Conservation and Recovery Act of 1976 (RCRA, which was amended in 1984) in that it aims at cleaning up existing waste dumps; RCRA's goal is to prevent future dump sites from being created. The Superfund law was passed in December 1980 after discoveries of waste dumps such as the ones at Love Canal (Niagara Falls, N.Y.) and the so-

called Valley of the Drums (Bullitt County, Ky.) during the late 1970s.

Financing Superfund

Superfund is the federal fund used to pay for cleaning up abandoned, uncontrolled hazardous waste sites. It was financed from 1981 through 1985 to the extent of nearly \$1.6 billion and was supplemented by 10% matching grants from the states. Eighty-six percent of the federal money was raised from a special tax imposed on petroleum and petrochemical companies and chemical manufacturers; the balance came from federal appropriations.

Superfund expired Sept. 30, 1985. During the time the law and its taxing authority were in force, EPA identified 20,766 potential hazardous waste sites in the U.S. and estimated that the total number of sites could reach 22,000.

These numbers represent private and government-owned chemical, mining, and radioactive waste sites, among others, such as municipal dumps containing hazardous materials.

The agency examined 13,058 sites and carried out further investigations at 4458 sites. EPA began 507 actions for the rapid removal of hazardous wastes deemed to present an immediate danger to human health and safety and the environment; the agency completed 458 of these actions. In addition, EPA and state governments were working on permanent solutions to problems posed by 448 hazardous waste sites, and in October it was announced that eight of these cleanups were completed.

By November, Congress had not passed any law reauthorizing Superfund, nor had it passed provisional legislation keeping the old law and its tax-

ing authority in force. Lee Thomas, EPA's administrator, said that with the approximately \$125 million his agency had left when Superfund expired, the only actions EPA could take would consist of site identification, emergency response to chemical spills and releases, and law enforcement to compel those responsible for the wastes at a site to clean it up.

As of November, the Senate had passed a bill providing \$7.5 billion for fiscal years 1986-90. This money is to be raised through broad-based taxes, including a 0.08% value-added tax (VAT) on almost all manufactured or imported goods. The House was considering but had not yet passed legislation calling for more than \$10 billion. Thomas said that EPA needed only \$5.3 billion to implement Superfund. He also warned that President Reagan might veto any Superfund reauthorization bill that contained provisions that the administration considered objectionable, such as excessively high funding levels and VAT. Nevertheless, many in the hazardous waste cleanup community expect reauthorization for much more funding than was provided for in the original law.

Two categories of contracts

Superfund and its pertinent regulations contain provisions for short-term, emergency cleanups of sites that pose imminent hazards to human health and the environment and for long-term, remedial cleanups for the permanent abatement of health and environmental hazards. To qualify for remedial cleanup, a site must be on the National Priorities List (NPL). A site at which an emergency response or cleanup was carried out need not be on the NPL. On the other hand, a site listed on the NPL may be subject to both emergency and remedial response.

Emergency and remedial cleanups should not be regarded as alternatives. A site that is cleaned up on an emergency basis may be a candidate for remedial cleanup as well, depending on the variety, degree, and distribution of the hazardous materials found there. But a site scheduled for remedial cleanup might not pose the sort of immediate hazard that requires an emergency response. Each mode of cleanup is a separate EPA contracting category.

Additional engineering contracts are let by state and local governments and by private companies that clean up dump sites, either voluntarily or under administrative or court orders. Contracts for long-term construction and cleanup work are awarded by the U.S. Army Corps of Engineers, state and local governments, and companies carrying out their own cleanups. All con-

tracts for Superfund activities must be implemented in keeping with guidelines set forth under Superfund and its attendant regulations, regardless of who awards them.

Superfund money is also spent on enforcement, which requires responsible parties to clean a site or reimburse the federal or state government for the costs of a cleanup. In cases in which the responsible parties cannot be identified or located, the fund absorbs the costs of cleanup.

Response and cleanup activities under the law are governed by the National Contingency Plan (NCP). The agency first published its regulatory document, the "National Oil and Hazardous Substances Pollution Contingency Plan," in July 1982—more than 18 months after Superfund became law (*Fed. Regist.* 1982, 47, 31180). Widely regarded as the Superfund bible, this document set forth the guidelines for implementing Superfund and mandated the compilation of the National Priorities List. The most recent revisions to the NCP were published last November (*Fed. Regist.* 1985, 50, 47912). Before the NCP was promulgated, cleanup work was done on an interim basis.

Identifying sites

Sites come to the attention of the authorities in a number of ways. For instance, owners and operators of facilities must have notified EPA of the existence of their facilities by June 1981. Section 103(c) of CERCLA allows certain exemptions. For instance, owners and operators who have notified the agency under another statute, such as RCRA, need not report again under CERCLA. In addition, facility owners and operators often are not penalized if they can offer good-faith, reasonable explanations for late notification. On the other hand, deliberate failure to notify EPA can result in civil and criminal penalties.

Otherwise, sites are identified through investigation and observation by government authorities, reports from citizens, and other sources. In recent years, aerial observation and geophysical surveying techniques have been useful for locating and characterizing hazardous waste sites.

Notices of releases of Superfund-targeted wastes or substances designated as hazardous by any federal law, such as RCRA or the Clean Water Act, are reported to the National Response Center of the U.S. Coast Guard by telephone. Such notices are required by Section 102 of CERCLA.

Remedial vs. emergency response

The larger portion of government contract and in-house funding and sci-

Listing a site on the NPL

The National Priorities List (NPL) uses a mathematical rating scheme known as the hazard ranking system (HRS) (*Fed. Regist.* 1982, 47, 31186). A site is rated according to its potential to release hazardous wastes that damage human health and the environment. Sites are also rated according to the potential for migration of wastes to groundwater, leachate toxicity, and air and soil contamination. The degree of hazard of the waste materials is also taken into account.

Points are awarded under HRS on the basis of these factors and related characteristics. If the total for a given site exceeds 28.5, it is proposed for inclusion on the NPL. Final inclusion comes after further scientific and engineering evaluation and a period of public comment. About 90% of sites proposed for the NPL are included eventually.

More than half the sites at which emergency response has taken place are never listed on the NPL. Even if an emergency response has been carried out, if the site does not score 28.5 points in the HRS process, no further work will be done. If no emergency is indicated, and the site does not score 28.5 HRS points, action is usually not taken.

entific, technical, and enforcement efforts is directed toward the permanent cleanup of hazardous waste sites. This is the remedial response program, and it is concerned with long-term remedies for threats to public health and the environment from uncontrolled hazardous waste sites. Threats prompting remedial response include potential releases of hazardous materials to air, surface water, and groundwater.

One current remedial action involves the Lone Pine site in Freehold, N.J. Lone Pine was a municipal waste site where organic compounds and heavy metals were dumped. The chemicals are to be contained—that is, not removed but prevented from migrating into surrounding soil, groundwater, and air. Contaminated groundwater is to be treated by air stripping and passage through activated carbon.

As of mid-October, 541 sites nationwide were included on the NPL and an additional 309 sites had been proposed for the list. On the basis of that rate of addition of sites to the list, EPA and other organizations forecast that the number of NPL sites could reach 2200 over the next several years. (The congressional Office of Technology As-

assessment puts the figure as high as 12,000.) As of September, engineering studies sponsored by EPA or state governments were in progress at 379 NPL sites, and remedial cleanup work was under way at 69 sites. Another 69 such studies were enforcement led, that is, private parties allegedly responsible for the presence of the contaminants at the sites complied with orders from federal or state authorities to clean up the sites.

By October EPA announced that eight sites had been cleaned up and would be proposed for deletion from the NPL. They include two sites in Pennsylvania, one of which required the removal of polychlorinated biphenyls (PCBs). But on Oct. 31, Rep. James Florio (D-N.J.), the author of the original Superfund law, expressed reservations about this information. Referring to an announcement made by EPA last spring that remedial actions had been completed at six other sites, Florio charged that those sites had been included on interim lists prepared before the NPL came into being. He also complained that one of those sites, located near Pittston, Pa., lost more than 100,000 gal of toxic waste to the Susquehanna River in late September after flooding caused by the torrential rains of Tropical Storm Gloria.

Critics of the Superfund program say that progress in remedial cleanups is slow. But it should be kept in mind that completing remedial cleanups has been hampered because the investigation, planning, and design phases can take two to three years before any actual cleanup work begins. Because of the physical and chemical complexity of each site, extremely thorough investigations and designs are needed to provide well-documented, cost-effective, permanent solutions.

By contrast, the emergency response program deals with the immediate removal of materials from sites that are found to pose an imminent danger to public health and welfare. This danger takes the form of fires, explosions, direct human contact with acutely toxic substances, and threats to drinking-water supplies. Between December 1980, when the Superfund program began, and April 1985, 507 emergency response actions were started, and 458 have been completed. Most emergency actions and interim remedial actions must be completed in six months or less and must cost no more than \$1 million each.

One recent emergency action involved a now-defunct pesticide-manufacturing facility in Omaha, Neb. It had been closed in 1982 by order of local authorities because of health and safety code violations. In July 1984, highly toxic insecticides and herbicides, in-



Hazardous wastes are removed from a Minnesota site

cluding toxaphene and Silvex, were removed and disposed of at a cost of \$1.7 million. Because of the presence of many open and leaking pesticide containers, surface spills, and improperly stored wastes, EPA and the Nebraska Department of Environmental Control determined that the site presented an immediate public health threat and ordered an emergency response.

A salient example of an emergency action involving explosive and flammable materials is found in the Chemical Control site in Elizabeth, N.J. This site also is listed on the NPL for remedial action. In 1980, an explosion and fire occurred at the site, and toxic materials were released to the atmosphere.

Remedial contracts

As of late November, five principal contracts that had been let by EPA for remedial response planning and engineering were in force. These contracts, called remedial engineering management (REM) contracts, are for planning, designing, and engineering the most technically and economically workable approaches to the permanent cleanup of abandoned hazardous waste sites. The contracts are called remedial planning-field investigation teams (REM/FIT, which is split into two separate contracts), REM II, REM III, and REM IV (Figure 1). In addition, there is a REM V procurement, administered by the Small Business Administration and valued at about \$2 million, for certain small and minority-owned businesses to participate in the program.

One purpose of the FIT component of REM/FIT is to determine whether a site should be proposed for the NPL. Under the REM component, the contractors provide technical services consisting of preliminary assessments, in-

spection, and remedial investigations and feasibility studies for remedial alternatives at uncontrolled hazardous waste sites.

A spokesman for one of the prime contractors notes that like REM/FIT, the subsequent contracts—REM II, REM III, and REM IV—call for remedial investigation and feasibility studies, remedial design, construction plans, laboratory analyses, the development of guidance documents, and numerous related activities. However, REM/FIT placed more emphasis on locating sites for the NPL, REM II on remedial design, and REM III and REM IV on plans and activities related to construction and cleanup.

In June, William Hedeman, then director of EPA's Office of Emergency and Remedial Response, explained the mechanism by which companies submitted bids for REM III and IV after the agency issued a request for proposals (RFP). He said that contract proposals were screened for technical merit and that EPA negotiated prices with companies passing the first screening for technical qualifications.

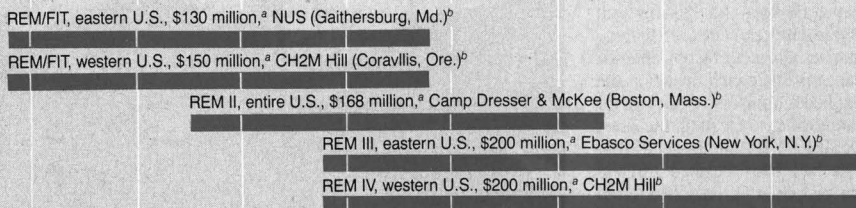
State and private initiatives

Like EPA, states and private interests are concerned with finding permanent solutions to the problem of abandoned, uncontrolled hazardous waste dumps. As of June, the states had spent a total of \$146.2 million to procure remedial services. States must go through the same contracting procedure that EPA uses—RFPs, screening of the proposals, and negotiating the final price with the firms showing the most technical merit.

States must be financially involved in any remedial action undertaken by the federal government. EPA will not sup-

FIGURE 1

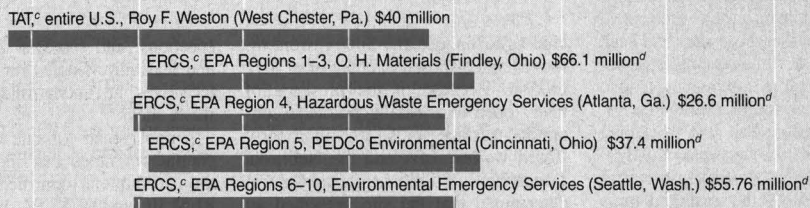
Ongoing remedial response contracts . . .



^aFunds for REM/FIT and REM II are obligated for the entire contracts, regardless of whether Superfund is reauthorized. The disbursement of funds could be delayed for REM III and REM IV if Superfund is not reauthorized.

^bPrime contractor. CH2M Hill subcontracted the FIT portion of REM/FIT to Ecology & Environment (Buffalo, N.Y.). Principal subcontractors for REM II are Roy F. Weston (West Chester, Pa.), Woodward-Clyde Associates (San Francisco, Calif.), Clement Associates (Arlington, Va.), ICF (Washington, D.C.), and C. C. Johnson & Associates (Silver Spring, Md.). Principal subcontractors for REM III are NUS, E. C. Jordan (Portland, Maine), Environmental Science & Engineering (Gainesville, Fla.), and ICF.

. . . and emergency response contracts



^cTAT = technical assistance teams; ERCS = emergency response cleanup services

^dApproximate contract value; funds for emergency responses are expected to remain available

Source: EPA

How the contractor evaluates a site

The remedial investigation and feasibility study (RI/FS) is the core of any remedial planning contract. It consists of an extensive technical investigation of a permanent solution to a contamination problem at an NPL site. Because no two sites are physically, chemically, and biologically alike, each RI/FS must address a particular site or cluster of sites.

The remedial investigation portion exhaustively investigates the factors that determine the lateral and vertical extent of contamination. It consists of a site survey, investigation, analysis, and laboratory and pilot studies. The document generated is the remedial investigation report.

Recently developed remote sensing and geophysical techniques have made it possible to speed up the identification of sites and to give a general idea of the site's location and spread of the wastes it contains. With that information, investigators have a better idea of how to proceed with the site survey and analysis.

The feasibility study component sets forth the nature of the remedial response to be conducted at the site, based on what was learned through the remedial investigation. It uses procedures that comply with applicable provisions of the National Contingency Plan. In this phase alternative remedies are considered and analyzed. Quantitative risk assessment is being used increasingly as a factor in the process of evaluating possible remedial action.

At the end of this study, a document sometimes called the record of decision is prepared. It serves as the technical basis for the remedial design.

In June 1985 EPA issued final guidelines for conducting an RI/FS: the "Guidance Document for Remedial Investigation Under CERCLA, EPA/540/G-85/002," and "Guidance Document for Feasibility Studies Under CERCLA, EPA/540/G-85/003."

port any remedial investigation or action unless the state supplies matching funds totaling at least 10%. If the site needing action is owned by a state or local government, the state must pay 50% of the remedial action costs.

In many cases, government authorities can determine who placed the wastes at a site—that is, who the potentially responsible parties are. The parties themselves often have notified EPA; in other cases, disposal sites are found through investigative work or citizen reports.

These parties frequently undertake remedial measures on their own. They may do so after an enforcement action—an order from the federal or state government or a court to clean up a site. Otherwise, they may do remedial work voluntarily. In either case, they must do all remedial investigation, planning, and cleanup work according to guidelines set forth by EPA (*Fed. Regist.* 1985, 50, 5034).

The program of action results from negotiations between the agency and the responsible parties. As long as EPA

or a state has approved a remedial program and the responsible parties are complying with the terms of their agreement with EPA or a state agency, they can contract for remedial planning, design, and construction services in whatever way they believe most advantageous.

3M (St. Paul, Minn.) is voluntarily carrying out a remedial program at a site east of St. Paul. During the 1940s and 1950s, 3M and several other companies had engaged an independent contractor to transport wastes to the site for disposal or open burning. The wastes mainly consisted of VOCs and heavy metals.

The company's plan, approved by EPA and the Minnesota Pollution Control Agency, called for pumping and treating contaminated groundwater from the shallow aquifer and plugging wells that tap portions of a slightly contaminated deeper aquifer. Concentrated wastes were to be removed and incinerated or disposed of in facilities meeting the requirements of RCRA.

Last June, Robert Paschke and Michael Santoro of 3M told the 78th Annual Meeting of the Air Pollution Control Association that waste excavation and removal have been completed. They said that the company has installed a network of monitoring wells to evaluate the effectiveness of remedial measures and to detect the migration of contaminants to shallow and deep aquifers. 3M has begun to submit monitoring reports to the state agency.

If the responsible parties do not come forward, or if they refuse to take action, then EPA or a state government will plan, design, and carry out the remedial measures and assess or sue the parties for reimbursement of all costs. Enforcement can be costly, especially if the parties are losing defendants in a lawsuit. In that case, responsible parties may be assessed up to three times what it cost the federal or state government to fund a remedial action. The U.S. General Accounting Office counsels these parties to take the initiative in doing their own remedial work; it will normally cost them far more if they must reimburse the federal or a state government for the cleanup, even if they are not assessed treble damages.

Industry initiative

That may be one reason a group of industry executives joined with environmental advocates and academicians to form Clean Sites, Inc. (CSI, Alexandria, Va.) in May 1984. CSI is a non-profit organization that supports and accelerates voluntary remedial action by responsible parties. At first, CSI's prospects appeared grim; it was unable to obtain site liability insurance because

that market had dried up suddenly.

Last Feb. 7, EPA signed a special agreement with CSI to commit Superfund money to protect it against third-party liability to the extent of \$5 million per site, but not to exceed \$10 million each fiscal year. This is similar to the indemnity accorded an EPA remedial investigation-feasibility study contractor. EPA included the condition that CSI must continue to seek insurance elsewhere. The agency's indemnification of CSI has caused considerable resentment among hazardous waste management businesses and trade associations because of what they perceive as a privileged status for CSI.

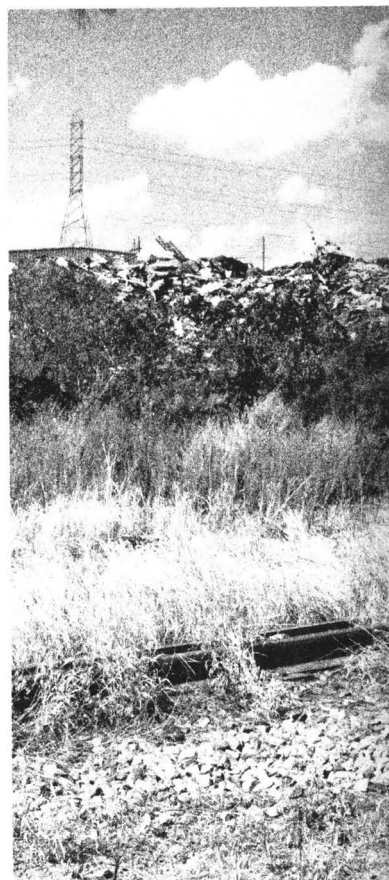
Another problem CSI has been facing—at least as of last spring—is underfunding. The company was to have received \$5 million. Half of that sum was to be contributed by the chemical industry and the other half by other industries and philanthropic organizations. The chemical industry supplied \$3 million, and recent contributions from outside the industry added \$500,000. CSI spokesmen say this level of funding is sufficient for now but there could be a money squeeze in the next few years. They have expressed hopes for a broadened base of contributions that would allow the expansion of CSI's activities.

Despite its relative youth and startup problems, CSI has made some gains. It is in the process of aiding responsible parties in assessing or working on more than 40 sites, including several large ones in Texas. And it has successfully mediated disputes among parties, or between parties and EPA, to get stalled remedial work back on track.

Construction phase

After the physical, chemical, and biological characteristics of a site have been defined and an engineering design for a permanent remedy is completed, the next phase is construction of the facilities to contain the wastes, treat them, or both. Scientific and engineering data and plans developed through remedial investigations and feasibility studies and remedial design based on the investigation govern which approaches are used.

There are several containment approaches, including control by grout curtains or slurry walls that isolate the site from groundwater. Other techniques include digging seepage basins or ditches and excavating, encapsulating, or dewatering contaminated soils. Guidelines for remedial construction have been issued in EPA's "Handbook for Remedial Action at Waste Disposal Sites," first published in June 1982. An updated version was published in November 1985.



Chemicals leaking from shredded drums (background) pose a threat to groundwater at this Florida site

Treatment procedures include pumping groundwater and leachate to the surface and treating them by chlorination, ozonation, and filtration through activated carbon. Wastes can be detoxified by activated sludge or rotating biological contactor treatment, chemical or bacterial degradation and decomposition, reverse osmosis, ion exchange, air stripping, and high-temperature incineration. These techniques are used mainly to control subsurface contamination plumes.

Containment facilities are installed and treatment usually is carried out at the site. The objective of these actions is to protect the groundwater, surface water, soil, and air in the vicinity from contamination by hazardous wastes that would migrate if the site remained uncontrolled.

Remedial response usually does not involve physical removal—that is, off-site destruction or transport and storage of wastes in a land disposal site that complies with RCRA regulations. Removal will be carried out if the EPA

TABLE 1
Contaminants found at Superfund sites

Chemical	Average percentage occurrence	Average concentration (ppb)
Lead	51.4	$\sim 3.09 \times 10^5$
Cadmium	44.7	2185
Toluene	44.1	$\sim 1.12 \times 10^6$
Mercury	29.6	1379
Benzene	28.5	16,582
Trichloroethylene	27.9	$\sim 1.03 \times 10^5$
Ethylbenzene	26.9	$\sim 5.4 \times 10^5$
Benzo[a]anthracene	12.3	$\sim 1.48 \times 10^5$
Bromodichloromethane	7.0	20
Polychlorinated biphenyls	3.9	$\sim 1.28 \times 10^5$
Toxaphene	0.6	12,360

Source: Presentation by William Eckel and Donald Trees, Viar and Company, and Stanley Kovell, EPA, at the National Conference on Hazardous Wastes and Environmental Emergencies

administrator determines that that approach provides the most technically feasible or cost-effective safeguards for human health and the environment.

The remedial response process requires the monitoring of soil, surface water, groundwater, and air. This is to be done during the actual response project and perhaps for as long as 30 years after remediation is complete. Remedial response also can involve federal and state governments paying for or sharing costs of relocating affected populations permanently, if the president or his designee deems such a move necessary.

Contracting for the construction phase works somewhat differently from that for REM projects. Instead of EPA, the environmental agency of the state in which the site is located publishes an RFP. The state then chooses the company offering the bid that most closely matches the RFP. Either the state agency concerned with remedial action or the U.S. Army Corps of Engineers may be the lead agency for handling the technical selection process. Corps of Engineers offices involved in Superfund construction are located in Kansas City, Mo., and Omaha, Neb.

Construction contracts are let site by site because of the need to tailor remedial construction projects to the characteristics of each site. For remedial engineering and construction purposes, a cluster of adjacent sites is treated as a single site.

Emergency response contracts

EPA has awarded five contracts for emergency response—one for technical assistance teams (TAT) and four for emergency response cleanup services (ERCS) (Figure 1). The contractors provide cleanup equipment, materials, and personnel to carry out immediate and planned removals of hazardous

waste. "Planned removal" is work at a site at which danger is not imminent but where waste containment or removal is to be carried out faster than at a site slated for remedial response. A planned removal is conducted only at the request of the governor of the state in which the site is located.

The technical assistance team consists of technical personnel who help EPA's on-site coordinator in preventing contamination and in containment, planning, community relations, monitoring, and arranging federal disaster assistance. Because of the emergency nature of the work, TAT and ERCS personnel are on call 24 hours a day and can be ordered on site within six hours of notification of an emergency.

Laboratory contracts

Under the contract laboratory program (CLP), 120 contracts for laboratory work under Superfund have been awarded to about 80 laboratories. The combined value of the individual contracts has been estimated at \$45 million. The CLP is the largest single laboratory program funded by EPA. Most of the laboratories are businesses for profit; a few belong to universities.

The laboratories are audited and monitored by EPA to ensure that they consistently provide high-quality standardized analytical services to a variety of clients in a given EPA region. The analytical methods run the gamut from gas chromatographic screens and wet chemistry to elaborate analyses requiring instrumentation such as gas chromatography-mass spectrometers (GC/MS) and even double-quadrupole mass spectrometers (GC/MS/MS).

Because a data base on the analyses has been developed, it is now possible to estimate the distribution and concentration of chemical contaminants at Superfund sites. William Eckel and

Donald Trees, scientists with Viar and Company (Alexandria, Va.)—contractors to EPA for the Sample Management Office—say these estimates of distribution and concentration arise from the analysis of nearly 3000 randomly selected samples from a total of 358 NPL and non-NPL sites. They discussed the estimates at the National Conference on Hazardous Wastes and Environmental Emergencies, which took place in Cincinnati, Ohio, in May and was organized by the Hazardous Materials Control Research Institute (Silver Spring, Md.).

Eckel and Trees presented lists of 218 compounds, metals, and ions that have been found in samples from Superfund sites. They gave information on frequency of detection and the average concentration and standard deviation for each compound. For example, among the volatile organics, ethylbenzene was found at more than 26% of the 358 sites, with an average concentration of nearly 540,000 ppb (Table 1). On the other hand, bromodichloromethane showed average concentration levels of only 20 ppb and was found at 7% of the sites. Eckel and Trees presented similar data for the other classes of contaminants such as pesticides, PCBs, and metals.

Funding uncertainties

Implementing Superfund is a nationwide operation that accounts for billions of dollars. Activities consist of emergency actions at hazardous waste sites that pose immediate threats to public health and the environment, permanent cleanups of hazardous waste sites, a huge laboratory program, and other efforts, such as policy studies. Most Superfund activities are started by EPA and state governments and later are contracted to private firms. Other work is being done entirely by the private sector either on a voluntary basis or as a result of enforcement actions.

But as this goes to press, businesses involved in implementing Superfund are experiencing uncertainties in funding. As of December, Superfund was in limbo; the original law and its taxing authority had expired. About \$125 million remaining from the time the law was in force, along with a possible congressional addition of \$60 million to EPA's hazardous waste budget, will keep site identification, emergency response, and enforcement activities going. The remedial engineering management contracts awarded in 1982 and 1984 will be carried out to completion. Unless Superfund is reauthorized, however, the resulting shortfall could delay the disbursement of funds for the new contracts and site cleanups.

—Julian Josephson

ES&T's 1986 Advisory Board



Russell F. Christman
Editor
University of North
Carolina



Dr. John H. Seinfeld
Associate Editor (air)
California Institute
of Technology



Dr. Philip C. Singer
Associate Editor (water)
University of North
Carolina

Russell F. Christman, editor, has announced the appointment of three new members to the *ES&T* advisory board. **Roy M. Harrison** is a reader in the department of chemistry at the University of Essex, Colchester, U.K. His research interests include aerosol studies and the uptake of aerosols by plants, pathways of organolead compounds, and the atmospheric chemistry of ammonia. **Walter J. Weber, Jr.**, is the chairman of the University Program in Water Resources at the University of Michigan. He has been active in the re-

search and development of processes for water and waste treatment and modeling of contaminant fate and transport for more than 25 years. **Richard G. Zepp** is affiliated with EPA's Environmental Research Laboratory, Athens, Ga. He is a research chemist specializing in the kinetics of photochemical and oxidation processes in aquatic environments.

Board members serve three-year terms. The last year of each member's term is noted in parentheses.



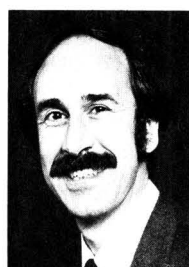
Dr. Marcia C. Dodge
EPA Environmental
Research Center
(1987)



Dr. Steven J. Eisenreich
University of Minnesota
(1986)



Dr. William H. Glaze
University of California
at Los Angeles
(1986)



Dr. Roy M. Harrison
University of Essex
(1988)



Dr. Michael R. Hoffmann
California Institute
of Technology
(1986)



Dr. Donald Mackay
University of Toronto
(1986)



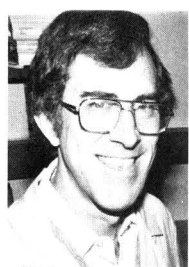
Dr. Jarvis L. Moyers
National Science
Foundation
(1987)



Dr. Kathleen C. Taylor
General Motors
Research Laboratories
(1987)



Dr. Walter J. Weber, Jr.
University of Michigan
(1988)



Dr. Richard G. Zepp
EPA Environmental
Research Laboratory
(1988)

Editorial policy

Environmental Science & Technology reports on aspects of the environment and its control by scientific, engineering, and political means. Contributed materials may appear as feature articles, critical reviews, current research papers, research notes, and correspondence. Central to the evaluation of all contributions is a commitment to provide the readers of *ES&T* with scientific information and critical judgments of the highest quality. For the convenience of authors, the specific nature of each type of contribution is outlined below.

Feature articles. A manuscript submitted for publication as a feature article should present useful discussion and opinion on important research directions in environmental science, developing technology, environmental processes, and social, political, or economic aspects of environmental issues. Each manuscript undergoes review by qualified peers as well as by the editors for the purpose of balance and elimination of inappropriate bias. Review criteria include significance of the scientific issue or process described, quality and succinctness of the text, and identification of potential research needs. Strict requirements for documentation of results, completeness of data, and originality, such as those applicable to research manuscripts, are not included in the review criteria for feature articles.

Critical reviews. Critical reviews are thoroughly documented, peer-reviewed assessments of selected areas of the environmental science research literature for the purpose of identifying critical research needs. Criteria for acceptability include current importance of the field under review, thoroughness of the literature coverage, clarity of text, and adequacy of research need identification.

Current research papers. The research pages of *ES&T* are devoted to the publication of critically reviewed papers concerned with the fields of water, air, and waste chemistry, and with other scientific and technical fields that are relevant to the understanding and management of the water, air, and land environments. Contributed research papers, in general, describe complete and fully interpreted results of original research.

Environmental Science & Technology seeks to publish pa-

pers of an original and significant nature. Originality should be evidenced by new experimental data, new interpretations of existing data, or new theoretical analysis of environmental phenomena. Significance will be interpreted with respect to the breadth of impact of the reported findings. Manuscripts reporting data of a routine nature that do not offer heretofore unavailable important information or do not substantially augment already available data will be declined publication in *ES&T*. The scope of the reported data in ambient monitoring studies should be such that broad conclusions applicable to more than the particular local scale are possible.

All research articles emphasizing analytical methodology for air or water analysis must include substantial application to environmental samples. *ES&T* faces some overlap with other journals in this area, and articles that do not contain, in the editors' judgment, a significant emphasis on environmental analysis will be returned to the authors for submission elsewhere.

Manuscripts should be prepared with strict attention to brevity. The vast majority of articles are expected to be fewer than four published pages. Processing time will be shortened if the editors do not have to return manuscripts to be condensed.

Notes and correspondence, as well as full-length papers, will be published in the research section. **Notes** are shorter research reports describing preliminary results of unusual significance or studies of small scope. Authors of Notes should be able to justify why it is not desirable to wait for a more complete report to be published as a full-length paper. **Correspondence** is a significant comment on work published in the research section of *ES&T*. Comments should be received within six months of date of publication of the original article. The authors of the original article ordinarily will be allowed to reply.

Send manuscripts to *Environmental Science & Technology*, 1155 16th St., N.W., Washington, D.C. 20036. Address feature manuscripts to Managing Editor; research manuscripts to Manager, Manuscript Office. Include a signed copyright transfer form, a copy of which appears on the inside back cover of this issue.

Current research author's guide

This manuscript preparation guide is published to aid authors in writing, and editors and reviewers in expediting the review and publication of research manuscripts in *Environmental Science & Technology*. For a detailed discussion with examples of the major aspects of manuscript preparation, please refer to *The ACS Style Guide* (1986).

Title

Use specific and informative titles. They should be as brief as possible, consistent with the need for defining the subject of the paper. If trade names are used, give generic names in parentheses. Key words in titles assist in effective literature retrieval.

Authorship

List the first name, middle initial, and last name of each author. Omit professional and official titles. Give the complete mailing address where work was performed. If present address of author is different, include the new information in a footnote. In each paper with more than one author, the name of the author to whom inquiries should be addressed

carries an asterisk. The explanation appears on the contents page.

Abstracts

An abstract, which will appear at the beginning of each paper, must accompany each manuscript. Authors' abstracts frequently are used directly for *Chemical Abstracts*. Use between 100 and 150 words to give purpose, methods or procedures, significant new results, and conclusions. Write for literature searchers as well as journal readers.

Text

Consult a current issue for general style. Assume your readers to be professionals not necessarily expert in your particular field. Historical summaries are seldom warranted. However, documentation and summary material should be sufficient to establish an adequate background. Divide the article into sections, each with an appropriate heading, but do not oversectionalize. The text should have only enough divisions to make organization effective and comprehensible without destroying the continuity of the text.

Keep all information pertinent to a particular section within that section. Avoid repetition. Do not use footnotes; include the information in the text.

Introduction. Discuss relationship of your work to previously published work, but do not repeat. If a recent article has summarized work on the subject, cite the summarizing article without repeating its individual citations.

Experimental. Apparatus: List devices only if of specialized nature. Reagents: List and describe preparation of special reagents only. Procedure: Omit details of procedures that are common knowledge to those in the field. Brief highlights of published procedures may be included, but details must be left to literature cited. Describe pertinent and critical factors involved in reactions so that the method can be reproduced, but avoid excessive description. Results and discussion: Be complete but concise. Avoid nonpertinent comparisons or contrasts.

Manuscript requirements

Three complete legible copies of the manuscript are required. They should be typed double or triple spaced on 22 × 28 cm paper, with text, tables, and illustrations of a size that can be mailed to reviewers under one cover. Duplicated copies will be accepted only if very clear.

If pertinent references are unpublished, furnish copies of the work or sufficient information to enable reviewers to evaluate the manuscript.

In general, graphs are preferable to tables if precise data are not required. When tables are submitted, however, they should be furnished with appropriate titles and should be numbered consecutively in Roman numeral style in order of reference in the text. Double space with wide margins, and prepare tables in a consistent form, each on a separate 22 × 28 cm sheet.

Submit original drawings (or sharp glossy prints) of graphs, charts, and diagrams prepared on high-quality inking paper. All lines, lettering, and numbering should be sharp and unbroken. If coordinate paper is used, use blue cross-hatch lines because no other color will "screen out."

Typed lettering does not reproduce well: Use black India ink and a lettering set for all letters, numbers, and symbols. On 20 × 25 cm copy, lettering should be at least 0.32 cm high—for example, with a Leroy lettering set, use template 120C and pen No. 0. Lettering on copy of other sizes should be in proportion. Label ordinates and abscissas of graphs along the axes and outside the graph proper. Do not use pressed wax for numbering or lettering; it rubs off in all the mailings and handlings necessary before receipt by the printer.

Photographs should be supplied in glossy print form, as large as possible, but preferably within the frame of 20 × 25 cm. Sharp contrast is essential.

Number all illustrations consecutively using Arabic numerals in the order of reference in the text. Include a typed list of captions and legends for all illustrations on a separate sheet.

If drawings are mailed under separate cover, identify by name of author and title of manuscript. Advise editor if drawings or photographs should be returned to the author.

Nomenclature

The nomenclature should correspond, as closely as possible, to that used by other ACS primary publications (refer to *The ACS Style Guide*).

Use consistent units of measure (preferably SI).

If nomenclature is specialized, include a "Nomenclature" section at the end of the paper, giving definitions and dimensions for all terms. Write out names of Greek letters and special symbols in margin of manuscript at point of first use. If subscripts and superscripts are necessary, place them accurately. Avoid trivial names. Trade names should be defined at point of first use (registered trade names should begin with a capital letter). Identify typed letters and numbers that could

be misinterpreted, for example, one and the letter "I," zero and the letter "O."

Formulas and equations

Chemical formulas should correspond to the style of ACS publications. Chemical equations should be balanced and numbered consecutively along with mathematical equations. The mathematical portions of the paper should be as brief as possible, particularly where standard derivations and techniques are commonly available in standard works.

Safety

Authors are requested to call special attention—both in their manuscripts and in their correspondence with the editors—to safety considerations such as explosive tendencies, precautionary handling procedures, and toxicity.

Acknowledgment

Include essential credits in an "Acknowledgment" section at the end of the text, but hold to an absolute minimum. Give meeting presentation data or other information regarding the work reported (for example, financial support) in a note following Literature Cited.

References

Literature references should be numbered and listed in order of reference in text. They should be listed by author, patentee, or equivalent. In the text, just the number should be used, or the name should be followed by the number. "Anonymous" is not acceptable for authorship. If the author is unknown, list the reference by company, agency, or journal source. Do not list references as "in press" unless they have been formally accepted for publication. Give complete information, using abbreviations for titles of periodicals as in the Chemical Abstracts Service Source Index, 1985.

For periodical references to be considered complete, they must contain authors' surnames with initials, journal source, year of issue, volume number, issue number (if any), and the first and last page numbers of the article. Consult *The ACS Style Guide* for reference style.

Supplementary material

Extensive tables, graphs, spectra, calculations, or other material auxiliary to the printed article will be included in the microfilm edition of the journal. Identify supplementary material as to content, manuscript title, and authors. Three copies of the supplementary material, one in a form suitable for photoreproduction, should accompany the manuscript for consideration by the editor and reviewers. The material should be typed on white paper with black typewriter ribbon. Computer printouts are acceptable if they are clearly legible. If individual characters for any of the material, computer or otherwise, are broken or disconnected, the material is definitely unacceptable.

Figures and illustrative material should preferably be original India ink drawings or matte prints of originals. Optimum size is 22 × 28 cm. Minimum acceptable character size is 1.5 mm. The caption for each figure should appear on the same piece of copy with the figure. Be sure to refer to supplementary material in text where appropriate.

Supplementary material may be obtained in photocopy or microfiche form at nominal cost. Material of more than 20 pages is available in microfiche only. Photocopy or microfiche must be stated clearly in the order. Prepayment is required. See instructions at the end of individual papers.

The supplementary material is abstracted and indexed by Chemical Abstracts Service.

Subscribers to microfilm editions receive, free, the supplementary material in microfiche form from individual papers in any particular issue. For information, contact Microforms Program at the ACS in Washington, D.C., or call (202) 872-4554.

Peer review in *ES&T*

Characteristics of *ES&T*

ES&T stands out among American Chemical Society journals in that it combines both a magazine and a journal. Only one other ACS publication contains this combination—our sister publication, *ANALYTICAL CHEMISTRY*. Because of the hybrid nature of our publication, it serves a large and diverse audience.

Central to the evaluation of all contributions to *ES&T* is a commitment to provide our readers with scientific information of the highest quality. The publication seeks the most significant, original, and broadly applicable types of articles for its current research section. A vast number of persons review original manuscript contributions and indicate in their evaluations the originality and scientific validity of the work, as well as the appropriateness of the material for our publication.

The editor and associate editors, who are located at the University of North Carolina and the California Institute of Technology, are fully responsible for all material published in *ES&T*. This policy is a general one applicable to all editors of American Chemical Society publications. The 10 members of the Advisory Board are chosen by the editor to provide input to *ES&T*'s operation. The members are chosen to represent various constituent groups in the research and reader communities and serve three-year terms. Although the editors seek advice and help from individuals in the scientific community and from advisory groups, it is ultimately the editors' responsibility to provide editorial direction, set editorial policies, and make individual publication decisions.

The Washington editorial staff handling the current research section is responsible for the day-to-day operation of the peer review system. All editorial staff members have chemistry or related science degrees.

General guidelines and overall editorial policies set by the editor form the basis for evaluating reviewers' comments on research articles submitted for the current research section.

A look at peer review

Each manuscript submitted to the current research section is assigned to a particular staff member who is then responsible for the manuscript—from choosing reviewers to communicating ultimate acceptance or rejection. The staff editor screens manuscripts to determine whether the papers may fall outside of *ES&T*'s scope. If there seems to be a question, the manuscript is immediately referred to the editor or an associate editor.

Reviewers are carefully selected, based on the subject matter of the paper, the experts available in a given area, and the editorial staff member's knowledge of the habits of proposed reviewers. Thus, known slow reviewers are avoided when possible. Potential reviewers for each paper are identified through various means, one of which involves a computer search of subjects that reviewers have indicated are their areas of expertise. Reviewers are normally asked to respond within three weeks, and if they are late, reminders are sent. Late review notifications are generated and dispatched as mailgrams on a weekly basis.

When the reviews come in, they are examined and evaluated by the staff editor. If the first two reviewers do not agree

on the disposition of the paper, a third reviewer is selected. If a review is deemed lacking in critical quality, that is, if the technical and scientific strengths or shortcomings of the work have not been adequately addressed, then a third review is also sought.

Copies of the reviews (at least two) and the manuscripts are always sent to the editor or an associate editor, who provides oversight for the entire operation and makes final decisions about manuscript disposition. The subject matter of the manuscript determines which editor will receive the file. Although all letters are written in the editorial office, the editors examine all materials and decide on the course of action, which is then conveyed to the staff editor.

If the editor or associate editor has recommended revision of the manuscript, the staff editor goes over the paper carefully in a "pre-edit" check to aid the author in revising the manuscript.

Tips for authors of papers submitted to *ES&T*

- Prepare your paper with the audience of the publication in mind. Papers prepared for other journals are likely to need some revision to make them suitable for *ES&T*.
- Clearly state in the introduction the purpose of the work and put the work in perspective with earlier work in the area. This may appear obvious, but authors often fail to clearly state the purpose and significance of their work.
- Write concisely. The vast majority of articles are expected to be fewer than five published pages. Long manuscripts are looked at much more closely and critically both by reviewers and editors. Do not repeat information or figures or tables that have appeared elsewhere. Use illustrative data rather than complete data where appropriate.
- Suggest names of possible reviewers for your paper. You may also suggest the names of persons who you do not want to review the paper. The editors try to use at least one reviewer who has been suggested by authors. This cannot be assured, however, since specific reviewers may not be available for reviewing or may already be overloaded.
- Follow the current research author's guide published in every January issue.

If your manuscript is rejected

- Read the reviews carefully. If the reviewers have "missed the point," as authors often claim, consider how the presentation can be clarified and improved to make the point clear. If reviewers have not understood, it is unlikely that readers will understand.
- Is the manuscript, after all, more suitable for another journal?
- Is the work sufficiently complete, or do you need to do more work before seeking publication?
- If you feel strongly that the paper has not been judged fairly, then carefully revise the manuscript taking into account the reviewers' criticisms and send the manuscript to the editorial office with a rebuttal letter asking that the manuscript be reconsidered. Provide an itemized list of changes made in the manuscript in response to reviewer comments, as well as objective rebuttals to the criticisms with which you do not agree.



All forward thinking environmental scientists depend on ES&T. They get the most authoritative technical and scientific information on environmental issues—and so can you! Have your own

subscription delivered directly to you each month!

YES! Enter my own subscription to *ENVIRONMENTAL SCIENCE & TECHNOLOGY* at the rate I've checked below:

Published Monthly One Year Rate	U.S.	Canada & Mexico	Europe	All Other Countries
ACS Members*	<input type="checkbox"/> \$ 28	<input type="checkbox"/> \$ 36	<input type="checkbox"/> \$ 44	<input type="checkbox"/> \$ 51
Nonmembers—Personal*	<input type="checkbox"/> \$ 42	<input type="checkbox"/> \$ 50	<input type="checkbox"/> \$ 58	<input type="checkbox"/> \$ 65
Nonmembers—Institutional	<input type="checkbox"/> \$164	<input type="checkbox"/> \$172	<input type="checkbox"/> \$180	<input type="checkbox"/> \$187

- Payment Enclosed (Payable to American Chemical Society)
 Bill Me Bill Company Charge my MasterCard VISA
 Diners Club/Carte Blanche

Card No. _____

Expires _____ Interbank No. _____ (MasterCard only)

Signature _____

Name _____

Title _____ Employer _____

Address Home Business _____

City, State, Zip _____

Employer's Business: Manufacturing, type _____

Academic Government Other _____

*Subscriptions at these rates are for personal use only. Subscriptions outside the US, Canada, & Mexico are delivered via air service. Foreign payment must be made in US currency by international money order, UNESCO coupons, US bank draft, or order through your subscription agency. For nonmember rates in Japan, contact Maruzen Co., Ltd.

Please allow 45 days for your first copy to be mailed. Redeem until December 31, 1986. 1986

MAIL THIS POSTAGE-PAID CARD TODAY!

3491X



All forward thinking environmental scientists depend on ES&T. They get the most authoritative technical and scientific information on environmental issues—and so can you! Have your own

subscription delivered directly to you each month!

YES! Enter my own subscription to *ENVIRONMENTAL SCIENCE & TECHNOLOGY* at the rate I've checked below:

Published Monthly One Year Rate	U.S.	Canada & Mexico	Europe	All Other Countries
ACS Members*	<input type="checkbox"/> \$ 28	<input type="checkbox"/> \$ 36	<input type="checkbox"/> \$ 44	<input type="checkbox"/> \$ 51
Nonmembers—Personal*	<input type="checkbox"/> \$ 42	<input type="checkbox"/> \$ 50	<input type="checkbox"/> \$ 58	<input type="checkbox"/> \$ 65
Nonmembers—Institutional	<input type="checkbox"/> \$164	<input type="checkbox"/> \$172	<input type="checkbox"/> \$180	<input type="checkbox"/> \$187

- Payment Enclosed (Payable to American Chemical Society)
 Bill Me Bill Company Charge my MasterCard VISA
 Diners Club/Carte Blanche

Card No. _____

Expires _____ Interbank No. _____ (MasterCard only)

Signature _____

Name _____

Title _____ Employer _____

Address Home Business _____

City, State, Zip _____

Employer's Business: Manufacturing, type _____

Academic Government Other _____

*Subscriptions at these rates are for personal use only. Subscriptions outside the US, Canada, & Mexico are delivered via air service. Foreign payment must be made in US currency by international money order, UNESCO coupons, US bank draft, or order through your subscription agency. For nonmember rates in Japan, contact Maruzen Co., Ltd.

Please allow 45 days for your first copy to be mailed. Redeem until December 31, 1986. 1986

MAIL THIS POSTAGE-PAID CARD TODAY!

680

3491X


**CALL
TOLL
FREE**
(800) 424-6747 (U.S. only)



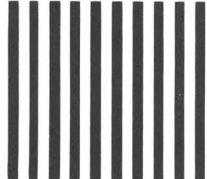
NO POSTAGE
NECESSARY
IF MAILED
IN THE
UNITED STATES

BUSINESS REPLY MAIL

FIRST CLASS PERMIT NO. 10094 WASHINGTON, D.C.

POSTAGE WILL BE PAID BY ADDRESSEE

American Chemical Society
Marketing Communications Department
1155 Sixteenth Street, N.W.
Washington, D.C. 20036-9976



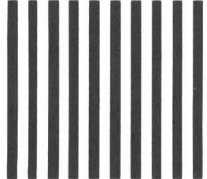

**CALL
TOLL
FREE**
(800) 424-6747 (U.S. only)

BUSINESS REPLY MAIL

FIRST CLASS PERMIT NO. 10094 WASHINGTON, D.C.

POSTAGE WILL BE PAID BY ADDRESSEE


American Chemical Society
Marketing Communications Department
1155 Sixteenth Street, N.W.
Washington, D.C. 20036-9976



NO POSTAGE
NECESSARY
IF MAILED
IN THE
UNITED STATES



professional consulting services directory

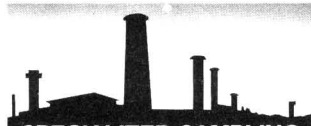


TRADITIONAL SOURCE SAMPLING

- Air Emissions Testing and Compliance
- Determination for Particulate and Gases
- Control Device Evaluation
- Particle Sizing Studies
- Resistivity Studies
- Specialized Analysis
- Method 1 Alternative
- 3-D Air Flow Studies

D. James Grove, P.E., Director
 PO Box 12291, Research Triangle Park, NC 27709 (919) 781-3550 or 1-800-ENTROPY

ENTROPY
 ENVIRONMENTALISTS INC.




SPECIALIZED SAMPLING

- (RCRA) Incinerator Testing
- Volatile Organic Compound (VOC) Testing
- Vapor Recovery Unit Compliance/Performance Testing
- Specialized Hydrocarbons Testing
- Testing of High Temperature and Pressure Sources

Walter S. Smith, P.E., Director
 PO Box 12291, Research Triangle Park, NC 27709 (919) 781-3550 or 1-800-ENTROPY

ENTROPY
 ENVIRONMENTALISTS INC.



CONTINUOUS EMISSIONS MONITORING (CEM) ENGINEERING

- Performance Specification Tests of Opacity, SO₂, NO_x, O₃, CO₂, CO, and TRS CEMS
- Stratification Tests (All Pollutants)
- CEM Performance Audits (RAA and CGA)
- Real-time Measurements Using Transportable CEM System
 - Boiler Tuning (NO_x)
 - Combustion Efficiency Studies
- Performance Tests of Gas Turbines (Method 20)

James W. Paeler, Director
 William G. DeWees, Associate Director
 PO Box 12291, Research Triangle Park, NC 27709 (919) 781-3550 or 1-800-ENTROPY

ENTROPY
 ENVIRONMENTALISTS INC.

Cenref Labs

BRIGHTON, CO (303) 659-0497
 LIBERAL, KS (316) 624-4292

ENVIRONMENTAL TESTING

Priority Pollutants • PCB's
 RCRA Hazardous Waste Analyses
 Drinking Water • Wastewater
 Pesticides • Sludge
 Engine Emission Monitoring



COMPLETE ANALYTICAL SERVICES GC/MS CAPABILITIES

- Screening & Analysis of Industrial & Hazardous Waste.
- Superfund & RCRA Requirements.
- Sampling to EPA Protocols.
- Toxicity Studies.


(516) 334-7770
 75 URBAN AVE, WESTBURY, NY 11590
NYTEST ENVIRONMENTAL INC.



COMPLETE ANALYTICAL SERVICES

- Gas Chromatography/Mass Spectroscopy
- Trace Metal Analyses - ICAP, AA, GFAA
- Drinking Water Analyses
- Industrial Hygiene Services
- Research and Development
- Environmental Field Sampling
- EPA Priority Pollutant Analyses

Brochure and/or fee schedule available on request
BARRINGER MAGENTA LTD.
 304 Carlingview Drive - Resdale - Ont - Canada L4B 6T5 675 3870
 US Office Denver CO 80401 (303) 232 8811



ENVIRODYNE ENGINEERS

a consulting engineering and sciences firm

- environmental engineering analytical chemistry priority pollutant analyses environmental monitoring and assessment hazardous waste monitoring hazardous waste management
- transportation engineering
- energy engineering
- construction management

12161 Lackland Road
 St. Louis, Missouri 63146
 (314) 434-6960

Baltimore / Chicago / New York



GROUNDWATER SPECIALISTS

- Computer modeling and code sales
- Groundwater modeling and field investigations
- RCRA and CERCLA investigations
- Water supply and water resource development
- LUS T investigations
- Mining Hydrology

209 Elden Street
 Suite 301
 Herndon, VA 22070

Denver Washington, DC Boston
 303/440-4556 703/435-4400 617/264-0550

THE CONSULTANTS' DIRECTORY

UNIT	Six Issues	Twelve Issues
1" X 1 col.	\$55	\$50
1" X 2 col.	110	100
1" X 3 col.	160	140
2" X 1 col.	110	100
2" X 2 col.	200	180
4" X 1 col.	200	180

Jay Francis
 ENVIRONMENTAL SCIENCE & TECHNOLOGY
 25 Sylvan Road South
 P.O. Box 231
 Westport, CT 06881
 Or call him at (203) 226-7131



ENVIROMED LABORATORIES, INC.

Sampling, Testing, & Consulting Services

- Priority Pollutants GC/MS, GC, AA
- RCRA-Hazardous Waste
- Animal Toxicity & Bioassay Studies
- Wastewater, Water & Sewage Analysis
- Permitt Preparation, Audits TOX, TOC
- PCB and Chlorinated Hydrocarbon Analysis
- Industrial Hygiene & Ambient Air Monitoring
- Ground Water Monitoring

414 W. Calif. Ruston La. 71270 (318) 255-0060
 1874 Dallas Dr. Baton Rouge, La. 70806 (504) 928-0232
 La. Toll Free 1-800-421-2993

CONSULTING GROUND-WATER GEOLOGISTS

ROUX ASSOCIATES INC

- RCRA Monitoring
- Superfund Response
- Site Evaluation
- Aquifer Clean Up
- Resource Development

11 STEWART AVENUE
 HUNTINGTON, NEW YORK 11743 516-678 7200
 1503 N. GRAVEL PIKE
 BERKSHIREVILLE, PA 18074 215-234-4900

CLASSIFIED SECTION

Clarkson University—Environmental Science and Engineering Program. Applications are invited for research assistantships and teaching assistantships in support of study at the Master's and Ph.D. levels. Superior applicants with B.S. and M.S. degrees from engineering and basic science disciplines are encouraged to apply. Currently, research assistantships exist in the following areas: process experimentation and modeling of contaminant fate and transport in groundwater systems; acid precipitation and acidic lake renovation; transport, bioavailability, and fate of toxic and nutrient pollutants in surface waters and sediments; removal of low-level organic and inorganic pollutants from drinking water supplies and industrial wastewaters. Full-time assistantships currently carry a \$9300 annual stipend plus full tuition. For further information and application write: Prof. William W. Clarkson, Department of Civil and Environmental Engineering, Clarkson University, Potsdam, NY 13676; an affirmative action/equal opportunity employer.

CLASSIFIED SECTION

DIRECTOR OF ECOLOGY DIVISION

Scientist to lead active Ecology Division in Environmental Planning, Ecology and Aquatic Toxicology. Responsibilities include Profit Center management, coordination with Regional Offices, Project Management, Marketing and Client Development. Additional experience in Wetlands Studies, Hazardous Waste and Reclamation desirable. Requires Ph.D. in Ecology or related Life Sciences, a minimum of ten years progressively responsible experience, including Business Development and people management. Previous work in Environmental Consulting, interaction with government and regulatory agencies and industry required.

HEALTH RISK ASSESSMENT SCIENTIST

Individual needed to work on interdisciplinary team performing exposure assessments, hazardous waste site risk assessments, and Superfund endangerment assessments. Position requires Master's degree or graduate level study in health/life sciences and at least 2 years of demonstrated experience in performance of multimedia human health and exposure assessments and integration with contaminant fate and transport analyses. Experience in proposal preparation and knowledge of environmental regulations desirable.

Interested applicants should submit their resume and salary requirements to:

ESE
ESE
ESE

**ENVIRONMENTAL SCIENCE
AND ENGINEERING, INC.**
Human Resources Department
P.O. Box ESE • Dept. EST
Gainesville, FL 32602
An RS&H Company
An Equal Opportunity Employer M/F

SCIENTISTS/ENGINEERS

\$23,170 - \$41,105 per annum

The U.S. Nuclear Regulatory Commission has positions available in the Division of Waste Management, Silver Spring, MD. These positions include:

- Environmental Engineer/Scientist
- Health Physicist
- Hydrologist
- Geochemist/Geophysicist
- Geoscientist
- Project Manager
- Technical Program Analyst
- Systems Performance Engineer/Analyst
- Geotechnical Engineer
- Nuclear Process Engineer

For immediate consideration, send Federal Employment Application Form (SF-171) or resume with salary requirements to: U.S. Nuclear Regulatory Commission, Division of Personnel, SPE: NMSS/ES/JAN, Washington, DC 20555.



**U.S. Nuclear
Regulatory Commission**

An Equal Opportunity Employer M/F/H
U.S. Citizenship Required

HEALTH PHYSICISTS ENVIRONMENTAL ENGINEERS

UNC Nuclear Industries, a prime operating contractor to the U.S. Department of Energy at Richland, WA, is embarking upon a major multi-year program to upgrade the NReactor. We are looking for a few top professionals to join our select technical team.

We have entry and mid-level professional positions in:

- Radioactive waste shipping and management, including DOT regulation compliance.
- Exposure reduction/ALARA efforts involving reactor operation and maintenance forces.
- Radiological support services including audit, development and presentation of radiological safety training material.
- Implementation of environmental and emergency preparedness plans, controls, procedures, and instructions in accord with all applicable standards.

The successful candidates will possess a degree and strong technical knowledge in one of the above areas, plus mature judgment and the ability to effectively interface with all levels of plant personnel.

If the above describes your background, and you are interested in being considered, please send resume, **salary history** and **salary requirements**, in confidence to: K.A. Bresnahan, Dept. JD, UNC Nuclear Industries, P.O. Box 490, Richland, WA 99352.

U.S. citizenship required (DOE security clearance preferred).

Equal employment opportunity is our pledge and our practice.



**UNC NUCLEAR
INDUSTRIES**

WESTERN RESEARCH INSTITUTE

ENVIRONMENTAL ENGINEER—MS/PhD Civil or Environmental Engineer or related discipline to perform research and mitigation services emphasizing water contamination. Experience with unit operations is required and broad hazardous waste background is desired.

CHEMIST-METALS ANALYSIS—BS/MS Chemist with minimum 3 years experience in metals analysis using graphite furnace AA and ICP. Require familiarity with EPA and RCRA methods. Prefer experience using PE-5000 AA spectrometer and performing EPA CLP inorganic analyses. Must have good communication skills.

ENVIRONMENTAL ORGANIC CHEMIST—MS/PhD Chemist to characterize organic hazardous wastes. Familiarity with RCRA/TSCA regulations is necessary, and industrial experience is desired.

GC/MS OPERATOR—BS Chemist or related field plus minimum 1 to 3 years experience in operation, maintenance, and some repair of Hewlett-Packard GC/MS systems, including software. Experience analyzing EPA, environmental, or related samples is preferred.

WRI offers career growth through contributions to basic and applied research programs emphasizing energy and environment. Our location offers an excellent quality of life in a university, small community atmosphere surrounded by abundant Rocky Mountain outdoor recreation. Send resume with salary expectations to **Manager, Human Resources, WESTERN RESEARCH INSTITUTE, University of Wyoming Research Corporation, P.O. Box 3395, University Station, Laramie, WY 82071.**

WRI is an equal opportunity employer.

SENIOR STACK TESTER

Applicants must be experienced in all EPA Methods and continuous monitoring. Lab and GC experience helpful. Send resume to: Pape & Steiner Environmental Services, 5801 Norris Road, Bakersfield, California 93308.

EOE/MF

DIRECTOR, CHEMISTRY LABORATORY

A managerial position responsible for directing an existing facility staffed with ten (10) chemists and technicians capable of performing 100,000 inorganic analysis a year of water, soil and plant samples using computer supported FIA, AA and AAS Instrumentation. The development of a complete organic laboratory is contemplated within the next two years. Requires a Master's degree in analytical organic chemistry and four years related experience, including two years at the supervisory level. Prefer knowledge and experience of analytical organic methods including operation and maintenance of GC, HPLC and GC/MS. Experience in planning, designing and construction of laboratories also desirable. Salary Range \$32,947 - \$49,420 commensurate with experience. For an official application and position dimensions, contact the South Florida Water Management District, Personnel Office, P.O. Box V, West Palm Beach, FL 33402 or call 305/686-8800 ext. 265 and ask for Karen. An official application must be received by the Personnel Office no later than 5:00 p.m. on February 8, 1986. Equal Opportunity Employer.

**USE THE
CLASSIFIED
SECTION**

Implications of a Gradient in Acid and Ion Deposition across the Northern Great Lakes States

Gary E. Glass*

Environmental Research Laboratory—Duluth, U.S. Environmental Protection Agency, Duluth, Minnesota 55804

Orie L. Loucks

Holcomb Research Institute, Butler University, Indianapolis, Indiana 46208

■ Average precipitation pH, 1979–1982, declines from west to east from 5.3 to 4.3 along a cross section of sites in Minnesota, Wisconsin, and Michigan. This answers questions about the seasonal and geographic pattern of anthropogenic acid precursor emissions and reaction products (SO_4^{2-} , NO_3^- , H^+ , NH_4^+) that increase from west to east. Except for higher concentrations of Ca^{2+} and Mg^{2+} observed at one site in the cultivated area of southwestern Minnesota, the contribution of soil-related metal cations to the total ions in solution is small (17%) and relatively uniform across the region. Significant seasonal and geographic patterns in precipitation chemistry and deposition values are observed. Close correspondence of the sums of strong acid anions with the sums of hydrogen and ammonium ions in precipitation is observed, indicating anthropogenic sources of sulfur and nitrogen oxides. Present atmospheric inputs show close chemical correspondence when precipitation chemistry values are compared to the resulting ionic composition of weakly buffered lakes in north central Wisconsin and northern Michigan. The wet deposition of total acidity in the middle and eastern part of the region is comparable to that of impacted sites in the Adirondacks and in regions of Scandinavia.

Introduction

Much research on the phenomenon of acidic precipitation has focused on the Eastern United States, eastern Canada, and the southern regions of Scandinavian countries (1–5). Munger and Eisenreich (6), reviewing the recent precipitation chemistry data on a continental scale, noted wide variations in elemental concentrations from one region to another, sometimes over relatively short distances. Gorham et al. (7) have examined the ionic correlation in the Eastern U.S. and noted the relationship of wet acidic loadings to precipitation pH. The transition from acid-dominated to base-dominated precipitation across the Great Lakes States (GLS) was not addressed in detail in these papers. In recognition of the large area of sensitive soils and of the abundance of low alkalinity surface waters in northern Minnesota, Wisconsin, and Michigan (8, 9), three precipitation monitoring sites were established in the Boundary Waters Canoe Area Wilderness of Minnesota and the northern highland region of Wisconsin. The possible effects of acidic deposition on this region are the concern of resource managers in these states and of scientists in general.

Research on which compounds contribute most to the differences in precipitation chemistry values found across this region offers the potential to understand the significance of regional and local variation in pH, ionic compositions, acid-forming precursors, and their reactive products (SO_4^{2-} , NO_3^- , H^+ , and NH_4^+). Soil- and agricultural-derived ions (10–12) also need to be considered as inputs to changes in surface water chemistry values relating to seasonal variations and historical changes in rainfall chemistry (9, 13–15). The objectives of this paper are, therefore, to report and evaluate the significance of geographic patterns in the ion composition of acidic and basic reactants in precipitation across the GLS region, to compare the potential significance of the snow period chemistry values with those of the rain period, to compare to wet deposition in other regions, and to compare the composition of precipitation with the resulting surface water.

Materials and Methods

Three precipitation monitoring sites were established in 1980 according to the protocol of the National Atmospheric Deposition Program (NADP) (16) bringing the total number of sites to eight in the western Great Lakes States (Table I). Weekly composite precipitation samples were collected by using Aerochem Metrics (Miami, FL) Model 301 automatic sensing wet/dry precipitation collectors. Field observations and measurements of environmental conditions were made according to NADP procedures (16), and a portion of the sample was used to measure pH and specific conductance. The remaining sample in the collection bucket was shipped to the Illinois Water Survey—Central Analytical Laboratory (CAL), Champaign, IL, for additional analyses. The concentrations of Ca, Mg, Na, and K were measured by using an Instrumentation Laboratory Model 353 atomic absorption spectrophotometer. Concentrations of sulfate, nitrate, chloride, and ammonium were measured colorimetrically on a Technicon Auto Analyzer II. Hydrogen ion was measured with an Orion Model 811 pH meter with Beckman electrodes and a Yellow Springs Instrument Co. alternating current conductance bridge was used with a glass microelectrode, $K = 1$, for specific conductance measurements. Field and laboratory data were key punched and reported back to site investigators by CAL for checking and quality assurance and eventually were published by the NADP as Quarterly Reports (17).

Table I. Average H⁺ Concentration, Volume Weighted, Expressed as pH, from Weekly Composite Samples (Measured at CAL) over a 3-year Period at Eight Sites across the Western Great Lakes States^a

site name location (N. lat., W. long.)	date site established	yearly average						snow period, Dec- March		rain period, April- Nov		all 3 years, Dec 1979-Nov 1982	
		Dec 1979-		Dec 1980-		Dec 1981-		pH	N	pH	N	pH	N
		Nov 1980		Nov 1981		Nov 1982							
Lamberton, MN; 44°14', 95°18'	Jan 2, 1979	4.99	31	5.38	33	5.45	36	5.01	15	5.27	85	5.25	100
Marcel, MN; 47°32', 93°28'	July 6, 1978	5.07	38	5.11	44	4.99	44	4.85	38	5.09	88	5.05	126
Fernberg, MN; 47°57', 91°30'	Nov 18, 1980	5.69	1	4.93	38	4.93	46	4.83	27	4.95	58	4.93	85
Spooner, WI; 45°49', 91°53'	June 3, 1980	5.11	22	4.80	27	4.91	42	4.69	19	4.92	72	4.90	91
Trout Lake, WI; 46°03', 89°39'	Jan 22, 1980	4.64	39	4.79	43	4.68	49	4.57	39	4.71	92	4.70	131
Douglas Lake, MI; 45°34', 84°41'	July 3, 1979	4.33	42	4.43	40	4.44	48	4.39	42	4.41	88	4.40	130
Wellston, MI; 44°13', 85°49'	Oct 10, 1978	4.33	44	4.32	43	4.40	49	4.37	46	4.35	90	4.35	136
Kellogg, MI; 42°25', 85°24'	June 26, 1979	4.33	38	4.32	37	4.33	44	4.39	35	4.32	84	4.33	119

^aThe number of samples in each average for the period Dec 1979–Nov 1982 is shown (N).

Table II. Analysis of the pH Differences between Field Site Investigators and Laboratory Results (CAL), as a Function of Precipitation Sampling Event Depth and in Comparison with Other Measured Ions for the 3-year Period 12/79–11/82

location	no. of samples	mean		Δ[H ⁺], site - CAL		slope of log [ion, μequiv/L] vs. log (precipitation depth)					
		pH, site	pH, CAL	μequiv/L	SD	H ⁺ , site	H ⁺ , CAL	SO ₄ ²⁻	NO ₃ ⁻	Ca ²⁺	Na ⁺
Lamberton, MN	84	4.63	5.33	18.9	38.7	+0.47	+0.63	-0.20	-0.27	-0.49	-0.59
Marcell, MN	114	4.88	4.99	2.9	8.2	-0.18	+0.30	-0.23	-0.22	-0.38	-0.60
Fernberg, MN	74	4.74	4.92	5.9	16.5	+0.09	+0.33	-0.22	-0.28	-0.45	-0.56
Spooner, WI	21	4.45	4.79	19.4	38.4	-0.14	+0.41	-0.15	-0.18	-0.35	-0.62
Trout Lake, WI	108	4.57	4.67	5.3	7.5	+0.08	+0.30	-0.13	-0.18	-0.33	-0.54
Douglas Lake, MI	117	4.30	4.39	9.4	21.7	+0.01	+0.23	-0.21	-0.36	-0.50	-0.60
Wellston, MI	115	4.16	4.35	24.7	55.9	+0.09	+0.37	-0.19	-0.18	-0.46	-0.62
Kellogg, MI	94	4.22	4.33	13.8	32.4	+0.11	+0.23	-0.13	-0.19	-0.32	-0.29

The data reported in this analysis were measured or obtained from CAL and the other individual site investigators in 1983. Analyses of normal wet side and dilute wet side precipitation samples were included, but trace precipitation and dryside samples were excluded. Over 900 pH values for weekly composites from the eight monitoring sites and over 5000 concentration values for the other ions were measured. Both the pH and specific conductivity measurements reported by the site investigators and by CAL have been used; the latter assure uniformity in technique and quality assurance for all chemical analyses (18, 19).

To summarize, the data have been grouped into periods approximately corresponding to the dominant seasons in this region, the "winter" period (December–March) when snow accumulation occurs, the "nonsnow" or rain period (April–November), spring–summer (April–July), and summer–fall (August–November). Wet deposition was calculated by using rain gauge measurements rather than sample bucket volumes as the latter underestimate total precipitation volumes by about 4 ± 2% over all sites. Of the 670 weekly composite samples, only 29 (<0.5%) had one or more missing values for individual ion measurements. Calculation of the missing ion values was computed by using a linear regression of log (concentration) vs. log (precipitation depth) for each individual sample using data for that site and time period so that a complete set of data was available as required for statistical analysis. Of a total of 6030 individual data points, 61 individual ion values were computed by using this procedure.

Results and Discussion

Regional Pattern in Precipitation pH. The geographic pattern of pH change from the 3 years of monitoring at eight sites is summarized in Tables I and II and in earlier maps by Hileman (20). In 1979–1980 pH ranged

from 4.99 in western Minnesota to 4.33 in lower Michigan, but in 1981–1982 it ranged from 5.45 to 4.33. These results illustrate several caveats that must be considered when comparing the yearly results. The weather during each period may vary from what is considered to be typical. The laboratory (CAL) measurements represent analyses of composite samples without added preservatives over a week old, with variable transit and storage time before analysis. Weekly samples with no record of rain or chemistry correspond to weeks with no precipitation for that monitoring site.

The laboratory data comparing snow period to rain periods at these sites show increases in hydrogen ion of about 0.2 pH unit at the Minnesota and Wisconsin sites in the winter. The more acidic Michigan sites show almost no seasonal differences. The regional gradient in pH is evident at all times and includes the entire range of precipitation pH observed in northern Europe (20–22).

The pH values measured at CAL are consistently higher (less acidic) than those measured in the field monitoring sites, which indicates the dynamic nature of H⁺ and the reactivity of substances in precipitation over time. These differences are attributable to biological activity, ion exchange, and reactivity of particulate materials such as soil particles with the reactions: M_x(CO₃)_y, M_xO_y, and M_xSi₂O₈ + xzH⁺ → xM^{z+} where M^{z+} = ΣNa⁺, K⁺, Ca²⁺, Mg²⁺, Al³⁺, Fe³⁺ (23, 24) over time. The analysis (Table II) of the differences between laboratory measurements of pH and the site pH shows (a) the differences at Lamberton, MN, are consistently greater by 0.7 pH unit than at the other locations and (b) for the seven locations not including Lamberton the average differences between CAL and site pH is 0.16 pH unit. This analysis uses all the observed differences between pH reported by CAL and site investigators pH, averaged by period and location. The increase in pH is equivalent to an approximate average reduction

Table III. Average Ion Concentration, Volume Weighted [Measured at CAL (in $\mu\text{equiv/L}$)], for the 2-year Period from Dec 1980 through Nov 1982 at All Eight NADP Sites

location	no. of samples	volume-weighted average ion concentration, $\mu\text{equiv/L}$										
		H ⁺	NH ₄ ⁺	SO ₄ ²⁻	NO ₃ ⁻	Cl ⁻	Ca ²⁺	Mg ²⁺	K ⁺	Na ⁺	$\Sigma(+)$	$\Sigma(-)$
Lamberton, MN	69	4	35	33	22	4	21	7	1	5	72	59
Marcell, MN	88	9	19	28	16	3	13	5	1	4	50	47
Fernberg, MN	85	12	18	31	16	3	10	5	1	3	49	48
Spooner, WI	71	14	31	42	22	3	14	4	1	3	67	67
Trout Lake, WI	93	19	20	37	19	2	10	3	1	2	56	58
Douglas Lake, MI	88	37	18	51	27	3	14	5	1	2	77	81
Wellston, MI	92	42	23	56	32	6	14	6	1	3	88	94
Kellogg, MI	81	46	25	64	30	4	14	5	1	3	94	98

of 12.5 $\mu\text{equiv/L}$ hydrogen ion for all samples between collection and analysis by CAL (Table II). The highest changes were seen in samples from Lamberton, MN, and Wellston, MI, reflecting their proximity to cultivated land with a high content of alkaline soil substances. The lowest changes were seen in samples from Marcell, MN, and Trout Lake, WI, reflecting surrounding forest cover with low input of ion-exchanging and neutralizing substances.

The differences in pH are also related to the mechanisms of atmospheric washout which usually show an inverse relationship of ion concentration to precipitation rate (9). Negative slopes are expected for ion concentration vs. precipitation volume (or depth) relationships for gaseous and particulate components of the atmosphere including soil-derived ions (Table II). Highly significant, negative slopes are observed at all sites for all anions and cations except NH₄⁺ and H⁺. Ammonium ion shows negative slopes at all sites that are not significantly different from zero except at Lamberton, MN, and Douglas Lake, MI. Hydrogen ion, in contrast, shows all positive slopes that are significantly different from zero for CAL measurements while measurements by site operators show nonsignificant zero slopes except for Lamberton, MN. Here the slope is significantly nonzero, positive, and indicates the dynamic nature of [H⁺] in precipitation chemistry.

The data on seasonal differences in Table I show that the sites in Minnesota and Wisconsin with a more acidic pH during the snow period, December–March, indicate a potential to accumulate greater acid concentrations in the winter snowpack than during the rain period. The accumulation of acids in the snowpack at the three Michigan sites to 44 $\mu\text{equiv/L}$ H⁺ was more than double the H⁺ concentration at the Wisconsin and Minnesota sites.

Is this pattern evident in Table I a long-standing or a relatively recent phenomenon? Estimates by Cogbill, Likens, and Butler (14, 15) show all stations north and west of the lower peninsula of Michigan reporting a pH above 5.5 in 1955–1956. Stensland and Semonin (13) have suggested that neutralizing substances from transported dust during the mid-1950s might have contributed to the elevation of pH measurements in the east central states during those years, but their analysis shows no anomalous calcium content in the northern Great Lakes region at that time. Both reviews of the earlier data seem to agree that the precipitation pH measurements of 5.5 and above represent a rural regional “prealteration state” for Minnesota and Wisconsin up until the mid-1950s. The published results for the 1965–1966 and 1975–1976 periods (13, 15) indicate that development of the region-wide gradient in pH has been a gradual one extending to Minnesota by the 1970s.

Seasonal and Geographic Pattern in the Ionic Composition of Acid-Forming Substances. Because precipitation pH is a measure of the resultant proton concentration after numerous reactions between acid-

forming precursors, ion exchange, and neutralization reactions with the specific mix of gaseous and particulate materials washed out of the atmosphere during a given precipitation event, the concentrations of the resultant reaction products, both anions and cations, need to be considered at each site. Strong acid precursor emissions result from fossil fuel combustion and ore smelting, causing strong acids to dominate the ionic composition of precipitation (26). Strong acids result from oxidation and hydration reactions in the atmosphere: SO_x, NO_x → H₂SO₄, HNO₃ (25, 26). The molar ratio of sulfate to nitrate ions in GLS precipitation ranges from an average low value of 0.8 occurring at Lamberton, MN, to a high of 1.12 at Kellogg, MI, and reflects the relative increase in sulfur oxide emissions in the east. These ratios compare with values 0.72 and 1.1 for Minnesota and Michigan, respectively, derived from state emission inventories for 1975–1978 (26). These major anion concentrations are indicative of strong acid precursors across the region. Individual site averages are given in Table III. The major cations, in addition to H⁺ in descending order of average concentration are NH₄⁺, Ca²⁺, Mg²⁺, K⁺, and Na⁺.

Ammonium (NH₄⁺) ion is an important and interesting reaction product of acid aerosols with gaseous ammonia, H₂SO_{4(s)} + NH_{3(g)} → (NH₄)₂SO_{4(s)} (11, 27). Ammonia neutralizes H⁺ in precipitation, but then ammonium ion serves as a major contributor to the acidic inputs to surface water due to microbial activity (nitrification) that occurs in surface water: NH₄⁺ + 2O₂ → NO₃⁻ + 2H⁺ + H₂O (24). In Table III, ammonium ion with hydrogen ion are the dominant cations, 66 ± 5%. These, with the base cations (Ca²⁺, Mg²⁺, Na⁺, and K⁺) are in ionic balance with sulfate, nitrate, and chloride anions at seven of the eight sites. An imbalance occurs at Lamberton, MN, where a 18% deficit in anions is due to unmeasured HCO₃⁻ and OH⁻ (23). The average concentration of the sum of base cations is 23 ± 4 $\mu\text{equiv/L}$ for all sites (Table III) and results from ion-exchange and acid neutralization reactions with H⁺ and from the washout and weathering of soil particles (23).

Both the geographical and seasonal patterns of volume-weighted average concentrations of ions in precipitation from atmospheric washout can be evaluated by using plots of the mean concentrations of ions from the eight monitoring sites as a function of time through a two-way analysis of variance (location by period). The data for the statistical analyses are for the 2 years of weekly composite samples for the period Dec 1980 through Nov 1982. Although data collection at some stations started in 1979, only the years with complete data from all eight stations could be used. To provide data for comparable periods, the 2 years were divided into six 4-month periods corresponding to the snow period (December through March), and two rain periods, spring–summer (April through July) and summer–fall (August through November).

Plots of the standardized means for concentrations

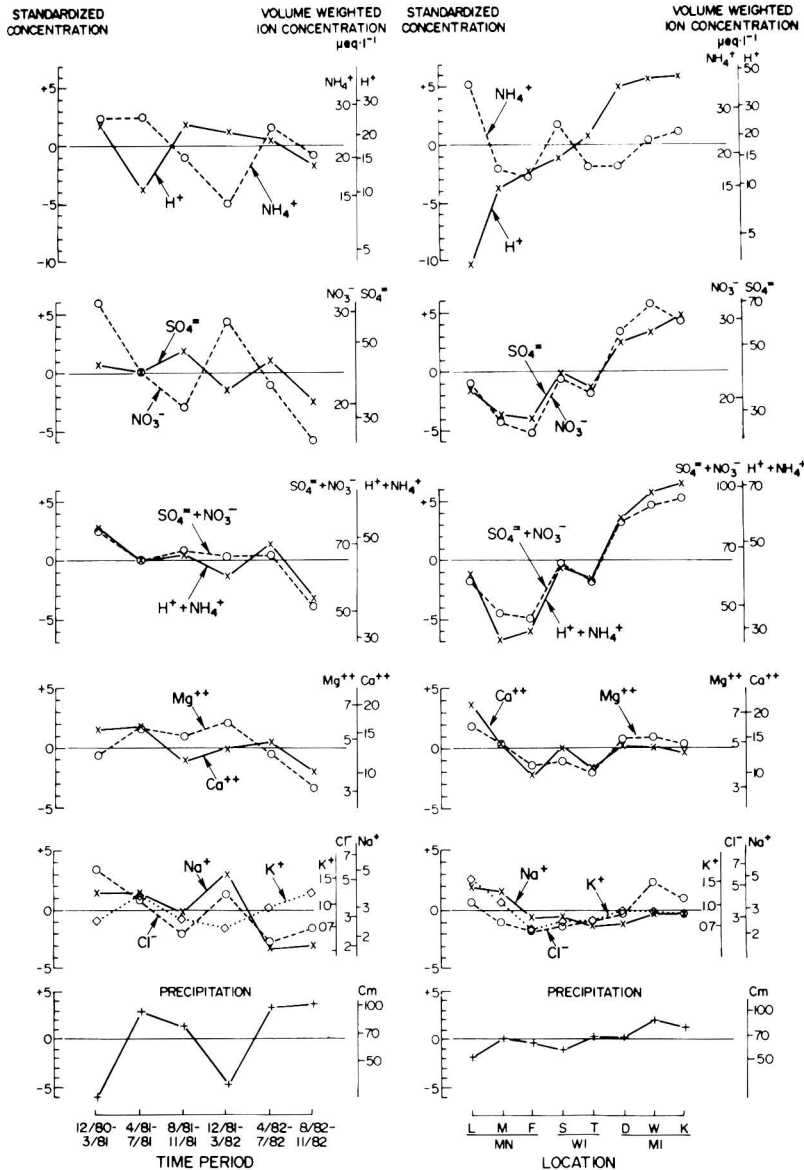


Figure 1. Standardized mean concentration (volume weighted, $\mu\text{equiv/L}$) of ionic substances in precipitation for six consecutive 4-month periods (2 years) beginning Dec 1980 to Nov 1982, showing seasonal patterns and regional gradient in concentrations for eight monitoring sites from southwestern Minnesota to south central Michigan.

(Figure 1) allow comparison of the mean responses relative to their pooled standard error where the standardized mean (for the period or site, i) =
$$\frac{\text{mean (for the period or site } i) - \text{overall mean}}{\text{standard error (of the mean for the period or site } i)}}$$

The standard error of the mean is based on the mean square error from the analyses of variance and is assumed to be equal to the standard error of the overall mean. In Figure 1, the left axis is in units of the standardized mean while the right axis is in units of log concentrations in microequivalents per liter. Differences of about 3 units in the standardized means are significant at the 5% level (using Tukey's HSD multiple comparison procedure (28)).

The NO_3^- concentrations illustrate a consistent but opposite seasonal pattern to K^+ concentrations and precipitation depth while Ca^{2+} and Mg^{2+} concentrations illustrate seasonal fluctuations of no statistical significance. The sum of $[\text{SO}_4^{2-}] + [\text{NO}_3^-]$ closely parallels the sum of $[\text{H}^+] + [\text{NH}_4^+]$, which is consistent with the observations of Brosset (27) and others (7, 25, 26), and indicates the dominance of anthropogenic sources of total atmospheric acidity in Europe and North America.

The model used for the two-way analysis of variance is resultant variation in response =
$$\text{variation in response by location} + \text{variation in response by period} + \text{variation due to random error}$$

Table IV. Analysis of Variance (Two Way) Giving Significance Level for Differences in Ion Concentrations, Depositions, and Precipitation between Locations and Periods

ion	significance levels for differences			
	concentrations		depositions	
	period	location	period	location
H ⁺	0.0014 ^a	<0.0001 ^c	0.0004	<0.0001 ^c
NH ₄ ⁺	<0.0001 ^c	<0.0001 ^c	<0.0001 ^c	0.031 ^a
SO ₄ ²⁻	0.045	<0.0001 ^c	<0.0001 ^c	<0.0001 ^c
NO ₃ ⁻	<0.0001 ^c	<0.0001 ^c	0.0001 ^c	<0.0001 ^c
Cl ⁻	0.0008 ^c	0.085	0.0081 ^b	0.0015 ^b
Ca ²⁺	0.077	0.012 ^d	<0.0001 ^c	0.0080 ^a
Mg ²⁺	0.0042 ^b	0.11	<0.0001 ^c	0.040 ^a
K ⁺	0.21	0.16	<0.0001 ^c	0.11
Na ⁺	0.0002 ^c	0.24	0.0018 ^b	0.27
H ⁺ + NH ₄ ⁺	0.0032 ^b	<0.0001 ^c	<0.0001 ^c	<0.0001 ^c
SO ₄ ²⁻ + NO ₃ ⁻	0.0026 ^b	<0.0001 ^c	<0.0001 ^c	<0.0001 ^c
precipitation	<0.0001 ^c	0.18		

^aSignificance level is <5%. ^bSignificance level is <1%.
^cSignificance level is <0.1%.

The significant differences by location and period are summarized in Table IV by using an analysis of variance *F* test (27). These results show (a) that consistent annual patterns in ion concentrations exist across the region, (b) that the variations in dominant anions (SO₄²⁻, NO₃⁻) and acid-formed cations (H⁺, NH₄⁺) and their sums are significantly larger than would occur by chance, and (c) that no patterns of statistical significance in the differences in ion concentrations of Ca²⁺, Mg²⁺, Na⁺, K⁺, and Cl⁻ between locations are larger than would be expected by chance.

The analysis of variance for differences in period and location across the GLS sampling sites (Table IV) shows that the pattern for variation in H⁺, NH₄⁺, SO₄²⁻, and NO₃⁻ and their sums has a probability of <1% of being random. The gradient in acidic reactants and products is consistent with the regional pattern in sulfur and nitrogen oxide emissions from sources in the region (29).

While a minor difference exists for Ca²⁺, no significant differences are found across the region for Cl⁻, Mg²⁺, K⁺, or Na⁺ despite the location of the Lambertton, MN, site in an agricultural region near alkaline soils. Lambertton, MN, exhibits the highest Ca²⁺ and NH₄⁺ concentrations, and both Spooner and Kellogg exhibit higher than average concentrations of NH₄⁺ (Figure 1). All of these sites are in agricultural areas where volatile, anhydrous ammonia is extensively used in field applications for fertilizer, although the Spooner site has forest to the north and east. In contrast to the drought-period results reported by Stensland and Semonin (13), the high calcium concentrations at Lambertton, MN, suggest that during periods of normal precipitation the effects of soil dust from agricultural activity are relatively localized. These results are consistent with the limited cross-regional data for

Minnesota obtained by Thornton and Eisenreich (10) and Munger (11), who reported a sharp decrease in cation concentrations from the Dakotas across Minnesota. Their data show that the highest values for calcium in precipitation occurred during periods when there existed extensive bare soil (especially in the winter) from agricultural activity. Verry (23) also has reported results for winter samples at Marcell, MN, to be affected by lack of snow cover and soil conditions upwind to the west. For the lower concentrations of SO₄²⁻ and NO₃⁻ at the western and northern sites in the GLS region, the concentrations of Ca²⁺ + Mg²⁺ exceed H⁺ but remain at less than 30% of SO₄²⁻ + NO₃⁻ and show the important influence that ion-exchange and neutralization reactions can have on the resultant pH. For the year as a whole, however, elevated concentrations of Ca²⁺ and Mg²⁺ from alkaline dust are not evident either at Marcell, MN, or at Spooner, WI, both of which are just beyond the edge of intensive agriculture.

Seasonal and Geographic Pattern in Wet Deposition. Since the potential for adverse effects on terrestrial resources is thought to be controlled by the total deposition of reactive substances (concentration × precipitation amount plus dry deposition), the average annual wet deposition of acidic and neutralizing substances is of major interest (Table V). Dry deposition would increase these values by 10% to more than 100%, depending upon many factors including atmospheric concentrations and conditions, receptor surface properties, and proximity to emission sources (5, 24, 30).

Even more than the above results for concentration show, total ionic deposition, similarly plotted by using standardized means, shows a strong seasonal pattern (Figure 2) and higher statistical significance (Table IV). The spring-summer and summer-fall precipitation peaks (Figure 1) in the region produce similar peaks in the deposition of other important chemical species during these periods, despite the higher average winter concentrations at some sites. The greater deposition of ammonium ion (NH₄⁺) compared to H⁺ in the central and western sites is evident in the deposition data for both location and time plots. The identical pattern observed for the sum of (SO₄²⁻ + NO₃⁻) deposition and the sum of (H⁺ + NH₄⁺) deposition (Figure 2) shows, however, that sulfur and nitrogen oxides are the major source of acidic reactants in the atmosphere of this region.

The relative difference in wet deposition of SO₄²⁻ and NO₃⁻ from the western sites to the eastern sites, comparing Lambertton, MN, to Kellogg, MI, is 40% and 55%, respectively. The west to east regional gradient in wet deposition is shown by the ratios of SO₄²⁻, NO₃⁻, and SO₄²⁻ + NO₃⁻ for Minnesota/Michigan sites and are 0.47, 0.53, and 0.49, respectively. These ratios can be compared with those derived from state emission inventories (26) of SO₂ and NO₂ (1975-1978) and are 0.30, 0.55, and 0.38, respectively. The nitrogen oxide emission/nitrate wet de-

Table V. Yearly Ion Deposition [Measured at CAL (in equiv/(ha • year))] Based on the 2-year Period from Dec 1980 through Nov 1982, Using Weekly Composite Samples from the Eight Precipitation Monitoring Sites

location	precip, cm	ion deposition, equiv/(ha-year)									
		H ⁺	NH ₄ ⁺	SO ₄ ²⁻	NO ₃ ⁻	Cl ⁻	Ca ²⁺	Mg ²⁺	K ⁺	Na ⁺	H ⁺ + NH ₄ ⁺
Lamberton, MN	62	23	220	210	140	23	130	43	9	29	240
Marcell, MN	78	72	150	220	130	20	98	35	8	30	210
Fernberg, MN	71	85	120	220	110	20	73	32	6	23	220
Spooner, WI	72	99	220	300	160	19	100	31	6	21	320
Trout Lake, WI	86	170	170	310	170	20	86	29	6	16	340
Douglas Lake, MI	72	260	130	370	200	24	100	38	8	18	390
Wellston, MI	88	370	200	490	280	53	120	49	9	25	570
Kellogg, MI	83	380	200	530	250	36	120	45	9	23	590

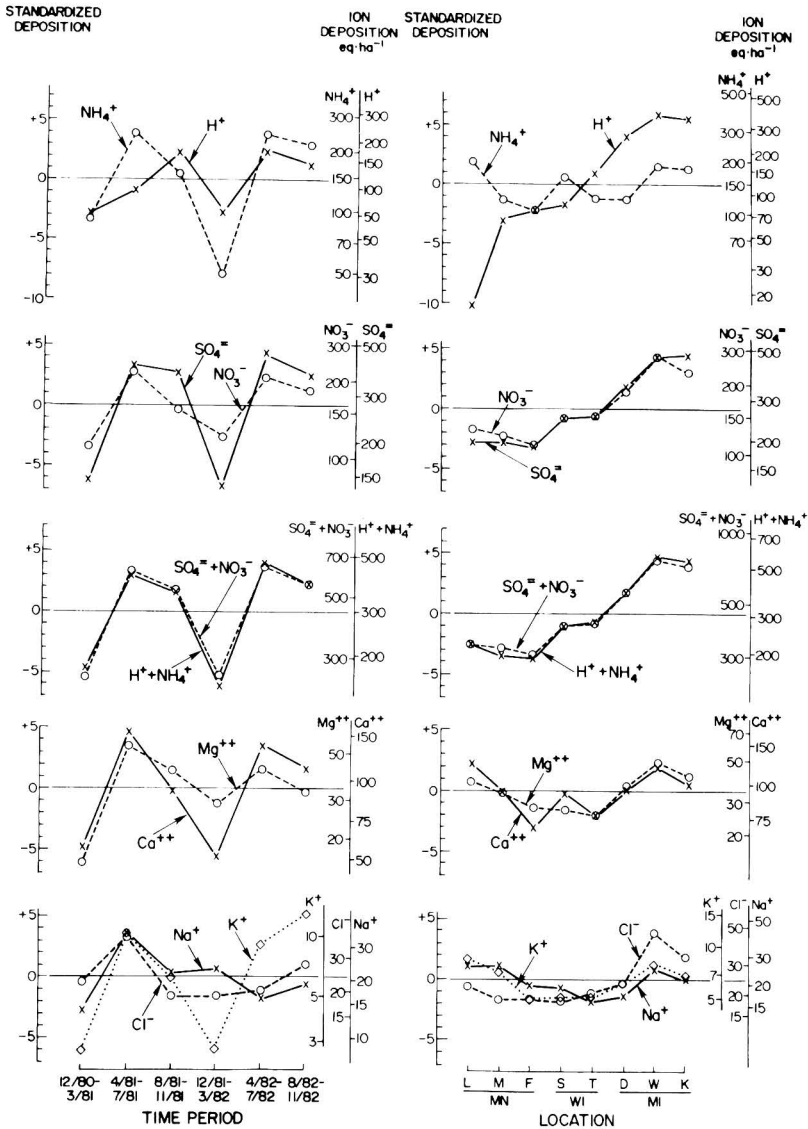


Figure 2. Standardized mean deposition (total ion, equiv/ha) for wet deposition of ionic substances in precipitation for six consecutive 4-month periods, Dec 1980–Nov 1982, showing strong rain period peaks and regional gradient in wet deposition from southwestern Minnesota to south central Michigan.

position ratios are in good agreement but sulfur wet deposition in Minnesota is greater than predicted from Minnesota sulfur oxide emission sources alone.

Comparison of Ca^{2+} deposition (Table V) with results for the middle 1950s (13) shows there has been little change since that time. The locational variation in deposition of Mg^{2+} , Ca^{2+} , Na^+ , K^+ , and Cl^- differ from random at a probability of less than 5%, and the acidic precursor products differ from random at less than 0.1% probability and show a strong positive increase with increased emissions in the east (26, 29).

The possible effect of precipitation anomalies on calculated deposition amounts during the 1979–1982 period was examined by comparing the measured amounts of precipitation at each site with the 40-year averages at the

site or at a nearby U.S. Weather Service station. Precipitation amounts were, statistically, very close to the normal with the exception of above normal precipitation at the Douglas Lake, MI, monitoring site during the April–October 1981 period. No other extreme wet or dry periods occurred.

Comparisons with Other Regions and Surface Water Chemistry. The data in Table VI show total wet deposition calculations for several sites outside of the Great Lakes States, allowing comparison with four other regions, two of them remote from emissions sources. Even the most westerly sites of the GLS region (Table V) show total quantities of acidifying substances appreciably greater than those of the two remote North American mountain regions. Several major industrial sources of SO_2 occur within a

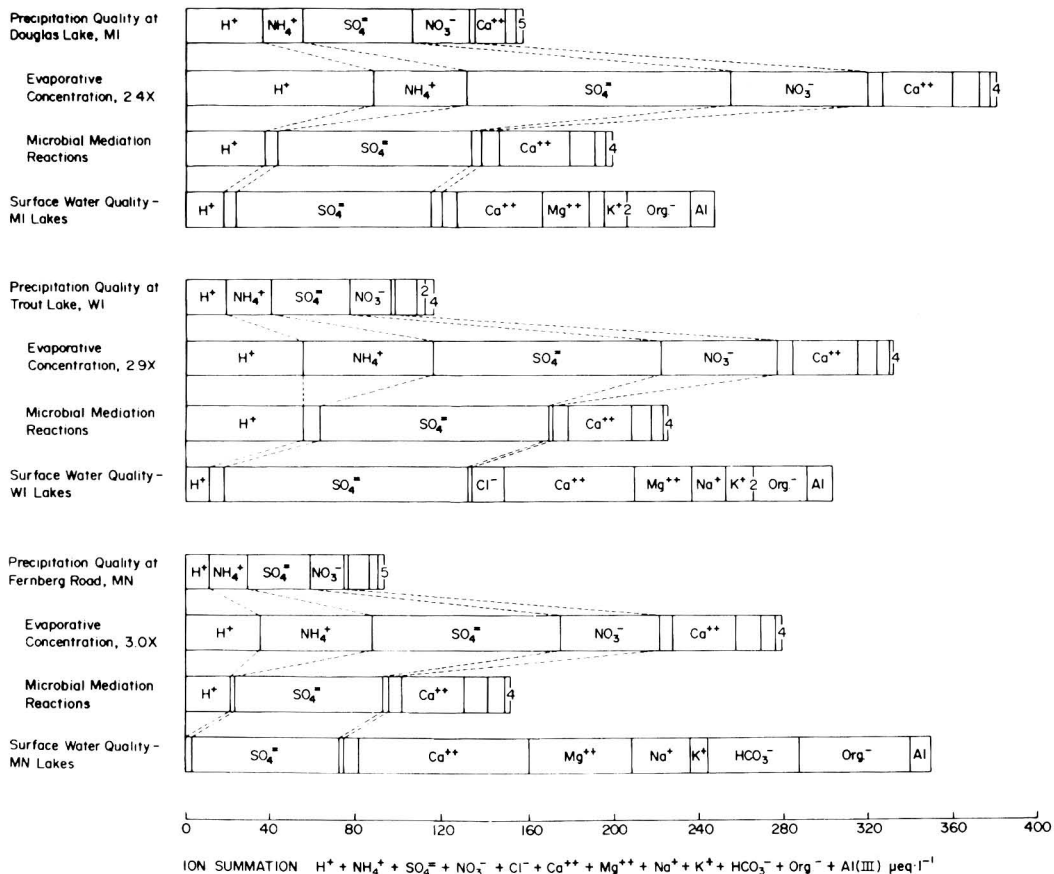


Figure 3. Annual average ion concentrations in precipitation at three monitoring sites in the western Great Lakes States showing the regional gradient between sites and expected concentrations after concentration by evaporation and microbial mediation reactions (see text) in comparison with the observed average water concentrations for eight weakly buffered lakes in each of the precipitation monitoring regions. Vertical bars indicate concentration boundary values for all ionic components, and numbers within the bars indicate overlap for low or zero ion concentrations.

300-km radius of Glacier National Park and may have contributed to the moderate levels of SO_4^{2-} and H^+ deposition observed at this otherwise remote site.

Of the three sites representing the Northeastern United States (Table VI), Aurora, NY (near Cornell University), an agricultural site, located downwind from major industrial areas in western New York, Ohio, and Pennsylvania, has the highest wet deposition of acid-forming substances of any U.S. site considered in this study, about 80% more than the Kellogg site in central Michigan. Because of higher precipitation, Hubbard Brook, NH, and Huntington, NY, show concentrations of acidic substances that, while similar to the values measured for the three Michigan sites, are higher in deposition.

The Narbuvollen site (Table VI), in east central Norway, an area similar to the northern GLS region with pine, spruce, and birch forests (9) and crystalline bedrock (3, 30), warrants further comparative study. Precipitation there averages about 42 cm annually (3), less than in the relatively dry regions of Minnesota, Wisconsin, and Michigan, and the wet depositions of acidic substances there measure lower amounts. However, in the vicinity of the Narbuvollen site significant alterations of water quality and fish populations have been reported and were attributed to the acidic inputs from the atmosphere (32).

The observed difference in aquatic effects, since the magnitude of wet-acidic inputs in Scandinavia is similar to the GLS, may be attributed to the differences in the duration of those inputs, hydrology (31), weathering rates of bedrock and soils (3), and other factors (5). Surface water quality alterations have been reported on a moderate scale in Norway for 30–60 years, and acidic deposition probably has occurred throughout this century (3). The evidence reviewed here indicates that region-wide, wet-acidic inputs to the GLS have had a duration in the order of only 20–30 years, but local emission sources using high-sulfur coal, ore smelting, and ore-sintering activities might have influenced some weakly buffered lakes at a much earlier time, without detection (34, 35).

The indications that present acidic atmospheric inputs have significantly altered the surface water chemistry of weakly buffered lakes in the GLS can be seen by comparisons of the ionic composition of precipitation across the region with those of the resultant lake water (8, 9, 31, 36, 37). The changes in water chemistry as precipitation is transformed into surface water during the inflow process can be complex involving physical, chemical, and biological processes and are illustrated in Figure 3 by using a stepwise mechanism (5, 33). Concentration by evaporation (5, 38) of ionic components, such as chloride, in precipitation up

Table VI. Annual Deposition of Major Anions and Cations Measured in Weekly Composite Precipitation Samples at NADP (Dec 1980–Nov 1982) and Other Sites Outside the Northern Great Lakes States

site name; location (lat., long.)	N	precip cm	equiv/(ha-year)									
			H ⁺	NH ₄ ⁺	SO ₄ ²⁻	NO ₃ ⁻	Cl ⁻	Ca ²⁺	Mg ²⁺	K ⁺	Na ⁺	H ⁺ + NH ₄ ⁺
Denali (McKinley National Park), AK; N63°43', W148°58'	73	29	9	6	28	7	13	10	12	5	16	16
West Glacier (Glacier National Park), MT; N48°31', W113°60'	73	68	52	23	89	43	14	30	17	5	14	75
Hubbard Brook, NH; N43°57', W71°42'	95	124	570	130	570	290	62	70	37	5	58	710
Huntington, NY; N43°58', W74°13'	94	100	420	150	490	250	28	80	30	6	27	570
Aurora, NY; N42°44', W76°40'	90	78	560	170	590	280	40	80	30	5	31	730
Birknes, Norway; ^a N58°, E8°		148	1000	620	1100	600	920	130	180	44	780	1600
Narbuvollen, Norway; ^a N62°, E11°		42	92	46	130	54		46	8			140

^a Mean annual values of 1977–1979 for daily bulk samples (3).

to 2–4 times can occur and varies from east to west across the GLS region, giving the predicted concentrations shown (Figure 3). For more reactive components, microbial activity or mediation reactions can be modeled by stoichiometry of oxidation–reduction reactions involving NH₄⁺ (nitrification processes adding acidity) and NO₃⁻/SO₄²⁻ (denitrification/reduction processes reducing acidity) where reaction of 1 equiv of each results in no overall change in acidity or alkalinity content (24, 33, 36). This reaction stoichiometry is used to account for the significant reduction in NH₄⁺ and NO₃⁻ concentrations, after evaporation, observed in surface water for the most weakly buffered lakes in the northern area of each region. The resulting ionic concentrations predicted for the surface water compare closely to the average ionic concentration values observed in weakly buffered, acidic lakes in northern Michigan and Wisconsin.

Increases in lake water concentrations of metal ions over those predicted by atmospheric input can occur by ion exchange, dissolution of sediment components, and weathering of soils and land use in the watershed yielding concentrations of base cations, aluminum, and corresponding bicarbonate, chloride, and organic anions (5). These data (Figure 3) indicate that, given the present differential in acidic inputs, the lake basins in the upper GLS must presently supply at least 20–60 µequiv/L acid-neutralizing substances (alkalinity) and ionic exchange substrate annually to precipitation inflow so that the pH may increase to 6.5 which is the minimum pH value considered safe for an abundance of freshwater aquatic life (39).

Summary and Conclusions

In a regional assessment of precipitation chemistry, care must be taken to consider a wide variety of potentially significant variables (5). Year-to-year differences in climatic trends, as well as potential local influences of topography, vegetation, and land use, may need to be evaluated. In this paper, local anomalies in precipitation composition have been considered in relation to long-term averages, both seasonal and annual. The effects of local sources of pollutants and local agricultural influences have been either minimized by site selection or treated systematically as part of the experimental design and analysis.

Despite variation in the wet deposition of substances during the 2–3-year study period, three conclusions can be drawn that are relevant to the aquatic resources at risk from acidic deposition in northern Michigan, Wisconsin, and Minnesota. First, the regional pH gradient from east

to west is influenced little by concentrations of ion-exchanging or neutralizing soil substances as indicated by relatively constant resultant concentrations of Ca²⁺, Mg²⁺, Na⁺, and K⁺ in precipitation. Although NO₃⁻ deposition is higher in this region compared to that of relatively remote sites, it ranges in wet deposition from 140 to 250 equiv/(ha-year) from west to east across the region. In comparison, SO₄²⁻ ranges from 210 to 530 equiv/(ha-year) reflecting total emission increases across the region and is in approximate equal molar ratios with NO₃⁻. The pattern in pH must be considered with [NH₄⁺] in assessing anthropogenic acid/precursor sources and implications for acidification of surface waters. Both can be attributed primarily to the resultant gradient in SO₄²⁻ + NO₃⁻ concentrations.

Second, these results show total wet-acidic deposition at the Michigan sites to be similar to those of the east central Adirondack region and portions of New England, while wet deposition of acidifying substances (H⁺ + NH₄⁺) in Michigan, Wisconsin, and Minnesota exceeds that of the interior of Norway and Sweden. Wet deposition of acidifying substances in Minnesota appears to be 2–10 times greater than that of unimpacted remote North American continental sites, but less than most sites where impacts have been observed. In northern Michigan and north central Wisconsin where there is close chemical correspondence between precipitation and weakly buffered surface water composition, acidification is observed. Studies of similarities and differences in the receiving landscape may be required to determine whether a continuation of the present loadings is inducing effects on resources similar to those observed in Scandinavia. The hydrology of lakes (31) in the Great Lakes region, differences in soil weathering rates (24), and the careful evaluation of historical change and loadings must be taken into account.

Finally, it may be possible to evaluate the regional importance of acidic deposition observed in the western Great Lakes States through comparisons with effects on aquatic chemistry and biotic resources now reported in areas of central Norway. The Norwegian sites have similar climate, bedrock, and soils and are receiving similar (or less) rainfall and wet-acidic deposition amounts. Surface water quality changes that are thought to have induced a decline of the local fishery in the most sensitive watersheds have been observed in the Norwegian study site. The apparent difference in biotic effects from central Norway to the Great Lakes States may be due to incomplete surveys in the Great Lakes States, differences in watershed charac-

terization, and the longer period of acidic deposition in Scandinavia.

Acknowledgments

We acknowledge and thank the following site investigators and NADP personnel for their assistance in providing and checking data for this report: Bill Dunn, Wellston, MI; John Goventz, Kellogg, MI; Bob Vanderkopel, Douglas Lake, MI; R. Becker, Trout Lake, WI; J. Chazin, Spooner, WI; Tony Strasser, Lamberton, MN; E. S. Verry, Marcell, MN; Ed Marsolek, Fernberg, MN; Jim Gibson and Van Baker, NADP, Natural Resources Ecology Laboratory, Ft. Collins, CO. We are grateful for the assistance of R. Becker for data gathering, quality assurance, and earlier drafts and of J. Rodgers and R. Lief for statistical calculations and interpretations, B. Halligan for drafting the figures, A. Schimpf and D. Glass for editing, and A. Hedin and T. Highland for typing the manuscript.

Registry No. NH₄⁺, 14798-03-9; H⁺, 12408-02-5; Ca, 7440-70-2; Mg, 7439-95-4; K, 7440-09-7; Na, 7440-23-5.

Literature Cited

- (1) Cogbill, C. V. *Water Air Soil Pollut.* **1976**, *6*, 407-413.
- (2) Drablos, D.; Tollan, A., Eds. "Ecological Impacts of Acid Precipitation"; SNSF Project: Oslo, Norway, 1980; pp 1-383.
- (3) Overrein, L. N.; Seip, H. M.; Tollan, A. "Acid Precipitation—Effects on Forest and Fish". SNSF, Oslo, Norway, 1980, SNSF Project Final Report, 1972-1980, pp 1-175.
- (4) Galloway, J. N.; Likens, G. E. *Atmos. Environ.* **1981**, *15*, 1081-1085.
- (5) Glass, G. E.; Brydges, T. G. *Proc. Symp. Acid Precip. Fishery Impacts Northeastern North America* **1982**, 265-286.
- (6) Munger, J. W.; Eisenreich, S. J. *Environ. Sci. Technol.* **1983**, *17*, 32A-42A.
- (7) Gorham, E.; Martin, F. B.; Litzau, J. T. *Science (Washington, D.C.)* **1984**, *225*, 407-409.
- (8) Glass, G. E. In "Ecological Impact of Acid Precipitation"; Drablos, D.; Tollan, A., Eds.; SNSF Project: Oslo, Norway, 1980; pp 112-113.
- (9) Glass, G. E.; Loucks, O. L. *U.S. Environ. Prot. Agency* **1980**, EPA-600/3-80-044, 1-186.
- (10) Thornton, J. D.; Eisenreich, S. J. *Atmos. Environ.* **1982**, *8*, 1945-1955.
- (11) Munger, J. W. *Atmos. Environ.* **1982**, *16*, 1633-1645.
- (12) Guiang, S. F.; Krupa, S. V.; Pratt, G. C. *Atmos. Environ.* **1984**, *18*, 1677-1682.
- (13) Stensland, G. J.; Semonin, R. G. *Bull. Am. Meteorol. Soc.* **1982**, *63*, 1277-1284.
- (14) Cogbill, C. V.; Likens, G. E. *Water Resour. Res.* **1974**, *10*, 1133-1137.
- (15) Likens, G. E.; Butler, T. J. *Atmos. Environ.* **1981**, *15*, 1103-1109.
- (16) Bigelow, D. S. "NADP Instruction Manual, Site Operation"; National Atmospheric Deposition Program, National Resources Ecology Laboratory, Colorado State University: Ft. Collins, CO, 1982; pp 1-29.
- (17) National Atmospheric Deposition Program "NADP Data Report: Precipitation Chemistry"; Colorado State University: Ft. Collins, CO, 1982; Vol. 5, pp 1-227.
- (18) Stensland, G. J.; Semonin, R. G.; Peden, M. E.; Bowersox, V. C.; McGurk, F. F.; Skowron, L. M.; Slater, M. J.; Stahlhut, R. K. Cal. National Atmospheric Deposition Program, Ft. Collins, CO, 1980, NADP Quality Assurance Report, pp 1-54.
- (19) Gibson, J. H. "NADP Quality Assurance Plan: Deposition Monitoring"; National Resources Ecology Laboratory, Colorado State University: Ft. Collins, CO, 1984; pp 1-39.
- (20) Hileman, B. *Environ. Sci. Technol.* **1982**, *16*, 325A.
- (21) Wright, R. F.; Dovland, H. *Atmos. Environ.* **1978**, *12*, 1755-1768.
- (22) OECD "The OECD Programme on Long Range Transport of Air Pollutants—Measurements and Findings", 2nd ed.; OECD: Paris, 1979; pp 1-328.
- (23) Verry, E. S. *Water Resour. Res.* **1983**, *19*, 454-462.
- (24) Schnoor, J. L.; Stumm, W. In "Chemical Processes in Lakes"; Stumm, W., Ed.; Wiley-Interscience: New York, in press.
- (25) Calvert, J. G., Ed. "SO₂, NO, and NO₂ Oxidation Mechanisms: Atmospheric Considerations"; Acid Precip. Ser., Butterworth: Boston, MA, 1984; Acid Precip. [Proc. Symp. Acid Precip. Am. Chem. Soc. Meet.], Vol. 3, pp 1-254.
- (26) National Research Council/National Academies of Science "Acid Deposition: Atmospheric Processes in Eastern North America, A Review of Current Scientific Understanding"; National Academy Press: Washington, DC, 1983; pp 1-375.
- (27) Brosset, C. In "Atmospheric Sulfur Deposition"; Shriner, D. S.; Richmond, C. R.; Lindberg, S. E., Eds.; Ann Arbor Science Publishers: Ann Arbor, MI, 1980; pp 145-152.
- (28) Sokal, R. R.; Rohlf, F. J. "Biometry", 2nd ed.; W. H. Freeman: San Francisco, CA, 1981; pp 244-251.
- (29) Altschuller, A. P. *Environ. Sci. Technol.* **1980**, *14*, 1337-1348.
- (30) Thompson, M. E.; Hutton, M. B. *Water Air Soil Pollut.* **1985**, *24*, 77-83.
- (31) Eilers, J. M.; Glass, G. E.; Webster, K. E.; Rogalla, J. A. *Can. J. Fish. Aquat. Sci.* **1983**, *40*, 1896-1904.
- (32) Drablos, D.; Sevaldrud, I. In "Ecological Impact of Acid Precipitation"; Drablos, D.; Tollan, A., Eds.; SNSF Project: Oslo, Norway, 1980; pp 354-355.
- (33) Stumm, W.; Morgan, J. J.; Schnoor, J. L. *Naturwissenschaften* **1983**, *70*, 216-223.
- (34) Conroy, N.; Hawley, K.; Keller, W.; Lafrance, C. *J. Great Lakes Res.* **1976**, *2* (Suppl. 1), 146-165.
- (35) Dickman, M.; Dixit, S.; Fortescue, J.; Barlow, B.; Terasmae, J. *Water Air Soil Pollut.* **1984**, *21*, 375-386.
- (36) Schnoor, J. L.; Palmer, W. D., Jr.; Glass, G. E. In "Modeling of Total Acid Precipitation Impacts"; Schnoor, J. L., Ed.; Ann Arbor Science Publishers: Ann Arbor, MI, 1983; pp 155-173.
- (37) Glass, N. R.; Glass, G. E.; Rennie, P. *J. Environ. Int.* **1980**, *4*, 443-452.
- (38) Geraghty, J. J.; Miller, D. W.; Van der Leeden, F.; Troise, F. L. "Water Atlas of the U. S."; Water Information Center, Inc., Port Washington, NY, 1973; pp 1-128.
- (39) U.S. EPA "Quality Criteria for Water"; Office of Water and Hazardous Materials, U.S. EPA: Washington, DC, 1976; pp 1-256.

Received for review July 5, 1983. Revised manuscript received April 1, 1985. Accepted July 10, 1985. This work was supported by the USEPA National Acid Precipitation Assessment Program through Cooperative Agreements CR809412 with the University of Minnesota, Duluth, and CR809484 with the Wisconsin Department of Resources and by Interagency Agreement A-D12F3581 with the USDA Forest Service, Duluth, MN. Manufacturers and trade names are given for identification, and no endorsement by the U.S. EPA is intended or should be implied.

Application of Mass-Transfer Theory to the Kinetics of a Fast Gas-Liquid Reaction: Chlorine Hydrolysis

E. Marco Aieta[†] and Paul V. Roberts*

Department of Civil Engineering, Stanford University, Stanford, California 94305

■ The short wetted-wall column is evaluated as a tool for quantifying the rate of a fast liquid-phase reaction, the hydrolysis of chlorine. In physical absorption experiments conducted at low pH such that the hydrolysis reaction does not proceed, the absorption of molecular chlorine from the gas phase into aqueous solution is measured, and the data are interpreted by using the penetration theory for mass transfer in a laminar falling film. The physical absorption data agree within 5.8% with the penetration theory. Chlorine hydrolysis experiments were conducted at pH 5.4 and 10.0, corresponding to first-order reversible and first-order irreversible kinetics, respectively. The observed rate constants at 293 K were $12.9 \pm 2.0 \text{ s}^{-1}$ at pH 5.4 and $12.7 \pm 1.8 \text{ s}^{-1}$ at pH 10. These results fall within the range of previously reported values at 293 K obtained by using temperature-jump and stopped-flow techniques.

Introduction

This paper describes a methodology for determining the kinetic parameters of fast reactions in solution. The procedure is applicable to reactions between a dissolving gas and an absorbing fluid or between a dissolving gas and a reactant in the absorbing fluid.

A variety of methods is available for the kinetic study of chemical reactions (1); the reaction half-life determines the appropriate experimental kinetic apparatus for initiating a reaction. For reactions with half-lives of about 20 s or longer the reaction can be initiated by simply mixing the reactants together at the appropriate concentrations. Flow methods, including quenching, continuous flow, and stopped flow, allow the study of reactions with half-times as short as 1×10^{-3} s. Newly developed laser flash photolysis techniques permit the study of gas-phase reactions with half-times of 1×10^{-9} s. Relaxation methods can be used for the study of chemical systems at equilibrium by perturbing the equilibrium with a sudden temperature or pressure change. Relaxation methods are not applicable to irreversible reactions, however.

The methodology presented here, based on enhancement of the interphase mass transfer by a fast liquid-phase reaction, permits the study of both reversible and irreversible liquid-phase reactions with half-times in the range from 1×10^{-2} to 1×10^{-5} s. In this paper, the chlorine hydrolysis reaction (reaction half-time $\sim 10^{-2}$ s) was studied and used as verification of the methodology. In the following paper (2), this technique is applied to the study of the kinetics of the chlorine-chlorite reaction (reaction half-time on the order of 10^{-5} s).

Previous Studies of Chlorine Hydrolysis

The chlorine hydrolysis reaction has been studied with several experimental approaches, including the short wetted-wall column, the laminar liquid jet, temperature-jump relaxation, and stopped-flow techniques (3-5).

In the present study, the chlorine hydrolysis reaction was studied under conditions for which the reaction was

first order with respect to chlorine and irreversible, as well as under conditions for which the forward reaction was first order and reversible. These conditions correspond to initial solution pH values of 10.0 and 5.4, respectively (3).

Theory

When a gas is brought into contact with a liquid, the gas is absorbed by the liquid until the liquid-phase dissolved gas concentration ultimately is in equilibrium with the gas-phase composition. This equilibrium is described by Henry's law (6).

When an absorbed gas reacts with the absorbing fluid or with a solute in the absorbing fluid, the rate of gas transfer may be increased over that for absorption without reaction. If the rate of liquid-phase reaction is great enough to consume the dissolved gas on a time scale comparable to the time constant for diffusion, then some degree of enhanced mass transfer will be observed. The magnitude of the increase in mass transfer depends upon the relative rates of reaction and diffusion. Measurements of the rate of gas absorption with and without chemical reaction can be used to determine the rate constant of the slow reaction step in the reaction mechanism that consumes the absorbed gas (6).

Film and Penetration Theories. Both the film theory (7, 8) and the penetration theory (9) have been used to describe mass transfer at a gas-liquid interface. A major difference between the two theories arises for the case of physical absorption, for which the penetration theory predicts that the mass flux should vary as the square root of the molecular diffusivity, whereas the film theory predicts that the mass flux should vary as the first power of the molecular diffusivity; in several experimental investigations (10, 11) the square-root dependency has been found more correct. For absorption with simultaneous liquid-phase chemical reactions, both models predict nearly identical results for the increase in mass flux due to the liquid-phase chemical reaction, and these predictions are in good agreement with experimental results.

Other gas-liquid mass-transfer models have been proposed that incorporated some of the basic characteristics of both the film theory and the penetration theory models, and have been applied to specific apparatus and geometries. Sherwood et al. (12) provided an excellent review of the development of these gas-liquid mass-transfer models. A thorough and concise treatment of the application of mass-transfer models to gas-liquid reactions has been presented by Danckwerts (6). In the present study, the short wetted-wall column was used for gas-liquid contacting. A cutaway of the short wetted-wall column and an idealization of the terminal velocity distribution profile are shown in Figure 1.

Mathematical Formulation of the Penetration Theory. The variation in time and space of the concentration of dissolved gas in the absence of liquid-phase chemical reactions is given by Fick's second law, subject to appropriate initial and boundary conditions. Analytical solutions have been developed for the special cases of gas absorption accompanied by first-order irreversible liquid-phase chemical reactions and instantaneous second-order

[†]Present address: Rio Linda Chemical Co., Sacramento, CA 95814.

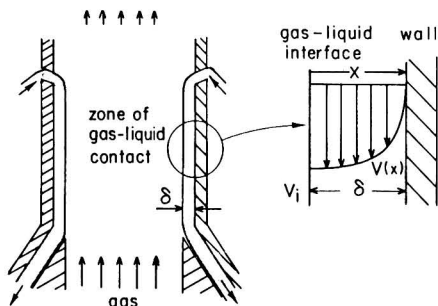
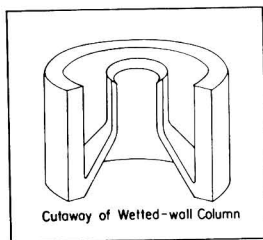


Figure 1. Cutaway of wetted-wall column and terminal velocity distribution in a falling laminar film.

irreversible liquid-phase chemical reactions (6). For the case of gas absorption with a simultaneous liquid-phase chemical reaction of general reaction order, approximate equations for the rate of gas absorption have been developed by Hikita and Asai (13). The development presented by Hikita and Asai (13) is applicable to any order irreversible reaction and, as suggested by Danckwerts (6), can be used to approximate the enhancement in gas absorption due to reversible liquid-phase reactions as well.

(1) **Physical Absorption.** In the absence of chemical reaction, the gas absorption rate can be predicted by applying the penetration theory to the conditions of a laminar film in a short wetted-wall column (6). The resulting relation for the mass-transfer coefficient in the absence of chemical reaction, k_L^* , is

$$k_L^* \left(\frac{h_c}{D_A} \right)^{1/2} = \left(\frac{2}{\pi^{1/2}} \right) \left(\frac{9g}{8\mu_w \rho_w} \right)^{1/6} \left(\frac{\Gamma}{\xi^{1/2}} \right)^{1/3} \quad (1)$$

By use of the nondimensionalized form of eq 1, variations in diffusivity, column height, viscosity and density due to solution composition changes, temperature variations, and column inlet-outlet changes are normalized so that results from different experiments can be compared directly. Substituting the viscosity and density for pure water at 20 °C (the reference condition used throughout the present study) into eq 1 yields the theoretical relationship:

$$k_L^* \left(\frac{h_c}{D_A} \right)^{1/2} = 7.787 \left(\frac{\Gamma}{\xi^{1/2}} \right)^{0.333} \quad (2)$$

which can be used to predict the mass-transfer coefficient as a function of liquid mass loading, Γ .

(2) **Physical Absorption with Simultaneous Liquid-Phase Chemical Reaction.** The solution developed by Hikita and Asai (13) is conveniently presented by forming two dimensionless groups, E and $M^{1/2}$, as first suggested by van Krevelen and Hofstijzer (14). The enhancement factor, E , is defined as the ratio of the time-averaged mass-transfer coefficient for gas adsorption with

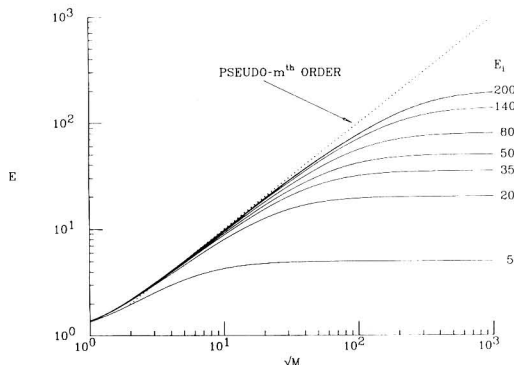


Figure 2. Effect of liquid-phase reaction on the rate of gas absorption.

liquid-phase chemical reaction, k_L , to the time-averaged physical absorption mass-transfer coefficient, k_L^* :

$$E = \frac{k_L}{k_L^*} \quad (3)$$

The second dimensionless group, $M^{1/2}$, is the ratio of the rate of chemical reaction to the rate of physical gas absorption, and for the general (m,n) th-order reaction case is given by (13)

$$M^{1/2} = \frac{\left[\left(\frac{2}{m+1} \right) k_{m,n} D_A A^{*(m-1)} B^{0(n)} \right]^{1/2}}{k_L^*} \quad (4)$$

The approximate solution of Hikita and Asai (13) for gas-liquid mass transfer enhanced by chemical reaction is given by the implicit function

$$E = \left[\gamma + \frac{\pi}{8\gamma} \right] \operatorname{erf}(2\gamma/\pi^{1/2}) + (1/2) \exp(-4\gamma^2/\pi) \quad (5a)$$

where

$$\gamma = M^{1/2} \left(\frac{E_i - E}{E_i - 1} \right)^{n/2} \quad (5b)$$

Equations 3-5b reduce to the analytical solution for the first-order irreversible case and agree closely (within 3%) with analytical solutions to the second-order, irreversible case (13). E_i , in eq 5b, is the enhancement factor based on the penetration theory solution for the case of instantaneous reaction of the dissolved gas with a dissolved reactant. If E_i is much greater than unity, the following approximation (6, 15) for E_i can be used:

$$E_i = \left(\frac{D_A}{D_B} \right)^{1/2} + \frac{B^0}{zA^*} \left(\frac{D_B}{D_A} \right)^{1/2} \quad (5c)$$

Figure 2 shows the enhancement factor, E , as a function of $M^{1/2}$ and E_i , as calculated from eq 3-5.

Figure 3 shows the form of the concentration profiles near the gas-liquid interface in the region where gas A and solute B are reacting. A comparison of the concentration profiles of Figure 3 to the corresponding regions in Figure 2 aids in the understanding of the physical significance of the family of curves of Figure 2. Figure 3a corresponds to an enhancement factor of unity, i.e., no reaction in the liquid phase due to short contact time or very slow reaction. Figure 3b corresponds to the diagonal upper limit of the family of curves of Figure 2, namely, the pseudo- m th-order region. The initial bulk fluid concentration of B at the gas-liquid interface can be considered constant,

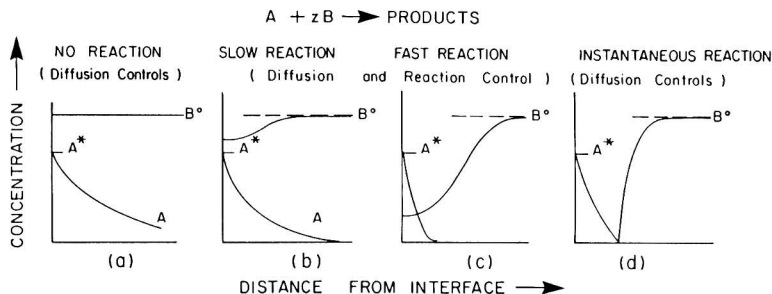


Figure 3. Concentration profiles at the gas-liquid interface for mass transfer with simultaneous liquid-phase reaction.

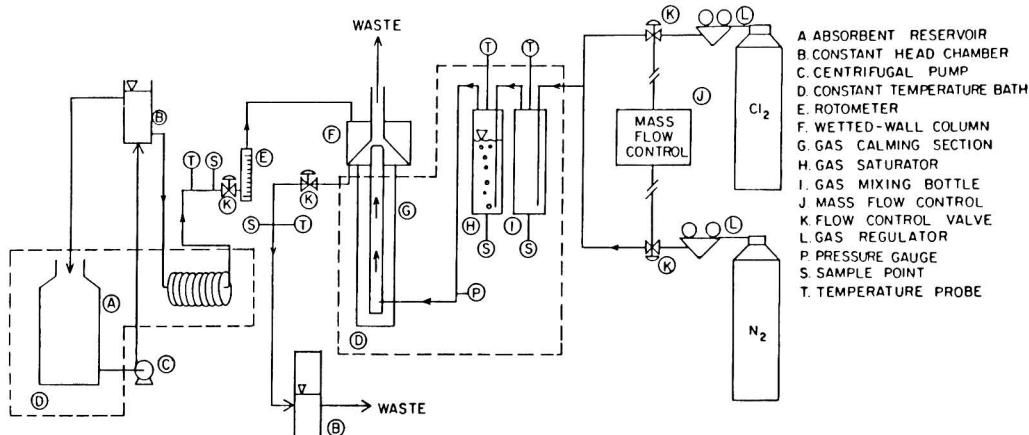


Figure 4. Schematic flow diagram.

and the rate of reaction is pseudo m th order in A with a rate constant k_m given by

$$k_m = k_{m,n}(B^0)^n \quad (6)$$

Figure 3c describes the intermediate case in which the reaction between dissolved gas and solute is fast and/or the initial bulk fluid concentration of B is low compared to that of A^* , such that the reaction depletes the concentration of B at the interface. Case 3c shows significant departure from the pseudo- m th-order case, with the reaction conditions approaching the instantaneous reaction enhancement factor asymptote of E_i (case 3d). The region of Figure 2 corresponding to case 3c is that area in which the curves for individual values of E_i begin to diverge from the diagonal pseudo- m th-order line. As can be seen in Figure 2, the larger the value of the ratio B^0/zA^* , and hence the larger the value of E_i (eq 5a), the larger $M^{1/2}$ must be to observe the deviation from the pseudo- m th-order case.

The final case to be considered is that of an instantaneous liquid-phase chemical reaction, depicted by Figure 3d and corresponding to the horizontal asymptotes of Figure 2. In case 3d, A and B react so rapidly that they do not coexist in the liquid phase. A sharp reaction plane develops that moves deeper into the liquid at longer contact times. The kinetics of the reaction are immaterial, and the rate of reaction is controlled by the rate at which A and B can diffuse to the reaction plane.

Experimental Apparatus and Methods

Wetted-Wall Column Construction. The short wetted-wall column was constructed from precision-bore glass tubing. The inner glass tube was 28 mm i.d., and the outer

glass tube was 78 mm i.d. (Figure 1). A plexiglass housing was fabricated to hold the column. The housing contained liquid inlet and outlet ports that were made of plexiglass and gas inlet and outlet tubes fabricated from a solid Teflon bar.

Fluid-Handling System. A schematic of the fluid-handling system used in the present study is shown in Figure 4. A general description of the system is given below. Unless otherwise noted, all materials were of either glass or Teflon.

Absorbing liquid was stored in a Nalgene carboy and maintained at constant temperature ($\pm 0.02^\circ\text{C}$) by recirculating water from a constant-temperature bath through glass heat exchangers immersed in the absorbing liquid. A centrifugal pump delivered absorbing liquid to a constant head chamber. The overflow from the constant head chamber was returned to the carboy. The fluid from the constant head chamber passed through a final glass heat exchanger immersed in the temperature-controlled water bath. Liquid flow rate was measured and controlled by a rotameter equipped with a precision control valve. The absorbing liquid then flowed to the short wetted-wall column for contact with the gas phase. A second precision flow-control valve was used to maintain the correct liquid level in the exit slot of the wetted-wall column. The liquid passed to another constant head chamber and then to waste.

Gas flow and composition were controlled by a dual-channel electronic mass-flow controller. The electronic gas mass-flow controller (MKS Baraton Model 254) was equipped with control valves (Tylan 251) and flow transducers (Tylan 256). The pressure regulators on the nitrogen (99.99%) and chlorine (99.99%) gas cylinders were

maintained at a nominal 240 kPa (20 psig). This setting was sufficient to supply adequate gas flow to operate the mass-flow controller while still maintaining atmospheric pressure within the wetted-wall column. The gas mixture passed through a gas mixing bottle and then through a gas saturator. Both of these water-jacketed gas bottles were temperature controlled by circulating water from the constant-temperature bath. After saturation with water vapor, the gas passed to a glass, water-jacketed calming section approximately 66 cm long and then into the wetted-wall column for contact with the liquid. The waste gas was water scrubbed and exhausted through a fume hood.

Analytical Equipment and Methods. The amperometric titrator used for chlorine determination was a Fischer-Porter Model 17-T2012 equipped with an Astra Scientific PT-D101 dual platinum-platinum external electrode system. Titrant used was 0.00564 N phenylarsine oxide, Baker chemical reagent grade. Titrant was delivered by a manually controlled Metrohm Digital Burette (Model E535) capable of accurate volume increments of 0.001 mL. The titrant was standardized according to *Standard Methods* (16, Section 409A) with amperometric end-point detection.

The determinations of fluid properties and chlorine solubility are described elsewhere (17, 18).

(1) **Chlorine Physical Absorption.** Physical absorption experiments were performed by absorbing chlorine gas from a chlorine-nitrogen gas mixture into 0.2 N hydrochloric acid. The hydrochloric acid used was Baker reagent grade 12 N hydrochloric acid diluted with deionized water. The hydrochloric acid served to suppress the chlorine hydrolysis reaction. These experiments were performed in the short wetted-wall column apparatus described above. The experiments were conducted at 293 K over a range of liquid loadings: $0.23 < \Gamma < 1.68 \text{ g}\cdot\text{cm}^{-1}\cdot\text{s}^{-1}$; under these conditions, the liquid film thickness, δ , was 0.02–0.04 cm, and the exposure time, t_e , was 160–48 ms. The mole fraction chlorine in the influent gas was 0.10. Samples were analyzed in triplicate for chlorine by amperometric titration (16, 19).

(2) **Chlorine Absorption with Liquid-Phase Chlorine Hydrolysis.** Chlorine hydrolysis experiments were performed by absorbing chlorine from a chlorine-nitrogen gas mixture into deionized water that had been adjusted to either pH 5.4 or pH 10.0. The pH adjustment was made with small amounts of hydrochloric acid for the pH 5.4 case and sodium hydroxide for the pH 10.0 case. The chosen pH values, 5.4 and 10.0, correspond to conditions under which the chlorine hydrolysis reaction is first order reversible and first order irreversible, respectively (3). These experiments were performed in the short wetted-wall column apparatus described. The range of mass-flow rates was $0.3 < \Gamma < 1.6 \text{ g}\cdot\text{cm}^{-1}\cdot\text{s}^{-1}$. The experiments were conducted at 293 K and 1 atm, with 0.10 mole fraction chlorine in the influent gas. Under these conditions the liquid film thickness, δ , was in the range 0.02–0.04 cm, the flow was laminar, and the surface was reasonably free of ripples. Samples were analyzed in triplicate for chlorine by amperometric titration (19).

Results and Discussion

Physical Adsorption. A log-log regression analysis of the results from the present study yielded the following equation for the physical absorption of chlorine gas into 0.2 M hydrochloric acid solution:

$$k_L^* \left(\frac{h_c}{D_A} \right)^{1/2} = 7.925 \left(\frac{\Gamma}{\xi^{1/2}} \right)^{0.38} \quad (7)$$

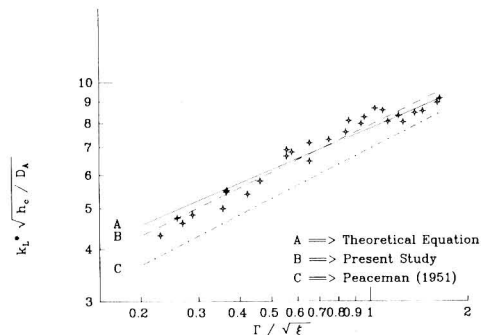


Figure 5. Transfer rate constant for physical absorption of chlorine into 0.2 N hydrochloric acid.

The 95% confidence interval for the exponent of eq 7 is 0.34–0.41, and the 95% confidence interval for the leading coefficient is 7.736–8.121. The coefficient of determination, r^2 , for this regression is 0.95.

Peaceman (15) reported the following equation based on experimental results on the desorption of carbon dioxide and chlorine from water using a short wetted-wall column similar to the experimental apparatus used in this study (corrected to 20 °C):

$$k_L^* \left(\frac{h_c}{D_A} \right)^{1/2} = 6.960 \left(\frac{\Gamma}{\xi^{1/2}} \right)^{0.4} \quad (8)$$

The theoretical relation for predicting k_L^* on the basis of the penetration theory (eq 2), the semiempirical relation (eq 8) developed from the work of Peaceman (15), and the semiempirical relation (eq 7) developed in this study are compared in Figure 5. Also shown are the experimental data points from the experiments. A Kolmogorov-Smirnov analysis (20) of the standardized residuals from the regression that produced eq 7 indicated that the residuals were normally distributed. The close approximation to the penetration theory achieved in this study is a significant improvement over the results obtained by Peaceman (15) and demonstrates that the penetration theory closely approximates the physical process of gas-liquid mass transfer in a short, wetted-wall column. The root mean square deviation of the observed values from the penetration theory prediction was equivalent to 5.8% in this study; the average deviation of the observed from the predicted values was only 0.1%, compared to 20% for the work of Peaceman (15).

Chlorine Absorption with Simultaneous Liquid-Phase Chlorine Hydrolysis. (1) **Methodology of Data Interpretation.** The results of the chlorine physical absorption experiments as described by eq 7 were used in computing the increase in mass-transfer rate for the cases of mass transfer with simultaneous liquid-phase chemical reaction. The ratio of the mass transfer coefficient with reaction to that without reaction (the enhancement factor, E , in eq 5c) was used as input to a mathematical algorithm described elsewhere (18) to determine the rate constant of the liquid-phase reaction.

For the absorption of chlorine gas into pure water at initial pH 5.4, the instantaneous enhancement factor, E_i , was calculated in the manner suggested by Danckwerts (6), using the chlorine hydrolysis equilibrium constants of Connick and Chia (21); the interfacial liquid-phase gas chlorine concentration was determined from the solubility of chlorine gas determined under the condition of these

experiments, as discussed elsewhere (17). The resultant E_i was multiplied by 1.15 to compensate for the effect of unequal diffusivities of the reacting species (6). The experiment with absorbing fluid initial pH of 10.0 was analyzed as a first-order irreversible reaction, which is equivalent to $E_i = \infty$.

In previous studies of the kinetics of gas-liquid reactions (15, 22, 23), the rate constant of the reaction was determined by fitting the enhancement factor, E , from all runs of an experiment to the type curves of Figure 2 and selecting a single value of the rate constant that represented the best fit for the experimental data. In this study, the estimation of the rate constant from experimental data was accomplished by fitting the enhancement factor, E , and the physical absorption mass-transfer coefficient, k_L^* , to the approximate equation of Hikita and Asai (13), eq 3 and 4. The data fitting and selecting of a rate constant were performed for each individual run of an experiment, and the arithmetic mean and standard deviation were calculated from the values of individual runs and reported for each experiment. This procedure permits a more rigorous error analysis (18) than was possible in previous work (15, 22, 23). The computer codes that were developed for this purpose have been presented elsewhere (18).

(2) Precision of Estimates. Evaluation of the rate constant in the manner described above facilitates the estimation of the precision of the methodology presented here. A sensitivity analysis indicated that the mathematical algorithm utilized in this study resulted in propagation of the random errors in the experimental procedures. The coefficient of variation for the calculated rate constant was 15–17%, whereas the random errors in the experimental procedures themselves account for variation on the order of 12–13%.

Chlorine Hydrolysis Rate Experiments. The chlorine hydrolysis rate constant was measured at 20 °C in two sets of experiments at pH 5.4 and 10.0, with the results interpreted by using the penetration theory in conjunction with first-order, reversible and irreversible kinetics, respectively. At each pH condition, experiments were carried out over a range of flow rates, such that the time of exposure varied from 50 to 200 ms; 23 experiments were conducted at pH 5.4 and 16 experiments at pH 10. The observed rate constants (mean \pm standard deviation) at pH 5.4 (reversible) and pH 10.0 (irreversible) were $12.9 \pm 2.0 \text{ s}^{-1}$ and $12.7 \pm 1.8 \text{ s}^{-1}$, respectively. The close agreement of the estimates obtained at the two conditions constitutes a strong confirmation of the accuracy of the methodology.

The observed enhancement factors for the chlorine hydrolysis were in the range $1.2 < E < 1.6$, and the corresponding values of $M^{1/2}$ (eq 27) were $0.65 < M^{1/2} < 1.5$. The system response can be characterized as pseudo m th order, corresponding to the region of Figure 2 near the origin and to the "slow reaction" case in terms of concentration profiles (Figure 3b). The calculated depth of penetration of chlorine into the aqueous film constituted less than 30% of the film thickness, δ , in all experiments, and less than 10% at the upper end of the flow rate range. The gaseous chlorine reactant was depleted to the extent of only 0.7–1.3%. It seems evident that short wetted-wall columns of the type used in this work are suitable for quantitating the rates of reactions much faster than chlorine hydrolysis at 293 K, in view of the relatively low values of $M^{1/2}$ and of fractional chlorine depletion observed in this work.

Comparison with Previous Studies. The first-order forward rate constants for the chlorine hydrolysis reaction determined in this study are compared with the results

Table I. First-Order Rate Constants for Chlorine Hydrolysis

k_1, s^{-1} ^a	temp, °C	technique	ref
2.32 ± 0.32	4.0	rapid mixing	24
3.36 ± 0.53	8.0	rapid mixing	24
5.60 ± 0.45	9.5	thermal continuous flow	5
8.5 ± 1.02^b	15.0	wetted-wall column	22
11.0 ± 1.0^b	20.0	temperature jump	4
15.4 ± 2.4	20.0	stopped flow	24
17.7 ± 0.7	20.0	temperature jump	24
12.9 ± 1.96^c	20.0	this study (first order, reversible)	
12.7 ± 1.84^d	20.0	this study (first order, irreversible)	
20.9 ± 1.20	25.0	laminar jet	3
15.4 ± 1.85^b	25.0	wetted-wall column	22
46.0 ± 5.52^b	40.0	wetted-wall column	22

^a Mean \pm standard deviation of the measurements. ^b Estimated standard deviation inferred from author's discussion. ^c Measured at pH 5.4, 23 replicates. ^d Measured at pH 10.0, 16 replicates.

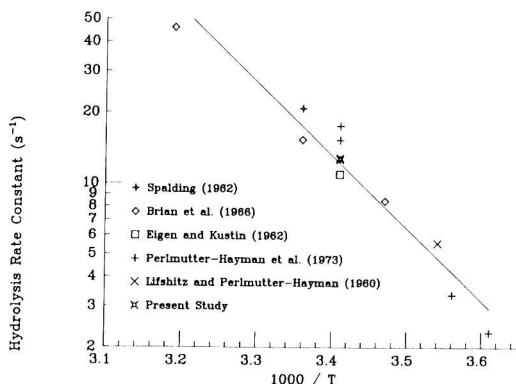


Figure 6. Chlorine hydrolysis rate constant as a function of temperature.

from the work of others in Table I. A rather wide range of values for the chlorine hydrolysis rate constant at 20 °C has been reported (3–5, 21, 22, 24). The kinetic methods used include temperature-jump relaxation and stopped-flow techniques, as well as the gas-liquid mass-transfer techniques described. Measurements with the conventional rapid mixing method have been restricted to temperatures lower than 20 °C because of their inability to deal with fast reactions.

If the data in Table I are analyzed according to the Arrhenius rate law by the regression of $\ln k_1$ vs. $1/T$, the activation energy is found to be $60.3 \text{ kJ}\cdot\text{mol}^{-1}$ with a 95% confidence interval of $49.4\text{--}71.2 \text{ kJ}\cdot\text{mol}^{-1}$. The preexponential factor is 6.76×10^{11} , and the coefficient of determination for the Arrhenius relation is $r^2 = 0.94$. The data from Table I and the resulting Arrhenius regression line are shown in Figure 6. The value of the chlorine hydrolysis first-order forward rate constant at 293 K predicted from all the data is 12.2 s^{-1} , approximately 5% lower than the results of this work, with a 95% confidence interval of $10.7\text{--}14.0 \text{ s}^{-1}$.

The agreement between the results of this study and of previous reports for the chlorine hydrolysis first-order forward reaction is quite good, as shown in Figure 6. The variation in the results (Table I) from the present study ($\pm 15\%$) was somewhat greater than the variation ($\pm 4\text{--}9\%$) reported by others using temperature perturbation techniques (4, 5, 24). The results of Brian et al. (22) show variability similar to that of this work, using similar ap-

paratus. The most precise value ($\pm 4\%$) reported for the chlorine hydrolysis first-order forward reaction at 20 °C is that of Perlmutter-Hayman et al. (21), who used a temperature-jump relaxation technique. However, Eigen and Kustin (4), using the same type of kinetic apparatus, reported a measured rate constant of $11.0 \pm 1.0 \text{ s}^{-1}$, substantially smaller than the value reported by Perlmutter-Hayman et al. (24), i.e., $17.0 \pm 0.7 \text{ s}^{-1}$. Perlmutter-Hayman et al. (24) discussed this discrepancy but offered no explanation for the difference in values, and the issue remains unresolved as to which of the results (4, 24) is more nearly accurate. The results of this work, obtained with the wetted-wall column, fall between the extremes of the data obtained with the temperature-jump technique (4, 24). Moreover, the present results are within 5% of the value predicted at 293 K by the Arrhenius-type regression (Figure 6) that synthesizes all of the data in Table I.

Potential Applications

The procedures and methods used in this study can be applied to other gas-liquid rapid reactions of environmental concern. The quantitation of the chlorine-chlorite reaction is the subject of the following paper (2). Two additional candidate systems for study are (a) the rate of reaction of ozone with liquid-phase organic and inorganic compounds and (b) the removal of sulfur and nitrogen oxides from offgases of coal-fired power plants by liquid absorption and liquid-phase chemical reaction.

The wetted-wall column or a similar apparatus can also be used to estimate the liquid-phase diffusivity of volatile organic compounds by either absorbing or desorbing the compound of interest (25). Subsequent analysis of the experimental data according to the penetration theory model would permit determination of the diffusivity from the observed mass-transfer coefficient.

Conclusions

This work has demonstrated the validity of the penetration theory as a predictor of the physical absorption of molecular chlorine into acidified aqueous solution in a laminar film, short wetted-wall column. The root mean square error was 5.8%. This close conformance to the penetration theory strengthens confidence in the methodology of quantitating the rate of fast reactions in the liquid phase by observing the enhancement of interphase transfer of a reactant introduced in the gas phase.

The rate of chlorine hydrolysis was studied by observing the enhancement of the transfer of molecular chlorine from the gas phase into water at appropriate pH values. The chlorine hydrolysis rate experiments were conducted at two pH conditions such that the kinetics were in the one case first order reversible and in the other case first order irreversible. The good agreement between the observed rate constants in the two cases, $12.9 \pm 2.0 \text{ s}^{-1}$ and $12.7 \pm 1.8 \text{ s}^{-1}$, respectively, also serves to confirm the accuracy of the methodology. Moreover, the rate constants from this work are in accord with the results of previous studies obtained with a variety of methods, principally relaxation techniques, for which the previously reported range at 293 K is 11.0–17.7 s^{-1} . From comparison of the results of this work with previous work, it appears that the wetted-wall-column methodology produces more consistent results for chlorine hydrolysis rates than do techniques of relaxation kinetics. There are grounds for confidence that the mass-transfer enhancement methodology can be employed by using the short, wetted-wall column to measure the rates of reactions considerably faster than chlorine hy-

drolysis. Moreover, the methodology presented here is applicable to both reversible and irreversible reactions, whereas relaxation methods are restricted to reactions at equilibrium.

Acknowledgments

Greg Arthur assisted with the experiments.

Glossary

A^*	equilibrium liquid-phase molecular chlorine concentration, $\text{mol}\cdot\text{L}^{-1}$
B^0	initial bulk fluid chlorite concentration, $\text{mol}\cdot\text{L}^{-1}$
D_A	diffusivity of molecular chlorine, $\text{cm}^2\cdot\text{s}^{-1}$
D_B	diffusivity of species B $\text{cm}^2\cdot\text{s}^{-1}$
E	enhancement factor = k_L/k_L^*
E_i	enhancement factor for instantaneous liquid-phase reaction
h_c	contact height of short wetted-wall column, cm
k_1	first-order reaction rate constant, s^{-1}
k_L	apparent liquid-side mass-transfer coefficient with reaction, $\text{cm}\cdot\text{s}^{-1}$
k_L^*	physical liquid-side mass-transfer coefficient, $\text{cm}\cdot\text{s}^{-1}$
$k_{m,n}$	reaction rate constant for (m,n)th-order reaction
$M^{1/2}$	ratio of chemical reaction rate to physical gas absorption rate as defined by eq 4
T	temperature, °C or K
t	time, s
t_e	time of exposure of liquid interface to gas phase, s
V_i	interfacial liquid velocity, $\text{cm}\cdot\text{s}^{-1}$
$V(x)$	velocity as a function of depth into the liquid film, $\text{cm}\cdot\text{s}^{-1}$
x	distance into liquid film, cm
z	stoichiometric factor
<i>Greek Symbols</i>	
Γ	mass-flow rate of liquid absorbent per unit wall perimeter, $\text{g}\cdot\text{cm}^{-1}\cdot\text{s}^{-1}$
δ	depth of liquid film, cm
μ	viscosity, $\text{g}\cdot\text{cm}^{-1}\cdot\text{s}^{-1}$
μ_w	viscosity of pure water at 20 °C, $\text{g}\cdot\text{cm}^{-1}\cdot\text{s}^{-1}$
ξ	$\rho\mu/\rho_w\mu_w$, dimensionless
ρ	density, $\text{g}\cdot\text{cm}^{-3}$
ρ_w	density of pure water at 20 °C, $\text{g}\cdot\text{cm}^{-3}$

Registry No. Cl_2 , 7782-50-5.

Literature Cited

- Moore, J. W.; Pearson, R. G. "Kinetics and Mechanism", 3rd ed.; Wiley: New York, 1981.
- Aieta, E. M.; Roberts, P. V. *Environ. Sci. Technol.*, following paper in this issue.
- Spalding, C. W. *AIChE J.* 1962, 8 (5), 685–689.
- Eigen, M.; Kustin, K. *J. Am. Chem. Soc.* 1962, 84, 1355–1361.
- Lifshitz, A.; Perlmutter-Hayman, B. *J. Phys. Chem.* 1960, 64, 1663–1665.
- Danckwerts, P. V. "Gas-Liquid Reactions"; McGraw-Hill: San Francisco, CA, 1970.
- Whitman, W. G. *Chem. Metall. Eng.* 1923, 29, 146–148.
- Lewis, W. K.; Whitman, W. G. *Ind. Eng. Chem.* 1924, 16 (12), 1215–1220.
- Higbie, R. *Trans. AIChE* 1935, 31, 365–389.
- Gilliland, E. R.; Sherwood, T. K. *Ind. Eng. Chem.* 1934, 26, 516–523.
- Vivian, J. E.; King, C. J. *AIChE J.* 1964, 10 (2), 221–227.
- Sherwood, T. K.; Pigford, R. L.; Wilke, C. R. "Mass Transfer"; McGraw-Hill: New York, 1975.
- Hikita, H.; Asai, S. *Int. Chem. Eng.* 1964, 4 (2), 332–340.
- van Krevelen, D. W.; Hofstijzer, P. *J. Chem. Eng. Prog.* 1948, 44, 529–536.
- Peaceman, D. W. Ph.D. Dissertation, Massachusetts Institute of Technology, 1951.
- American Public Health Association "APHA-AWWA-WPCF Standard Methods for the Examination of Water and Wastewater", 14th ed.; APHA: Washington, DC, 1976.
- Aieta, E. M.; Roberts, P. V. *J. Chem. Eng. Data*, in press.

(18) Aieta, E. M. Ph.D. Dissertation, Stanford University, Stanford, CA, 1984.
 (19) Aieta, E. M.; Hernandez, M.; Roberts, P. V. *J. Am. Water Works Assoc.* 1984, 76, 64-70.
 (20) Sokal, R. R.; Rohlf, F. J. "Biometry"; W. H. Freeman: San Francisco, CA, 1969.
 (21) Connick, R. E.; Chia, Y.-T. *J. Am. Chem. Soc.* 1959, 81, 1280-1284.
 (22) Brian, P. L. T.; Vivian, J. E.; Piazza, C. *Chem. Eng. Sci.* 1966, 21, 551-558.
 (23) Gilliland, E. R.; Baddour, R. F.; Brian, P. L. T. *AIChE J.* 1958, 4 (2), 223-230.

(24) Perlmutter-Hayman, B.; Wieder, H.; Wolff, M. H. *Isr. J. Chem.* 1973, 11 (1), 27-36.
 (25) Himmelblau, D. M. *Chem. Rev.* 1964, 64, 527-550.

Received for review June 11, 1984. Revised manuscript received April 26, 1985. Accepted August 13, 1985. This work was funded by the U.S. Environmental Protection Agency under Research Grant R-808686. It has not been subjected to the Agency's required peer and administrative review and therefore does not necessarily reflect the views of the Agency; no official endorsement should be inferred.

Kinetics of the Reaction between Molecular Chlorine and Chlorite in Aqueous Solution

E. Marco Aieta[†] and Paul V. Roberts*

Department of Civil Engineering, Stanford University, Stanford, California 94305

■ The kinetics of the aqueous phase reaction between molecular chlorine and chlorite ion was studied experimentally by measuring the enhancement of chlorine transfer from the gas phase. The results were interpreted by using the penetration theory of mass transfer, in conjunction with the assumption that the reaction is second order overall, being first order with respect to both chlorine and chlorite. The second-order rate constant was determined as a function of temperature and solution ionic strength. These experiments indicated that the reaction rate constant at 293 K and zero ionic strength is $1.62 \times 10^4 \text{ M}^{-1}\text{s}^{-1}$. The reaction rate constant increased with increasing temperature, having an activation energy of 39.9 $\text{kJ}\cdot\text{mol}^{-1}$, and decreased with increasing ionic strength. A collision theory interpretation of the observed rate indicates that the steric factor is on the order of unity, suggesting that nearly every collision of sufficient energy results in reaction, regardless of the relative orientation.

Introduction

The reaction between dissolved molecular chlorine and aqueous chlorite represents a potential route for generating chlorine dioxide, a promising alternative to chlorine for disinfection in water and wastewater treatment (1-6). Chlorine dioxide commonly is generated by acid activation of aqueous chlorite or by contacting aqueous chlorite with aqueous chlorine under conditions such that the predominant reaction is between chlorite ion and hypochlorous acid (1-4). The latter method, which is most common in U.S. practice, affords an acceptably high yield on the basis of the chlorite reactant, but, as usually practiced, requires an excess of chlorine (1) and can result in the formation of substantial amounts of byproduct chlorate (4).

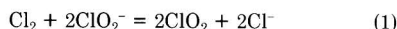
There is some evidence that the yield and purity of the chlorine dioxide product can be enhanced by contacting chlorine gas directly with concentrated chlorite solution (7), thus minimizing the amounts of unconverted chlorine and chlorite and of byproduct chlorate. Important benefits could be gained from choosing conditions to maximize the yield and purity of the chlorine dioxide generated for water treatment. Improving the yield, especially that based on chlorite, decreases the cost of treatment. Decreasing the amount of unreacted chlorine present in the product reduces the extent of reactions between chlorine and organic

constituents in the water being treated, thus minimizing the potential formation of halogenated organic byproducts. Reducing the amounts of chlorite and chlorate helps alleviate concern regarding possible adverse health effects of chlorine dioxide use in water treatment.

To realize these potential benefits of improved chlorine dioxide generation, the kinetics of the reaction between molecular chlorine and aqueous chlorite, as well as the chemistry and kinetics of competing reactions, must be understood. This paper is intended to elucidate and quantify the kinetics of the reaction between dissolved molecular chlorine and chlorite ion in aqueous solution, as pertains to chlorine dioxide generation for water treatment.

Chlorine-Chlorite Reaction and Mechanism

Stoichiometry. In the oxidation of aqueous chlorite by chlorine or hypochlorous acid, both chlorine dioxide and chlorate appear as products. In acid solution, where the chlorine is present mainly as dissolved molecular chlorine gas, the stoichiometries of the two reactions are



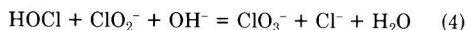
and



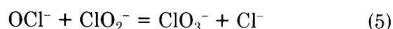
In solutions near neutral pH, where chlorine is present largely as hypochlorous acid, the stoichiometries are



and



In alkaline solutions, where the chlorine is present as hypochlorite ion, the reaction is very slow and the only product formed is chlorate ion:



Mechanism. Taube and Dodgen (8), using radioactive chlorine, provided significant insight into the reaction mechanisms of the oxidation of chlorite by chlorine (or hypochlorous acid), the reduction of chlorate by chlorite ion (and the reverse reaction), and the disproportionation of chlorous acid. The observations of Taube and Dodgen led them to postulate an unsymmetrical intermediate that was common to all three reaction mechanisms. Subsequent work by Emmenegger and Gordon (9) has amplified and

[†]Present address: Rio Linda Chemical Co., Sacramento, CA 95814.

refined the mechanism proposed by Taube and Dodgen (8), but their original findings remain as the foundation for many of the subsequent studies of the kinetics and mechanisms of aqueous chlorine chemistry.

From the dependence of the product ratio of chlorine dioxide to chlorate on experimental conditions, the following consensus has emerged (8, 9):

(1) The reaction between chlorite ion (or chlorous acid) and chlorine (in acid or neutral solution) is second order overall, being first order in both chlorine and chlorite;

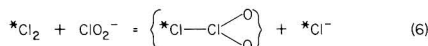
(2) Acidic conditions favor the formation of chlorine dioxide, whereas under neutral and alkaline conditions, chlorate is the primary reaction product;

(3) For a given pH value, an increase in chlorite concentration results in relatively more chlorine dioxide production;

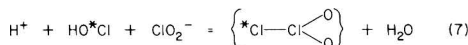
(4) Higher chloride ion concentrations favor the formation of chlorine dioxide relative to chlorate, especially at acidic pH;

(5) Proportional increases in all reactant concentrations favor the formation of chlorine dioxide relative to chlorate.

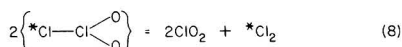
The mechanism for the chlorine-chlorite reaction proposed by Taube and Dodgen (8) as consistent with experimental observations will be presented. The chlorine atoms with asterisks trace the fate of the chlorine originally present as molecular chlorine or hypochlorous acid. Hypothetical, metastable intermediate species are enclosed in brackets. For the reaction of chlorite with molecular chlorine



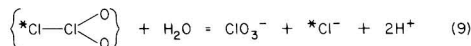
and with hypochlorous acid



The metastable intermediate can decompose to form either chlorine dioxide



or chlorate ion



This mechanism satisfies the experimental observations discussed above according to the following rationale. The metastable intermediate, $\{Cl_2O_2\}$, can decompose by either a first-order process, reaction 9, to give chlorate ion or by a second-order process, reaction 8, to give chlorine dioxide. The formation of the intermediate, $\{Cl_2O_2\}$, is, in either case, the rate-limiting step in the mechanism as determined from the observed rate law (9). Reaction conditions that promote the formation of higher concentrations of the intermediate will favor the product chlorine dioxide over the product chlorate ion.

Emmenegger and Gordon (9) have shown that the rate of oxidation of chlorite by molecular chlorine, reaction 6, is considerably faster than the oxidation by hypochlorous acid, reaction 7. Therefore, reaction conditions that favor molecular chlorine as opposed to hypochlorous acid result in higher intermediate concentrations. Higher hydrogen ion concentrations and chloride ion concentrations shift the chlorine hydrolysis equilibrium (10) toward increased molecular chlorine concentration. These reaction conditions are in fact those that are observed experimentally to produce relatively more chlorine dioxide (11). An excess of chlorite also promotes higher concentrations of the intermediate, as does increasing the absolute concentrations

of all reactants, while maintaining the same reactant ratios, resulting in proportionally more chlorine dioxide.

The $\{Cl_2O_2\}$ intermediate must be asymmetric, since the chlorine atoms of the reactants remain distinct, as demonstrated by Taube and Dodgen (8). The intermediate also appears in the mechanisms of the reduction of chlorate by chloride ion and in the mechanism of the disproportionation of chlorous acid. In studies by Hong and Rapson (12) and Kieffer and Gordon (13) on the kinetics and stoichiometry of the disproportionation of chlorous acid, more details were added to the mechanism that was originally proposed for this reaction by Taube and Dodgen (8), but $\{Cl_2O_2\}$ remains the predominant intermediate complex in the mechanistic pathway that leads to chlorine dioxide. This intermediate may, indeed, be a common factor in much of aqueous oxochlorine chemistry.

Rate. Although the stoichiometry and mechanism of the chlorine-chlorite reaction are well established, very little work has been done to quantify the rate of the reaction. Emmenegger and Gordon (9) suggested that, even at 0 °C and reactant concentrations of 10^{-3} M, the reaction is too rapid to be studied by conventional kinetic methods. It follows that a study of the kinetics of the chlorine-chlorite reaction at concentrations (3 M) and temperatures (20–30 °C) typically used in water treatment would not be possible with currently available rapid kinetic techniques. The expedient approach of slowing the ClO_2 -forming reaction by reducing the reactant concentrations is not feasible in this instance, because competing reactions are favored at lower concentration.

Experimental Section

Approach. Experiments were performed using the laminar flow short wetted-wall column as a gas-liquid contact device. This experimental apparatus was designed to conform to the assumptions of the penetration theory of gas absorption accompanied by the liquid-phase reaction (10–14). The amount of chlorine gas absorbed into 0.2 N HCl (physical absorption only) was compared to the amount of chlorine gas absorbed into a sodium chlorite solution (absorption with the liquid-phase reaction). The increase in chlorine absorption, due to the liquid-phase reaction, was used to estimate the rate of the chlorine-chlorite reaction at the temperature and ionic strength of the experiment. The mathematical theory, experimental apparatus, analytical procedures, and the method of data reduction and analysis have been described elsewhere (10, 14).

Two aspects of the stoichiometry and reaction mechanism of the chlorine-chlorite reaction are crucial to the experimental approach taken here. The first observation is that the rate-limiting step is the formation of the intermediate $\{Cl_2O_2\}$ and that the rate of formation is faster when the chlorine is present as molecular chlorine. In aqueous systems at equilibrium, molecular chlorine is the dominant chlorine species only in very acidic solutions. Above pH 4, however, the chlorine hydrolysis equilibrium is shifted far to the right, and the dominant chlorine species at equilibrium are hypochlorous acid and hypochlorite ion. In the present study, chlorine gas was contacted with aqueous sodium chlorite solution in a gas-liquid system. As shown by Emmenegger and Gordon (9), the rate of reaction of the dissolved molecular chlorine gas with the chlorite ion is much faster than the rate of chlorine hydrolysis. Hence, the chlorine molecule reacts preferentially with the chlorite ion, and the reaction solution pH does not influence the rate of reaction in a gas-liquid system as it has been shown to do in a liquid-liquid system. The second observation is that, as shown

Table I. Summary of Chlorine-Chlorite Reaction Experimental Conditions

EXP ^a	N ^b	B ⁰ , M	A* × 10 ³ , M	I, M	μ × 10 ² , g/(cm·s)	ρ, g/cm ³	T, °C	pH	D _{Cl₂} × 10 ⁵ , cm ² /s	D _{ClO₂⁻} × 10 ⁵ , cm ² /s	E _i
T1	28	1.06	5.72	1.42	1.31	1.077	20	9.5	0.99	1.08	195
P ^c	6	0.12	7.21	0.12	1.03	1.006	20	7.8	1.25	1.36	18
T2	16	0.12	7.15	0.17	1.02	1.008	20	9.2	1.27	1.38	19
T3	25	1.04	8.43	1.39	1.58	1.080	10	9.7	0.79	0.86	129
T4	12	3.18	3.44	4.26	2.04	1.228	20	9.5	0.64	0.69	961
T5	19	1.06	4.08	1.42	0.95	1.074	30	9.6	1.41	1.54	273

^aEXP = experimental series. ^bN = number of runs. ^cPurified sodium chlorite was used.

Table II. Composition of Sodium Chlorite Reactant Mixtures

component	% by weight ^a	
	commercial grade	purified
sodium chlorite	78.7	96.1
sodium chloride	3.3	1.0
sodium nitrate	12.0	1.2
sodium chlorate	1.9	0.1
other sodium salts	4.1	1.6
total	100.0	100.0

^aDry basis.

by the overall stoichiometries (reactions 1 and 2), 2 mol of chloride ion are formed per mole of molecular chlorine reacting with chlorite ion. Accordingly, the amount of chlorine gas absorbed and reacted with aqueous chlorite can be determined by measuring the increase in liquid-phase chloride ion concentration. Chloride was analyzed by potentiometric titration using an automatic potentiograph and digital buret system (Metrohm, Models E536 and E535) with a silver sulfide selective ion electrode and a double-junction reference electrode (Orion Models 94-16 and 90-02) and 0.025N NaNO₃ titrant.

Conditions. The gas-phase mixture consisted of 0.1 mole fraction of chlorine in nitrogen at atmospheric pressure. The chlorine gas interfacial concentration, A*, was determined from chlorine solubility measurements (15). The absorbing fluid was deionized water which contained a known concentration of sodium chlorite, B⁰.

The experimental conditions for the chlorine-chlorite reaction experiments are summarized in Table I. In each of the six experimental series (column 1) a number N of individual experiments (6 < N < 28) was conducted over a 3-fold range of flow rates (approximately 4–12 mL/s). The temperature and ionic strength were held constant for a given series; temperature was held at 10, 20, or 30 °C at a constant ionic strength I = 1.42 M, whereas ionic strength was set at 0.17, 1.42, or 4.26 M at a constant temperature of 20 °C. The base case (20 °C and 1.42 M) corresponds to typical conditions for chlorine dioxide generation in water treatment.

In all but one experiment, the sodium chlorite was of commercial grade (Hoechst technical grade). A small

amount of purified sodium chlorite (96.1% NaClO₂) was prepared for one experimental series (EXP P) to determine if there was a measurable effect on the reaction rate due to the impurities of the commercial-grade sodium chlorite. The purification procedure consisted of preparing a saturated solution of the commercial-grade material at 35 °C, cooling the solution under vacuum to 15 °C, and collecting the recrystallized product. The compositions of the sodium chlorite materials used in this study are shown in Table II.

The pH of the chlorite solution of each experiment was adjusted to below pH 10 with hydrochloric acid in order to suppress the second-order reaction between dissolved chlorine and hydroxide ion (16). For the purified sodium chlorite experiment no pH adjustment was necessary.

Data Analysis. For each experiment, the enhancement factor, E, was evaluated as the ratio of the observed mass transfer rate to the transfer rate anticipated in the absence of chemical reaction (ref 10, eq 3). The rate constant k_{m,n} for the chemical reaction was then evaluating by fitting the observed enhancement factor E to an approximate solution for mass transfer with chemical reaction in a wetted-wall column (ref 10, eq 5). The fitting procedure is an adaptation of the Levenberg-Marquardt algorithm (ref 14, Appendix B). For this evaluation procedure, the reaction was presumed to be first order with respect to both chlorine and chlorite (m = n = 1), and E_i was calculated by using eq 5C of ref 10 and the values of D_A, D_B, B⁰, and A* from Table I.

Results

Experimental values of the second-order rate constant, k₂, are reported in Table III. Each result is the composite of a number N of individual experiments, carried out over an approximately 10-fold range of liquid flow rates (14). The values of k₂ are on the order of 10⁴ (M⁻¹s⁻¹). The weighted average experimental error, as gauged from the coefficients of variation (Table III, last column), was 17%. The standard error of estimate was in all cases less than 10% of the mean.

Discussion

Sensitivity Analysis. A systematic sensitivity analysis was undertaken (14) to ascertain the effects of errors in

Table III. Summary of Experimentally Determined Second-Order Rate Constants of the Chlorine-Chlorite Reaction

EXP ^a	N ^b	I, M	T, °C	rate constant, M ⁻¹ s ⁻¹	standard deviation M ⁻¹ s ⁻¹	standard error, M ⁻¹ s ⁻¹	95% CI ^c × 10 ⁻⁴ , M ⁻¹ s ⁻¹	CV, ^d %
T1	28	1.42	20	1.31 × 10 ⁴	0.22 × 10 ⁴	0.04 × 10 ⁴	1.23–1.40	16.5
P	6	0.12	20	1.49 × 10 ⁴	0.30 × 10 ⁴	0.12 × 10 ⁴	1.19–1.79	20.2
T2	16	0.17	20	1.69 × 10 ⁴	0.36 × 10 ⁴	0.09 × 10 ⁴	1.50–1.88	21.5
T3	25	1.39	10	0.55 × 10 ⁴	0.15 × 10 ⁴	0.03 × 10 ⁴	0.49–0.61	26.6
T4	12	4.26	20	1.16 × 10 ⁴	0.28 × 10 ⁴	0.08 × 10 ⁴	0.98–1.33	24.3
T5	19	1.42	30	1.67 × 10 ⁴	0.25 × 10 ⁴	0.06 × 10 ⁴	1.55–1.79	14.9

^aEXP = experimental series. ^bN = number of runs. ^cCI = confidence interval. ^dCV = coefficient of variation = standard deviation/mean.

input variables on the accuracy of the experimentally determined rate constants, k_2 (Table III).

The uncertainties in estimating k_2 arising from possible systematic errors in fluid viscosity and density, flow rates, and gas-phase composition all are believed to be on the order of 1%. The estimation of k_2 is more sensitive to potential errors in estimating the diffusivity of sodium chlorite and the Henry constant of chlorine; uncertainties regarding the value of these two parameters may affect the reported k_2 values by as much as 5%. The Henry constant for chlorine was determined directly (15) under conditions simulating as closely as possible those of the chlorine-chlorite reaction experiments, to minimize the error from this source.

Rate Expression. The rate-limiting step of the chlorine-chlorite reaction mechanism is the formation of the reactive intermediate $\{\text{Cl}_2\text{O}_2\}$ from Cl_2 and ClO_2^- . Emmenegger and Gordon (9) found that the overall reaction order for the chlorine-chlorite reaction was 2.1 ± 0.1 . When the steady-state approximation is applied to the intermediate $\{\text{Cl}_2\text{O}_2\}$ in the reaction mechanism (eq 6), the overall rate of reaction is given by

$$\text{rate} = k_2[\text{Cl}_2][\text{ClO}_2^-] \quad (10)$$

The results of the present work are consistent with a reaction rate equation incorporating first-order dependence on both chlorine and chlorite, and second order overall. Hence, the results are consistent with the mechanism proposed by Taube and Dodgen (8) as well as with the data of Emmenegger and Gordon (9).

The chlorine-chlorite experiments undertaken in the present study were designed to determine the value of the second-order rate constant, as well as its dependence on the ionic strength and composition of the aqueous solution, on the reaction temperature, and on the purity of the sodium chlorite solute.

Effect of Ionic Strength. At ionic strengths greater than 0.01 M, the logarithm of the reaction rate constant should be a linear function of the first power of ionic strength for reactions involving a neutral molecule and an ion (17). The chlorine-chlorite reaction falls into this category.

Experimental series T1, T2, and T4 reported in Table III (a total of 56 experiments) were all performed at 20 °C, but the absorbing liquids were of different ionic strengths. A regression analysis of the natural logarithms of the second-order rate constants of the chlorine-chlorite reaction from these experiments vs. ionic strength yielded the relationship

$$\ln \left(\frac{k_2}{k_{2,0}} \right) = -0.085I \quad (11)$$

where $k_{2,0}$ is the second-order rate constant determined by extrapolation to zero ionic strength and is $1.62 \times 10^4 \text{ M}^{-1}\text{s}^{-1}$. The 95% confidence interval for the zero ionic strength second-order rate constant is 1.49×10^4 – $1.76 \times 10^4 \text{ M}^{-1}\text{s}^{-1}$. The 95% confidence interval for the slope in eq 11 is -0.046 to -0.124 . This relationship is shown in Figure 1 together with the means of the experimental data and the respective standard deviations.

Effect of Temperature. The rate of the chlorine-chlorite reaction increased with increasing temperature, in agreement with the Arrhenius relationship

$$k_2 = A_r \exp(-E_a/RT) \quad (12)$$

Regression of $\ln(k_2)$ vs. $1/T$ gives $-E_a/R$ as the slope and $\ln(A_r)$ as the intercept. The data from series T1, T3,

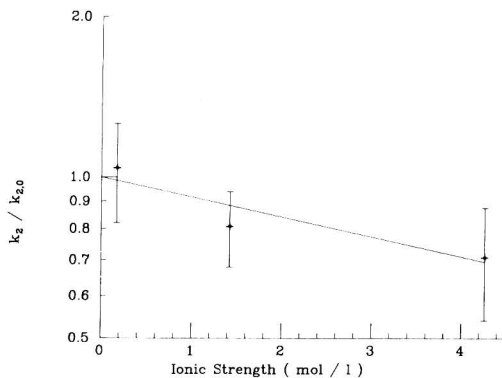


Figure 1. Effect of ionic strength on the second-order rate constant of the chlorine-chlorite reaction.

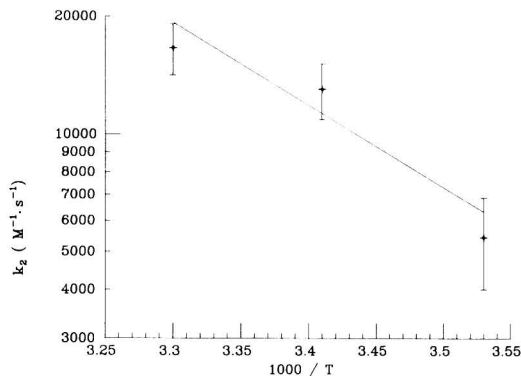


Figure 2. Effect of temperature on the second-order rate constant of the chlorine-chlorite reaction.

and T5—a total of 72 experiments all at $I = 1.4 \text{ M}$ (Table III)—for the second-order rate constant of the chlorine-chlorite reaction at 20, 10, and 30 °C, respectively, were used to determine the parameters of the Arrhenius expression. A regression analysis of $\ln(\text{rate})$ vs. $1/T$ yielded

$$k_2 = 1.31 \times 10^{11} \exp \left(\frac{-39.9 \text{ kJ}\cdot\text{mol}^{-1}}{RT} \right) \quad (13)$$

Equation 13 is plotted in Figure 2 along with the mean of the experimental data points and their respective standard deviations. The 95% confidence interval for the activation energy is 35.6–45.2 $\text{kJ}\cdot\text{mol}^{-1}$.

Effect of Sodium Chlorite Purity. Experimental series P and T2 can be compared to determine the effects of impurities in the sodium chlorite feed solution on the second-order rate constant. For series T2, the sodium chlorite used was an untreated technical-grade product (Table II), representative of the type and quality of material generally sold for water treatment use (80% NaClO_2). For series P, the sodium chlorite was purified from the technical-grade product. The concentrations of the sodium chlorite for experiments P and T2 were the same, but the ionic strength of the sodium chlorite solution used for experiment T2 was slightly greater than that used for experiment P owing to the presence of impurities in the technical-grade material.

The second-order rate constants determined from these experiments are presented in Table III along with their standard deviations; the two second-order rate constants

do not differ significantly at the 95% confidence level. It can be concluded that, within the variation of the method, there is no statistically significant difference between the second-order rate constant observed when the sodium chlorite solution is made from unpurified technical-grade material and the second-order rate constant observed when the sodium chlorite solution is made from purified technical-grade material.

This conclusion was not tested at other sodium chlorite liquid-phase concentrations because of the large amounts of chemical required and the extremely low recoveries of purified sodium chlorite.

Collision Theory Interpretation. In terms of the collision theory of bimolecular reactions (17), the Arrhenius expression (eq 12) can be written as

$$k_2 = pZ \exp[-E_a/(RT)] \quad (14)$$

The factor Z represents the frequency of collisions or encounters between the reacting molecules. The product $p \exp[-E_a/(RT)]$ can be interpreted as the fraction of encounters that results in reaction, where p represents the fraction of encounters that has the correct orientation for reaction to take place and $\exp[-E_a/(RT)]$ represents the fraction of encounters that has sufficient energy to result in reaction.

The temperature dependence of the chlorine-chlorite reaction, as determined above, can be used to estimate the steric factor p for encounters between chlorine molecules and chlorite ions in solution. The frequency factor Z has been estimated to have a value on the order of $1 \times 10^{11} \text{ M}^{-1}\text{s}^{-1}$ for bimolecular reactions in solution (17). For the chlorine-chlorite reaction the factor $\exp[-E_a/(RT)]$ is on the order of 1×10^{-7} , if the activation energy is $39.9 \text{ kJ}\cdot\text{mol}^{-1}$ (eq 13). If k_2 is on the order of 1×10^4 , as observed in this work, the steric factor p evaluated from eq 14 is on the order of unity, indicating that the reaction between chlorine molecules and chlorite ions in solution occurs at nearly every encounter or collision of sufficient energy, irrespective of relative orientation.

Application to Chlorine Dioxide Generation for Water Treatment. Previous studies (7, 18) have demonstrated that a high yield of chlorine dioxide can be obtained when chlorine gas is contacted directly with concentrated aqueous chlorite. Chlorine dioxide yields of 95–99% were reported for a continuous, full-scale system in which chlorine gas was contacted with 2 M chlorite solution in a packed-bed reactor affording a residence time of a few seconds. This virtually complete reaction of chlorite was obtained with only a slight excess (approximately 3–4 mol %) of chlorine, and negligible quantities of chlorate were found in the reactor product stream under optimum conditions. Such nearly ideal reactor performance can be attributed to the extremely rapid rate of the reaction between molecular chlorine and concentrated aqueous chlorite, as shown in this paper; the formation of chlorine dioxide proceeds to completion so rapidly that competing reactions do not occur to an appreciable extent.

Conclusion

The second-order rate constant for the molecular chlorine-chlorite ion liquid-phase reaction was determined and found to have plausible temperature and ionic strength dependencies as interpreted by the collision reaction rate theory.

The penetration theory of gas absorption accompanied by liquid-phase reaction was used in analyzing experimental results to determine the kinetic parameters of the second-order reaction between molecular chlorine and chlorite ion. The successful application of the penetration

theory to this rapid chemical reaction was accomplished through the use of the laminar flow, short wetted-wall column.

The results of this research contribute to the understanding of the oxochlorine chemistry relevant to chlorine dioxide generation for water treatment. The reaction between molecular chlorine and chlorite ion in aqueous solution was found to proceed extremely rapidly, with a second-order rate constant on the order of $10^4 \text{ M}^{-1}\text{s}^{-1}$. Under the conditions of chlorine dioxide generation for water treatment (2 M ClO_2^-), the reaction between molecular chlorine and aqueous chlorite is approximately 1000-fold faster than chlorine hydrolysis. This difference offers a plausible explanation for the high yield of chlorine dioxide obtained when chlorine gas is contacted directly with concentrated chlorite solution.

This research also exemplifies how the experimental approach and apparatus used in the study of chlorine-chlorite reaction can be applied to other gas-liquid systems in which an absorbing gas undergoes a rapid reaction in solution.

Acknowledgments

Henry Taube advised us regarding the mechanism of the chlorine-chlorite reaction. Greg Arthur assisted with the experiments.

Glossary

A_r	preexponential factor in Arrhenius expression
A^*	equilibrium liquid-phase molecular chlorine concentration, $\text{mol}\cdot\text{L}^{-1}$
B^0	initial bulk fluid chlorite concentration, $\text{mol}\cdot\text{L}^{-1}$
D_{Cl_2}	diffusivity of molecular chlorine in water, $\text{cm}^2\cdot\text{s}^{-1}$
$D_{\text{ClO}_2^-}$	diffusivity of sodium chlorite in water, $\text{cm}^2\cdot\text{s}^{-1}$
E_a	activation energy, $\text{kJ}\cdot\text{mol}^{-1}$
E_i	enhancement factor for instantaneous liquid-phase reaction
I	ionic strength, $\text{mol}\cdot\text{L}^{-1}$
K_H	chlorine hydrolysis equilibrium constant, M
k_1	first-order reaction rate constant, s^{-1}
k_2	second-order reaction rate constant, $\text{M}^{-1}\cdot\text{s}^{-1}$
$k_{2,0}$	zero ionic strength second-order rate constant, $\text{M}^{-1}\cdot\text{s}^{-1}$
$k_{m,n}$	reaction rate constant for (m,n)-th-order reaction
m	reaction order with respect to chlorine
n	reaction order with respect to chlorite
p	fraction of molecular encounters with correct orientation for reaction
R	universal gas constant ($8.31441 \text{ J}\cdot\text{K}^{-1}\cdot\text{mol}^{-1}$)
T	temperature, K
Z	frequency coefficient for encounters between reacting molecules, $\text{M}^{-1}\cdot\text{s}^{-1}$

Greek symbols

μ	viscosity, $\text{g}\cdot\text{cm}^{-1}\cdot\text{s}^{-1}$
ρ	density, $\text{g}\cdot\text{cm}^{-3}$

Registry No. ClO_2^- , 14998-27-7; Cl_2 , 7782-50-5.

Literature Cited

- Gall, R. J. In "Ozone/Chlorine Dioxide Oxidation Products of Organic Materials"; Rice, R. G.; Cotruvo, J., Eds.; Ozone Press International: Cleveland, OH, 1984; pp 356–382.
- Sussman, S. In "Ozone/Chlorine Dioxide Oxidation Products of Organic Materials"; Rice, R. G.; Cotruvo, J., Eds.; Ozone Press International: Cleveland, OH, 1984; pp 344–355.
- Miller, G. W.; Rice, R. G.; Robson, C. M.; Scullin, R. L.; Kühn, W.; Wolf, H. "An Assessment of Ozone and Chlorine Dioxide Technologies for Treatment of Municipal Water Supplies". U.S. EPA, Cincinnati, OH, 1978, EPA-600/2-78-147.
- Masschelein, W. J. "Chlorine Dioxide: Chemistry and Environmental Impact of Oxochlorine Compounds"; Ann Arbor Science: Ann Arbor, MI, 1979.

- (5) National Research Council "Drinking Water and Health"; National Academy Press: Washington, DC, 1980; Vol. 2.
- (6) Symons, J. M.; et al. U.S. EPA, Cincinnati, OH, 1981, EPA-600/2-81-156.
- (7) Aieta, E. M.; Roberts, P. V.; Hernandez, M. J.—*Am. Water Works Assoc.* 1984, 76 (1), 64-70.
- (8) Taube, H.; Dodgen, H. J. *Am. Chem. Soc.* 1949, 71, 3330-3336.
- (9) Emmenegger, F.; Gordon, G. *Inorg. Chem.* 1967, 6, 633-635.
- (10) Aieta, E. M.; Roberts, P. V. *Environ. Sci. Technol.*, preceding paper in this issue.
- (11) Gordon, G.; Kieffer, R. G.; Rosenblatt, D. H. In "Progress in Inorganic Chemistry; Lippard, S. J., Ed.; Wiley-Interscience: New York, 1972; Vol. 15, pp 201-286.
- (12) Hong, C. C.; Rapson, W. H. *Can. J. Chem.* 1968, 46, 2053-2060.
- (13) Kieffer, R. G.; Gordon, G. *Inorg. Chem.* 1968, 7, 235-244.
- (14) Aieta, E. M. Ph.D. Dissertation, Stanford University, Stanford, CA, 1984.
- (15) Aieta, E. M.; Roberts, P. V. *J. Chem. Eng. Data*, in press.
- (16) Spalding, C. W. *AIChE J.* 1962, 8 (5), 685-689.
- (17) Moore, J. W.; Pearson, R. G. "Kinetics and Mechanism", 3rd ed.; Wiley: New York, 1981.
- (18) Aieta, E. M.; Roberts, P. V. In "Chemistry in Water Reuse"; Cooper, W. J., Ed.; Ann Arbor Science Publishers: 1981; Vol. 1, pp 429-452.

Received for review June 11, 1984. Revised manuscript received April 26, 1985. Accepted August 13, 1985. This work was funded by the U.S. Environmental Protection Agency under Research Grant R-808686. It has not been subjected to the Agency's required peer and administrative review and therefore does not necessarily reflect the views of the Agency; no official endorsement should be inferred.

Effects of Nonreversibility, Particle Concentration, and Ionic Strength on Heavy Metal Sorption

Dominic M. Di Toro,* John D. Mahony, Paul R. Kirchgraber, Ann L. O'Byrne, Louis R. Pasquale, and Dora C. Piccirilli

Environmental Engineering and Science Program and Chemistry Department, Manhattan College, Bronx, New York 10471

■ The reversible component partition coefficient for nickel and cobalt sorbed to montmorillonite and quartz is shown to be a function of particle concentration. Resuspension and dilution experiments appear to exclude explanations that rely on nonseparated particles and/or complexing ligands associated with the particles. A particle interaction model is presented that assumes the existence of an additional desorption reaction that results from particle-particle interactions. The model is in conformity with the experimental results. The observed partition coefficient decrease with increasing ionic strength is a result of the decrease in the classical, low particle concentration limit, partition coefficient. The particle-particle interaction is independent of ionic strength.

Introduction

The extent of heavy metal sorption is a critical component in the evaluation of fate in natural water systems. Adsorption at trace concentrations is usually quantified by the slope of the (linear) isotherm, i.e., the distribution or partition coefficient, π . It is well established that the magnitude of the partition coefficient is a function of particle properties such as particle size (1), the nature of the oxide coating (2), organic carbon content (3), and zero point of charge (4) and of chemical variables such as pH (5), ionic strength (6), and the concentration of complexing ligands (7, 8). Such effects can usually be rationalized within the frameworks of solution and surface chemistry.

Less well understood is the desorption reaction. The conventional desorption tests for heavy metals are extractions using concentrated solutions (9-11). This is in contrast to the usual desorption tests for organic chemicals in which the same aqueous phase is used for both adsorption and desorption to directly test reversibility. Heavy metal desorption into various extraction solutions has been found to be incomplete, suggesting that the reaction is not completely reversible (e.g., see ref 12). The

usual finding is that substantial quantities of the heavy metals remain associated with the particle even at extractant concentrations (~0.1 M) that should displace all the physically adsorbed metal (see ref 13 for a review and other references). The desorption literature (11-22) contains almost no data that include adsorption and desorption isotherms using the same aqueous phase. The purpose of this paper is to analyze adsorption-desorption isotherm data and examine reversible component sorption as a function of pH, ionic strength, and particle concentration.

Nickel and cobalt montmorillonite sorption data are presented below which demonstrate that reversibility is not complete and varies as a function of chemical (pH and ionic strength) and physical (particle concentration) variables. A method for analyzing adsorption-single desorption isotherms which yields the partition coefficients of the reversible and resistant components (23) is applied in order to isolate the behavior of reversibly sorbed heavy metal.

Perhaps the most puzzling phenomenon exhibited by heavy-metal and organic chemical partitioning is the effect of the particle concentration itself. It has been noted that the partition coefficient tends to decrease with increasing particle concentration (24), in some cases quite dramatically. It is as if, for the analogous partitioning in gas-water systems, Henry's constant is dependent upon the volume of the gas phase. Since such behavior has not been noted for other phase distribution coefficients, a certain amount of skepticism attends these observations in particle-water systems. Although the effects of particle concentration on the partition coefficient are not infrequently noted (25-27), they are usually explained as either experimental artifacts or as the result of an improper chemical system description which ignores, for example, the presence of other important but unobserved phases such as colloidal particles or dissolved organic carbon (28).

This paper presents the results of simple resuspension and dilution experiments that strongly suggest the effect is not due to experimental artifacts or hidden variable fluctuations. A model is proposed that suggests that the classically conceived partition coefficient is indeed descriptive of reversible sorption at low particle concentra-

* Address correspondence to this author at the Environmental Engineering and Science Program.

tions but that as particle concentration is increased above a certain concentration, which is chemical and sorbent specific, the reversible partition coefficient starts to decrease and eventually its magnitude is dependent only on particle concentration and independent of the specific sorbate-sorbent or auxiliary aqueous-phase parameters such as ionic strength. It is suggested that physical rather than chemical factors are controlling in this regime.

Materials and Methods

Initial experiments indicated that buffered aqueous phases are necessary since pH cannot be controlled in the usual fashion by addition of acid or base to the reactors during equilibration. The reasons are (1) that a desorption step must follow the adsorption equilibration which requires that the vessel be a centrifuge tube, making pH adjustments difficult, and (2) that multiple vessels are required for an isotherm. Both inorganic (borate and carbonate) and organic (sulfonic acid) buffers that were found to be noncomplexing with respect to nickel were used for the experiments. Differential pulse polarographic analysis was employed to measure the presence of any complexation between the metal and these buffers. No change in the half-wave potential for the metal ion alone compared with that for the metal ion in the presence of the buffer was observed. This method is somewhat more sensitive than those previously used for this purpose (29). Finally, the similar adsorption-desorption results obtained by using quite different buffers suggest that complexing is not occurring to a significant extent. This is discussed in detail below.

Adsorption-desorption isotherms were obtained by the following procedure. The aqueous phase, containing buffered distilled water and metal of known concentration tagged with ^{63}Ni or ^{60}Co , was combined with montmorillonite or quartz particles to a volume of 9 mL in a 20-mL centrifuge tube. The sorbents employed were montmorillonite (Wards Scientific) and α -quartz particles (Min-U-Sil 5, Penn. Glass Sand Corp.) and were used as received. The initial metal concentration in the systems ranged from 3.3 to 200 $\mu\text{g/L}$; the sediment concentrations studied were 5, 10, 30, 100, 300, and 1000 mg/L for montmorillonite and 200–10000 mg/L for quartz. The buffers were kept at the minimum effective level to maintain pH during the course of the experiment (10^{-3} M). The following buffers were employed: sodium bicarbonate (pH 7); TAPS ([2-hydroxy-1,1-bis(hydroxymethyl)ethyl]amino]-1-propanesulfonic acid) (29) (pH 8); sodium tetraborate (pH 8–10); sodium carbonate (pH 10–11). The capped tubes were agitated until adsorption equilibrium was reached. A sample of the sediment-aqueous phase mixture was removed, and the total metal concentration, c_{Ta} , was determined by liquid scintillation counting. The system was then centrifuged (6000–12000g for 15–20 min), and the metal concentration of the aqueous phase, c_a , was similarly determined. The sorbed concentration at adsorption equilibrium is calculated by difference: $r_a = (c_{\text{Ta}} - c_a)/m$, where m is the adsorbent concentration.

For desorption steps, the contaminated aqueous phase is carefully removed, leaving the sedimented solids in the tube, and uncontaminated aqueous phase is added to achieve a total volume that produces the same particle concentration as initially present at adsorption. The capped tube is agitated until desorption equilibrium is achieved. A sample of sediment-aqueous phase mixture is removed and analyzed yielding c_{Td} . After centrifugation an aqueous phase sample is removed and analyzed for c_d . The sorbed concentration is obtained by difference, $r_d = (c_{\text{Td}} - c_d)/m$.

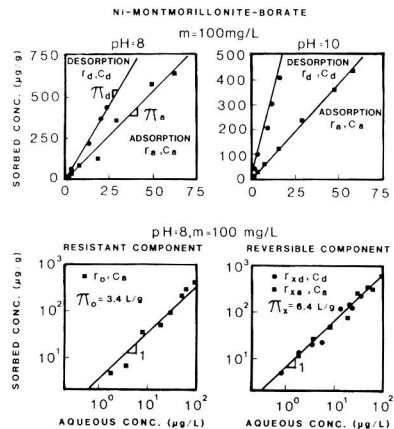


Figure 1. Adsorption-desorption isotherm examples (top). Conformity to component model assumptions (bottom).

In order to check our experimental procedures, we have examined the behavior of particle-free but otherwise identically configured experiments and found no evidence of precipitation. No adsorption-desorption differences were found if, preceding the adsorption step, a particle agitation, centrifugation, replacement of supernant, and resuspension are performed. Thus, the particle separation is efficient in the sense that only an insignificant fraction of sorbing particles is not removed by the centrifugation.

Analysis Framework

The two-component model of adsorption-desorption (23) is designed to interpret incompletely reversible behavior. Sorbed chemical, r_a , is assumed to be the sum of a reversibly sorbed component described by a linear isotherm; $r_x = \pi_x c_a$, and a resistant component that adsorbs following a linear adsorption isotherm; $r_0 = \pi_0 c_a$, but resists desorption over the time periods characteristic of experimental desorption equilibration (hours to days). The component partition coefficients π_x and π_0 can be calculated from the adsorption, π_a , and single desorption "partition coefficient", π_d , by using the relationships given in ref 23.

For each experimental condition a complete adsorption and desorption isotherm is generated by using four to eight duplicated concentrations over the range 3.5–200 $\mu\text{g/L}$. The partition coefficients are determined as the log average of the ratios: $\pi_a = r_a/c_a$ and $\pi_d = r_d/c_d$. These are used to compute π_x and π_0 . The experimental log standard deviations are used to compute the log standard errors of π_x and π_0 which are presented in the subsequent figures as error bars if they exceed the symbol size. Figure 1 illustrates the isotherm data and the conformity to the component model assumptions.

Kinetics

The kinetics of metal sorption are usually found to be rapid (30). For the nickel-montmorillonite-borate system both adsorption and desorption kinetics were examined by generating isotherms at varying adsorption and desorption times. No significant change in π_a is observed for adsorption times of up to 5 days.

A more important question is the effect of increasing desorption time, since incomplete reversibility may be the result of insufficient desorption time. No significant change in π_x or π_0 occurs for desorption times of up to 5 days. Thus, the component concentrations seem to be in

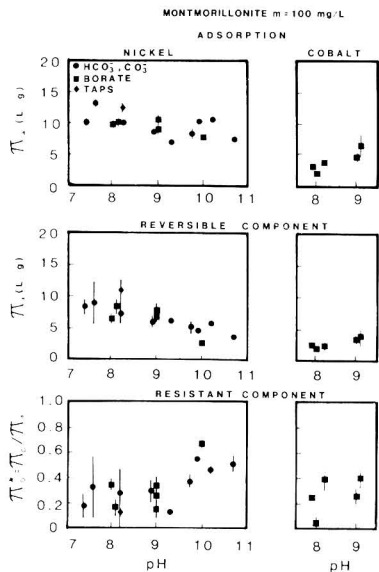


Figure 2. Effect of pH on adsorption (top), reversible (middle), and resistant (bottom) component partition coefficient.

metastable equilibrium for time scales of up to 5 days, and no substantial kinetic effects were observed. At long desorption times incomplete reversibility persisted.

Effect of pH and Buffering

The strong effect of pH on metal adsorption is well-known and the subject of numerous experiments and models (5, 6, 31, 32). The usual focus is the shape of the curve of percent metal sorbed vs. pH and, in particular, the pH at which adsorption begins. Since sorption is only important at a pH above this "pH edge", pH values above the edge and at low montmorillonite concentrations, $m = 100$ mg/L, were employed. Full adsorption-desorption isotherms were generated by using different buffers in order to detect possible complexing effects. The results, shown in Figure 2, suggest a slight decrease in π_a and π_x , together with an increase in resistant component fraction, π_o/π_a , at pH ~ 9.5 which corresponds to the pK of Ni-(OH)⁺ (33). Less extensive cobalt data exhibit the reverse trend with increasing π_a and π_x between pH 8 and pH 9 and no significant change in resistant fraction.

In summary, no major pH effects were noted for either nickel or cobalt. Significant (20–60%) nonreversibility persisted throughout the pH range investigated with no apparent complexing effects due to the buffers.

Particle Concentration Effects: Isotherms, Resuspension, and Dilution Experiments

In contrast to the effects of kinetics and pH, a significant relationship exists between partition coefficients and montmorillonite or quartz particle concentration. Adsorption isotherms at pH 9 (borate) for Ni-clay at $m = 30$ –1000 mg/L, cobalt-clay for $m = 100$ and 1000 mg/L, and Ni-quartz for $m = 600$ and 10,000 mg/L (Figure 3) clearly show the effect of varying particle concentration.

The inverse relationship found between particle concentration and partition coefficient is certainly a most unexpected result, and additional experiments were performed in order to rule out any artifacts. The most popular explanation of this phenomenon is to invoke an additional complexing or sorbing agent associated with the

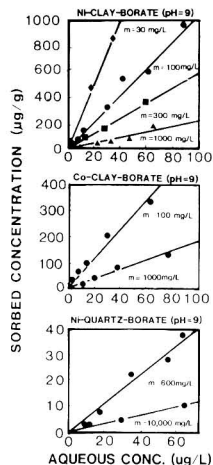


Figure 3. Adsorption isotherms at various particle concentrations.

particles which experimentally appears to be dissolved—it is not removed by the particle separation technique—but actually complexes (if it is a ligand such as dissolved organic carbon (28)) or sorbs (if it is colloidal particles (27, 41)) some dissolved chemical. If it is assumed that the concentration of the third phase increases with the concentration of added particles, then in fact an apparent reduction in partition coefficient is consistent with increasing particle concentration since the experimentally determined "dissolved" concentration is actually the sum of the truly dissolved and the additional sorbed or complexed chemical.

The experiments described below were designed to specifically exclude an additional complexing agent as an explanation. The design was based upon the desire to change only the particle concentration while all else was maintained constant. Two experimental designs were developed which are in a sense the inverse of each other: a resuspension procedure and a dilution procedure.

Resuspension Experiment. For the resuspension experiment, replicate controls and experimental vessels are prepared. After adsorption equilibrium is achieved, the particles and supernatant are separated by centrifugation, and only in the experimental vessels, a portion of the supernatant is removed. The volume of supernatant in the control vessels is not changed. Then the particles are resuspended into the supernatant and equilibrated, after which measurements of the total and dissolved nickel are made. In both the experimental and control vessels the particles are resuspended into the same supernatant with which they were in equilibrium. If a dissolved third phase is present which is not separated by centrifugation, then its concentration is not changed by the partial removal of supernatant in the experimental vessels. The only modification is that the particle concentration is increased in the experimental vessels since the supernatant volume is decreased.

The results for both the controls and the experimental vessels are shown in Table I for montmorillonite and quartz particles. The montmorillonite controls behaved as expected: the dissolved nickel concentration at both adsorption and resuspension equilibrium are essentially equal, and their ratio is unity. For the quartz experiments a slight decrease occurred in the controls presumably due to lack of complete equilibrium. The experimental vessels for all experiments clearly exhibit the particle concentra-

Table I. Resuspension Experiment, with Borate Buffer, pH 9. Aqueous Ni Concentrations ($\mu\text{g/L}$)

Montmorillonite					
control vessels			experimental vessels		
adsorption, $m = 100 \text{ mg/L}, c_a$	resuspension, $m = 100 \text{ mg/L}, c_{rs}$	ratio, c_{rs}/c_a	adsorption, $m = 100 \text{ mg/L}, c_a$	resuspension, $m = 243 \text{ mg/L}, c_{rs}$	ratio, c_{rs}/c_a
72.6	72.2	1.00	74.7	97.3	1.30
38.9	37.8	0.97	36.8	40.4	1.10
15.9	17.0	1.07	19.1	23.4	1.23
6.18	6.33	1.02	5.32	5.87	1.10
av 1.017			av 1.182		
Quartz					
control vessels			experimental vessels		
adsorption, $m = 1000 \text{ mg/L}, c_a$	resuspension, $m = 1000 \text{ mg/L}, c_{rs}$	ratio, c_{rs}/c_a	adsorption, $m = 1000 \text{ mg/L}, c_a$	resuspension, $m = 2430 \text{ mg/L}, c_{rs}$	ratio, c_{rs}/c_a
102.	91.9	0.901	87.3	96.0	1.10
46.8	41.6	0.889	38.3	43.7	1.41
20.1	19.0	0.945	19.7	20.4	1.04
10.1	9.32	0.923	9.80	11.9	1.21
av 0.914			av 1.123		
Quartz					
control vessels			experimental vessels		
adsorption, $m = 1000 \text{ mg/L}, c_a$	resuspension, $m = 1000 \text{ mg/L}, c_{rs}$	ratio, c_{rs}/c_a	adsorption, $m = 1000 \text{ mg/L}, c_a$	resuspension, $m = 3750 \text{ mg/L}, c_{rs}$	ratio, c_{rs}/c_a
72.3	61.2	0.846	74.9	87.5	1.17
36.0	32.6	0.906	30.3	36.2	1.195
16.1	13.9	0.863	17.5	24.5	1.40
9.10	8.16	0.897	8.29	12.0	1.45
av 0.878			av 1.303		

tion effect. Similar results were obtained for PCB (35). The result of increasing particle concentration is apparently to decrease the partition coefficient. This causes nickel to desorb from the particles, thereby increasing the dissolved nickel concentration. The average ratio of resuspension to adsorption dissolved concentrations increases in all cases whereas the average ratio for the controls is either equal to or less than one.

Dilution Experiment. The dilution experiment is designed to decrease the particle concentration without any other alteration. Three parallel sets of vessels are employed: a control, an experimental vessel, and a vessel to supply additional supernatant with which to dilute the experimental vessel. After adsorption equilibrium, the supernatant from the third vessel is obtained by centrifugation, and this particle-free supernatant is added to the experimental vessel. If no experimental fluctuations were present, this supernatant should have the same dissolved nickel concentration as the experimental and control vessels since they are identically configured. Note that the experimental vessel is not centrifuged. The particle dilution is achieved by adding additional (identical) supernatant. The vessels are then equilibrated, the total and aqueous concentrations are measured, and a comparison is made between the controls and experimental aqueous concentrations. Again if a dissolved third phase existed, it would have the same concentration in both the experimental and control vessels. As shown in Table II the aqueous concentrations in the experimental vessels decrease as predicted. The particle concentration is decreased by dilution, so that the partition coefficient increases, and more nickel is removed from solution. In all the resuspension and dilution experiments, pH fluctuations were not significant ($\Delta\text{pH} < 0.3$).

Both these experimental designs specifically exclude the possibility of a dissolved third phase since if it were present

Table II. Dilution Experiment with Ni-Montmorillonite (pH 9, Borate Buffer)

Total Ni Concentrations, $c_T, \mu\text{g/L}$			
control/supernatant vessels, $m = 500 \text{ mg/L}$	exptl vessels, $m = 500/188 \text{ mg/L}$		
249/263	261/166		
266/264	270/161		
269/266	275/163		
Dissolved Ni Concentrations, $c_d, \mu\text{g/L}$			
control/supernatant vessels, $m = 500 \text{ mg/L}$	exptl vessels, $m = 188 \text{ mg/L}$	exptl to control vessel ratio	
115/105	103	0.898	
118/98.0	89.3	0.756	
98.1/98.7	83.4	0.850	
		av 0.835	
Partition Coefficients, L/kg^a			
control/supernatant vessels, $m = 500 \text{ mg/L}$	exptl vessels, $m = 188 \text{ mg/L}$		
2330/3009	3191		
2510/3387	4259		
3480/3390	5083		
av 3017 \pm 494	av	4178 \pm 949	
$^a \pi = (c_T - c_d)/(mc_d)$.			

its concentration would be the same in both the experimental and control vessels so that its presence could not affect the difference in partitioning observed at differing particle concentrations. In fact, any hypothesis that attempts to explain the results via an increased desorption of complexing ligands (34) or an increased adsorption of competing cations just transfers the problem to explaining

why the changes in ligand or cation concentrations occur with increasing particle concentration for an aqueous phase that is initially in equilibrium with the particles.

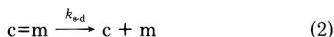
Another explanation for the particle concentration effect is flocculation or at least some agglomeration of the sediment particles. The result would be to decrease the overall surface area of the adsorbent, leading to a reduction in the partition coefficient in higher sediment concentration systems. Extensive microscopy of representative clay and quartz suspensions including the resuspension experiments was carried out. In all cases, both the size and distribution of particles was essentially constant. These results appear to rule out particle size alteration as a means of accounting for the particle concentration effect in our experiments.

A Particle Interaction Model. The resuspension and dilution experiments strongly suggest that it is the presence of particles themselves, and not a surrogate variable, that is influencing the extent of reversible partitioning. Thus, it appears reasonable to expect that particle interactions somehow affect sorption. We suggest the following model for the sorption of the reversible component:

adsorption

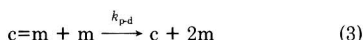


spontaneous desorption



which are the conventional adsorption-desorption reactions, and we hypothesize that an additional desorption reaction exists:

particle interaction induced desorption



where c is the dissolved chemical concentration, $c+m$ is the reversibly sorbed chemical concentration, and m is the particle concentration. The reaction rate constants for these reactions, k_{ads} , k_{sd} , and k_{pd} , are indicated. Particle interaction induced desorption (eq 3) assumes that a binary interaction between particles causes desorption to occur. The mechanism that prompts this desorption is uncertain at present.

For these three reactions at equilibrium, the reversible partition coefficient is

$$\pi_x = \frac{[c+m]}{[c][m]} = \frac{k_{ads}}{k_{sd} + mk_{pd}} \quad (4)$$

A useful normalization of this expression is

$$\pi_x = \frac{\pi_{xc}}{1 + m\pi_{xc}/\nu_x} \quad (5)$$

where $\pi_{xc} = k_{ads}/k_{sd}$, the classical partition coefficient, and $\nu_x = k_{ads}/k_{pd}$, which is the slope of the π_x vs. m relationship at large particle concentration:

$$\pi_x \cong \nu_x/m \quad m \gg \nu_x/\pi_{xc} \quad (6)$$

Figure 4 presents Ni-montmorillonite data and the π_x relationship, eq 5. For a tentative assignment of $\pi_o^* = 0.4$, which assumes that the resistant fraction is independent of m —the data are too scattered for a more refined hypothesis—the resulting $\pi_a = \pi_x + \pi_o^*$ relationship is compared to the observations in Figure 4 as well.

These π_x data and those for the Co-montmorillonite and Ni-quartz are fit to eq 5 by using a nonlinear least-squares fit of $\log \pi_x$ vs. $\log m$ to estimate π_{xc} and ν_x . The results are given in Table III (individual data sets). The resulting ν_x values are essentially equal for the three systems. A

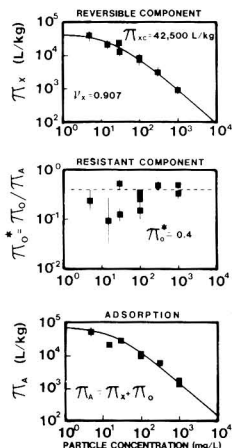


Figure 4. Partition coefficients vs. particle concentration (nickel, montmorillonite, borate buffer, pH 8). Reversible component (top): data (symbols) and eq 5 using parameters as indicated. Resistant component (middle) and adsorption partition coefficient (bottom).

Table III. Least-Squares Parameter Estimates^a of π_{xc} and ν_x (pH 9, Borate Buffer)

system	individual data sets			joint data set
	no. of points	π_{xc} , L/g	ν_x	π_{xc} , L/g
Ni-clay	10	42.5 (7.3)	0.907 (0.078)	45.5 (9.9)
Co-clay	2	6.44	0.773	5.83 (2.2)
Ni-quartz	5	1.22 (0.36)	0.677 (0.20)	1.08 (0.18)

^a Estimated value (standard error of estimate).

four-parameter least-squares fit, constant ν_x , and an individual π_{xc} for each system yield the same result within the standard error estimates (Table III, joint data set). The results are shown in Figure 5 for the three systems. A normalized plot of

$$\frac{\pi_x}{\pi_{xc}} = \frac{1}{1 + m\pi_{xc}/\nu_x} \quad (7)$$

vs. $m\pi_{xc}/\nu_x$ illustrates that these data are well represented by eq 7 and that each system has data in both the range of m for which π_x is essentially constant and for which π_x varies inversely with particle concentration.

Two observations are worthy of note. At low particle concentrations $m \ll \nu_x/\pi_{xc}$, so that $\pi_x \cong \pi_{xc} = k_{ads}/k_{sd}$, the classical reversible partition coefficient. It is a function of both the nature of the sorbate (Ni-clay, $\pi_{xc} = 45$ L/g; Co-clay; $\pi_{xc} = 5.8$ L/g) and the sorbent (compare Ni-clay to Ni-quartz; $\pi_{xc} = 1.1$ L/g) as would be expected. The surprising result is that ν_x is essentially independent of both sorbate type and sorbent properties (Table III, individual data sets). Since $\nu_x = k_{ads}/k_{pd}$ is the ratio of adsorption to particle-induced desorption rate, the fact that it is constant suggests that its magnitude is physically rather than chemically determined. This would be the case if, for example, both the adsorption rate and particle interaction induced desorption rate were functions of hydrodynamic factors.

Following this idea and assuming that k_{ads} is constant, the extent of reversible partitioning is determined by the magnitude of the two desorption mechanisms. The data in Figure 5 can be interpreted as follows. For small particle concentrations, the rate of spontaneous desorption exceeds

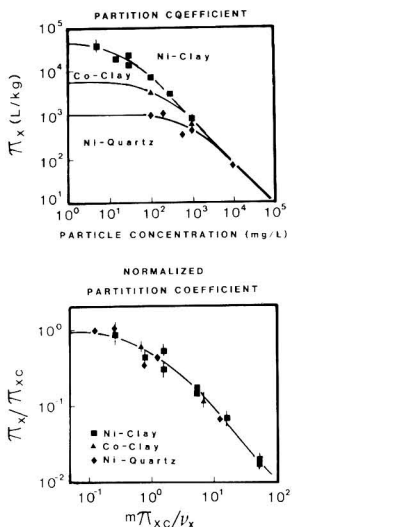


Figure 5. Reversible component partition coefficient vs. particle concentration (top) data (symbols) and eq 5 using parameters as indicated in Table III (joint data set). Normalized plot of all data (symbols) and eq 7.

the rate of particle interaction induced desorption (which is small due to the low particle concentrations), and spontaneous desorption dominates the total desorption rate. Spontaneous desorption is expected to be a function of the strength of the chemical and electrostatic bonding, and so it is chemical and surface specific. The spontaneous desorption rate is smallest for Ni-clay, yielding the highest reversible partition coefficient at small m , followed by Co-clay and Ni-quartz (left-hand side of Figure 5). However, as m increases, the rate of particle interaction induced desorption increases for all systems. Since the spontaneous desorption rate is smallest for Ni-clay, the particle interaction desorption rate, mk_{p-d} , becomes comparable to k_{s-d} for this system first, and the Ni-clay reversible partition coefficient starts to decrease at relatively small particle concentrations $m \sim 20$ mg/L. However, the partitioning of Co-clay and Ni-quartz systems, with their larger spontaneous desorption rates, are unaffected at these particle concentrations. As m increases further (~ 150 mg/L), however, mk_{p-d} approaches k_{s-d} for Co-clay, and π_x for this system starts to decrease. Not until $m \sim 800$ mg/L for the Ni-quartz system is mk_{p-d} comparable to k_{s-d} for this system.

Hence, π_x is a specific chemically determined constant, π_{xc} , for each system until m reaches ν_x/π_{xc} for that system at which point $mk_{p-d} = k_{s-d}$ and the additional particle interaction induced desorption causes π_x to start decreasing. For large $m \gg \nu_x/\pi_{xc}$, the spontaneous desorption rate is overwhelmed by the particle interaction induced desorption, and $\pi_x \approx \nu_x/m$ which is constant for the all sorbate-sorbent pairs. Hence, all π_x curves eventually meet at high particle concentrations as shown in Figure 5. Note that at $m = 1000$ mg/L the three systems have virtually the same π_x and the pattern continues for Ni-quartz at $m = 10000$ mg/L. This is a consequence of the virtually constant $\nu_x = 0.68-0.91$ found experimentally.

Ionic Strength Effects

Metal-clay sorption is known to decrease significantly as ionic strength increases (36, 37). This effect is examined at two particle concentrations ($m = 100$ and 1000 mg/L)

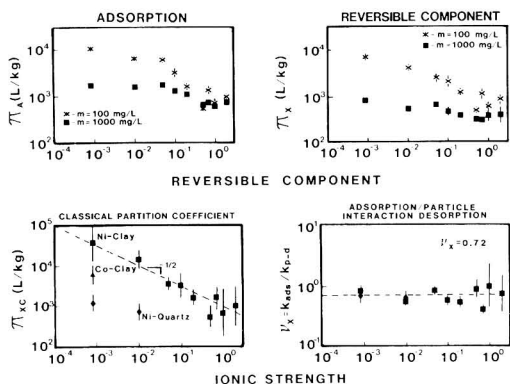


Figure 6. Partition coefficients vs. ionic strength, pH 9. (Top) Adsorption (left) and reversible component (right) at two particle concentrations for Ni-montmorillonite-borate buffer. (Bottom) Particle interaction model parameters vs. ionic strength. Classical partition coefficient (left) and ν_x (right) for systems as indicated.

using adsorption and desorption isotherms as before (pH 9, borate buffer). The component partition coefficients are shown in Figure 6. At the low ionic strength of the buffer, the effect of particle concentration is clearly in evidence. However, as ionic strength is increased by adding NaNO_3 , π_a and π_x at both particle concentrations tend to become equal.

The reversible component partitioning can be analyzed by using the particle interaction desorption model. By use of the observed π_x at $m = 100$ and 1000 mg/L and eq 5 in the form

$$\frac{1}{\pi_x} = \frac{1}{\pi_{xc}} + \frac{m}{\nu_x} \quad (8)$$

π_{xc} and ν_x can be computed at each ionic strength. They are shown in Figure 6 together with the Co-clay data and Ni-quartz data. Once again the influence of the chemical factors, ionic strength and the specific sorbate-sorbent pair, is clearly seen for the estimated classical partition coefficient, π_{xc} .

On the other hand, the estimates of ν_x are essentially constant and independent of ionic strength and the identity of the sorbate-sorbent pair. This is further support for the idea that $\nu_x = k_{ads}/k_{p-d}$ and, therefore, reversible partitioning at large particle concentrations, is physically controlled.

Discussion and Conclusions

The data and analysis presented above suggest that the adsorption partition coefficient is not the proper quantification of the classical reversible model on the basis of adsorption and spontaneous desorption reactions. Rather it is confounded by incomplete reversibility and particle concentration effects. Only by properly accounting for these additional mechanisms can observed adsorption partition coefficients be understood. We offer no framework for the interpretation of incomplete reversibility other than to suggest that the component model allows a separation to be made that isolates both the resistant, π_r , and reversible, π_x , partition coefficients.

Reversible partitioning appears to be strongly affected by particle concentration. The resuspension and dilution experiments are difficult to explain in any other way. The hypothesis that two desorption mechanisms are involved leads to an expression, eq 5, which conforms to observations (Figure 5) and involves two parameters: π_{xc} , the

classical reversible partition coefficient, and ν_x , which we suggest is physically controlled. The finding that ν_x is essentially constant for the experiments presented above (Table III and Figure 6) and that its magnitude for heavy-metal sorption ($\nu_x \sim 0.5-1.0$) is essentially the same as that found for the reversible component sorption of a hexachloro-PCB isomer to various natural lake sediments and clays $\nu_x = 0.68 \pm 0.26$ (39) and for a large collection of neutral hydrophobic organic chemical data (40) is both remarkable and mystifying. The particle concentration-adsorption partition coefficient relationship found for PCBs from field observations in Saginaw Bay, $\nu_x = 0.3$ (39), suggests that this finding is not just a laboratory curiosity but has wider applicability.

Acknowledgments

We are pleased to acknowledge the support of Thomas P. O'Connor of the Office of Marine Pollution Assessment, NOAA, and Victor J. Bierman and John F. Paul of the EPA Research Laboratory, Narragansett, RI. This investigation is the theoretical portion of more practically directed projects currently under way. The support of our group at Manhattan College, Sue Blakeney, Elizabeth Comerford, Elaine Dwyer, John Sowa, and Mark Tallman, and our colleagues John Connolly, James Mueller, Donald O'Connor, John Jeris, Robert Thomann, and Richard Winfield is also appreciated, as is Herbert Allen's (Drexel University) suggestion that we use "good" buffers.

Registry No. Ni, 7440-02-0; Co, 7440-48-4; montmorillonite, 1318-93-0; quartz, 14808-60-7.

Literature Cited

- (1) Duursma, E. K.; Gross, M. G. In "Radioactivity in the Marine Environment"; National Academy of Science: Washington, DC, 1971; p 147.
- (2) Oakley, S. M.; Nelson, P. O.; Williamson, K. J. *Environ. Sci. Technol.* **1982**, *15*, 474.
- (3) Salim, R. *Water Res.* **1983**, *17*, 423.
- (4) James, R. O.; Healy, T. W. *J. Colloid Interface Sci.* **1972**, *40*, 65.
- (5) Hohl, H.; Stumm, W. *J. Colloid Interface Sci.* **1976**, *55*, 281.
- (6) Mattigod, S. V.; Gibali, A. S.; Page, A. L. *Clay Clay Miner.* **1979**, *27*, 411.
- (7) Benjamin, M. M.; Leckie, J. O. *Environ. Sci. Technol.* **1982**, *16*, 162.
- (8) Garcia-Miragaya, J.; Page, A. L. *Soil Sci. Soc. Am. J.* **1976**, *40*, 658.
- (9) Farrah, H.; Pickering, W. F. *Water Air Soil Pollut.* **1978**, *9*, 491.
- (10) Engler, R. M.; Brannon, J. M.; Rose, J.; Bigham, G. In "Chemistry of Marine Sediments"; Yen, T. F., Ed.; Ann Arbor Science: Ann Arbor, MI, 1977; p 163.
- (11) van der Weijden, C. H.; Arnoldus, M. J. H. L.; Meurs, C. J. *Neth. J. Sea Res.* **1977**, *11* (2), 130.
- (12) Pickering, W. F. In "Zinc in the Environment"; Nriagu, J. O., Ed.; Wiley-Interscience: New York, 1980; Part I, p 72.
- (13) Forstner, U.; Wittmann, G. T. W. "Metal Pollution in the Aquatic Environment"; Springer-Verlag: Berlin, New York, 1979.
- (14) Murray, C. N.; Murray, L. In "Radioactive Contamination of the Marine Environment"; International Atomic Energy Agency: Vienna, 1973; p 105.
- (15) Kharkar, D. P.; Turekian, K. K.; Bertine, K. K. *Geochim. Cosmochim. Acta* **1968**, *32*, 285.
- (16) Evans, D. W.; Cutshall, N. H. In "Radioactive Contamination of the Marine Environment"; International Atomic Energy Agency: Vienna, 1973; p 125.
- (17) Rozell, T. C.; Andelman, J. B. *ACS Symp. Ser.* **1971**, No. 106, 280.
- (18) Bothner, M. H.; Carpenter, R. In "Radioactive Contamination of the Marine Environment"; International Atomic Energy Agency: Vienna, 1973; p 73.
- (19) Duursma, E. K. In "Estuarine Chemistry"; Burton, J. D.; Liss, P. S., Ed.; Academic Press: New York, 1976; p 159.
- (20) Karimian, N.; Cox, F. R. *Soil Sci. Soc. Am. J.* **1978**, *42*, 757.
- (21) Patel, B.; Patel, S.; Pawar, S. *Estuarine Coastal Mar. Sci.* **1978**, *7*, 49.
- (22) Singh, S. S. *Can. J. Soil. Sci.* **1979**, *59*, 119.
- (23) Di Toro, D. M.; Horzempa, L. *Environ. Sci. Technol.* **1982**, *16*, 594.
- (24) O'Connor, D. J.; Connolly, J. P. *Water Res.* **1980**, *14*, 1517.
- (25) Aston, S. R.; Duursma, E. K. *Neth. J. Sea Res.* **1973**, *6*, 225.
- (26) Schell, W. R.; Sibley, T. H.; Sanchez, A. L.; Clayton, J. R. NTIS, Springfield, VA, 1980, NUREG/CR-0803.
- (27) Benes, P.; Majer, V. "Trace Chemistry of Aqueous Solutions"; Elsevier, New York, 1980.
- (28) Voice, T. C.; Rice, C. P.; Weber, W. J., Jr. *Environ. Sci. Technol.* **1983**, *17*, 513.
- (29) Good, N. E.; Winget, G. D.; Winter, W.; Connolly, T. N.; Izawa, S.; Singh, R. M. M. *Biochemistry* **1966**, *5*, 467.
- (30) Zasoski, R. J.; Burau, R. G. *Soil Sci. Soc. Am. J.* **1978**, *42*, 372.
- (31) Davis, J. A.; Leckie, J. O. *J. Colloid. Interface Sci.* **1978**, *67*, 90.
- (32) Bowden, J. W.; Posner, A. M.; Quirk, J. P. *Aust. J. Soil Res.* **1977**, *15*, 121.
- (33) Baes, C. F., Jr.; Mesmer, R. E. "The Hydrolysis of Cations"; Wiley: New York, 1976.
- (34) Griffin, R. A.; Au, A. K. *Soil Sci. Soc. Am. J.* **1977**, *41*, 880.
- (35) Di Toro, D. M.; Horzempa, L. In "Physical Behavior of PCB's in the Great Lakes"; Mackay, D.; Paterson, S.; Eisenreich, S. J.; Simmons, M. S., Eds.; Ann Arbor Science: Ann Arbor, MI, 1982; p 89.
- (36) McBride, M. B. *Clay Clay Miner.* **1978**, *26*, 101.
- (37) Egozy, Y. *Clay Clay Miner.* **1980**, *28*, 311.
- (38) Stumm, W.; Morgan, J. J. "Aquatic Chemistry", 2nd ed.; Wiley-Interscience: New York, 1981; p 681.
- (39) Di Toro, D. M.; Horzempa, L. M.; Casey, M. M.; Richardson, W. L. *J. Great Lakes Res.* **1982**, *8*, 336.
- (40) Di Toro, D. M. *Chemosphere*, in press.
- (41) Schwend, P. M.; Wu, S. *Environ. Sci. Technol.* **1985**, *19*, 90.

Received for review June 22, 1984. Revised manuscript received May 21, 1985. Accepted July 26, 1985.

Vertical Transport Processes of an Acid-Iron Waste in a MERL Stratified Mesocosm

Mary Frances Fox,* Dana R. Kester, and Carlton D. Hunt

Graduate School of Oceanography, University of Rhode Island, Kingston, Rhode Island 02881

■ The vertical transport of the Fe particles formed after an acid-Fe waste mixes with seawater and the impact of the waste on the trace metal composition of seawater were examined in a stratified tank (2 m diameter and 5 m deep) at the MERL facility of the University of Rhode Island. Two acid-Fe waste additions were made to one of the stratified tanks at concentrations comparable to those observed after the initial dispersion of the waste in the ocean (10^5 dilution); a second stratified tank was maintained as a control. The removal of the Fe waste from the water column was due to settling of the Fe particles through the pycnocline; biological transport of the Fe particles was not an important removal mechanism. The kinetic behavior of the Fe particles was different after the two waste additions; gravitational settling was the rate-limiting step after the first addition, whereas flocculation was the rate-limiting step after the second waste addition. The first acid-Fe waste addition apparently altered the properties of the seawater, possibly stripping organic substances from the water column. This alteration in the characteristics of seawater changed the distribution of Pb and V between the "dissolved" and particulate forms. Both Pb and V showed a strong correlation with Fe, suggesting scavenging of these metals by the Fe particles. Cu and Cd show remarkable independence from the behavior of Fe.

Introduction

The impact of chemicals disposed in the marine environment is an important issue for waste management practices. Field studies were conducted at a deep water dumpsite off the coast of New Jersey (DWD-106) to determine the fate of an acid-Fe industrial waste, a byproduct in the production of titanium dioxide (Table I). When this waste mixes with seawater, the acid is rapidly neutralized by the carbonate and borate buffers in seawater, and hydrous Fe oxide precipitates. The water column at DWD-106 is 2000 m deep; thus, the primary fate of the waste is dispersion and vertical transport through the water column rather than incorporation into the sediments.

In initial field work at DWD-106 discrete samples were analyzed to determine the concentration of Fe, Pb, Cu, and Cd in the water column at several time intervals after the dump (1). These studies showed elevated Fe levels in the surface water above the seasonal thermocline for ~30 h after the dump. Pb, which was present primarily in the particulate phase, showed strong correlation with Fe, whereas the distribution of Cd present primarily in the dissolved phase was not correlated with Fe. The results for Cu were intermediate between those of Pb and Cd, showing a weak correlation with Fe. Analysis of these data was complicated by the limited number of samples obtained in the acid-Fe waste plume.

To better understand the dispersion of the acid-Fe waste plume, the concentration of Fe in the plume was measured in real time by using a continuous pumping system and an automated system for the analysis of Fe (2). This system provided information on the horizontal and vertical gradients of Fe in the waste plume. A vertically uniform concentration of Fe was found in the surface

Table I. Chemical Properties of E.I. du Pont de Nemours Acid-Fe Waste

property	value
density, g/mL ^b	1.20
total dissolved solute, g/L ^a	240
total suspended solids, g/L ^a	1.5
total organic carbon, mg/L ^a	960
pH ^a	0.01
alkalinity, equiv/L ^a	-4.50
chloride, M ^a	5.36
sulfate, M ^a	0.0083
hydrogen ion, M ^a	0.98
iron, M ^b	0.80
titanium, M ^a	0.063
aluminum, M ^a	0.063
manganese, M ^a	0.031
vanadium, M ^b	0.0074
chromium, M ^a	0.004
lead, M ^b	0.00044
copper, M ^b	0.00013
cadmium, M ^b	0.0000013

^a Based on Sept 10, 1970, EPA Region III discharge permit and application. These data are not internally consistent. The pH and [H⁺] could be in error if the measurement were made on an instrument not suitable for pH < 0. If the alkalinity is correct, the [H⁺] is 1.6 equiv/L, pH -0.2. ^b Based on analyses in our laboratory.

waters above the seasonal thermocline within 3 h of the dump; Fe was not detected below the seasonal thermocline at any time after the dump. Continuous horizontal profiles showed dispersion of the waste plume in the first 48 h after the dump; after this time the surface signature of the plume was "lost". The lateral distribution of waste observed at several time intervals after the dump fit a constant diffusion velocity model (3). This model predicted that if horizontal dispersion was the only removal mechanism, the Fe concentration in the surface water should persist above detectable limits (~0.1 μmol/kg) for several weeks after the dump. In all our field studies the waste plume was not detected after 55 h.

To resolve the questions that remained after the field studies and to assess the long-term impact of the waste plume on the marine environment, a new approach was taken. An experiment was performed at MERL (Marine Ecosystems Research Laboratory) at the University of Rhode Island. MERL is a special facility that provides small-scale controlled ecosystems for experimental manipulation. To simulate the water column at the deep water dumpsite, two of the MERL tanks that are normally operated as a well-mixed homogeneous planktonic ecosystem were stratified with a pycnocline (4). Acid-Fe was added to one of the stratified tanks; the second was maintained as a control.

The MERL mesocosm allowed us to address questions that could not be resolved from field studies:

(1) What is the removal mechanism of the Fe particles from the surface water? Our field studies suggest that horizontal dispersion is not the only removal mechanism. Is biological transport an important removal process? Is the seasonal thermocline a significant barrier to the settling of the Fe particles through the water column?

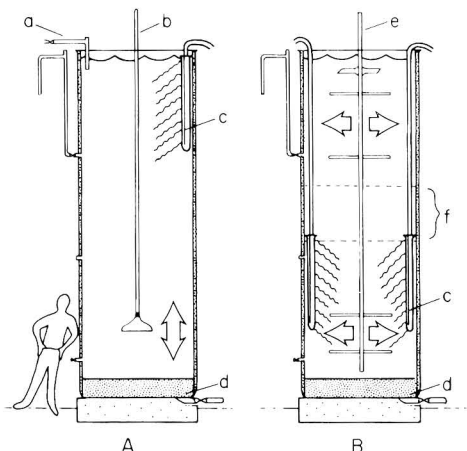


Figure 1. Physical configuration of conventional well-mixed MERL mesocosm (A) and stratified MERL mesocosm (B). (a) Seawater feed, (b) plunger mixer, (c) heat exchanger, (d) benthos, (e) rotary mixer, (f) pycnocline, $\Delta T = 10^\circ\text{C}$, $\Delta S = 3\text{‰}$. Redrawn from Donaghay and Klos (8).

(2) To what extent are metals other than Fe removed from seawater and the waste plume by the hydrous Fe oxide?

Experimental Design

The MERL tanks (4, 5) used in this experiment were 2 m in diameter and 5 m deep containing a 50 cm layer of sediment and associated benthic organisms which were collected from lower Narragansett Bay (Figure 1). The sediments were important to maintain the nutrient regeneration required to sustain the planktonic ecosystem in the stratified tank. The tanks were initially filled with seawater ($\sim 30\text{‰}$ salinity, $T \sim 18^\circ\text{C}$) from Narragansett Bay with the prevailing phytoplankton and zooplankton species present. The two stratified tanks were operated as a closed system and were not inoculated with additional plankton during the experiment. The upper 2 m of the water column was maintained at ambient temperature; the bottom 2 m was cooled with heat exchangers to produce a 10°C temperature differential between the surface and bottom layer (Figure 2a). NaCl (Baker reagent grade) was added to the bottom layer to increase the salt content by $\sim 3\text{ g/kg}$ (Figure 2b). In addition to enhancing the pycnocline, the salt difference was used as a conservative tracer to monitor mixing across the pycnocline. Cross pycnocline mixing accounted for a 1.5% exchange of water between the surface and bottom layer in the 7 weeks of the experiment (6). Daily temperature and salinity profiles were made in the control and experimental tanks by using a YSI Model 33 temperature-salinity probe (Yellow Springs Instrument Co., Yellow Springs, OH). Discrete salinity samples were drawn biweekly in the surface and bottom layer to calibrate the YSI probe. A detailed salinity profile using discrete samples was made through the pycnocline 280 h after the start of the experiment. All discrete salinity samples were analyzed with an inductive salinometer (Industrial Instruments, RS-7B).

Detailed fluorescence profiles in the region of the thermocline were obtained throughout the experiment to assess the importance of the pycnocline to the distribution of marine organisms (Figure 2c). All fluorescence measurements were made on a Turner Model 111 fluorometer using a modification of the technique of Lorenzen (7).

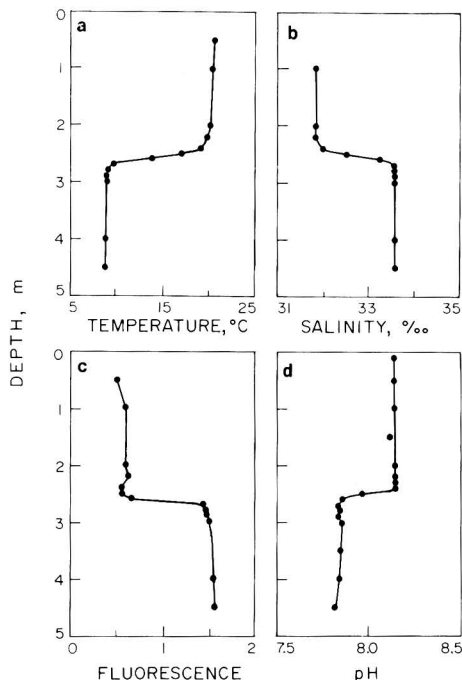


Figure 2. Vertical temperature, salinity, fluorescence, and pH profiles of stratified mesocosm at $t = 280\text{ h}$ (pH profile at $t = 1150\text{ h}$).

These profiles consistently showed a significant fluorescence gradient across the pycnocline. The magnitude and range of variation in fluorescence in the bottom layer was consistent with the values obtained in MERL tanks that were maintained as well-mixed systems. However, fluorescence values in the surface water of the stratified tank were significantly lower than those observed in the bottom layer or in well-mixed tanks and showed only minor variations during the entire experiment (8). Visually the surface water of the stratified tanks resembled clear, low particulate seawater, and this clarity was maintained in the control tank throughout the experiment.

The higher observed fluorescence in the bottom water relative to the surface water indicated increased productivity in the lower layer of the tank. Increased productivity and respiration in the bottom layer caused an increase in the partial pressure of CO_2 and a corresponding decrease in pH (9). The importance of pH measurements became apparent at the end of the experiment; thus, a detailed pH profile was obtained in the control and experimental tank 1150 h after the start of the experiment (Figure 2d). The pH measurements were made by using an Altex combination pH electrode and a Corning Model 111 digital pH meter. At this time the pH values in the surface layer of the control and experimental tanks were almost identical (pH control 8.15; pH experimental 8.13). In the bottom layer the pH values were lower with a greater range (pH control 7.85; pH experimental 7.97). The greater divergence of pH values in the bottom layer is probably due to the impact of the waste on benthic organisms in the experimental tank. The pH gradient across the pycnocline was maintained throughout the experiment; the magnitude of the gradient varied with time and experimental conditions.

To simulate the concentration of Fe observed in the waste plume after the initial rapid dilution in the wake of

Table II. Summary of Acid-Iron Waste Additions

date	time	designation	h	mL of waste added	T(Fe) added, mmol
July 2, 1981	1400	first addition	0	50	40
July 3, 1981	1630	first addition	25	20	16
July 13, 1981	1430	second addition	260	65	52

a barge, acid-Fe waste was added to the experimental tank to achieve a 100000 dilution. To avoid excessive localized concentrations the waste was diluted 100:1 with seawater prior to introduction into the tank. During the experiment there were two major additions of waste to the tanks (Table II). The first addition was made over a 2-day period since an initial objective was to study the effects of a steady-state concentration of the Fe floc on the marine environment. The rapid removal of the Fe particles from the water column led to a reassessment of the experimental design and the experiment was revised to study the removal of Fe with time. When Fe levels in the experimental tank returned to background levels, a second waste addition was made to the experimental tank (260 h after the initial addition).

Water samples for total and particulate trace metal analyses (Fe, Cu, Cd, Pb, and V) were siphoned directly into the sample bottles by using a Teflon sampling tube to avoid contamination. The partitioning of these trace metals between the particulate and dissolved phases and their removal from the water column were studied. The particulate fraction is defined as the fraction that is retained on a 0.4- μ m Nuclepore filter. The "dissolved" metal values were obtained by difference. Discrete filtered metal samples were analyzed for Cu and Cd at several time intervals to confirm the difference data. The average difference between the discrete filtered values and the values obtained by difference for 11 samples is 0.3 ± 1.5 nmol/kg for Cu and -0.06 ± 0.09 nmol/kg for Cd. Due to the fragile nature of the Fe colloidal particles, a portion of the Fe is not retained on the 0.4- μ m filter. Thus, the dissolved Fe does not reflect the true solubility of Fe; at times the reported values exceed the solubility limit for Fe in seawater. The total and discrete dissolved metal samples with the exception of total Fe samples were concentrated by using the Co-APDC coprecipitation technique (10). The particulate metals were determined by acid digestion (5 mL of 3.0 N HNO₃) of the filtrate retained on a 0.4- μ m Nuclepore filter (11). All metal analyses were made on a Perkin-Elmer atomic absorption spectrometer using a graphite furnace (Table III). The total suspended matter (TSM) was determined by the weight difference observed on a Nuclepore filter after vacuum filtration of 200 mL of water sample. The filters were washed with 5 mL of quartz subboiled water to remove the dissolved salts and air-dried for 24 h (12).

Results and Discussion

Iron Removal from the Surface Water. The variation of Fe with time in the surface water of the experimental tank was used to follow the fate of the waste in the tank. There were similarities and divergences in the behavior of the waste following the two acid-Fe waste additions. Following both additions there was a depletion of total Fe from the surface layer with Fe levels reaching background levels within 200 h (~8 days); however, the time dependence of the Fe removal was different. Fe profiles obtained after the second waste addition demonstrate the time dependence of the removal process (Figure 3). Immediately after the waste addition there was an

Table III. Summary of Analytical Procedures Used for Total, "Dissolved", and Particulate Metal Samples

metal	designation	preconcn	treatment	atomic absorption spectrometer
Fe	total	none	direct injection	PE 5000
Fe	dissolved	Co-APDC		PE 5000
Fe	particulate	filtration	acid digestion	PE 2000
Cu	total	Co-APDC		PE 5000
Cu	dissolved	Co-APDC		PE 5000
Cu	particulate	filtration	acid digestion	PE 2000
Cd	total	Co-APDC		PE 5000
Cd	dissolved	Co-APDC		PE 5000
Cd	particulate	filtration	acid digestion	PE 2000
Pb	total	Co-APDC		PE 5000
Pb	particulate	filtration	acid digestion	PE 2000
V	total	Co-APDC		PE 5000
V	particulate	filtration	acid digestion	PE 5000

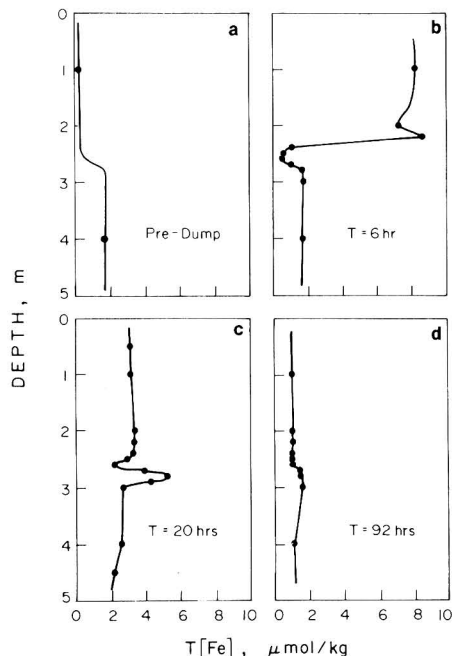


Figure 3. Vertical profiles of Fe concentrations in the experimental tank at several times after the second waste addition. Maxima and minima are observed in the pycnocline that represent regions of accumulation and depletion of iron ranging from colloidal to filterable sizes. A more extensive time series of high-resolution profiles would be needed to examine this phenomenon.

increase in the total Fe concentration in the surface layer from the background level of 0.01-8.0 μ mol/kg with a small maximum observed at the top of the pycnocline (Figure 3b). The profile below the pycnocline (>2.5 m) was similar to that observed before the waste addition, indicating that Fe particles had not penetrated the pycnocline. This interpretation is confirmed by a mass budget calculation for the system; 97% of the total Fe in the water column was in the surface water with the remaining 3% distributed between the pycnocline and the bottom layer. Twenty hours after the waste addition the total Fe in the surface layer decreased to 3.0 μ mol/kg with significant structure in the pycnocline, a minimum at 2.6 m and a maximum at 2.8 m (Figure 3c). Mass budget calculations show almost

50% Fe removal; 65% of the Fe remaining in the water column was in the surface layer, 16% in the pycnocline, and 19% in the bottom layer. Ninety-two hours after the waste addition, 80% of the Fe added had been removed. There was a more homogeneous distribution of Fe throughout the water column and a smooth Fe gradient through the thermocline (Figure 3d). These time series observations indicate that the pycnocline was not a significant barrier to the removal of Fe from the surface layer for periods of tens of hours.

The visual behavior of the particles formed after the two waste additions was different. After the first waste addition large (~1 mm diameter) flocculant particles formed within 1 h. These particles were visually evident for 36 h; there was minimal attachment of the Fe floc on the walls and surfaces within the tank. In contrast, the Fe particles observed after the second addition were smaller and there was accumulation on the walls and surfaces of the tank. Mass budget calculations indicated that the total loss of Fe to the walls and exposed surfaces was less than 4% of the total Fe added to the tank. Within 36 h Fe particles were not visually evident in the surface water or attached to the surfaces. These observations suggests that the first waste addition altered the properties of the seawater, possibly stripping organic substances from the water column. A thin organic film was observed on the walls and exposed surfaces following the first waste addition.

A possible removal mechanism of Fe from the water column was assimilation by organisms. Two approaches were used to determine if there was significant uptake of the Fe waste by the planktonic species in the tank. Throughout the experiment samples were drawn for phytoplankton and zooplankton counts from the surface and bottom layer of the control and experimental tank (13). Zooplankton samples were analyzed for trace metal composition. No uptake of metals in the tissues of these organisms was observed during the experiment. In addition dialysis bags containing the species *Skeletonema costatum* were suspended in the surface layer of the control and experimental tank after the second waste addition. Samples drawn at regular intervals after the waste addition showed no significant difference in the trace metal composition of the samples exposed to the waste and those drawn from the control tank. Thus, biological assimilation of the waste was not a removal mechanism in this experiment.

The removal of Fe particles from the surface layer was due to the settling of the particles through the pycnocline. The rate of removal can be controlled by either of two competitive processes: gravitational settling or the flocculation of Fe particles (14). If flocculation is rate limiting, then the removal will depend on the collision of small Fe particles to form Fe clusters. This process will follow second-order kinetics

$$d[\text{Fe}]/dt = -k_2[\text{Fe}]^2$$

where [Fe] is the concentration of Fe as small particles and k_2 is the second-order rate constant. If flocculation is rapid, then gravitational settling of the Fe clusters is rate limiting and the removal will follow pseudo-first-order kinetics

$$d[\text{Fe}]/dt = -k_1[\text{Fe}]$$

where [Fe] represents the concentration of particulate Fe which varies with time and k_1 is the first-order rate constant.

Our experimental results indicated different removal mechanisms for the two waste additions (Figure 4). After the first waste addition the removal followed first-order kinetics, indicating that gravitational settling was the

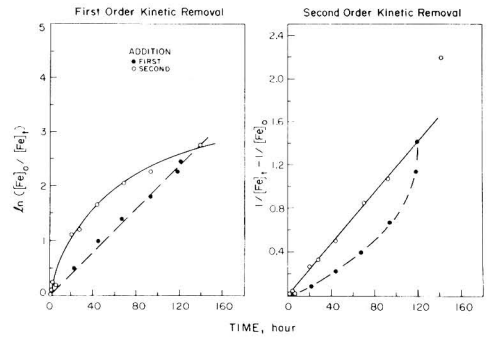


Figure 4. Kinetic behavior of Fe particles in the surface layer of the experimental tank. First-order kinetics (gravitational settling, the rate limiting step). (●) First addition; (○) second addition. Second-order kinetics (flocculation, the rate-limiting step). (●) First addition; (○) second addition.

Table IV. Vertical Flux of Fe from the Surface Layer of the Experimental Tank

time, h	Fe flux after first addition, $\text{mmol m}^{-2} \text{h}^{-1}$	Fe flux after second addition, $\text{mmol m}^{-2} \text{h}^{-1}$
1-21	0.38	0.89
21-44	0.20	0.14
44-68	0.10	0.06
68-92	0.06	0.02

rate-limiting step. After the second waste addition the removal followed second-order kinetics, indicating that flocculation was rate limiting for the first 140 h.

A significant difference in the two removal processes observed after the first and second waste addition is that for first-order kinetic removal (gravitational settling being rate limiting) the half-life, τ , of Fe in the surface water is independent of concentration

$$\tau = \frac{\ln 2}{k_1}$$

For a second-order kinetic removal (flocculation being rate limiting) the time to reduce the initial concentration by half varies inversely with the initial concentration, $[\text{Fe}]_0$

$$\tau = 1/(k_2[\text{Fe}]_0)$$

This dependence or lack of dependence of the half-life on the Fe concentration was reflected in the vertical flux of Fe from the surface layer after the two waste additions (Table IV). For the first waste addition the flux decreased by half within each 24-h period. For the second waste addition the initial flux was more than twice as great as that observed after the first addition. However, after the first 24 h the flux was dramatically reduced and was consistently less than that observed after the first waste addition. The vertical flux of Fe from the surface layer can be used to calculate a settling velocity for the Fe particles formed after the two waste additions. The settling velocity was calculated by dividing the flux observed during a specific time period by the average Fe concentration in the surface layer during this time. There was no significant difference in the settling velocity calculated for the first and second day following the first waste addition. For the first day ($t = 1-21$ h) the settling velocity was 1.5 m/day; for the second day ($t = 21-44$ h) the velocity was 1.3 m/day. Thus, when gravitational settling is rate limiting, the removal of Fe from the surface layer is not concentration dependent. In contrast to the first

Table V. Summary of Particulate and Total Metal Data for Control Tank

metal	depth, m	P(M), nmol/kg	T(M), nmol/kg	P(M), nmol kg ⁻¹ / T(M), nmol kg ⁻¹	P(M), mg kg ⁻¹ / TSM, mg kg ⁻¹
Fe ^a	1.0	0.17 ± 0.02	0.17 ± 0.02	1.0	0.005
Fe ^a	4.0	1.6 ± 0.4	1.4 ± 0.7	1.1	0.014
Pb	1.0	0.4 ± 0.2	1.2 ± 0.1	0.33	0.04 × 10 ⁻³
Pb	4.0	0.6 ± 0.2	1.5 ± 0.2	0.40	0.02 × 10 ⁻³
V	1.0	1 ± 2	42 ± 2	0.02	0.03 × 10 ⁻³
V	4.0	4 ± 2	49 ± 5	0.08	0.03 × 10 ⁻³
Cu	1.0	1.8 ± 1.9	19 ± 3	0.09	0.06 × 10 ⁻³
Cu	4.0	3.0 ± 1.0	20 ± 3	0.15	0.03 × 10 ⁻³
Cd	1.0	0.01 ± 0.02	0.5 ± 0.1	0.02	0.06 × 10 ⁻⁵
Cd	4.0	0.04 ± 0.02	0.5 ± 0.1	0.08	0.07 × 10 ⁻⁵
TSM ^a	1.0	2.0 ± 0.5			
TSM ^a	4.0	6.2 ± 1.1			

^aFe units are μmol/kg; TSM units are mg/kg.

addition, the settling velocity observed within the first 24 h after the second addition was greater, 3.2 m/day. Thus, the flocculation that produced the second-order removal of waste in the second experiment resulted in more rapidly settling particles. After the first day the settling velocity was similar to that observed after the first waste addition, 1.3 m/day.

Alteration in the Characteristics of Seawater. There were significant differences in the distribution of Fe, Pb, and V between the dissolved and particulate phase after the two waste additions (Figure 5a-c). The times of the waste addition were evident from the sharp increase in Fe at *t* = 0 and *t* = 260. After the first waste addition there was a sharp increase in both particulate and dissolved Fe; following the second addition the increase was primarily in particulate phase (70% of the total Fe). A similar but more dramatic change in the distribution of Pb and V between the particulate and dissolved phase was observed. After the first addition 34% of Pb and 52% of V were present in the particulate phase; for the second addition 90% of Pb and 88% of V were present in the particulate phase. This increase in the particulate phase of Fe, Pb, and V after the second waste addition indicated that the first waste addition significantly altered the water column characteristics. If organic substances were stripped from the water column during the first waste addition, they would be unavailable to form metal-organic complexes and colloidal aggregates or to stabilize the colloidal Fe particles.

The removal of Pb and V from the water column was consistent with the removal of Fe; however, the dissolved phase of both metals was stripped from the surface layer of the stratified tank after the first waste addition. The dissolved phase refers to the fraction that is not retained on a 0.4-μm Nuclepore filter. This effect was most dramatic for V. Prior to the first acid-Fe waste addition only dissolved V was observed in the surface layer of the tank (40 nmol/kg); the addition of the waste produced a 40 nmol/kg increase in particulate V. Particulate V returned to a nondetectable background level (<1.0 nmol/kg) ~200 h after the dump. The steady-state concentration of dissolved V observed after the first waste addition was 15 nmol/kg. This represented a 60% removal of dissolved V by the Fe floc. Dissolved Pb was also stripped from the water column (30% removal). The dissolved Pb levels, which were calculated by difference, were within the experimental uncertainty (0.2 nmol/kg) after the first waste addition; statistically significant dissolved Pb values were not observed after the second waste addition. These results suggested that the complexation of Pb and V by organic substances increased the soluble fraction of these metals in the water column. If the initial acid-Fe waste addition stripped organics from the water column, this

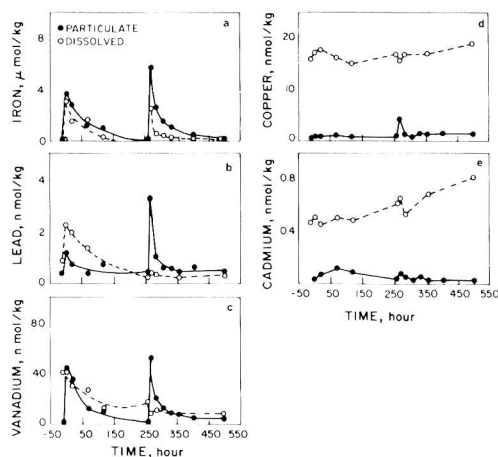


Figure 5. Variation of particulate and dissolved Fe, Pb, V, Cu, and Cd in the surface (*Z* = 1 m) layer of the experimental mesocosm with time after the waste additions. (●) Particulate metal; (○) dissolved metal.

soluble fraction of Pb and V could have been lost. The disposal of Fe waste significantly changed the trace metal composition of the seawater.

In contrast to the behavior of Pb and V, particulate and dissolved Cu and Cd showed remarkable independence from the addition of the acid-Fe waste and subsequent flux of hydrous Fe particles through the tank (Figure 5d,e). The waste produced a slight increase in the total concentration of Cd and Cu, primarily in the particulate phase, immediately after the waste addition. However, within 20 h the concentration of these two metals returned to background levels (Table V). The consistent upward trend in total Cu and Cd indicates input to the tanks from the surroundings. The behavior of Cd is consistent with previous observations in natural and controlled ecosystems (12, 15). The behavior of Cu is complex. In previous experiments in a homogeneous well-mixed MERL tank, Cu that was added in the dissolved form of CuSO₄ was strongly adsorbed on naturally occurring particles showing distribution coefficients in the range 10⁴-10⁵ and a half removal time of 6-10 days at 20 °C (16). In contrast, the variation of Cu in a coastal transect across the New York Bight was conservative with salinity, suggesting no removal from the water column (17). Our results in a stratified MERL tank showed that Cu was not adsorbed on the Fe particles. The complex behavior of Cu in marine systems suggests that the speciation of Cu may be an important factor determining its immunity to adsorptive processes

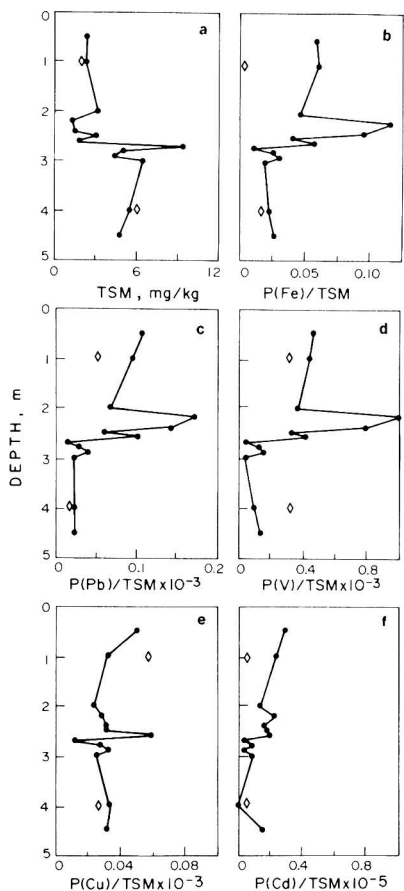


Figure 6. Vertical profiles at $t = 280$ h of the total suspended matter (TSM); the ratio of particulate Fe to TSM, $P(\text{Fe})/\text{TSM}$; $P(\text{Pb})/\text{TSM}$; $P(\text{V})/\text{TSM}$; $P(\text{Cu})/\text{TSM}$; $P(\text{Cd})/\text{TSM}$. (●) Experimental; (◇) control.

as well as biological toxicity.

The time series observations of metal partitioning between the particulate and dissolved phase demonstrate that the particulate phase was more important after the second addition; thus, it is of interest to examine the nature of the particulate phase after the second waste addition. Detailed vertical profiles of temperature, salinity, fluorescence, total suspended matter (TSM), and total and particulate metals were made 20 h after the second waste addition. The TSM profile showed a pronounced maximum at the base of the pycnocline (Figure 6a). An average of five observations of TSM in the control tank at several time intervals throughout the experiment showed that the TSM in the surface and bottom layer of the experimental tank were comparable to those observed in the control tank (Table V).

To better understand the composition of the TSM, one can examine the mass ratio of a particular metal to the TSM. A comparison of the particulate Fe to TSM ratio, $P(\text{Fe})/\text{TSM}$, in the experimental tank showed that particles in the surface layer are enriched in Fe relative to the control tank, whereas particles in the bottom of the tank were similar in composition to those observed in the control tank (Figure 6b). Particles with a high $P(\text{Fe})/\text{TSM}$ ratio are predominantly inorganic phases whereas particles with a lower $P(\text{Fe})/\text{TSM}$ ratio are biogenic particles (18).

The $P(\text{Fe})/\text{TSM}$ was high relative to the control in the surface layer 20 h after the second waste addition. A maximum value of $P(\text{Fe})/\text{TSM} = 0.12$ was observed at the top of the pycnocline. This maximum did not coincide with the TSM maximum at 2.7 m, but represented an accumulation of Fe particles in a region of minimal mixing. The TSM maximum at 2.7 m was not due to particulate Fe from the acid-Fe waste dump. The sharp fluorescence gradient was observed at this depth, suggesting that the TSM maximum represented an accumulation of planktonic organisms at the base of the pycnocline.

Further insight into the nature of the particulate phase can be obtained from a similar analysis of the composition of the TSM for Pb, V, Cu, and Cd. The vertical structure observed in the profiles for $P(\text{Pb})/\text{TSM}$ and $P(\text{V})/\text{TSM}$ were similar to that observed for $P(\text{Fe})/\text{TSM}$ (Figure 6c,d). There was a strong correlation between $P(\text{Fe})$ and $P(\text{V})$ and $P(\text{Pb})$. For the first addition the correlation coefficient for the regression of $P(\text{Fe})$ vs. $P(\text{V})$ was 0.998; for $P(\text{Fe})$ vs. $P(\text{Pb})$ the coefficient was 0.869. For the second addition the correlation between $P(\text{Fe})$ and $P(\text{V})$ was the same (0.995); $P(\text{Pb})$ showed a stronger correlation, 0.959. These data suggested that Pb and V were scavenged by the Fe particles. The scavenging of Pb by Fe is consistent with our field observations.

In contrast to Pb and V, Cu and Cd were present predominantly in the dissolved fraction. The vertical profiles of $P(\text{Cu})/\text{TSM}$ were strikingly different from those obtained for $P(\text{Fe})/\text{TSM}$ (Figure 6e,f). There was no distinct maximum at the top of the pycnocline (2.2 m). The $P(\text{Cu})/\text{TSM}$ profile showed some structure at the base of the pycnocline, a maximum at 2.6 m and a minimum at 2.7 m. The same structure was present in the $P(\text{Cd})/\text{TSM}$ profile, but the gradients were smaller. The concentration of Cu and Cd associated with the particulate phase was similar in the bottom of the control and experimental tank (Table V). There was a slight depletion of $P(\text{Cu})/\text{TSM}$ in the top of the experimental tank; however, there was significant variation in partitioning of Cu between the particulate and soluble phases in the control tank. The $P(\text{Cd})/\text{TSM}$ ratio in the surface layer of the experimental tank 20 h after the waste addition was significantly higher than that observed in the control tank. Elevated Cd concentrations have been observed in field studies immediately after an acid-Fe waste dump (1).

Conclusion

Field studies failed to resolve the question of the vertical processes controlling the removal of acid-Fe waste from the water column and the impact of the waste on the chemical properties of seawater. These questions were addressed in an experiment performed in a stratified MERL tank, which allowed the study of the vertical processes controlling Fe removal without considering horizontal advection and diffusion. The vertical flux of Fe was due to settling of the Fe particles through the pycnocline. Biological transport of the waste was not an important removal mechanism.

Two competitive processes control the rate of Fe removal from the surface water: flocculation of the Fe particles and gravitational settling through the pycnocline (14). If flocculation is rapid, then gravitational settling is the rate-limiting step, and the removal follows pseudo-first-order kinetics. If aggregation of the Fe particles is slow, then flocculation is the rate-limiting step, and the removal follows second-order kinetics. For the first waste addition, gravitational settling was the rate-limiting step; the calculated settling velocity was 1.5 m/day. The first waste addition altered the chemical properties of seawater,

possibly stripping organic substances from the water column, and the removal of Fe after the second addition was second order with respect to Fe. The settling velocity calculated within the first 24 h when flocculation was rate limiting was 3.2 m/day.

There were significant differences in the behavior of the trace metals added with the waste and those already present in the seawater. After the first addition, Fe, Pb, and V were equally distributed between the dissolved and particulate forms; after the second addition the particulate form was dominant. There was a strong correlation in the behavior of Pb and V with Fe, suggesting that these metals were scavenged by Fe particles. The dissolved form of Pb and that of V were stripped from the water column after the waste additions. A possible explanation for these observations is that the first waste addition stripped dissolved organic substances from the water column. Pb and V could form soluble organic complexes and/or colloidal aggregates with these species during the first waste addition. The organic species that enhance the soluble fraction of these metals had been stripped from the water column after the initial waste addition and were not available for complexation after the second waste addition. In contrast to Pb and V the behavior of Cu and Cd was independent of the acid-Fe waste addition. There was only a minor increase in total Cu and Cd after the waste addition, and these metals were not scavenged by the Fe floc.

This experiment in the stratified MERL tank allowed us to understand the processes controlling the removal of Fe from the surface water after a simulated dump and to characterize the changes in the trace metal composition of seawater. The alteration in the properties of the seawater observed after the initial acid-Fe waste dump is an important consideration in the control of ocean dumping. If acid-Fe waste is consistently dumped in a region where lateral exchange is not rapid, the properties of the seawater and the subsequent behavior of the waste can be significantly altered.

Acknowledgments

We are grateful to several people for their assistance in this work: Michael Pilson and Candice Oviatt for their assistance with the overall design of the experiment; Percy Donaghay for his invaluable help with the sampling strategy and the experimental design; Eric Klos for the technical design and maintenance of the stratified tanks; Douglas Huizenga and Wayne Warren for their assistance in the trace metal sampling and analyses.

Registry No. TiO₂, 13463-67-7; Fe, 7439-89-6; Cu, 7440-50-8; Cd, 7440-43-9; Pb, 7439-92-1; V, 7440-62-2.

Literature Cited

- (1) Kester, D. R.; Hittinger, R. C.; Mukherji, P. In "Ocean Dumping of Industrial Wastes"; Ketchum, B. H.; Kester, D. R.; Park, P. K., Eds.; Plenum Press: New York, 1981; pp 215-232.
- (2) Brown, M. F.; Kester, D. R.; Dowd, J. M. In "Wastes in the Ocean: Chemical and Sewage Wastes"; Duedall, I. W., Ketchum, B. H., Park, P. K., Kester, D. R., Eds.; Wiley-Interscience: New York, 1983; Vol. 1, pp 157-169.
- (3) Csanady, G. T. In "Ocean Dumping of Industrial Wastes"; Ketchum, B. H.; Kester, D. R.; Park, P. K., Eds.; Plenum Press: New York, 1981; pp 109-129.
- (4) Klos, E. G., University of Rhode Island, unpublished results, 1985.
- (5) Nixon, S. W.; Alonso, D.; Pilson, M. E. Q.; Buckley, B. A. In "Microcosm in Ecological Research"; Giesy, J. P., Ed.; Augusta, GA, 1980; DOE Symp. Ser., pp 818-849.
- (6) Fox, M. F.; Kester, D. R. In "Wastes in the Ocean"; Kester, D. R., Bunt, W. V., Capuzzo, J. M., Park, P. K., Duedall, I. W., Eds.; Wiley-Interscience: New York, 1985; Vol. 5, pp 171-185.
- (7) Lorenzen, C. J. *Deep-Sea Res.* **1966**, *13*, 223-227.
- (8) Donaghay, P. L.; Klos, E. G. *Mar. Ecol.: Prog. Ser.*, in press.
- (9) Brewer, P. G.; Goldman, J. C. *Limnol. Oceanogr.* **1976**, *21*, 108-117.
- (10) Boyle, E. A.; Edmond, J. M. *Anal. Chim. Acta* **1977**, *91*, 189-197.
- (11) Mukherji, P.; Kester, D. R. In "Wastes in the Ocean: Chemical and Sewage Wastes"; Duedall, I. W., Ketchum, B. H., Park, P. K., Kester, D. R., Eds.; Wiley-Interscience: New York, 1983; Vol. 1, pp 141-155.
- (12) Hunt, C. D.; Smith, D. L. *Can. J. Fish. Aquat. Sci.* **1983**, *40*, 132-142.
- (13) Hunt, C.; Donaghay, P. L. *Eos (Madrid)* **1985**, *65*, 938.
- (14) Stumm, W.; Morgan, J. J. "Aquatic Chemistry"; Wiley-Interscience: New York, 1981; pp 647-653.
- (15) Sanschi, P. H.; Li, Y. H.; Carson, S. R. *Estuarine Coastal Mar. Sci.* **1980**, *10*, 635-654.
- (16) Hunt, C. University of Rhode Island, unpublished results, 1985.
- (17) Hanson, A. K., Jr.; Quinn, J. G. *Can. J. Fish. Aquat. Sci.* **1983**, *40*, 151-161.
- (18) Hong, H. S.; Kester, D. R. *Estuarine Coastal Shelf Sci.*, in press.

Received for review October 1, 1984. Revised manuscript received March 29, 1985. Accepted July 12, 1985. This work was supported by National Oceanic and Atmospheric Administration Grant NA79-AA-D-00033.

Aromatic Hydrocarbons in New York Bight Polychaetes: Ultraviolet Fluorescence Analyses and Gas Chromatography/Gas Chromatography-Mass Spectrometry Analyses

John W. Farrington,* Stuart G. Wakeham, Joaquim B. Livramento, Bruce W. Tripp, and John M. Teal

Departments of Chemistry and Biology, Woods Hole Oceanographic Institution, Woods Hole, Massachusetts 02543

■ Polychaetes collected from New York Bight sediments near sewage sludge and harbor dredge spoil dump sites contained a series of diaromatic-tetracyclic hydrocarbons of apparent triterpenoid origin. Microbial processes in sewage sludge are a likely source of these compounds. These octahydrochrysenes were much more abundant in the polychaetes than were the fossil fuel and combustion-derived polycyclic aromatic hydrocarbons which were found in the sediments, presumably because they are more available for biological uptake. If the polychaetes had been analyzed only by the spectrofluorometric techniques often used for screening samples for petroleum contamination, then grossly inaccurate results for aromatic hydrocarbon content would have been obtained. Therefore, UV fluorescence must be used in a hierarchical approach, with more sophisticated procedures available to verify the petrogenic nature of the hydrocarbons.

Numerous papers and reviews have set forth the difficult task of measuring for petroleum hydrocarbons in samples from aquatic ecosystems (1-6). Some monitoring programs such as MARPOLMON (7) and the Georges Bank Monitoring Program (8) have opted to employ a UV fluorescence method for screening samples to detect the presence of petroleum hydrocarbons in water, sediments, or organisms. This method of analysis is easy to employ and provides rapid results in comparison to the more time consuming and costly but more specific glass capillary gas chromatography (GCGC) or glass capillary gas chromatography mass spectrometry (GCMS) analyses.

However, it has been recommended that the UV fluorescence screening method is best employed not alone but in a hierarchical approach to monitoring for petroleum pollution (8, 9). If UV fluorescence screening indicates elevated concentrations of petroleum hydrocarbons, then further, more detailed analyses should be applied to the samples to verify the petrogenic nature of the hydrocarbons. We present aromatic hydrocarbon data for polychaetes from the New York Bight and Buzzards Bay, MA, which illustrate the advisability of the hierarchical approach and one pitfall inherent in UV fluorescence methods if used alone.

Methods

Samples of polychaetes were obtained by box coring with a MK III box corer (Ocean Instruments, San Diego, CA) during *R/V Oceanus* cruises 26 and 46 to the New York Bight and a *R/V Asterias* cruise in Buzzards Bay. Station locations and dates of sampling for the New York Bight are given in Table I. Polychaetes were separated from the sediment by seawater sieving through 1-mm mesh screens immediately after box coring. Polychaetes were picked from the screens and frozen until analysis several weeks later. Aromatic hydrocarbons were isolated from the polychaetes by using an aq. alkaline extraction procedure modified from Warner (10). Hydrocarbons were isolated from the digestion extract by column chromatography on an alumina over silica gel column (9). The fractions containing aromatic hydrocarbons were analyzed

by UV fluorescence spectrometry using a Perkin-Elmer MPF 3 UV fluorescence instrument and general procedures described previously (11). Single wavelength excitation-emission scan and synchronous excitation-emission scan modes were employed. No. 2 fuel oil was also subjected to the same analytical procedures.

The aromatic hydrocarbon fractions from the polychaetes were also analyzed by GCGC and GCMS. Descriptions of the procedures used for extraction, column chromatography, GCGC, and GCMS and more example chromatograms are published elsewhere (9, 12).

Results and Discussion

UV fluorescence spectra are given in Figure 1. Both single wavelength excitation-emission and synchronous scan excitation-emission spectra indicate the presence of elevated concentrations of two-ring and possibly three-ring aromatic hydrocarbons in the polychaetes from the stations in the New York Bight. The PAH fractions determined by GCGC and GC/MS from Buzzards Bay polychaetes had spectra which were very similar to the blanks, indicating little if any aromatic hydrocarbons were present. The spectra of the polychaetes from the New York Bight station were similar to the UV fluorescence spectra for No. 2 fuel oil and some light crude oils (Figure 1) (11). The intensity of the fluorescence signal for aromatic hydrocarbons decreased in samples with increasing distance from the sewage sludge and harbor dredge materials dump sites in the New York Bight. This is consistent with gradients in fossil fuel hydrocarbon pollution, both PAH from combustion sources and PAH from petroleum, in sediments in the area (13-15). Thus, the UV fluorescence data support the expectation that polychaetes living in sediments containing elevated PAH concentrations might also have elevated concentrations of PAH, unless enzymes are induced that will metabolize the hydrocarbons once they are taken up by the polychaetes (16).

We analyzed the column chromatography fraction containing the PAH by quantitative GCMS in order to obtain concentrations of individual or groups of PAH in the polychaetes. Computer-assisted quantitative measurements of substituted naphthalenes, phenanthrene, substituted phenanthrenes, and other compounds present as major aromatic hydrocarbons in the sediment of the area (15, 17) revealed only low concentrations of a few PAH (Table I). These amounts are insufficient to account for the intensity of the fluorescence signal. The fluorescence intensity of the compounds in the aromatic hydrocarbon fraction of the polychaetes was calculated relative to chrysene by using both single wavelength excitation and synchronous scan excitation-emission procedures. These data are given in Table II for samples from *R/V Oceanus* 46 (1978) cruise samples.

Further analysis by GCMS provided the answer to this apparent paradox. The total ion plot from GCMS of the PAH fraction from the polychaete sample nearest the dump sites is presented in Figure 2. Note the major peak indicated by the arrow; the spectrum for this peak is given in Figure 3. The compound has been assigned the octa-

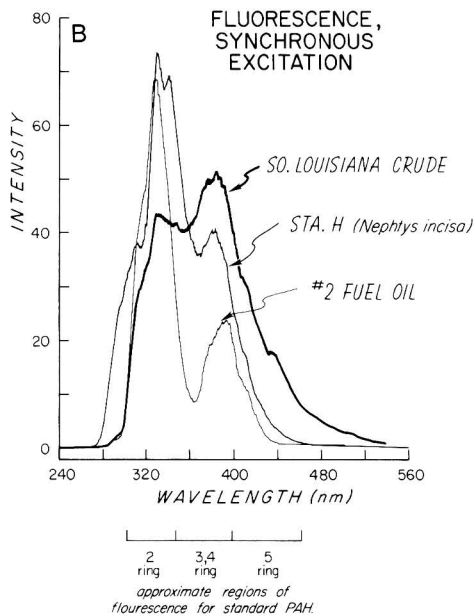
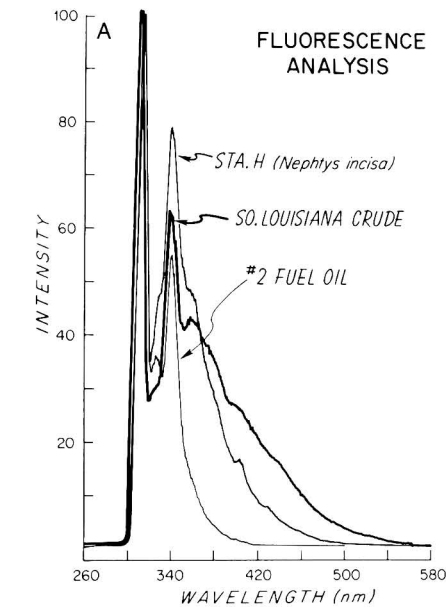


Figure 1. UV fluorescence spectra of aromatic hydrocarbons in oils and polychaetes. (A) Single wavelength excitation (310 nm); (B) synchronous scanning of excitation and emission, 40 nm offset.

hydrochrysene structure indicated in Figure 3 on the basis of evidence from conjunction with PAH from the Messel Shale, which contains this compound, and by comparison with mass spectra and GC data of the authentic compound (18). Selected ion scans of m/z 290 and 292 (Figure 4) and examination of mass spectra reveal the presence of several other structurally related partially aromatized triterpenoid compounds in the polychaetes. We can only provide a rough estimate of the concentrations of these compounds from GCMS analyses because we lack calibration curves from injection of known amounts of authentic compounds.

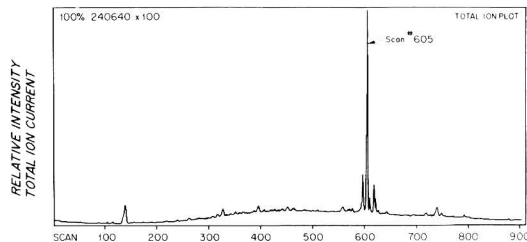


Figure 2. Total ion chromatogram (GCMS analysis) of the aromatic hydrocarbon/alkene fraction of *Nephtys* from station Oc-H in the New York Bight.

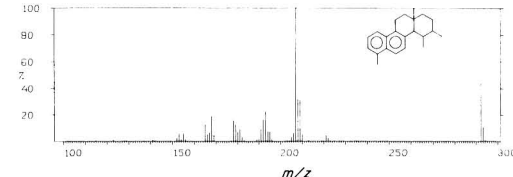


Figure 3. Mass spectrum (electron impact) of scan 605 in Figure 2.

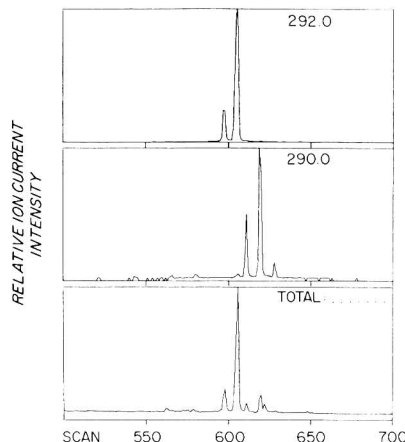


Figure 4. Selected ion (m/z 292 and 290) and total ion chromatograms for station Oc-H *Nephtys* aromatic hydrocarbon/alkene fraction.

However, rough estimates from applying response factors for phenanthrene, fluoranthene, and pyrene give approximately $(1-5) \times 10^{-6}$ g/g dry weight total m/z 292 octahydrochrysenes in the Station H *Nephtys*. These estimated concentrations are 2 orders of magnitude higher than concentrations of naphthalenes, phenanthrene, fluoranthene, and pyrene (Table II).

Analyses of surface sediments from the New York Bight stations confirm the presence of the octahydrochrysenes, but in concentrations much less than fossil fuel or combustion PAH (17). It is not clear why the polychaetes contain a predominance of the octahydrochrysene in comparison to other PAH. Other diagenetic PAH present in some other sediments (18, 19) were not found in the polychaetes, which is intriguing and suggests something relatively unique about the octahydrochrysenes, their precursors, reactions yielding the octahydrochrysenes, or some combination of the preceding.

The octahydrochrysenes in the PAH fraction from the polychaetes have UV fluorescence spectra similar to those for substituted naphthalenes. Since substituted naphthalenes are among the more predominant aromatic hydrocarbons in No. 2 fuel oil and some light crude oils (6),

Table I. Concentrations (10^{-9} g/g Dry Weight) of Selected Aromatic Hydrocarbons in Polychaetes^a from New York Bight Surface Sediments

station	month/year	naphthalene series, at m/z^b				phenanthrene/anthracene series, at m/z^b			fluoranthene, m/z^b 202	pyrene, m/z^b 202
		128	142	156	170	178	192	206		
Oc-L (40°23'N, 72°37'W)	6/77	c	c	c	c	1.0	5.0	8.8	1.5	3.8
Oc-L	5/78	1.2	c	c	c	c	c	c	4.6	7.2
Oc-LL (40°04'N, 73°29'W)	5/78	c	17	c	c	2.0	1.7	c	5.0	5.2
Oc-M (40°17'N, 73°47'W)	6/77	c	c	c	14	14	31	90	58	200
Oc-M	5/78	1.2	0.5	1.4	4	6.9	14	33	20	80
Oc-H (40°26'N, 73°48'W)	6/77	c	c	8.0	6.0	5.5	12	19	8.5	27
Oc-H	5/78	2.2	5.6	28	29	11	c	c	15	54

^aMixed species of polychaetes were analyzed in 1977; *Nephtys incisa* samples were analyzed in 1978. ^b m/z 128, naphthalene; m/z 142, methylnaphthalenes; m/z 156, dimethyl- or ethylnaphthalenes; m/z 170, trimethyl-, ethyl-, dimethylnaphthalenes; m/z 178, phenanthrene; m/z 192, methylphenanthrenes/methylanthracenes; m/z 206, dimethyl- or ethylphenanthrenes/anthracenes by quantitative glass capillary GCMS. ^cNot detected at 0.1×10^{-9} g/g dry weight.

Table II. UV Fluorescence Data for Aromatic Hydrocarbons in *Nephtys spp.* from New York Bight Surface Sediments

station	10^{-6} g of chrysene equivalents ^a /g dry weight	
	single λ excitation	synchronous scan
Oc 46-LL	0.86	0.62
Oc 46-M	27	19
Oc 46-H	60	40

^aMethods given in ref 7 adapted for organisms.

the UV fluorescence spectra of the PAH fraction from the New York Bight polychaetes gives a false indication of the presence of elevated concentrations of petroleum hydrocarbons, a result consistent with the expectation that the samples should be contaminated with petroleum given their geographical location near a source of petroleum input. However, the octahydrochrysenes are not from petroleum pollution but apparently result from early diagenesis reactions which transform unidentified precursor compounds to the observed structures by as yet unknown reaction pathways (18, 19).

Our favored hypothesis for the presence of the measured concentrations of octahydrochrysene in the polychaete is as follows: (i) the octahydrochrysenes are produced by microbial processes in the sewage sludge from precursors yet to be identified; (ii) the octahydrochrysenes are more readily taken up by the polychaetes because they are more biologically available relative to PAH bound to particulate matter from combustion processes, but perhaps equally available as PAH from petroleum inputs (17); (iii) once incorporated into the body of the polychaete the octahydrochrysenes are less readily metabolized by mixed-function oxidase or aryl hydrocarbon hydroxylase enzymes (cytochrome P-450 systems) than are PAH from petroleum sources. Regardless of the source, the presence of 10^{-6} g/g dry weight levels in the polychaetes which are thought to possess capabilities to respond to PAH elevations in tissue or habitat (16) raises the interesting question as to why the concentrations of octahydrochrysenes have not been reduced to lower concentrations by metabolism. Perhaps this is due to structural specificity (20).

Alternative hypotheses that we cannot discount are (i) the polychaetes biosynthesize the octahydrochrysenes or (ii) the gut flora of the polychaetes biosynthesize these compounds. In both cases, the precursor(s) would have to be associated with sludge or some other input to the New York Bight. A New York Bight sludge or dredge spoils origin for the octahydrochrysenes or precursors

would explain the measured concentration gradients. It is less likely, but possible that stress due to pollution of the polychaetes habitat influence de novo biosynthesis in polychaetes in a manner that produces the observed gradients in concentration.

Given the small number of samples of organisms subjected to detailed analyses for hydrocarbon concentrations and compositions—especially for aromatic hydrocarbons—there may be a few more surprises of the sort we have encountered in our analyses of these polychaete samples. We think that our results clearly support the need for application of detailed analyses for individual PAH compounds by GCMS when UV fluorescence analyses screening by samples indicate apparently elevated concentrations of petroleum in samples. Furthermore, our results raise interesting questions regarding specificity of PAH metabolism in polychaetes and/or biological availability of various types of PAH in benthic ecosystems. Finally, the polychaetes and their habitat seem to offer good systems for further studies of precursor-product relationships for the origin of octahydrochrysenes during early diagenesis.

Acknowledgments

We thank the officers, crew, and fellow scientists of *R/V Oceanus* cruises 26 and 46 for their assistance in sample collection. N. M. Frew conducted the GCMS analyses.

Registry No. Fluoranthene, 206-44-0; pyrene, 129-00-0; naphthalene, 91-20-3; methylnaphthalene, 1321-94-4; phenanthrene, 85-01-8; methylphenanthrene, 31711-53-2; methylanthracene, 613-12-7; octahydro-3,4,7,12a-tetramethylchrysene, 74229-82-6.

Literature Cited

- (1) Connell, D. W.; Miller, G. J. *Crit. Rev. Environ. Control* 1980-1981, 11, 37-162.
- (2) Wakeham, S. G.; Farrington, J. W. In "Contaminants and Sediments I"; Baker, R., Ed.; Ann Arbor Science Publishers, Inc.: Ann Arbor, MI, 1980; pp 3-32.
- (3) Farrington, J. W. In "Petroleum in the Marine Environment"; Petrakis, L.; Weiss, F. T., Eds.; American Chemical Society: Washington, DC, 1980; Adv. Chem. Ser. No. 185, pp 1-22.
- (4) "Petroleum in the Marine Environment"; U.S. National Academy of Sciences Press: Washington, DC, 1975.
- (5) Mackie, P. R.; Hardy, R.; Whittle, K. J.; Bruce, C.; McGill, A. S. In "Polynuclear Aromatic Hydrocarbons"; Bjorseth, A.; Dennis, A. J., Eds.; Battelle Press: Columbus, OH, 1980; pp 379-393.
- (6) Neff, J. M. "Polycyclic Aromatic Hydrocarbons in the Aquatic Environment"; Applied Science Publishers, Ltd.: London, 1979.

- (7) IOC-UNESCO, 1982, Report of Fourth Session of the Working Committee for the Global Investigation of Pollution in the Marine Environment.
- (8) Science Applications, Inc., report to Minerals Management Service, U.S. Department of Interior, Washington, DC, 19838, Report SAI/JRB-045-03.
- (9) Farrington, J. W.; Davis, A. C.; Frew, N. M.; Rabin, K. S. *Mar. Biol.* 1982, 66, 15-26.
- (10) Warner, J. S. *Anal. Chem.* 1976, 48, 578-583.
- (11) Wakeham, S. G. *Environ. Sci. Technol.* 1977, 11, 272-276.
- (12) Farrington, J. W.; Tripp, B. W.; Teal, J. M.; Millie, G.; Tjessem, K.; Davis, A. C.; Livramento, J. B.; Hayward, N. A.; Frew, N. M. *Toxicol. Environ. Chem.* 1982, 5, 331-346.
- (13) Farrington, J. W.; Tripp, B. W. *Geochim. Cosmochim. Acta* 1977, 41, 1627-1641.
- (14) LaFlamme, R. E.; Hites, R. A. *Geochim. Cosmochim. Acta* 1978, 42, 289-303.
- (15) Boehm, P. D.; Steinhauer, W.; Brown, J. Battelle New England Marine Research Laboratory, Duxbury, MA, 1984, report to National Oceanic and Atmospheric Administration.
- (16) Lee, R. F. *Mar. Biol. Lett.* 1981, 2, 87-105.
- (17) Farrington, J. W.; Teal, J. M.; Tripp, B. W.; Livramento, J. B.; McElroy, A., report to U.S. Department of Energy, Washington, DC, 1983, Report DOE/EV/04256-04.
- (18) Spyckerelle, C. Ph.D. Dissertation, L'Universite Louis Pasteur de Strasbourg, Strasbourg, France, 1975.
- (19) Wakeham, S. G.; Schaffner, C.; Giger, W. *Geochim. Cosmochim. Acta* 1980, 44, 415-429.
- (20) Stegeman, J. in "Polycyclic Hydrocarbons and Cancer"; Gelboin, H. V.; Ts'ao, P. O. P., Eds.; Academic Press: New York, 1981; Vol. 3, Chapter 1, pp 1-60.

Received for review November 5, 1984. Revised manuscript received June 26, 1985. Accepted July 26, 1985. This work was supported by Contract DE-AC02-77EV04256 A007 from the U.S. Department of Energy and Interagency Agreement AA550-1A7-20 between the U.S. Department of Energy and the U.S. Department of the Interior, Bureau of Land Management. Contribution No. 5798 from the Woods Hole Oceanographic Institution.

Products and Quantum Yields for Photolysis of Chloroaromatics in Water

David Dulin, Howard Drossman, and Theodore Mill*

Physical Organic Chemistry Department, SRI International, Menlo Park, California 94025

■ Photolysis of chlorobenzene, 2- and 4-chlorobiphenyl, and 2- and 4-chlorobiphenyl ethers in water with 250-300-nm light produce corresponding phenols or, in the case of 2-chlorobiphenyl ether, dibenzofuran exclusively. Quantum yields in most cases are very similar to those reported in hexane for the reduction process. 1,2,4-Trichlorobenzene and 2,3,7,8-tetrachlorodibenzodioxin (TCDD) photolyze much less efficiently in water than in hexane. A common pathway for photolysis of monochloroaromatics involving aryl cations accounts well for the experimental observations. C-O rather than C-Cl cleavage in TCDD may be a major pathway for its loss. Half-lives for photolysis of these chloroaromatics in sunlight in water range from 460 days to 5 days; TCDD photolyzes in water with a half-life of about 4-5 days in summer at 40° latitude.

Introduction

Polychlorinated biphenyls (PCBs) and polychlorinated dioxins (PCDs) now are widely distributed in the water and soil, and because of their possible toxicity and/or carcinogenicity, they may pose significant human health hazards to large populations (1-3). Their wide distribution probably results from both widespread use or production patterns and relatively low reactivity in the environment (4, 5).

The importance of understanding the environmental pathways for PCBs and dioxins has prompted a variety of studies to examine chemical reactivity, physical transport, and biotransformation in water, sediment, and soil, but quantitative data useful for environmental assessment are either lacking or in conflict; information on transformation pathways is notably incomplete.

Available data and inspection of the chemical structures of PCBs and PCDs suggest that they sorb strongly to sediments, may volatilize from water, resist hydrolysis and biotransformation, but probably photolyze in sunlight. This report describes a study of the photolysis of chlorobenzenes, chlorobiphenyls, chlorobiphenyl ethers, and tri- and tetrachlorodioxins in water or water-acetonitrile to

measure photolysis quantum yields, assesses the effects of solvent, especially water, on reactivity and reaction pathways, and provides a quantitative basis for estimating sunlight photolysis rate constants (k_{pE}). In addition systematic measurement of quantum yields in water may lead to a predictive scheme for estimating quantum yields for other chlorinated aromatics.

Background

Chlorobenzene is the simplest, best-studied chloroaromatic (6-10). Our present understanding of the process is that chlorobenzene photodissociates via the triplet state to the phenyl and chlorine radical pair followed by their reactions with solvent. Quantum yields in organic solvents are ~0.3; a similar value is found in the gas phase (11). The triplet state of chlorobenzene has enough energy (86 kcal mol⁻¹) to efficiently cleave the Ph-Cl bond, $D(C-Cl)$ 85 kcal mol⁻¹ (12). Reduction is the dominant pathway in all H-atom-donating solvents including hexane and methanol, but in the latter case about 25% anisole also forms by substitution of chlorine by methoxy. Recently Tissot et al. (9, 10) reported that photolysis of chlorobenzene in water-acetonitrile gives phenol via the short-lived (30 ns) triplet state.

Reported values of quantum yields (ϕ) for photolysis of chlorobenzene and biphenyls in organic solvents show a striking pattern (12-19): chlorobenzenes all have $\phi > 0.01$ (18) but only ortho-substituted biphenyls have ϕ values ≥ 0.002 . Usually chlorine substitution in only the 3-, 4-, or 5-positions causes ϕ values to fall below 0.01 (15, 17, 19, 20). Moreover, all of these reactions give solely or mainly the reduced product in organic solvents.

Photochemical studies on chlorinated diphenyl ethers, dibenzofurans, and dibenzodioxans reveal similar chemistry to that observed with PCBs and chlorobenzenes (21-23). Reductive dehalogenation occurs in organic solvents, but no apparent relationship was found between substitution patterns and photolysis rates using light > 290 nm (Rayonet reactor) (21). However, *o*-chlorine is preferentially lost from polychloro ethers, and some dibenzo-

Table I. Photolysis of Chlorobenzene in Aerated Water^a

10 ⁴ [CB], M	[additives]	time, min	% conversion CB	10 ⁶ k _p ^b s ⁻¹	10 ³ k _{CB} ^b s ⁻¹	φ _{CB} ^b	products, % ^c
1.57	1% AN	540	28	3.20 ± 0.15	1.12 ± 0.01	0.37	55% phenol, ^d 112% chloride ion, ^e 2% acetanilide
1.57	1% AN, 0.05 M NaOH		25	2.50 ± 0.05	1.32 ± 0.55	0.52	phenol
1.57	1% AN	600	44		1.67 ± 0.09		32% phenol
1.57	1% AN, 0.01M <i>i</i> -PrOH	600	38		1.57 ± 0.05		37% phenol
1.95	0.1% AN, pure O ₂ , 254-nm light ^f	60	57		24.0 ± 1.8		58% phenol in 15 min; 20% in 60 min
1.95	0.1% AN, no O ₂ , 254-nm light ^f	60	58		23 ± 2		36% phenol in 15 min; 45% in 60 min
3.04	pure MeOH		19	2.43 ± 0.19	0.778 ± 0.048	0.26	benzene, 7% anisole
3.04	pure MeOH		18	2.63 ± 0.34	0.735 ± 0.037	0.25	

^a Photolyses performed in merry-go-round with 450-W medium pressure Hg lamp; 7–10 time points measured for each value of k_p or k_{CB}.
^b Phenol actinometer. ^c Product yields (product/ΔCB) × 100. ^d Actual amount of phenol found. ^e Measured with Cl⁻ ion specific electrode.
^f Photolyzed with Pen-ray low-pressure lamp with >90% emission at 254 nm.

furans form as minor products.

Experimental Procedures

Materials. Chlorobenzene, trichlorobenzene, chlorobiphenyls, and 2-hydroxybiphenyl were 99% pure commercial compounds used as is. The chlorobiphenyl ethers were synthesized at Dow Chemical Co. and were >95% pure judged by high-performance liquid chromatography (HPLC). 2,3,7-Trichloro- and 2,3,7,8-tetrachlorodibenzo-dioxins (TrCDD and TCDD) were supplied by Dow Chemical Co. and were >99% pure by capillary column GC. Water used in the experiments was purified by a Millipore Milli-Q system. Solvents were reagent or chromatography grade.

Photolyses. Most photolyses were performed in a carousel apparatus (Ace Glass) using a Hanovia 450-W mercury lamp filtered only with a Corning 7-54 glass filter to remove light below ~230 and above ~410 nm. The emission spectrum was measured with a Jarrell-Ash 0.25-m spectral monochromator with a 6-in. diffraction grating blazed for 300 nm; light was monitored with an IP28 photomultiplier tube which has a nearly linear response between 220 and 400 nm. Absolute line intensities were estimated relative to that at 313 nm. The 313-nm line intensity was measured with a *p*-nitroacetophenone/pyridine actinometer (24) through a K₂CrO₄ isolation filter solution with a measured 98% cutoff of non-313-nm light. The phenol actinometer was calibrated against a 2.0 × 10⁻³ M hydrazoic acid (HN₃) actinometer (25). HN₃ solutions absorb light uniformly from 248 to 280 nm and thereafter with diminished intensity to 313 nm.

Photolysis solutions were made up in 10-mL quartz cylindrical tubes sealed with Teflon-lined caps. The path length in the tube was estimated to be 10.1 mm by the method of Zepp (26); 4 mL of solution was photolyzed in each tube. Kinetic measurements were based on 7–10 time points in which ln [C]_t was regressed with time *t* to give the slope k_p.

Analyses. Most analyses were performed on a C₁₈-reverse-phase HPLC column with acetonitrile–water solvent and 254- or 280-nm UV detection. TCDD and TrCDD were analyzed on a 10 m × 0.25 mm fused silica DB-5 capillary column (J & W Scientific) fitted to a HP5840A chromatograph with a ⁶³Ni electron capture detector at 302 °C; a 5% methane–95% argon carrier was used at 0.93 cm⁻³ min⁻¹. Chlordane was used as internal standard. UV spectra were measured on a HP5480 UV/vis spectrometer. GC/mass spectrometry was performed on a Ribermag Model R10-10C mass spectrometer.

Chloride ion was measured with a Cl⁻ ion selective electrode against a double-junction reference electrode.

Samples were prepared by photolyzing 25 mL of solution (in six 5-mL quartz tubes), combining the solutions, and reducing the volume to 2 mL (weighed) with a rotary evaporator. All glassware used in these experiments was washed several times with Millipore Milli-Q water to obtain low blank readings.

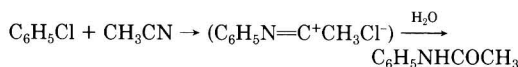
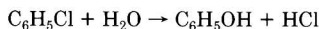
Spectral Data. All spectra were measured on an HP1090 ultraviolet spectrometer with a diode array detector. Absorbances were computed at desired wavelengths by the spectrometer and printed out on individual spectral plots. Most solutions were measured in 1.00 ± 0.01 cm quartz cells at 25 °C.

Detailed spectral listings for each compound discussed here can be obtained from T. Mill.

Results

Chlorobenzene (CB). Chlorobenzene absorbs significant amounts of light only below 300 nm with ε(max) at 264 nm = 180 M⁻¹ cm⁻¹ and ε at 297 nm = 0.12 M⁻¹ cm⁻¹ in water. Therefore, photolyses were performed with a filtered and calibrated multiwavelength 450-W medium-pressure mercury lamp.

A series of experiments was performed with chlorobenzene dissolved in aerated water containing 1% acetonitrile and added isopropyl alcohol, sodium hydroxide, or humic acid. Phenol is the principal product formed under all photolysis conditions in water; exclusion of oxygen had little effect on rates or products. We found several other products attributed to further photolysis of phenol along with acetanilide, the product of substitution of chlorine by acetonitrile. No benzene was detected under any conditions in water. Results of these experiments are listed in Table I.



Quantum yields for photolysis were estimated by photolyzing separately chlorobenzene and phenol solutions and measuring loss of each as a function of time. Phenol was used as a secondary actinometer because it absorbs in the same spectral region as CB and is easy to analyze. Rate constants for loss of chlorobenzene and phenol (k_{CB} and k_p) were estimated from regression of the first-order equation for several time points

$$\ln (C_0/C_t) = kt \quad (1)$$

and, when combined with summed products of UV spectral absorbances and light intensities (∑I_λε_λ) and the quantum

Table II. Phenol Production in Photolysis of 1.57×10^{-4} M Chlorobenzene in Water^a

time, min	ΔCB , $\text{M} \times 10^5$	phenol, $\text{M} \times 10^5$	theor phenol, $\text{M} \times 10^5$ ^b	(obsd/theor) $\times 100$ ^c
0	0	0	0	
120	1.31	0.67	1.09	62
240	2.40 ^c	1.25	1.86	67
360	3.32	1.59	2.40	66
540	4.82	1.92	2.88	67

^a Experiment 1 in Table I. ^b Estimated from eq 3 and values in Table I for k_p and k_{CB} . ^c Calculated value using $k_{\text{CB}} = 1.12 \times 10^{-5} \text{ s}^{-1}$.

Table III. Photolysis of 1,2,4-Trichlorobenzene (TCB)^a

com- pound	[TCB] ^b	solvent	photolysis time, h	% conversion	ϕ ^{c,d}
TCB	1.22 (-4)	H ₂ O (10% AN)	72	49	0.043
TCB	1.00 (-4)	H ₂ O (10% AN), degassed	217	52	0.018
TCB	1.00 (-5)	H ₂ O (10% AN), degassed	216	72	0.025
TCB	2.32 (-4)	hexane	24	95	0.21

^a Photolyses performed with a 450-W mercury source. ^b Powers of ten in parentheses. ^c Values based on phenol actinometer $\phi = 0.050$ with a multiwavelength 450-W Hg source. ^d Six-ten time points were used to calculate k_{TCB} and k_p ; probable error in the ϕ value is $\pm 30\%$.

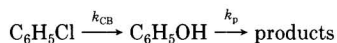
yield for photolysis of phenol ($\phi_p = 0.050$), gives the quantum yield for photolysis of CB (ϕ_{CB}):

$$\phi_{\text{CB}} = \phi_p (k_{\text{CB}}/k_p) (\sum I_{\lambda} \epsilon_{\lambda P} / \sum I_{\lambda} \epsilon_{\lambda \text{CB}}) \quad (2)$$

The value of ϕ_{CB} is large and varies only slightly from 0.37 in water to 0.50 in 0.05 M NaOH. In MeOH, ϕ is 0.26. Quantum yield data also are listed in Table I.

The major product of photolysis of chlorobenzene in water is phenol under all conditions. No benzene was detected, and we estimate that benzene must be less than 1% of the phenol formed. Since phenol formation was nearly the same under pure O₂ or N₂, phenol oxygen must come from water, not O₂. The reaction is only slightly sensitive to pH: a 10⁵-fold increase in [OH⁻] led only to a 50% increase in rate.

To learn if phenol is the principal intermediate formed from chlorobenzene, we performed a kinetic analysis of the sequence



If loss of CB is accounted for entirely by formation of phenol, then the concentrations of phenol at any time t is given by eq 3 (27) (we can ignore acetanilide formation

$$[\text{C}_6\text{H}_5\text{OH}]_t = \frac{[\text{C}_6\text{H}_5\text{Cl}]_0 k_{\text{CB}}}{k_p - k_{\text{CB}}} (e^{-k_{\text{CB}}t} - e^{-k_p t}) \quad (3)$$

Table IV. Photolysis of Chlorobiphenyls and 2-Hydroxybiphenyl in Aerated Water^a

CBP	$10^6[\text{CBP}]$, M	[additives]	photolysis time, h	% conversion	$10^5 k_p$, $\text{s}^{-1 b,c}$	$10^5 k_{\text{CBP}}$, $\text{s}^{-1 c}$	ϕ_{CBP}	products ^d
2-CBP	8.00	10% AN	8	98	2.33 ± 0.16	11.2 ± 0.75	0.29	no BP
2-CBP	8.00	25% AN	8	94	2.33 ± 0.16	9.68 ± 0.16	0.25	no BP
2-CBP	10.0	10% AN	2	50	2.77 ± 0.12	9.62 ± 0.09	0.20	33-35% 2-HOBP in 30 min
2-CBP	8.00	10% AN, HA ^e	2	68	2.77 ± 0.12	8.83 ± 0.13	f	9.5% 2-CH ₃ C(O)NHBP plus 4 products from 2-HOBP
4-CBP	10.0	10% AN	90	91	0.99 ± 0.082	0.36 ± 0.011	0.0020	4-HOBP, products; 90% Cl ⁻¹
2-HOBP	10.8	none	2	21	2.77 ± 0.16	76.8 ± 7.3	0.11	4 products by HPLC

^a All solutions photolyzed with 450-W mercury light (see Table II). ^b Rate constant for loss of phenol. ^c Seven-twelve time points were used to estimate k_p and k_{CBP} . ^d BP is biphenyl. ^e 5 mg of humic acid L⁻¹. ^f No estimate possible since about 50% of light absorbed by HA.

since it constitutes only 2% of chlorobenzene lost). Table II shows analyses of experiment 1 in Table I using eq 3 and indicates that, at conversions of CB to 31%, the amount of phenol formed corresponds only to 62-67% of the amount expected if phenol were the only intermediate. The theoretical yield of phenol decreases from 83% to 60% for conversions of 8-31% of chlorobenzene.

Acetanilide and phenol account for about 65-70% of photolyzed chlorobenzene but HPLC analyses of photolyzed solutions of CB, phenol, and benzene (photolyzed at 254 nm) all showed very polar products eluting with the solvent front. However, we are unable to quantitate the amounts owing to lack of identification and detector response factors.

1,2,4-Trichlorobenzene (TCB). We have measured the value of ϕ for TCB in water at 1.0×10^{-4} M and at 1.0×10^{-5} M to check if there may be solubility or aggregation effects on photolysis of TCB in water; the reported solubility of TCB is 1.6×10^{-4} M (30 mg L⁻¹) (28). The results of several experiments, summarized in Table III, show that over a 10-fold change in concentration ϕ changes only by a factor of 2 and indicates no major aggregation effects. Comparison of the values of ϕ under nitrogen and air indicates that oxygen accelerates photolysis (0.043 vs. 0.013). One measurement was made in hexane at 2.3×10^{-4} M where TCB photolyzed about 5 times faster than in aerated water with a ϕ value of 0.21, the same as reported by Ruzo et al. (15).

Product studies on photolyzed TCB solutions in water gave no evidence either for dichlorophenols or for dichlorobenzenes. No product study was performed on hexane solutions where we assume dichlorobenzenes are the main or sole products.

2- and 4-Chlorobiphenyls and Chlorobiphenyl Ethers. We performed a series of experiments with 2- and 4-chlorobiphenyls and 2- and 4-chlorobiphenyl ethers (2- or 4-CBP and 2- or 4-CBPE) which parallel those performed with chlorobenzene. Solutions of CBPs in 10 or 25% AN-H₂O were photolyzed along with phenol as actinometer by using the same unfiltered 450-W mercury lamp. Products and quantum yields were measured and are listed in Table IV. 2-Chlorobiphenyl photolyzes in water to give mostly 2-hydroxybiphenyl and its photolysis products as well as about 10% 2-acetylbiphenyl, formed by the reaction of acetonitrile with 2-CBP.

We found no biphenyl by HPLC, but the detection limit is 10% of the photolyzed 2-CBP. A trace was detected but not quantitated in the GC/MS. Biphenyl is photolytically stable under these conditions. We found negligible effects of additional AN or humic acid on the rate of photolysis, but since humic acid absorbed about half the light in the experiment without much affect on rate, some sensitized photolysis may have occurred. 2-Hydroxybiphenyl, the major product, photolyzes 9 times faster than 2-CBP. Therefore, we used the same kinetic analysis as we used

Table V. Photolysis of Chlorobiphenyl Ethers (CBPE)^a

CBPE	concn, M	solvent	% conversion	$\phi^{b,c}$	products
2	9.8×10^{-6}	water-10% AN, degassed	37	0.19	89% dibenzofuran
2	1.02×10^{-5}	water-10% AN	33	0.19	70% chloride ion
2	1.24×10^{-4}	hexane, degassed	65	0.97	84% biphenyl ether, 16% dibenzofuran
4	1.89×10^{-4}	water-10% AN	94	0.63	4-hydroxybiphenyl ether and 95% chloride ion
4	2.0×10^{-4}	hexane	50	0.50	

^aAll photolyses performed with 450-W mercury lamp; five to nine time points used to estimate k_p and k_{CBPE} . ^bPhenol actinometer ($\phi = 0.05$) used. ^cStandard error in ϕ is $\pm 33\%$.

Table VI. Photolysis of TCDD and TrCDD in Sunlight and at 313 nm

cmpd	solvent	source	$10^7[\text{TCDD}]_0$, M	time, h	% conversion	$10^6k(\text{tcdd})$, s^{-1} ^a	$10^6k(\text{PNA})$, s^{-1} ^{a,b}	ϕ^c
TCDD	water-AN (90:10)	313 nm	3.61	24	62	14.6 ± 0.9	2.75 ± 0.09	0.0022
TCDD	water-AN (90:10)	sun	3.61	26.3 ^d	49	6.94 ± 0.63	59.4 ± 6.1	0.0007
TCDD	hexane	313 nm	3.36	4	66	76.1 ± 2.1	5.17 ± 1.13	0.049
TrCDD	hexane	313 nm	1.71	70	61	203 ± 48	25.5 ± 0.28	0.20

^aFive to seven time points were used to estimate water constants. ^bActinometers had different concentrations of pyridine in PNA. ^cStandard estimated error in ϕ is $\pm 42\%$. ^dSunlight hours.

for chlorobenzene and found 80–97% of the theoretical yield of 2-hydroxybiphenyl when 1×10^{-5} M 2-CBP was photolyzed for 120 min and analyzed at 30-min intervals. In a parallel experiment chloride ion analysis gave over 90% of the expected chloride ion.

We performed only a few experiments with 4-CBP to measure its quantum yield and chloride ion production. The quantum yield in water-acetonitrile is only 0.002, close to that reported in organic solvents (15). Chloride ion production was nearly quantitative. No biphenyl was detected, and the major product is 4-hydroxybiphenyl identified by GC/MS (see Table IV).

2- and 4-chlorobiphenyl ethers (CBPE) photolyze efficiently in water to liberate nearly quantitative amounts of chloride ion and form either dibenzofuran or 4-hydroxybiphenyl ether, respectively. We measured the quantum yield of 2-CBPE in hexane and water under air and argon and the yields of products (Table V). 2-CBPE photolyzes almost 5 times more efficiently in hexane than in water. In hexane the major product is biphenyl ether (80%); dibenzofuran is formed in less than 20% yield. However, in water 2-CBPE photolyzes almost exclusively to give dibenzofuran (90%); only very small amounts of another product presumed to be the 2-hydroxybiphenyl ether were observed (see Table V). 4-CBPE photolyzes 3 times more efficiently than the 2-isomer and gives a single product in water identified as the corresponding phenol. 4-CBPE photolyzes almost equally fast in hexane as in water.

2,3,7,8-Tetrachlorodibenzodioxin (TCDD) and 2,3,7-Trichlorodibenzodioxin (TrCDD). The low solubility of TCDD in water, reported as 0.2 ppb or 6.2×10^{-10} M (29), required that we use 50:50 water-acetonitrile as solvent with less than 1×10^{-6} M TCDD. The spectrum of TCDD in acetonitrile shows a strong absorbance centered at 309 nm ($\epsilon = 7020 \text{ M}^{-1} \text{ cm}^{-1}$); in hexane the maximum is at 304 nm ($\epsilon = 5640 \text{ M}^{-1} \text{ cm}^{-1}$).

Quantum yield measurements were performed on 3.7×10^{-7} M TCDD solution in 50:50 water-acetonitrile. Analyses of these solutions by GC showed no loss by absorption to walls with time in the dark. Photolyses were performed at 313 nm and in sunlight. PNP/Py actinometers (24) were used to estimate photon fluxes and to calculate the quantum yields. Data are summarized in Table VI. The quantum yield for TCDD in water-acetonitrile is 7×10^{-4} in sunlight and 2.2×10^{-3} at 313 nm. In hexane ϕ is 4.9×10^{-2} or 20 times larger than in water. No products were detected in hexane by GC under

conditions where authentic trichlorodioxin (TrCDD) was easily detected.

Other workers report finding small yields of trichloro (TrCDD) and dichloro congeners on photolysis of TCDD in organic solvents (30). To check the possibility either that TrCDD photolyzes so much faster than TCDD that its steady concentration is below the detection limit or that TCDD photolyzes by another pathway, we measured the spectrum of TrCDD and its quantum yield at 313 nm in hexane where reductive cleavage of C-Cl to C-H should be facile. The absorbance of TrCDD at 313 nm is $2400 \text{ M}^{-1} \text{ cm}^{-1}$, compared to $4100 \text{ M}^{-1} \text{ cm}^{-1}$ for TCDD; the maximum for TrCDD lies near 304 nm where $\epsilon = 2900 \text{ M}^{-1} \text{ cm}^{-1}$. The quantum yield for photolysis of 1.7×10^{-7} M TrCDD in hexane is 0.20 or about 4 times larger than for TCDD (see Table VI). Thus, the rate of photolysis of TrCDD at 313 nm will be more rapid than for TCDD by almost a factor of 3 and will form only in small concentrations under steady illumination.

Kinetic analysis of the sequence



using eq 3 with measured values of k_1 and k_2 at 313 nm of 8.60×10^{-5} and $2.22 \times 10^{-4} \text{ s}^{-1}$, respectively (Table VI), and $[\text{TCDD}]_0$ of 3.40×10^{-7} M gave 6.1×10^{-8} M TrCDD in 60 min; the conversion of TCDD is 27% at 60 min. Since as little as 3×10^{-8} M TrCDD was detectable by GC (10 pg in 1 μL) and we found none at 60 min, we tentatively conclude that some other process such as C-O cleavage also may be important. It is of some interest that the parent dibenzodioxin is nearly as unstable in light as is TCDD or TrCDD (31).

Sunlight Photolysis of Chloroaromatics. Many chloroaromatics absorb sunlight and will photolyze at rates which we can estimate from the relations (32)

$$\text{rate} = k_{pE}[\text{C}] \quad (4)$$

$$k_{pE} = \phi k_a = \phi \sum L_\lambda \epsilon_\lambda \quad (5)$$

where k_a is the light absorption constant, k_{pE} is the photolysis rate constant in sunlight, ϕ is the quantum yield, L_λ is the solar flux (in 2.3×10^{-3} einstein $\text{cm}^{-2} \text{ s}^{-1}$) over a wavelength interval λ , and ϵ_λ is the average extinction coefficient over the same wavelength interval.

We have used quantum yields and measured spectral data for several reactive chloroaromatics to calculate maximum values for k_{pE} at 40° latitude in summer season in surface waters. These data are shown in Table VII. We

Scheme I. Pathways for 2-CBPE

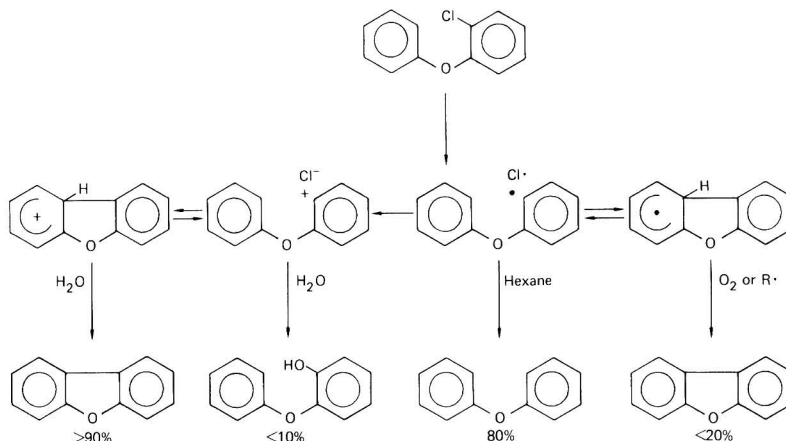


Table VII. Calculated Sunlight Photolysis Rate Constants for Chloroaromatics in Surface Water at 40° L in Summer

chloroaromatic	k_2 , day ⁻¹ ^a	ϕ^b	k_{pE} , day ⁻¹ ^c	$t_{1/2}$ ^d
CB	3.0 (-5)	0.37	1.1 (-5)	170 years
1,2,4-TCB	9.7 (-5)	0.043	4.2 (-6)	450 years
2-CBP	3.7 (-4)	0.29	1.1 (-4)	18 years
4-CBP	0.115	0.002	2.3 (-4)	8.2 years
2,4,2',4'-PCB	0.553	0.10 ^e	0.055	13 days
2-CBPE	0.043	0.12	0.19	3.6 days
4-CBPE	0.0055	0.63	0.0035	200 days
TCDD	76	0.0022	0.15	6 days

^a Calculated from $\sum \epsilon_i L_i$ for summer season. See text and ref 3.
^b Measured value in water (this work) or from published value.
^c Calculated from ϕk_a . ^d $t_{1/2} = 0.69/k_p$. ^e In hexane (15).

also performed a series of photolyses in winter sunlight or simulated sunlight on aqueous solutions of some of these same chloro aromatics to measure rate constants (k_{pE}) for comparison with calculated values of k_{pE} to confirm both spectral and quantum yield information. Table VIII summarizes the results.

Photolyses of 2-CBPE and 2,2',4,4'-TCBP in sunlight and simulated sunlight gave rate constants (k_p) appreciably different from k_p values calculated from eq 5. In the case of 2-CBPE the measured value is about 10 times larger, and in the case of 2,2',4,4'-TCBP the measured value is about 4 times smaller. Both compounds have weak tailing absorption above 300 nm where sunlight intensity became significant. As a result calculations become very sensitive to the exact values of ϵ which are difficult to measure in water.

We should also note that, for many of the chloro aromatics which absorb weakly above 300 nm, indirect photolysis by energy transfer and free radical reactions (33, 34) from dissolved humic acids in natural waters may lead to much faster reactions than will direct photolysis.

Discussion

One of the most important results from this study is our finding that photolyses of all monochloroaromatics (except 2-CBPE) in water are nearly as efficient as in hydrocarbons but give predominately or exclusively the corresponding phenols as primary products. No evidence was found for reduction to benzene, biphenyls, or biphenyl ethers even when good H-atom donors such as humic acid and isopropyl alcohol (35, 36) were present. These results indicate that the reaction pathway is substantially altered on going

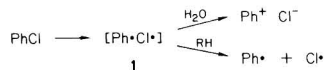
Table VIII. Photolysis of Chlorinated Biphenyls and Biphenyl Ethers in Winter Sunlight at 40° L in Surface Waters

compound	10 ⁵ concn, M	ϕ	k_{pE} (calcd), s ⁻¹ ^a	k_{pE} (measd), s ⁻¹ ^b	$t_{1/2}$ (measd), days
2-CBPE	1.43	0.19	3.1 (-9)	3.4 (-8)	240
4-CBPE	1.80	0.68	3.7 (-8)	<2 (-8) ^c	>400
2,4-DCBP	1.40	0.052 ^c	5.7 (-11)	<2 (-8) ^c	>400
2,4,4'-TCBP	0.57	0.25 ^d	2.2 (-8)	6 (-8)	133
2,2',4,4'-TCBP	0.57	0.19 ^c	2.1 (-7)	5 (-8)	170

^a From $\sum L_i \epsilon_i$; L_i values for 40° L winter season; value in parentheses is power of ten. ^b Photolyzed with xenon lamp for 379 h, equivalent to 16 winter days. ^c From ref 15 in hexane. ^d From ref 17 in hexane. ^e No change in 16 days.

to largely water solvent. Ring closure of 2-CBPE to benzofuran, participation in reactions by acetonitrile, and the lack of significant effect of pH on the quantum yield for chlorobenzene point to phenyl or aryl cations as initial and common intermediates.

To accommodate these features as well as the lack of large solvent effects on quantum yield, we propose that the initial steps in all solvents are the same: (1) excitation to the first excited singlet state followed by either (2) homolytic cleavage of the C-Cl bond or (3) intersystem crossing to the triplet state which also leads to homolytic C-Cl bond cleavage. Chlorobenzene illustrates the process.



The radical pair 1 may diffuse apart either as a radical species in nonpolar media including alcohols or (following electron transfer) as ionic species in water. In hydrocarbons each radical abstracts the H atom from the solvent to form a reduced aromatic and HCl; in water the phenyl or biphenyl cation is rapidly scavenged by available nucleophilic species including, in this case, water and acetonitrile (37).



This mechanism also is more consistent with our observations than one in which the triplet state is the electrophilic species (9, 10) because (1) lack of an oxygen effect

on rates for CB and CBPE indicates that the triplet state lifetimes are too short to be intercepted by solvent (10, 38), (2) lack of pH effect with CB indicates that the intermediate is indiscriminate in its reaction with nucleophiles, a property more likely found in the phenyl cation than a triplet, and (3) near invariance of the quantum yield on going from water to hexane for several chloroaromatics is most consistent with a common primary step, namely C-Cl cleavage.

For 2-CBPE, cyclization to dibenzofuran must proceed via a radical or ionic intermediate; the much higher proportion of furan formed in water compared to hexane again is more easily explained by formation of a cation intermediate in water where proton removal by water from the cyclized intermediate is sufficient to form dibenzofuran; in hexane another radical or oxygen is needed to effect this step. The processes are shown in Scheme I.

Results with polychlorinated aromatics are less clear-cut. TCB and TCDD both photolyze much more efficiently in hexane than in water, and we have not identified any products from aqueous photolysis. Possibly polychlorinated aromatic cations are too destabilized to form readily. In the case of TCDD, cleavage of one Ar-O bond is an alternative pathway as observed in the parent dibenzodioxin (31). This pathway is not important with either 2-chlorobiphenyl ether or 4-chlorobiphenyl ether.

3,4-Dichloroaniline is reported to rapidly photosolvololyze in water to an aryl cation (39) and is more reactive in water than in hexane where a radical process occurs.

Table VII illustrates how spectral overlap of solar irradiance with absorption spectra of chloroaromatics dramatically affects rates: chlorobenzene photolyzes over 100 times more efficiently than TCDD, but because it absorbs almost no solar photons, its half-life in sunlit surface water is over ten thousand times longer. Similar comments apply to the other weakly absorbing biphenyls or biphenyl ethers.

The environmental fate of many chlorinated aromatics especially those with weak or absent solar absorption spectra will be to volatilize from water to the troposphere where either HO· radical oxidation or sorption to particulate will occur. We estimate that for mono- or dichloro aromatics half-lives in atmospheric HO· oxidation will be about 3-5 days; tri- or tetrachloro aromatics will be about half as reactive toward the HO· radical (40).

Photolysis of chloroaromatics in water produces phenols that might react further to form much more toxic benzofurans or dioxins. This possibility arises mostly in polychlorinated biphenyls and biphenyl ethers where 2-chloro-2'-hydroxybiphenyls may photocyclize. Direct photolytic formation of benzofurans as in the case of 2-chlorobiphenyl ether appears to be a common feature of reactions of biphenyl ethers having 2-chloro substituents and deserves further attention. The competition between cyclization and hydroxylation in water or reduction in organic solvents depends on several factors that require quantitative evaluation before we can make reliable estimates of furan production.

Acknowledgments

We thank David Thomas for identification of many reaction products by GC/MS, Brock Neely of Dow Chemical Co for generous samples of chlorobiphenyl ethers, and Ronald Spangord and Dan Combes for TCDD and TrCDD samples and analyses.

Registry No. TCDD, 1746-01-6; CB, 108-90-7; TCB, 120-82-1; 2-CBP, 2051-60-7; 4-CBP, 2051-62-9; 2-CBPE, 2689-07-8; 4-CBPE, 7005-72-3; 2-HOBP, 90-43-7; 4-HOBP, 92-69-3; TrCDD, 58802-17-8; 2,4,2',4'-PCB, 2437-79-8; 2,4-DCBP, 33284-50-3; 2,4,4'-TCBP,

7012-37-5; C₆H₅OH, 108-95-2; dibenzofuran, 132-64-9.

Literature Cited

- (1) Hileman, B. *Environ. Sci. Technol.* **1983**, *17*, 11a.
- (2) Poiger, H.; Schlatter, C. *Chemosphere* **1983**, *12*, 453.
- (3) Rawls, R. L. *Chem. Eng. News* **1983**, *61* (23), 37.
- (4) Corbet, R. L.; Muir, D. C. G.; Webster, G. R. B. *Chemosphere* **1983**, *12*, 523.
- (5) Ward, C. T.; Matsumara, F. *Arch. Environ. Contam. Toxicol.* **1978**, *7*, 349.
- (6) Pinhey, J. T.; Rigby, R. D. G. *Tetrahedron Lett.* **1969**, 1267.
- (7) Fox, M. A.; Nichols, W. C.; Lemal, D. M. *J. Am. Chem. Soc.* **1973**, *95*, 8164.
- (8) Arnold, D. R.; Long, P. C. *J. Am. Chem. Soc.* **1977**, *99*, 3361.
- (9) Tissot, A.; Boule, P.; Lemaire, J. *Chemosphere* **1983**, *12*, 859.
- (10) Tissot, A.; Boule, P.; Lemaire, J. *Chemosphere* **1984**, *13*, 381.
- (11) Ichimura, T.; Mori, Y. *J. Chem. Phys.* **1973**, *58*, 288.
- (12) Bunce, N. H.; Bergsma, J. P.; Graff, W. De; Kumar, Y.; Ravanal, L. *J. Org. Chem.* **1980**, *45*, 3708.
- (13) Bunce, N. J.; Kumar, Y. *Chemosphere* **1978**, *7*, 155.
- (14) Bunce, N. J. *Chemosphere* **1982**, *11*, 701.
- (15) Ruza, L. O.; Zabik, M. J.; Schuetz, R. D. *J. Am. Chem. Soc.* **1974**, *96*, 3809.
- (16) Choudhry, G. G.; Sundstrom, G.; Ruza, L. O.; Hutzinger, O. *J. Agric. Food Chem.* **1977**, *25*, 1371.
- (17) Bunce, N. J.; Kumar, Y.; Ravanal, L.; Safe, S. *J. Chem. Soc., Perkin Trans. 2*, **1978**, 880.
- (18) Bunce, N. J.; Hayes, P.; Lemke, D. *Can. J. Chem.* **1983**, *61*, 1103.
- (19) Nishiwaki, T.; Shinoda, T.; Anda, K.; Hida, M. *Bull. Chem. Soc. Jpn.* **1982**, *55*, 3569.
- (20) Ruza, L. O.; Safe, S.; Zabik, M. J. *J. Agric. Food Chem.* **1975**, *23*, 594.
- (21) Crosby, D. G.; Wong, A. S.; Plimmer, J. R.; Woolson, E. A. *Science (Washington, D.C.)* **1971**, *173*, 748.
- (22) Choudhry, G. G.; Hutzinger, O. *Residue Rev.* **1982**, *84*, 115.
- (23) Crosby, D.; Moilanen, K. N. *Science (Washington, D.C.)* **1977**, *195*, 1337.
- (24) Dulin, D.; Mill, T. *Environ. Sci. Technol.* **1982**, *11*, 815.
- (25) Shapiro, D.; Trieninin, A. *J. Phys. Chem.* **1973**, *77*, 1195.
- (26) Zepp, R. G. *Environ. Sci. Technol.* **1978**, *12*, 327.
- (27) Frost, A. A.; Pearson, R. G. "Kinetics and Mechanism"; Wiley: New York, 1953; p 153.
- (28) "Technical Data Bulletin for 1,2,4-Trichlorobenzene, Organic Chemicals Development"; Dow Chemical USA, Midland, MI, 1978.
- (29) Crummett, W. B.; Stehl, R. H. *Environ. Health Perspect.* **1973**, *15*, 230.
- (30) Desideri, A.; Domenico, A. D.; Vanzati, R.; Tancioni, P.; Muccio, A. *Boll. Chim. Farm.* **1979**, *118*, 274.
- (31) Plimmer, J. R.; Klingbiel, U. I.; Crosby, D. G.; Wong, A. S. *Adv. Chem. Ser.* **1973**, No. 120, 44.
- (32) Mill, T.; Mabey, W. R.; Bomberger, D. C.; Chou, T.-C.; Hendry, D. G.; Smith, A. H. "Laboratory Protocols for Evaluating the Fate of Organic Chemicals in Air and Water", 1981, EPA Report EPA 600/3-82-022.
- (33) Zepp, R. G.; Baughman, G. L.; Schlozhauser, B. F. *Chemosphere* **1981**, *10*, 109.
- (34) Baxter, R. M.; Carey, J. H. *Nature (London)* **1983**, *306*, 575.
- (35) Pohlman, A.; Mill, T. *Soil. Sci. Soc. Am. J.* **1983**, *47*, 1923.
- (36) Scaiano, J. C.; Stewart, L. C. *J. Am. Chem. Soc.* **1983**, *105*, 3609.
- (37) Scaiano, J. C.; Nguyen, K.-T. *J. Photochem.* **1983**, *23*, 269.
- (38) Turro, N. "Modern Molecular Photochemistry"; Benjamin/Cummings Publishing Co., Inc.: Menlo Park, CA, 1978; p 354.
- (39) Miller, G. C.; Miller, M. J.; Crosby, D. G.; Sontum, S.; Zepp, R. G. *Tetrahedron* **1979**, *35*, 1797.
- (40) Davenport, J.; Hendry, D. G.; Gu, L.; Mill, T., SRI, unpublished results, 1984.

Received for review November 9, 1984. Revised manuscript received April 29, 1985. Accepted July 29, 1985.

A Comparative Study of Combustion in Kerosene Heaters

Trudy Lionel, Richard J. Martin, and Nancy J. Brown*

Applied Science Division, Lawrence Berkeley Laboratory, University of California, Berkeley, California 94720

■ The combustion characteristics of radiant, convective, and multistage kerosene heaters have been determined and compared. Two types of experiments were conducted. In the first of these, composition and temperature were measured as a function of axial position in the heater to determine the progress of combustion. In the second type, composition, fuel consumption rate, temperature, pressure, and exhaust stream mass flow rate were measured in an exhaust manifold to ascertain the effect of heater type and heater operating conditions on exhaust gas composition. Fuel consumption was sensitive to wick height, wick age, and volume of fuel in the tank. Heater design strongly influenced emission rates. The convective and multistage heaters produced the smallest amounts of CO (per kilojoule). The radiant heater produced the largest amounts of CO and the smallest amounts of NO_x. The convective heater produced the largest amounts of NO_x. Results were compared with chamber and other laboratory studies, and agreement among the various studies was found to be quite satisfactory.

Introduction

Energy conservation can be achieved in the home environment by modifications of ventilation, insulation, and heating. The use of space heaters in residences has become more popular as the cost of central heating has increased. Kerosene heaters offer a truly portable alternative to electric, natural gas, or oil-fired heaters; however, their unvented design necessitates consideration of the effects of combustion emissions in the indoor environment. The rate of air infiltration is closely coupled to emission levels in affecting the indoor air quality.

Descriptions of the emissions produced by kerosene heaters have involved three types of experiments: laboratory studies characterizing exhaust concentrations (1), environmental chamber studies (2-4), and field studies in houses (5-7). The indoor air pollutants carbon monoxide (CO), sulfur dioxide (SO₂), oxides of nitrogen (NO_x = NO₂ + NO), carbon dioxide (CO₂), unburned hydrocarbons and particulates have been detected.

Emissions of NO_x were first detected in laboratory studies (1) in the exhaust of radiant and convective types of kerosene heaters. In order to simulate the operation of kerosene heaters, environmental chamber "test rooms" were constructed to control ventilation rates to values expected in residences. In two separate chamber studies (3, 4), occupational health standards for CO₂ and ambient air quality standards for NO₂ were exceeded for both radiant and convective types of kerosene heaters. Radiant heaters also produced cautionary levels of CO in small rooms. Leaderer (3) measured levels of SO₂ in excess of ambient air quality standards. Traynor et al. (4) observed that reducing wick heights led to reduced rates of combustion but increased CO and formaldehyde emissions rates.

The next step in characterization of kerosene heater pollutant emissions was to examine their concentrations in actual residences. In a typical Japanese living room, the decay process of NO₂ generated from a convective heater was found to follow first-order kinetics (7). A study in a Canadian test house (5) indicated that operation in

large ventilated rooms produced more acceptable, lower concentrations of CO and NO_x than in small rooms. An extensive study (6) of over 300 residences in Connecticut indicated that concentrations of CO₂, NO₂, and SO₂ exceeded ambient standards during peak exposures. In homes with an additional combustion source such as a gas stove or a second kerosene heater, higher NO₂ concentrations were detected.

In this paper we will compare the combustion characteristics of radiant, convective, and multistage kerosene heaters. All heaters have a wick (first stage) to introduce kerosene to the primary combustion chamber (second stage) where much of the combustion occurs. Experiments have been performed to ascertain the effects of heater design and heater operating conditions on exhaust gas composition.

Experimental Section

Description of Apparatus. An exhaust and sampling manifold was designed and positioned above the kerosene heater in order to completely mix the products of combustion while producing no effect upon the burning characteristics (see Figure 1). Measurements were carried out with each heater positioned such that its top was at the same height as the bottom of the exhaust manifold. Probe ports were located in the manifold at three different axial positions, 5 cm apart. Each position had two tapped ports 90° apart to permit probing at different radial positions. In addition, samples could be obtained from inside the heaters by inserting probes through openings in the structure. The multistage heater was modified to allow vertical probing through any of three tapped ports located at and near the heater top. Probe repositioning was possible while a heater was operating; however, the uncertainty in positioning was approximately 0.2 mm in the sampling manifold and approximately 2.0 mm inside a heater.

Samples were withdrawn through probes constructed from 3.0 mm o.d. × 2.0 mm i.d. quartz tubing with tips narrowed to an orifice diameter of 0.3-0.5 mm. In general, straight probes were used, with the exception of sampling done at the top of the second stage of the multistage heater where it was necessary to bend the quartz tubing to reach the flame zone. The probes were connected by filtered heated Teflon lines to either a gas chromatograph, a nondispersive infrared analyzer, a chemiluminescence analyzer, or a pulsed fluorescence analyzer. Each analyzer was equipped with a pump for sample extraction. Combustion products detected were hydrocarbons, particulates, CO₂, NO₂, SO₂, CO, NO, O₂, and N₂. Additional diagnostic information was obtained from a series of measurements characterizing physical parameters, e.g., temperature, pressure, fuel consumption, and flow velocity.

Fuel uniformity was assured by the purchase of two barrels of kerosene (Union Oil K-1). The fuel was analyzed at the University of California microchemical analysis and mass spectrometer laboratories. The elemental composition was determined which yielded a kerosene carbon-hydrogen mass ratio of 6.38 and a sulfur content of 0.04% by weight. The limit of detectability for nitrogen was 0.01 mass %; nitrogen in excess of this amount was not reported.

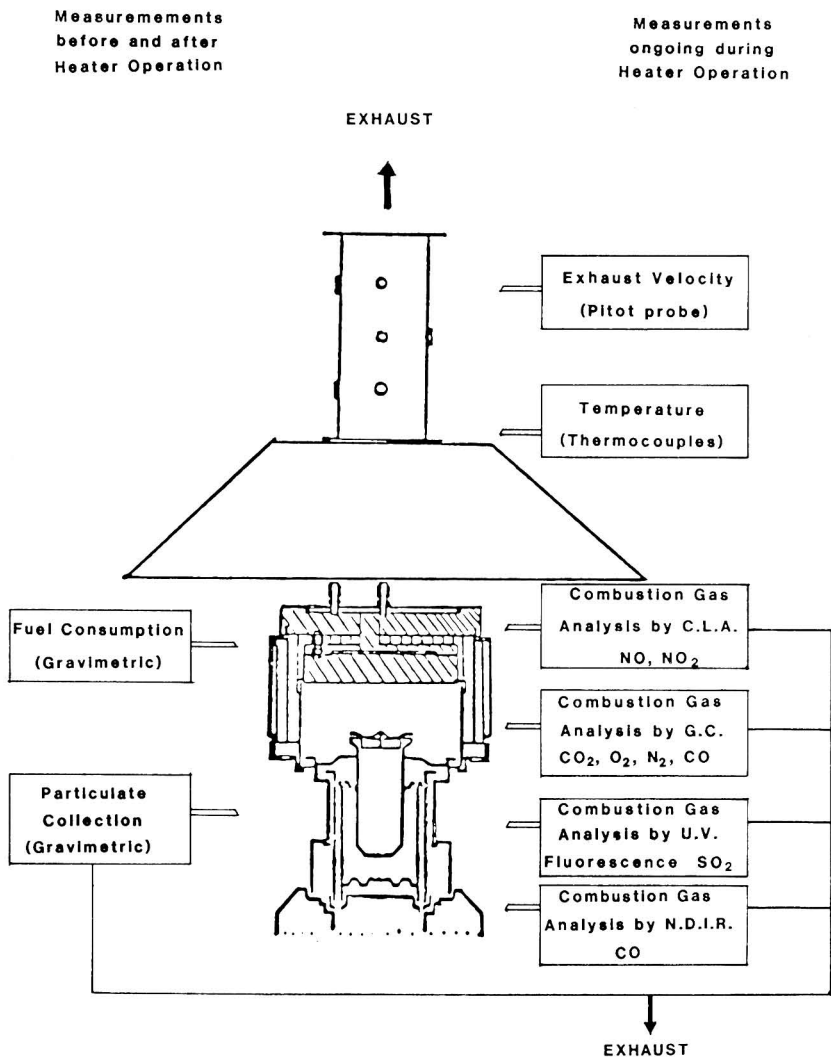


Figure 1. Schematic diagram of experimental apparatus: C.L.A., chemiluminescence analyzer; G.C., gas chromatograph; N.D.I.R., nondispersive infrared analyzer.

Chemical Analysis. Oxides of nitrogen were measured with a chemiluminescence analyzer (CLA), Thermo-Electron Model 14A, modified with heated sample capillaries to minimize H₂O condensation. Calibration was carried out with standards of NO₂ in N₂, NO in N₂, and a very dilute mixture of the two oxides in N₂. These standards were independently verified by the Industrial Hygiene Laboratory of the California State Department of Health. Analyzer linearity was checked by dilution of standard mixtures with N₂ to prepare concentrations down to the very low ppm range. The measurements of NO_x and NO made on the kerosene heater are sensitive to within 0.1 ppm.

Total hydrocarbons, CO₂, CO, O₂, and N₂ were measured with a gas chromatograph (GC), Hewlett-Packard Model 5880A. In order to measure CO₂, CO, O₂, and N₂, a temperature programmed series/bypass configuration was prepared with Porapak Q and Molecular Sieve 5A columns attached to a thermal conductivity detector. At the same time, samples were analyzed for total hydrocarbon content

with a flame ionization detector. Carbon monoxide was only detectable to approximately 100 ppm by this method. Water was determined by difference and compared well with the values predicted from the stoichiometry of kerosene combustion. Both pure gases and prepared mixtures simulating combustion exhaust concentrations were used to calibrate for atmospheric pressure sampling. Chromatograms of gas samples were integrated and compared with the calibrations automatically. The precision of the gas chromatograph measurements was better than 2% for oxygen and nitrogen at their atmospheric concentration levels. At levels found in the emissions, CO₂ and CO could be detected to better than 2% precision. Hydrocarbons could be detected at better than 3% precision.

Carbon monoxide was detected in the very low ppm range with a nondispersive infrared analyzer (NDIR), Bendix Model 8501-5CA. Calibration was achieved by comparison with a standard of CO in N₂. The concentration of the calibration gas was also verified at the Industrial Hygiene Laboratory of the Department of Health.

Analyzer linearity was again confirmed by dilution with N₂, and the sensitivity of measurements of CO was within 0.1 ppm.

Sulfur dioxide was measured with a pulsed fluorescence analyzer, Thermo-Electron Series 40, calibrating with standards of SO₂ in N₂. It was necessary to ensure that H₂O present in the combustion emissions did not interfere with detection by solution of SO₂ or by quenching of fluorescence (8).

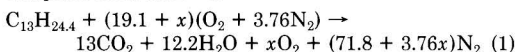
Particulates were deposited by rotary oil pump suction through a 0.5- μ m Teflon filter (Millipore) attached to a sampling probe, and weighed on an electronic balance (Mettler Model AE163) with precision to 0.02 mg.

Physical Measurements. Fuel consumption rate was measured gravimetrically by a triple-beam balance, with precision to 1 g in 20 kg. Temperatures were measured both in the exhaust manifold and in the heater interiors. Chromel-alumel thermocouples, with exposed junctions and 1.0-mm bead diameters were used for all temperature measurements. Reported data are not corrected for radiation or conduction losses. Radiation error will be completely negligible in the exhaust manifold where temperatures are below 520 K. In the heater combustion chambers, where peak temperatures do not exceed 1120 K, radiation error is likely to be less than 10 deg. In the third stage of the multistage heater, temperatures are expected to reach 1470 K at the flame front. Here the radiation loss from the thermocouple junction and particulate adhesion to the thermocouples could induce much larger measurement errors. Static pressures in the naturally aspirated heater and in the exhaust manifold varied less than 0.02 mmHg from the local barometric pressure of approximately 740 mmHg. Air flow rates were not monitored since air is entrained into all three kerosene heaters at the base and above the wick in the convective and multistage designs. The heater would have had to be placed in a fairly large chamber to monitor air inflow and not alter the combustion characteristics. Exhaust gas mass flow rate in the exhaust manifold was determined from measured velocities, temperatures, and pressures. Velocity was measured by a 3.17 mm o.d. Pitot probe aligned at various locations where the flow was fully developed in the manifold. Differential pressures were measured with a Dwyer-Microtector manometer. Sensitivity of the manometer was 0.01 mm of the water column height, resulting in better than 10% precision for the measured velocity.

Results and Discussion

Experiments were performed on radiant, convective, and multistage heaters to acquire an understanding of the combustion occurring. The experiments were of two types. In the first type composition and temperature were measured at different spatial locations in the heater to determine the progress of combustion as a function of axial position. In the second type, composition, temperature, pressure, and exhaust gas mass flow rate were measured in the exhaust manifold to ascertain the effect of heater type and heater operating conditions on exhaust gas composition.

It is useful to indicate the overall stoichiometry of kerosene burning. The balanced chemical equation for complete combustion is



The chemical formula for kerosene is determined from the elemental analysis and the fact that the average number of carbon atoms per hydrocarbon in kerosene is 13. The symbol x in the above balanced reaction is the number of

moles of excess oxygen present, which can be determined from the measured exhaust concentrations of N₂, O₂, and CO₂, after assuming complete combustion.

Combustion Characteristics. The kerosene heaters selected for study consist of three major parts. The first of these is the wick, which is a circular ring of woven fiberglass, where fuel evaporation occurs. Temperatures immediately above the wick area are on the order of 470 K. The wick is enclosed by two concentric perforated metal cylinders, which are in turn enclosed by a Pyrex cylinder in the radiant and multistage heaters. A significant amount of combustion occurs in the region between the metal cylinders. Temperatures in the chamber rise quickly from approximately 470 K directly over the wick to 1070 K and remain between 1070 and 1170 K up to the top of the cylinder. The third section of the heater functions to mix the products of combustion and increase the residence time available for combustion. In the radiant design, this section is the space surrounding the combustion chamber and enclosed on all but one side by reflective surfaces to radiate heat outward. In the convective and multistage heaters, the third section is a closed cylinder, either constructed of metal and enclosing the combustion chamber (convective) or constructed of glass and placed on top of it (multistage). Within the third section, products of incomplete combustion remaining after second stage burning are converted to CO₂ and H₂O. Mixing is improved, and the opportunity for more complete combustion is enhanced. Temperatures are higher in the multistage heater's third section than in the second section. Temperatures as high as 1332 K have been measured near the flame contours. Above the contours, at the top of this section, temperatures are nearly uniform at approximately 870 K in both the convective and multistage heaters. The third section temperatures do vary radially near the flame contour, as this is where the buoyancy-driven mixing of combustion products and dilution air is initiated.

Air and fuel mixing in these and other heaters in the U.S. marketplace is accomplished by natural convection and diffusion. Most of the air enters from a series of holes located at the heater base, below the wick. A large column of air enters within the area enclosed by the wick; a large volume fraction of this center air flow is not mixed with fuel or products of combustion until the third section or later. Air is also entrained from the base of the heater around the exterior wall of the outermost metal cylinder, flowing upward to be used for combustion in the second section combustion chamber and for cooling the exterior walls of the heater. In the multistage heater, additional air is introduced through holes located near the boundary of the second and third sections. Mixing of fuel and oxidizer is enhanced by various flow diversion structures at the top of the combustion chamber ranging from a circular coil and umbrella-shape in the radiant heater to a cone and disc in the multistage heater. In the convective and multistage designs, flaming combustion continues up into the third section, about the periphery of the flow diversion disk. A series of temperature measurements in the multistage heater indicate that the flow field is axially symmetric over the wick, in most of the second section, and at the end of the third section, but not at the interface between the second and third sections.

An understanding of the combustion characteristics of the newer design multistage heater can be obtained by reviewing the results of experiments of the first type which are summarized in Table I. The data in Table I were taken at a fixed radial position from variable axial positions in the heater, as shown in Figure 2. The axial profile,

Table I. Multistage Heater Axial Profile

position ^a	ϕ^b	CO ₂ , %	O ₂ , %	N ₂ , %	HC, % ^c	CO, %	NO _x , ppm	NO ₂ , ppm	NO, ppm	temp, K
1		~5.2	~10.0	~65.1	0.114	~0.37	16.9	8.5	8.4	
2	2.64	5.23	13.4	75.4	0.0016	0.019	21.8	13.5	8.2	1080
3 ^c	14.1	0.98	19.1	75.7	ND ^d	0.016	1.5	0.1	1.4	1210
4		12.0	2.77	77.9	0.0201	1.40	18.8	2.1	16.6	1330
5	2.20	6.40	11.6	77.3	ND	0.049				
6	1.99	7.06	10.9	76.8	ND	ND	11.9	1.6	10.2	
7	2.02	7.04	11.2	77.9	ND	ND	10.0	ND	10.2	
8	1.92	7.18	10.4	75.6	ND	ND	12.6	2.0	10.5	
9	1.84	7.56	9.94	76.0	ND	ND				950

^a See Figure 2. ^b (Air/fuel)/(air/fuel)_{stoichiometric} estimated from measured O₂ and N₂ and assuming complete combustion. ^c Outside of flame contour, inflow of dilution air. ^d Nondetectable. ^e HC, hydrocarbons.

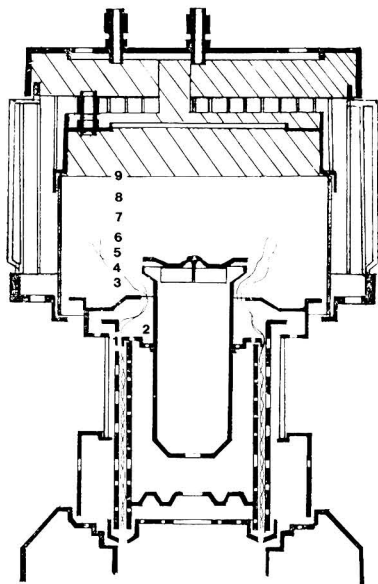


Figure 2. Schematic diagram showing the axial probing positions in a cross section of the multistage heater. The flaming combustion zone is indicated by wavy lines which pass through position 4.

which will be described, is in a region of strong gradients. Measurements of temperature and composition at these positions are therefore likely to represent an average over more than one probe diameter, rather than a particular value at a point. In these experiments, hydrocarbons, CO₂, NO₂, NO, CO, N₂, and O₂ were measured. The quantity ϕ , the inverse-equivalence ratio, is defined in the usual way of (air/fuel)/(air/fuel)_{stoichiometric} and is determined from measured CO₂, O₂, and N₂. The calculated equivalence ratio is somewhat in error when CO concentrations are appreciable. Tabulated values of ϕ are computed after assuming complete combustion and are useful for quantifying the large amount of dilution air present. It was not possible to measure composition at axial positions directly above the wick in the combustion chamber. This is due to interference by hydrocarbons, consisting of a wide range of products of incompletely combusted kerosene, which condense in probes and make quantitative analysis of the gaseous products of combustion very difficult.

The first entry in Table I is representative of the area above the wick and near the top of the combustion chamber, where the temperature is approximately 1070 K. Relatively large CO and hydrocarbon concentrations are found, which indicate incomplete combustion at this location (position 1 in Figure 2). A large NO_x concentration

Table II. Symmetry of Product Composition Inside Third Stage

position	ϕ	CO ₂ %	O ₂ , %	N ₂ , %
near top third stage	1.84	7.56	9.94	76.0
rotated 90°	1.75	8.05	9.81	77.2
above flame third stage	2.02	7.04	11.16	77.9
rotated 90°	1.85	7.53	10.03	76.6
rotated 180°	1.79	7.85	9.76	76.7

results from the formation of most of the NO_x before the third section, and the contributing NO₂ and NO concentrations are nearly equal. The second entry in the table indicates the conditions toward the center of the heater out of the flaming zone and influenced by the central air column dilution. The third entry is representative of composition at the beginning of the convection section just below and outside the flame. Here products of combustion have been mixed with a relatively large amount of dilution air as reflected in the large value for the equivalence ratio. Note that the CO concentration is still appreciable. The entry designated 4 is for a sample taken from the convective section inside the flame contour, where hydrocarbons and CO are relatively abundant and the NO_x is present mainly as NO. Compositions are next indicated at position 5, above the flame contour in a region of more dilution than the previous entry. Within experimental error, the data reveal that the CO → CO₂ burnout occurs between positions 4 and 6. The next four entries in the table are, to within experimental uncertainty, nearly equivalent. They indicate that (1) combustion is complete, with no measurable CO and hydrocarbons (detected with the GC), and (2) after passage through the flame zone, the NO_x along this axis is mostly present as NO.

To investigate symmetry inside the third section of the multistage heater, measurements were made at various points around an axis, at fixed radial positions above the flame zone. Figure 2 indicates the positioning of the probe for these experiments, corresponding to the axial locations designated by positions 7 and 9. Compositions were the same as positions 7 and 9 in Table I, and axial symmetry was found. Examination of Table II, where these data are summarized, reveals that the products of combustion are quite well mixed before reaching the top of the third section. Combustion is again nearly complete as evidenced by hydrocarbon and CO concentrations below the limit of GC detectability.

Measurements in the Exhaust Manifold. Prior to conducting experiments to determine the effect of operating parameters on final gas composition, measurements were performed to verify reproducibility of the heater combustion and to determine the uniformity of conditions in the sampling manifold. Early measurements were performed with the exhaust manifold open to the laboratory above the level of the sample ports; in later mea-

Table III. Summary of Fuel Consumption Rates

heater and wick position	no. of data	fuel consumption rate, g/h	heat release ^a rate, kJ/h	manufacturer's rating, kJ/h
radiant, high	3	191 ± 6	8250 ± 260	10 100
convective, high	3	258 ± 13	11 100 ± 560	13 800
multistage high	15	360 ± 14	15 600 ± 600	18 500
medium	4	320 ± 26	13 800 ± 1120	
low	3	299 ± 27	12 900 ± 1170	

^a Kerosene heat content = 43.2 kJ/g; 1.000 kJ/h = 0.948 Btu/h.

surements, the manifold was connected to an externally directed vent. Radial temperature and velocity profiles were measured in the exhaust duct, to determine whether conditions were uniform. The temperature profile, shown in Figure 3, was measured 15.2 cm downstream of the manifold inlet. The profile was nearly uniform across much of the central region and exhibited steeper gradients near the wall. The shape of the profile is typical of turbulent flow in circular ducts. When the exhaust manifold was open, the velocity profile consisted of flow rates measured at the lower limit of a simple Pitot tube with an uncertainty of ±10%. However, when the exhaust was directed externally and a new Prandtl-type differential pressure probe was used, the measured values were very close to flow rates computed from fuel consumption and measured CO₂ concentrations.

Emissions in the heater exhaust were also examined at different positions in the manifold to test for uniformity of mixing. Measurements of combustion product gases at different radial and axial positions were found to be most uniform with the multistage heater and less for the convective design. The radiant heater was least uniform because it is designed to radiate some heat asymmetrically outward, rather than allowing the hot gases to rise uniformly upward by convection.

All three heaters are designed to allow the wick position to be altered to modify the heat output. Adjustment is over a much greater range in the multistage heater than with the radiant and convective heaters and is designed to be reproducible by the use of a graduated scale next to the wick height adjustment.

A good indication that the heater operates reproducibly is the consistency of fuel consumption rate measurements. Table III summarizes fuel consumption rates for three different heaters and shows the effect of different wick heights on the fuel consumption data. The data indicate that the fuel consumption rate and hence the heat release rate vary directly with wick position in the multistage heater. The largest measured deviation from the mean fuel consumption rate is only 5% for heaters with wicks in the high position. Reasons for the greater deviation in the medium and low settings will be discussed subsequently. As the wick height is reduced, less fuel is delivered for evaporation and combustion, thus reducing the heat release rate. The range of adjustment in heating rate is seen from

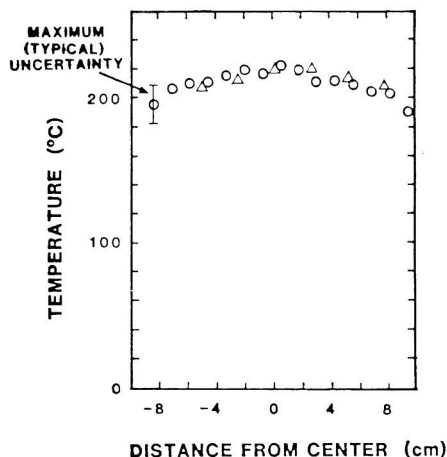


Figure 3. Temperatures (in °C) as a function of distance from the center line (cm) of the exhaust stack, measured with a 0.10-cm diameter inconel-sheathed chromel-alumel thermocouple. Symbols represent insertion through the top left port (O) or top right port (Δ); maximum typical uncertainty is 20 °C.

the data to be approximately 20%, which is lower than the manufacturer's specification of 30%. The average heat release rate (15 600 kJ/h) for this multistage heater is 16% lower than the manufacturer's claim of 18 500 kJ/h. The radiant heater (rated at 10 100 kJ/h) and the convective heater (rated at 13 800 kJ/h) are found to be similarly low in heat output (11% and 16%, respectively) at their maximum wick settings.

When the multistage heater was relatively new, a set of experiments was performed to ascertain the effect of different wick heights on combustion. These experiments yielded heat release rates closer to manufacturer's specifications. The variation in wick height between the low and high positions produced differences in heat release rates of 30% in accord with the manufacturer's specification. When experiments of this type were repeated several months later, using the same, but aged wick, it was not possible to reproduce the earlier results. Thus, wick aging affects the burning rate and emission concentrations. Exhaust measurements for the multistage heater operating with a newer wick are summarized in Table IV, and those for the same heater with an aged wick are given in Table V. Carbon monoxide was measured with the NDIR analyzer for the experiments with the aged wick. Samples for all the exhaust measurements were extracted from the topmost port of the exhaust manifold, with the probe positioned along the center line.

In Table IV, the fuel consumption, CO₂ concentration, and NO concentrations increase with wick height. The air dilution in the manifold expressed in terms of inverse-equivalence ratio decreases with increasing wick height since the combustion products are a larger part of the bulk flow. Wick position also alters the combustion zone ap-

Table IV. Multistage Heater Exhaust Measurements

wick height	fuel consumption, g/h	φ	emissions ^a					exhaust temp., K
			CO ₂ , %	O ₂ , %	N ₂ , %	NO, ppm	NO ₂ , ppm	
high	356	8.4	1.65	18.4	76.8	2.4	ND ^b	490
high	348	8.4	1.67	18.5	77.5	2.4	ND	490
medium	303	9.1	1.56	18.8	78.0	1.9	0.1	470
low	271	9.7	1.44	18.7	77.0	1.5	0.2	450

^a As measured in exhaust manifold. ^b Nondetectable.

Table V. Multistage Heater Exhaust Measurements

wick height	fuel consumption, g/h	ϕ	emissions ^a						exhaust temp., K
			CO ₂ , %	O ₂ , %	N ₂ , %	CO, ppm	NO, ppm	NO ₂ , ppm	
high ^b	370	10.3	1.39	19.9	77.8	0.7	2.1	0.8	460
high	342	10.1	1.41	19.3	78.0	1.4	1.7		470
high	338	10.2	1.40	19.1	78.3		1.6	1.0	450
low	323	11.2	1.28	20.0	78.2	1.1	1.6	0.7	440
low	316	10.0	1.46	19.2	80.1	1.2	1.7	0.8	440
med ^c	294	10.4	1.36	19.2	78.2	2.3	1.3	0.8	450
low	269	12.5	1.14	19.6	78.4	4.4	1.1	1.1	450

^a As measured in exhaust manifold. ^b Fuel tank completely full at beginning of experiment. ^c Very low fuel tank an end of experiment.

Table VI. Comparison of Heaters

heater ^b	fuel consumption, kJ/h	ϕ	emission rates, ^a ($\mu\text{g}/\text{kJ}$)				temp, K
			CO ₂	CO	NO	NO ₂	
radiant	8040	12.8	85000				390
	8160	13.8	81000	130	1.7	5.6	400
convective	11300	10.5	78000				440
	11600	11.1	76000	8.0	16.3	5.6	430
multistage	14800	10.1	72000	4.6	6.0		470
	14600	10.2	75000		5.7	5.6	450
	16000	10.3	77000	2.4	7.5	4.3	460

^a Emission rate ($\mu\text{g}/\text{kJ}$) computed from measured exhaust concentrations and fuel consumption. ^b All measurements performed with wick in high position.

pearance. There is an obvious lowering of the bottom of the luminous portion of the flame from the third stage, down into the top of the second stage as the wick height is decreased. In general, the newer the wick, the greater the fuel consumption for a given wick setting.

Table V summarizes data for fuel consumption, CO, NO, and NO₂, taken in the exhaust manifold for the multistage heater. The data are given in descending order of fuel consumption and include data for aged wicks, different wick heights, and different amounts of fuel in the tank. Fuel consumption and flame appearance are influenced by the amount of fuel in the tank. Most experiments were performed when the fuel tank was neither filled to capacity nor nearly empty. Filling the tank to capacity increases fuel consumption. In Table V, for the cases when heater fuel consumption was in excess of 300 g/h, CO concentrations appear to be unaffected by fuel consumption rate; however, the CO emissions are much higher for the lowest value of the fuel consumption rate. The measured NO concentration varies directly with fuel consumption rate. This is illustrated in Figure 4 where NO emissions expressed in terms of micrograms per kilojoule of fuel are plotted vs. fuel consumption. A straight line is drawn through the data for clarity and to indicate the approximate linear relationship. The dependence of NO on fuel consumption is nearly first-order behavior. The measured NO₂ concentrations show a curious lack of systematic behavior, and thus, total NO_x does not vary significantly with total fuel consumption.

Calculated values for SO₂ in the exhaust of the multistage heater, based upon the sulfur concentration in the fuel, are 3 ppm. We did not detect any SO₂ in the exhaust of the multistage heater. Particulate sampling experiments were performed in the exhaust manifold by using 0.5- μm pore size filter elements and a sampling flow rate of approximately 14 L/min. Particulate mass captured during experiments with each of the heaters in operation never exceeded ambient capture levels. Suitable equipment for detecting or capturing very fine particles was not available.

Table VI contains a summary of the combustion characteristics of all three heaters. The amount of air dilution

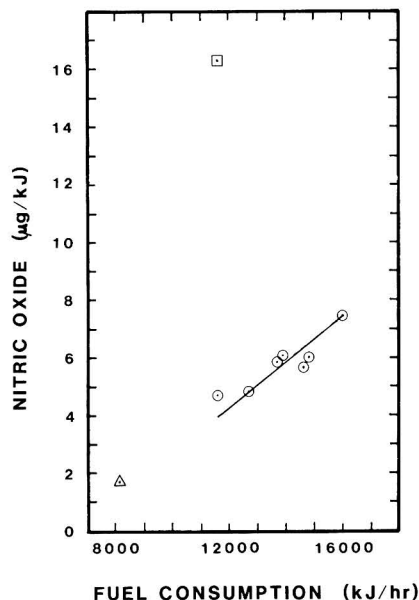
NITRIC OXIDE VS FUEL CONSUMPTION

Figure 4. Nitric oxide emission rates ($\mu\text{g}/\text{kJ}$) as a function of fuel consumption in (kJ/h). Data are not adjusted for ambient concentrations. The probe is located at the center line of the exhaust manifold. Symbols represent the multistage heater (O), the radiant heater (Δ), and the convective heater (\square).

in the exhaust stack, as indicated by the values of inverse-equivalence ratio, is inversely related to the fuel consumption rate. The amount of CO₂ emitted to the exhaust per kilojoule heat output is listed for the heaters and is based upon measured CO₂, O₂, and N₂ concentrations, exhaust flow rates, and fuel consumption rates. If one assumes complete combustion and the stoichiometry

Table VII. Comparison of Heaters

heater ^b	fuel consumption, kJ/h	emission rates ^a μg/kJ		
		CO	NO	NO ₂
radiant	8160	125 ± 0.6	1.4 ± 0.7	3.7 ± 1.0
convective	11600	0.8 ± 0.5	15.5 ± 0.5	3.0 ± 0.8
multistage	14800	1.0 ± 0.5	5.7 ± 0.5	
	14600		5.3 ± 0.5	2.8 ± 0.8
	16000	1.7 ± 0.5	7.2 ± 0.5	2.2 ± 0.8

^aEmission rate (μg/kJ) computed from exhaust measurements (adjusted for background levels) and fuel consumption. ^bAll measurements performed with wick in high position.

given in eq 1, the CO₂ emission rate is calculated to be 73000 μg of CO₂/kJ of fuel consumed. The experimentally determined values for CO₂ for the multistage heater agree with the calculated values to within 5%, and the experimentally determined CO₂ values for the convective heater agree with the calculated value to within 7%. Agreement is less satisfactory for the radiant heater, and we attribute this to greater uncertainties in the measured exhaust flow rates.

Table VI also displays the computed emission rates of the noxious pollutants: CO, NO, and NO₂. All data are normalized to fuel consumption but were not adjusted for ambient levels of the pollutant species. The CO emission rates were largest for the radiant heater and smallest for the multistage heater. The multistage and convective heaters are designed with a third section which allows products of incomplete combustion time for further oxidation. In this third section, there are elevated temperatures and sufficient residence time to assure the nearly complete burnout of CO to CO₂. Unadjusted NO emission rates are greatest for the convective heater and least for the radiant heater; NO₂ emission rates for each of three heaters are similar. Total NO_x follows the same order with respect to heater type as observed for NO. Since the fuel analysis indicated no measurable fuel nitrogen content, one must assume that the NO is formed from the thermal Zeldovich mechanism and that the flame temperature must be the important variable which determines the extent of NO production. Since the air entrainment and hence dilution factors at various stages of the combustion process are different for the three heaters, and since combustion occurs throughout the various regions of each heater, variations in flame temperatures must also occur. Additionally, radiant heat loss during the initial stages of combustion in the multistage and radiant heaters could serve to reduce peak temperatures in the burnout region downstream.

It is important to question whether or not NO₂ is actually present or is an artifact of sampling. It has been

pointed out by Cernansky (9) that sampling from relatively cool post flame regions where radial concentrations are not significant should result in no sample modification due to radical reactions within the sampling system. A possible explanation for the existence of NO₂ in the exhaust manifold is that it is formed near the combustion zone upstream from the exhaust, from turbulent mixing of cold dilution air with the combustion products. The mixing process involves the entrainment of cold air, which quenches radicals, and allows the NO₂ to form from radical reactions with NO (10). The formation of NO₂ from NO under combustion conditions has been verified experimentally by Cernansky and Sawyer (11). In addition, the results of chamber studies of kerosene heaters indicate reasonably large concentrations of NO₂.

As previously stated, the emission rates reported in Table VI were not adjusted for background levels of the pollutant species. Ambient concentrations were measured at a single point near the heater during each experiment; however, no measurements were made to verify that the values were uniform in the space surrounding the heater. If the single point measurements are used to represent an average background concentration for each species, the computed emission rates reported in Table VI will be in excess by up to 7.2, 0.8, and 2.8 μg/kJ for CO, NO, and NO₂ respectively. In a few cases, the individual adjustments are substantial compared to the uncorrected values. Furthermore, when the exhaust and ambient levels differ by less than 5%, the adjustment itself may be miscalculated by 1 order of magnitude or more due to lack of measurement precision. Table VII presents the data shown in Table VI after correction for background levels (assuming that the single-point ambient measurements were representative). Also included is an estimate of the uncertainty in these adjusted values.

Comparison of Tables VI and VII shows that, for NO and NO₂, the adjustments did not alter conclusions about the relative source strengths of the three heaters. However, the ambient CO measurements were so similar to the exhaust manifold measurements taken from the convective and multistage heaters that no differences can be distinguished between these models, within experimental uncertainty. It is clear from these results that determining pollutant emission rates from exhaust manifold measurements is difficult when ambient concentrations approach the expected source concentrations from the dilute product stream.

In order to compare our results with those of the investigators, we have converted our uncorrected emission rates (Table VI) to steady-state concentrations in a chamber of fixed ventilation rate using a technique given by Traynor et al. (12). It has been assumed that all comparisons are made for a constant value of the heat output

Table VIII. Steady-State Indoor Pollutant Levels

study	heater	heat release rate, kJ/h	CO, ppm	NO, ppm	NO ₂ , ppm	NO _x , ppm
A ^a (Lionel)	multistage ^b	15100	1.8	3.1	1.8	4.9
	convective	11600	4.2	8.0	1.8	9.8
	radiant	8160	68.3	0.8	1.8	2.6
B (3)	convective	5870	11.7	5.7	4.6	10.3
	radiant	6760	30.6	<0.1	1.6	1.6
C (4)	convective	7850	4.8	12.2	4.1	16.3
	radiant	8250	37.6	0.6	1.3	1.9
D ^a (1)	convective	8070				21.6
	radiant	9430				2.9
health			35 ^c		0.25 ^d	

^aEntries computed from exhaust manifold measurements and estimated ventilation parameters. ^bAverage of three experiments. ^cEPA ambient air quality standard for CO (1-h average not to be exceeded more than once a year). ^dCalifornia short-term (1 h) standard for NO₂.

rate (kJ/h), and our measurements and those of others have been scaled accordingly. The following expression was used to determine the equivalent steady-state concentrations:

$$(X_i)_{ss} = \frac{1}{\rho_i} \frac{Q}{V} E_i \quad (2)$$

where E_i = emission rate of species i ($\mu\text{g}_i/\text{kJ}$), Q = common energy release rate (kJ/h), V = volumetric air flow rate ($\text{m}^3_{\text{air}}/\text{h}$), ρ_i = density of i at STP ($\mu\text{g}_i/\text{m}^3$), and X_i = volume fraction of i ($\text{m}^3_i/\text{m}^3_{\text{air}}$) with values chosen for $Q = 8080$ kJ/h and $V = 13.5$ m^3/h . The steady-state concentrations are then compared with the results of environmental chamber studies (3, 4) and one laboratory study (1). Our own results and those of others are summarized in Table VIII.

It is likely that the heaters of a given type are fabricated by different manufacturers and differ in design subtleties. Although each of the heaters has a different heat release rate, the indicated steady-state concentrations are normalized to a heater of 8080 kJ/h heat output. The general results observed by other investigators concur with our own findings. The radiant heater emits greater concentrations of CO than the other types of heater. The NO steady-state concentrations are greatest for the convective heater and least for the radiant heater. The radiant heater loses significant heat by radiation to the room. Reduced NO formation is thereby associated with lower temperature in regions where NO formation occurs. There is some disagreement among investigators regarding NO₂ concentrations emitted from the convective heater; however, trends in total NO_x concentrations are in agreement for radiant and convective heaters.

Although there are no standards for indoor air, the illustrated, steady-state CO concentrations produced from the radiant heater do exceed standards for outdoor ambient air. All heaters exceed the California short-term (1 h) standard for NO₂ (4). Without sufficient ventilation, carbon dioxide concentrations are of concern in all combustion appliances.

Summary and Conclusions

The combustion characteristics of radiant, convective, and multistage kerosene heaters have been determined and compared. Two types of experiments were conducted. In the first of these, composition and temperature were measured as a function of axial position in the heater to determine the progress of combustion. In the second type, composition, fuel consumption rate, temperature, pressure, and exhaust stream mass flow rate were measured in an exhaust manifold to ascertain the effect of heater type and

heater operating conditions on exhaust gas composition. Fuel consumption was sensitive to wick height, wick age, and volume of fuel in the tank. Heater design strongly influenced emission rates. The convective and multistage heaters produced the smallest amounts of CO (per kilojoule). The radiant heater produced the largest amounts of CO and the smallest amounts of NO_x. The convective heater produced the largest amounts of NO_x. Results were compared with chamber and other laboratory studies, and agreement among the various studies was found to be quite satisfactory.

Acknowledgments

We express our gratitude to Dr. Amos Newton and Dr. Donald Lucas for their many valuable contributions to this research.

Registry No. CO, 630-08-0; NO_x, 11104-93-1.

Literature Cited

- (1) Yamanaka, S.; Hirose, H.; Takada, S. *Atmos. Environ.* **1979**, *13*, 407-412.
- (2) Kweller, E. R.; Cuthrell, W. prepared for Consumer Product Safety Commission, by Center for Consumer Product Technology, National Engineering Laboratory; National Bureau of Standards, Washington, DC, unpublished results, March 1980.
- (3) Leaderer, B. P. *Science (Washington, D.C.)* **1982**, *218*, 1113-1115.
- (4) Traynor, G. W.; Allen, J. R.; Apte, M. G.; Girman, J. R.; Hollowell, C. D. *Environ. Sci. Technol.* **1983**, *17*, 369-371.
- (5) Clarkson, S. G.; Tom, B. L.; Babcock, A. J.; Mehkeri, K. A. *Proc.-APCA Annu. Meet.* **1984**, 77th.
- (6) Leaderer, B. P.; Stolwijk, J. A. J.; Zagraniski, R. T.; Qing-Shan, M. *Proc.-APCA Annu. Meet.* **1984**, 77th.
- (7) Yamanaka, S. *Environ. Sci. Technol.* **1984**, *18*, 566-570.
- (8) Lucas, D.; Morrow, M. D.; Brown, N. J. *Symp. (Int.) Combust., [Proc.]* **1984**, 20th.
- (9) Cernansky, N. P. In "Experimental Diagnostics in Gas Phase Combustion Systems"; Zinn, B. T., Ed.; American Institute of Aeronautics and Astronautics: New York, NY, 1977; Vol. 53, pp 83-102.
- (10) Bowman, C. T. *Prog. Energy Combust. Sci.* **1975**, *1*, 33-45.
- (11) Cernansky, N. P.; Sawyer, R. F. *Symp. (Int.) Combust., [Proc.]* **1975**, 15th, 1039-1050.
- (12) Traynor, G. W.; Anthon, D. W.; Hollowell, C. D. *Atmos. Environ.* **1982**, *16*, 2979-2987.

Received for review December 27, 1984. Revised manuscript received June 7, 1985. Accepted July 23, 1985. This research was supported by the Assistant Secretary of Conservation and Renewable Energy, Office of Energy Systems Research, Energy Conservation and Utilization Technology Division of the U.S. Department of Energy, under Contract DE-AC03-76SF00098.

Photochemical Transformation of Pyrene and Benzo[*a*]pyrene Vapor-Deposited on Eight Coal Stack Ashes

Robert A. Yokley, Arlene A. Garrison, E. L. Wehry,* and Gleb Mamantov*

Department of Chemistry, University of Tennessee, Knoxville, Tennessee 37996

■ The photochemical decomposition of pyrene and benzo[*a*]pyrene, as adsorbates deposited from the vapor phase, has been examined on eight coal stack ashes of diverse origin and properties. Similar studies using alumina, silica gel, controlled-porosity glass, and graphite adsorbents also have been performed. Phototransformation of the adsorbates proceeds more slowly on any of the ash substrates than on alumina, silica, or glass surfaces. Those ashes relatively high in carbon and/or iron content are especially effective at suppressing photodegradation of adsorbed pyrene or benzo[*a*]pyrene. This relationship appears, at least in part, to be associated with the relatively dark colors of those ashes. The apparent acidity of ash surfaces does not appear to be related to the rate of phototransformation of adsorbed polycyclic aromatic hydrocarbons.

Introduction

The ultimate fate of environmental polycyclic organic matter is a subject of substantial concern, as reflected in the recent appearance of several lengthy reviews of the topic (1-5). Much of this interest arises from observations that the mutagenicity of organic extracts from sampled airborne particulate matter cannot be related solely to the presence of polycyclic aromatic hydrocarbons (PAH) (6). Chemical transformation products of PAH have been implicated as possible contributors to the mutagenicity of extracts from atmospheric particles (2, 4, 6). Thus, there is a need for information regarding the nature and efficiency of degradation of particle-associated PAH.

It is presumed that PAH formed in combustion processes are released into the atmosphere in the vapor phase and then condense on the surface of atmospheric particles (7, 8). It has become apparent that the extent to which adsorbed PAH undergo chemical reactions (both in the absence and in the presence of light) is strongly dependent upon the nature of the particulate substrate upon which they are adsorbed (1-4, 9-19).

We have previously reported that the PAH benzo[*a*]pyrene, pyrene, anthracene, and fluoroanthene are much less photochemically reactive when adsorbed on Illinois State Line fly ash than on activated alumina (11, 12). The question as to whether or not such behavior is general for PAH, rather than a consequence of special characteristics of that particular fly ash, was not addressed in that investigation. Moreover, bulk elemental analyses and relevant physical data (e.g., porosity measurements) for the Illinois fly ash were unavailable. In this investigation, we have examined the photochemical reactivity of pyrene and benzo[*a*]pyrene (BaP) adsorbed on eight coal stack ashes, for which considerable chemical and physical characterization has been undertaken. Several other adsorbents, including alumina, silica gel, controlled pore size glass, and flaked graphite, have also been utilized. As in our previous investigations (11, 12), each PAH has been deposited on the various adsorbent surfaces from the vapor phase, rather than by adsorption from a liquid solution of the PAH in question, in order to avoid possible artifacts from modification of adsorbent surfaces by solvents and to simulate, as closely as feasible under laboratory conditions, the

postulated model for deposition of combustion-produced PAH onto particulate surfaces (7, 8).

Experimental Section

Materials. Six ashes (from combustion of eastern Appalachian (EA), east Tennessee (ET), western Kentucky (WK), and Illinois (IL) bituminous coals; New Mexico (NM) subbituminous coal; Texas (TX) lignite) were obtained from the Oak Ridge National Laboratory. All six ashes were obtained from electrostatic precipitators of coal-fired steam plants (20). A seventh ash was a commercially available analytical standard (AR) obtained from Alpha Resources, Stevensville, MI; the type of coal from which this ash was produced is unknown. An eighth ash was obtained from the electrostatic precipitators of a steam plant burning Kaneb (KA) coal. The plant was not operating properly at the time of sampling; thus, this ash is unusually high in carbon content. The KA ash is less well characterized than the other seven.

Other adsorbents included the following: alumina (neutral, Brockmann activity I); silica gel; controlled porosity glass (100-Å average pore diameter, obtained from Pierce Chemical Co., Rockford, IL); flaked graphite (Southwestern Graphite Co., Burnet, TX). Pyrene and BaP were obtained from commercial sources and purified, when necessary, by vacuum sublimation. All coal ashes were sieved to pass a 45-µm screen and stored in the dark until used.

Deposition Technique. Pyrene or BaP was deposited on an adsorbent from the vapor phase using a diffusion cell-expanded adsorbent bed technique described previously (21). Prior to deposition, each adsorbent was degassed by passing dry nitrogen over the adsorbent in the expanded bed at 427 (for pyrene studies) or 459 K (for studies with BaP) for 24 h.

Illumination Technique. Illumination cells of two distinctly different designs were used: a rotary quartz cell (12) and a fluidized-bed photoreactor (22). Similar results were obtained for the two reactor cell designs. Due to difficulties associated with agglomeration of ash particles and a tendency for them to adhere to the walls of the fluidized-bed reactor, the rotary photoreactor was used for a majority of these studies. All samples illuminated in the rotary cell were in contact with air throughout the period of illumination. The illumination source was a Cermax LX300UV xenon illuminator operated at 180-320 W and situated 34-38 cm from the photolysis cell. To avoid thermolysis of adsorbed PAH by the intense near-infrared output of this lamp, the light beam was passed through 20 cm of water in a cell situated between the lamp and sample cell. When a thermocouple was placed in the illumination cell, it was observed that the temperature of adsorbent samples rose by less than 10 °C over 24-h illumination periods under these conditions. Chemical actinometry (23) indicated the radiant intensity to which samples were exposed to be approximately 0.7 W/cm².

Analytical Procedures. The general procedure consisted of measuring the extent of apparent photodecomposition of the adsorbed PAH produced by illumination

Table I. Photodegradation of Pyrene Adsorbed on Various Substrates^a

adsorbent	initial [Py], $\mu\text{g/g}$	final [Py], $\mu\text{g/g}$	% change ^b	reactivity classification ^c
silica gel	317 \pm 41	68 \pm 6	79	++
alumina	186 \pm 1	ND ^d	>99	++
controlled-pore glass	318 \pm 10	45 \pm 3	86	++
graphite	583 \pm 5	580 \pm 12	<1	0
EA	212 \pm 7	241 \pm 24	-14	0
ET	44 \pm 2	42 \pm 9	5	0
WK	30 \pm 8	29 \pm 10	3	0
IL	449 \pm 29	420 \pm 10	6	0
NM	176 \pm 11	180 \pm 17	-2	0
TX	375 \pm 2	244 \pm 8	35	+
AR	186 \pm 19	64 \pm 10	66	++
KA	96 \pm 5	89 \pm 3	7	0

^a As 95% confidence limits ($N = 4$) for extractable pyrene (Py). All illuminations for 24 h. Abbreviations for ashes as under Experimental Section. ^b Calculated from mean concentrations of extractable pyrene before and after illumination. ^c (0) little or no reactivity (<10% decomposition); (+) moderate reactivity (10-50% decomposition); (++) high reactivity (>50% decomposition). All substrates for which "initial" and "final" 95% confidence limits overlap assigned (0). ^d ND, not detected.

Table II. Photodegradation of Benzo[a]pyrene Adsorbed on Various Substrates^a

adsorbent	initial [BaP], $\mu\text{g/g}$	final [BaP], $\mu\text{g/g}$	% change ^b	reactivity classification ^c
silica gel	85 \pm 12	6 \pm 2	93	++
alumina	394 \pm 6	158 \pm 12	60	++
controlled-pore glass	227 \pm 4	10	96	++
graphite	29 \pm 11	33 \pm 9	-14	0
EA	118 \pm 8	108 \pm 4	8	0
ET	25 \pm 2	26 \pm 3	-4	0
WK	25 \pm 2	22 \pm 5	12	0
IL	31 \pm 6	27 \pm 1	13	0
NM	43 \pm 2	40 \pm 9	7	0
TX	53 \pm 3	25 \pm 3	53	++
AR	56 \pm 1	46 \pm 1	18	+
KA	42 \pm 3	35 \pm 4	17	0

^a As 95% confidence limits ($N = 4$) for extractable BaP. All illuminations for 24 h. Abbreviations for ashes as under Experimental Section. ^b Calculated from mean concentrations of extractable BaP before and after illumination. ^c (0) little or no reactivity (<10% decomposition); (+) moderate reactivity (10-50% decomposition); (++) high reactivity (>50% decomposition). All substrates for which "initial" and "final" 95% confidence limits overlap assigned (0).

for 24 h. Thus, after deposition of a PAH on an adsorbent, that adsorbent was subdivided; part of the adsorbent was subjected to illumination while the remainder was stored in the dark as a control. The "illuminated" and "dark" samples were then each divided into four portions, and each of the individual portions was subjected separately to micro-Soxhlet extraction (in the dark) for 24 h with methanol or toluene as extractant. Subdividing samples after illumination or dark storage but before extraction was necessary because PAH often cannot be recovered quantitatively from coal ash by extraction (24, 25). When samples were subdivided prior to extraction, the results of each analysis could be expressed in terms of the 95% confidence interval for the mean recovery of quadruplicate extractions. The extracts were analyzed for their PAH content by ultraviolet absorption or fluorescence spectrometry.

Other Techniques. Surface area and porosity measurements were carried out via Brunauer-Emmett-Teller (BET) nitrogen adsorption using computer-controlled instrumentation designed for this purpose at the Oak Ridge National Laboratory. Diffuse reflectance spectra were measured on a Cary 14L spectrophotometer equipped with a diffuse reflectance attachment. Color assignments were made by using Munsell soil color charts (26). Estimates of the acidity or basicity of adsorbent surfaces were made by contacting 1 g of each adsorbent with 30 mL of distilled water, stirring the slurry for 1 min, allowing the adsorbent to settle to the bottom of the container, and measuring the pH of the water above the suspended adsorbent with a glass pH electrode. Bulk carbon analyses for the ashes were performed by Galbraith Laboratories, Inc. (Knoxville, TN); bulk analyses for other elements were performed by ion microprobe mass analysis at the Oak Ridge National Laboratory (20).

Results and Discussion

Experimental results for photodegradation of pyrene and BaP on silica gel, alumina, controlled-pore glass, flaked graphite, and the eight stack ashes are compiled in Tables I and II, respectively. On the basis of these results, each PAH is assigned a "reactivity classification" on each adsorbent for qualitative comparison purposes, defined as

follows: (0) little or no photochemical reactivity; (+) moderate photochemical reactivity; (++) high photochemical reactivity, based on a 24-h illumination period. BaP did not undergo detectable nonphotochemical degradation when adsorbed on any of the substrates listed in Table II, even under prolonged dark storage (e.g., 653 days for silica gel and 463 days for NM ash). Pyrene underwent detectable nonphotochemical transformation only when adsorbed on AR ash, but this nonphotochemical reaction did not proceed to a detectable extent in 1 day; thus, the "photochemical" results for pyrene on AR ash (Table I) do not appear to be an artifact caused by the simultaneous occurrence of a dark reaction.

It is clear from Tables I and II that both pyrene and BaP undergo efficient phototransformation when adsorbed on silica gel, alumina, controlled-pore glass, and TX and AR ashes. However, virtually no reactivity is observed for either PAH on any of the other six stack ashes or on flaked graphite surfaces. Obviously, the nature of the adsorbent plays a major role in determining the susceptibility of an adsorbed PAH to photochemical transformation. In general, the two PAHs are less readily photodecomposed when adsorbed on any of the stack ashes than as adsorbates on alumina, silica gel, or controlled-pore glass. However, there are significant differences between ashes in terms of their ability to suppress photolysis of PAH; the PAH are much more photoreactive on the TX and AR ashes than on any of the other ashes.

The nature of the differences between the stack ashes responsible for the differing photoreactivities of adsorbed pyrene and BaP is of obvious interest. Coal ash is a complex inhomogeneous mixture of many particle sizes, shapes, and colors (27, 28). It generally consists of three different major types of particles: mineral (mullite-quartz or glassy), magnetic (magnetite or other iron oxides), and graphitic carbon. Coal ash contains virtually every element in the periodic table. The dominant elements are Si, Al, O, and Fe, along with significant concentrations of C, Ca, K, Mg, and Ti. Some trace elements are distributed more or less uniformly in individual particles, while others (such as Cr, Pb, and Tl) tend to be more concentrated at particle surfaces than in particle interiors (27, 29). Bulk elemental analyses and aqueous extract pH values for the ashes used

Table III. Bulk Elemental Composition and Aqueous Extract pH Values for Coal Stock Ashes^a

element	KA	EA	NM	ET	TX	WK	IL	AR
Si		23.4	28.1	30.0	25.7	23.4	22.7	29.0
Al		13.6	13.1	15.5	7.5	10.1	9.1	11.4
C	2.8	1.8	1.0	0.5	0.5	0.3	0.3	0.3
Fe		10.9	2.5	1.7	3.4	16.9	16.5	4.0
Ca		1.0	4.2	0.2	14.5	1.3	2.4	2.9
Mg		0.8	0.7	1.8	1.9	0.4	0.6	0.8
Na		0.3	1.4	0.2	0.4	0.2	1.7	0.8
K		2.4	0.6	2.0	0.5	2.2	1.6	0.9
pH	6.4	8.2	11.9	4.7	10.8	4.4	3.3	11.4
pyrene photochemistry	0	0	0	0	+	0	0	++
BaP photochemistry	0	0	0	0	++	0	0	+

^a As weight percentages of the elements. Percent carbon only available for KA ash. Analyses for all elements but C from ref 20.

in this work are compiled on Table III (except for KA, for which only a bulk carbon analysis was obtained), along with the reactivity categories for pyrene and BaP photolysis, as defined in Tables I and II.

Examination of Table III reveals that the two stack ashes on which adsorbed pyrene and BaP are most reactive are relatively low both in carbon and in iron. Those ashes on which pyrene and BaP are very resistant to photodegradation tend to be relatively high in carbon (KA), iron (WK, IL), or both carbon and iron (EA). The only significant exception to this trend is the ET ash, which is relatively low in both iron and carbon (by comparison with the remaining ashes) and yet very effectively suppresses photodecomposition both of pyrene and BaP. It also is noteworthy that both PAH are extremely resistant to photolysis when adsorbed on flaked graphite.

Considerable emphasis has been devoted to the carbon content of the ashes because of observations that carbonaceous coal ash particles exhibit a very high affinity for PAH. Griest et al. (30-32) have noted that the sorptivity of ash particle size fractions and subfractions increases with increasing carbon content, in part because the carbonaceous ash particles tend to exhibit larger specific surface areas than mineral or magnetic ash particles. There appear to be specific chemical interactions between carbonaceous particle surfaces and adsorbed PAH (25, 30-32), the precise nature of which has yet to be elucidated. Whether these chemical interactions are relevant to the apparent ability of adsorbents of high carbon content to suppress photochemical transformation of adsorbed PAH (or whether the apparent relationship is adventitious) is not yet clear.

It is noteworthy that, in a series of careful extraction recovery studies using ¹⁴C-labeled BaP, Griest and Tomkins found that the recovery of nonphotochemical degradation products of BaP was greater from mineral or magnetic ash particles than from carbonaceous particles (32). This observation is consistent with the findings reported in this study for photochemical transformation. Of course, the possibility exists that degradation products (such as quinones) are in fact formed from PAH molecules adsorbed on carbonaceous particles, but they fail to be recovered in appreciable yield by extraction because they are strongly bound to those particles. Such factors cannot, however, rationalize the obvious differences reported here between high-carbon and low-carbon adsorbents in terms of quantity of extractable PAH before and after illumination.

It appears likely that the apparent relationship of C and Fe content of stack ashes with the ability of those ashes to suppress PAH photodegradation is partially (but not fully) due to the fact that the high C and/or Fe ashes are darkest in color, while the TX and AR ashes (upon which both pyrene and BaP undergo relatively efficient photo-

Table IV. Color Designations of Adsorbents

adsorbent	Munsell designation ^a	color description ^a	photo-reactivity	
			pyrene	BaP
silica gel	N 9/0	white	++	++
alumina	N 9/0	white	++	++
controlled-pore glass	N 9/0	white	++	++
graphite	N 3/0	very dark gray	0	0
EA	5Y 5/1	gray	0	0
ET	5Y 8/1	white	0	0
WK	2.5Y 3/2	very dark grayish brown	0	0
IL	10YR 3/2	very dark grayish brown	0	0
NM	5Y 5/1	gray	0	0
TX	5Y 7/2	light gray	+	++
AR	5Y 6/2	light olive gray	++	+
KA	5Y 3/1	very dark gray	0	0

^a From ref 26.

transformation) are strikingly light in color. If an adsorbing substrate is relatively porous and highly colored, it is possible for an adsorbed molecule to be "filtered" from the incident light. Such an "inner filter effect" (33) has previously been presumed to play a major role in the photodegradation (or lack thereof) of PAH adsorbed on particulate surfaces (1), but evidence for the significance of the effect has been lacking.

Reliable specification of the color of a particulate substrate is difficult to achieve. We have approached a qualitative description of the stack ash colors by use of Munsell soil color charts (see Table IV), with more quantitative information being obtained by diffuse reflectance spectrophotometry of the adsorbents. As seen in Table IV, those adsorbents on which pyrene and benzo[a]pyrene exhibit efficient photodegradation are without exception white or light gray in color, while (with one exception) the substrates on which the PAH are very resistant to photolysis are dark in color. The one major exception to this general trend is the ET ash, which is relatively light in color but nonetheless proves to be a substrate on which neither PAH undergoes detectable phototransformation.

These conclusions are reinforced in Figure 1, which shows the diffuse reflectance spectra of several of the adsorbents in the 240-400-nm wavelength region (pyrene absorbs strongly in the 270-340-nm region; BaP absorbs strongly in the 270-300- and 340-390-nm wavelength regions; the photolysis source exhibits virtually no output at wavelengths below 270 nm). As seen in Figure 1, the WK, KA, and NM ashes (all of which are substrates on which pyrene and BaP undergo little or no photodecomposition) are relatively strongly absorbing, whereas silica and the TX ash (adsorbents on which both PAH photodecompose relatively efficiently) are appreciably less

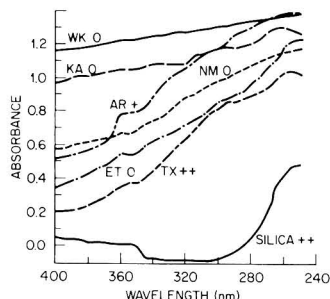


Figure 1. Diffuse reflectance spectra of seven adsorbents. The "reactivity category" [(0), (+), and (++)] for photodegradation of benzo[a]pyrene adsorbed on each substrate is indicated.

Table V. BET Surface Areas and Porosity Characteristics of Selected Adsorbents

adsorbent	sp surface area, m ² /g	pore-size range, Å ^a	sp pore volume, mL/g ^a	pore shape ^b
controlled-porosity glass	125.0	100	3.8	spherical
graphite	4.43	100-1000	7.0	slit
ET	4.01	100-1000	3.0	slit
KA	3.15	100-1000	3.8	slit
TX	2.61	100-1000	5.0	slit
AR	0.84	100-1000	1.8	slit

^a Determined from the Kelvin equation (34). ^b Determined from hysteresis of adsorption-desorption isotherms (34).

efficient absorbers of light in the 270-370-nm wavelength region. Again, the ET ash fails to conform to this overall trend; it actually absorbs less strongly than the AR ash through much of this spectral region, yet PAH adsorbed on ET ash resist photolysis whereas they undergo detectable photodecomposition when adsorbed on AR. Note also that the NM and AR ashes exhibit comparable absorbances throughout much of the spectral region, yet the PAH exhibit detectable photoreactivity on AR but not NM.

In order for an inner filter phenomenon to affect the photolysis of an adsorbed compound, the adsorbent must be porous as well as strongly absorbing, so that adsorbate molecules can penetrate into pores and be "shielded" from the incident light by the adsorbent. Therefore, adsorption-desorption isotherms (BET nitrogen technique) were measured to assess the pore-size distributions of many of the adsorbents. Surface areas were measured by using the multipoint BET method (34, 35). The shapes of the isotherms were used to calculate the pore volumes per gram of adsorbent and pore-size ranges; these relationships are embodied in the Kelvin equation (34-38). The results are listed in Table V. Inclusion of the controlled pore glass sample serves as a check of the method, inasmuch as this material is known to be characterized by a narrow diameter distribution of spherical pores centered about 100 Å. The results indicate that while the porosity characteristics of the different stack ashes (and other adsorbents) are somewhat different, all adsorbents contain a sizable number of pores in the 100-1000-Å diameter range. Assuming average molecular areas for pyrene and BaP of 90.0 and 108.0 Å², respectively (37), it appears safe to conclude that all stack ashes are sufficiently porous for an inner filter effect mechanism to be operative. While these results, in conjunction with the color assignments and reflectance spectra of the adsorbents, do not unambiguously "prove"

the significance of inner filter effects, it seems highly improbable that the relationships between absorbent color and the photoreactivity of adsorbed PAH can be totally coincidental. On the other hand, the fact that PAH photolysis on ET ash proceeds with much lower efficiency than inner filter considerations would predict is undoubtedly indicative of the importance of other chemical and/or physical factors in the phototransformation of particle-associated organic compounds.

One chemical parameter that has previously been considered relevant to the problem is the apparent acidity or basicity of the adsorbent surface. In a comparison of the photodegradation rates of anthracene and phenanthrene adsorbed on two coal ashes, Dlugi and Güsten (16) observed that the PAH underwent much more rapid decomposition when adsorbed on an "acidic" ash (aqueous extract pH 5.65) than as adsorbates on an "alkaline" ash surface (pH 9.3). In contrast, we observe that the only two ashes on which pyrene and BaP undergo detectable photolysis are apparently quite alkaline (TX, pH 10.8; AR, pH 11.4; see Table III). At the same time, pyrene and BaP resist photodegradation when adsorbed on strongly (NM) and weakly (EA) alkaline ashes (Table III), as well as on strongly (IL, WK) and weakly (KA) acidic ashes. Our results, considered along with those of Dlugi and Güsten (16), show no obvious relationship between apparent surface acidity (as estimated from pH values of aqueous extracts) and the photoreactivity of adsorbed PAH. It is very interesting, however, that the acidic ash examined by Dlugi and Güsten was much lighter in color than the alkaline ash ("beige" vs. "grayish black"). Thus, their observations are entirely consistent with ours in noting that phototransformation of adsorbed PAH proceeds much more rapidly on the more lightly colored ash.

Conclusions

- (1) Pyrene and benzo[a]pyrene are more resistant to photochemical transformation when adsorbed on any of the eight stack ashes examined in this study than as adsorbates on alumina, silica gel, or controlled-porosity glass.
- (2) Different coal stack ashes stabilize adsorbed pyrene and BaP to degradation with different efficiencies.
- (3) Pyrene and BaP exhibit no detectable phototransformation over 24-h illumination periods when adsorbed on any ash that is greater than 10% iron and/or 0.5% carbon. Likewise, the two PAH exhibit no detectable photoreactivity when adsorbed on flaked graphite.
- (4) The color, reflectance spectral characteristics, and porosity parameters for the ashes are generally consistent with significant inner filter suppression of photolysis of adsorbed organic compounds by the highly colored, porous ash substrates. Only one of the eight ashes investigated yields results seriously at variance with this general relationship.
- (5) There is no obvious relationship between the apparent acidity or basicity of an adsorbent surface and the susceptibility to photodegradation of adsorbed pyrene or BaP.
- (6) Nonphotochemical transformations of pyrene and BaP on coal ash appear sufficiently slow that their environmental significance should be virtually negligible, unless significant concentrations of copollutant species such as ozone or nitric acid also are present (39, 40).

Acknowledgments

We thank D. A. Lee for the surface area and porosity measurement, J. S. Krueger and R. J. Engelbach for assistance in photochemical studies, and W. H. Griest for

communication of results prior to publication.

Registry No. BaP, 50-32-8; Fe, 7439-89-6; C, 7440-44-0; alumina, 1344-28-1; pyrene, 129-00-0; graphite, 7782-42-5.

Literature Cited

- (1) Nielsen, T.; Ramdahl, T.; Bjørseth, A. *Environ. Health Perspect.* **1983**, *47*, 103.
- (2) Pitts, J. N., Jr. *Environ. Health Perspect.* **1983**, *47*, 115.
- (3) Edwards, N. J. *J. Environ. Qual.* **1983**, *12*, 427.
- (4) Van Cauwenbergh, K.; Van Vaeck, L. *Mutat. Res.* **1983**, *116*, 1.
- (5) Nikolaou, K.; Masclet, P.; Mouvrier, G. *Sci. Total Environ.* **1984**, *32*, 103.
- (6) Chrisp, C. E.; Fisher, G. L. *Mutat. Res.* **1980**, *76*, 143.
- (7) Natusch, D. F. S.; Tomkins, B. A. In "Polynuclear Aromatic Hydrocarbons"; Jones, P. W.; Freudenthal, R. I., Eds.; Raven Press: New York, 1978; p 145.
- (8) Eiceman, G. A.; Vandiver, V. J. *Atmos. Environ.* **1983**, *17*, 461.
- (9) Thomas, J. F.; Mukai, M.; Tebbens, B. D. *Environ. Sci. Technol.* **1968**, *2*, 33.
- (10) Fox, M. A.; Olive, S. *Science (Washington, D.C.)* **1979**, *205*, 582.
- (11) Korfmacher, W. A.; Natusch, D. F. S.; Taylor, D. R.; Mamantov, G.; Wehry, E. L. *Science (Washington, D.C.)* **1980**, *207*, 763.
- (12) Korfmacher, W. A.; Wehry, E. L.; Mamantov, G.; Natusch, D. F. S. *Environ. Sci. Technol.* **1980**, *14*, 1094.
- (13) Korfmacher, W. A.; Mamantov, G.; Wehry, E. L.; Natusch, D. F. S.; Mauney, T. *Environ. Sci. Technol.* **1981**, *15*, 1370.
- (14) de Mayo, P. *Pure Appl. Chem.* **1982**, *54*, 1623.
- (15) Sancier, K. M.; Wise, H. *Atmos. Environ.* **1981**, *15*, 639.
- (16) Dlugi, R.; Güsten, H. *Atmos. Environ.* **1983**, *17*, 1765.
- (17) Beck, G.; Thomas, J. K. *Chem. Phys. Lett.* **1983**, *94*, 553.
- (18) Daisey, J. M.; Low, M. J. D.; Tascon, J. M. D. *Polynucl. Aromat. Hydrocarbons: Int. Symp., 8th*, in press.
- (19) Taskar, P. K.; Solomon, J. J.; Daisey, J. M. *Polynucl. Aromat. Hydrocarbons: Int. Symp., 8th*, in press.
- (20) Lauf, R. J. "Application of Materials Characterization Techniques to Coal and Coal Wastes"; Oak Ridge National Laboratory: Oak Ridge, TN, 1981; ORNL/TM-7663.
- (21) Miguel, A. H.; Korfmacher, W. A.; Wehry, E. L.; Mamantov, G.; Natusch, D. F. S. *Environ. Sci. Technol.* **1979**, *13*, 1229.
- (22) Daisey, J. M.; Lewandowski, C. G.; Zorz, M. *Environ. Sci. Technol.* **1982**, *16*, 857.
- (23) Pitts, J. N., Jr.; Cowell, G. W.; Burley, D. R. *Environ. Sci. Technol.* **1968**, *2*, 435.
- (24) Griest, W. H.; Caton, J. E. In "Handbook of Polycyclic Aromatic Hydrocarbons"; Bjørseth, A., Ed.; Marcel Dekker: New York, 1983; p 95.
- (25) Griest, W. H.; Yeatts, L. B.; Caton, J. E. *Anal. Chem.* **1980**, *52*, 199.
- (26) "Munsell Soil Color Charts"; Kollmorgen Corp.: Baltimore, MD, 1975.
- (27) Fisher, G. L.; Natusch, D. F. S. In "Analytical Methods for Coal and Coal Products"; Karr, C., Jr., Ed.; Academic Press: New York, 1979; Vol. 3, p 489.
- (28) Hulett, L. D.; Weinberger, A. J. *Environ. Sci. Technol.* **1980**, *14*, 965.
- (29) Linton, R. W.; Williams, P.; Evans, C. A., Jr.; Natusch, D. F. S. *Anal. Chem.* **1977**, *49*, 1514.
- (30) Griest, W. H.; Tomkins, B. A. *Sci. Total Environ.* **1984**, *36*, 209.
- (31) Griest, W. H.; Caton, J. E. In "Polynuclear Aromatic Hydrocarbons: Chemical Analysis and Biological Fate"; Cooke, M.; Dennis, A. J., Eds.; Battelle Press: Columbus, OH; 1981; p 719.
- (32) Griest, W. H.; Tomkins, B. A., Oak Ridge National Laboratory, Oak Ridge, TN, personal communication, Nov 1984.
- (33) Wehry, E. L. In "Analytical Photochemistry and Photochemical Analysis"; Fitzgerald, J. M., Ed.; Marcel Dekker: New York, 1971; p 173.
- (34) Gregg, S. J.; Sing, K. S. W. "Adsorption, Surface Area, and Porosity"; Academic Press: New York, 1982.
- (35) Shields, J. E.; Lowell, S. *Am. Lab.* **1984**, *16* (11), 81.
- (36) de Boer, J. H.; Linsen, B. G.; van der Plas, T.; Zondervan, G. J. *J. Catal.* **1965**, *4*, 649.
- (37) Schure, M. R. Ph.D. Dissertation, Colorado State University, Fort Collins, CO, 1981.
- (38) Schure, M. R.; Soltys, P. A.; Natusch, D. F. S.; Mauney, T. *Environ. Sci. Technol.* **1985**, *19*, 82.
- (39) Jäger, J.; Rakovic, M. *J. Hyg., Epidemiol., Microbiol., Immunol.* **1974**, *18*, 137.
- (40) Grosjean, D.; Fung, K.; Harrison, J. *Environ. Sci. Technol.* **1983**, *17*, 673.

Received for review February 14, 1985. Accepted July 1, 1985. This work was supported in part by the Office of Health and Environmental Research, U.S. Department of Energy (Contract AS05-81ER6006).

Contribution of Gulf Area Natural Sulfur to the North American Sulfur Budget

Menachem Luria,*† Charles C. Van Valin, Dennis L. Wellman, and Rudolf F. Pueschel

Air Quality Division, Air Resources Laboratory, National Oceanic and Atmospheric Administration, Boulder, Colorado 80303

■ To evaluate the contribution of natural sulfur compounds from the Gulf of Mexico to the overall North American sulfur budget, two series of air sampling flights were performed over the gulf area. Total aerosol mass load and sulfate concentration data indicate, in agreement with our previous findings on gas-phase products, that these observations can be divided into two categories. One group of measurements was taken under offshore airflow and the other under onshore flow conditions. From the measurements performed under "clean" (onshore) flow, average inside boundary layer SO_4^{2-} concentrations were evaluated. Using these data, together with our previously reported dimethyl sulfide levels, we developed a simple model to estimate the sulfur flux transported northward from the gulf area. Upper and lower limits of this contribution are estimated at 0.25 and 0.04 Tg (S) year⁻¹, respectively. Although this quantity is relatively low compared with the national U.S. anthropogenic emission, it has significance for the global sulfur cycle, and it can cause a significant acidification of cloud water.

Introduction

The large continuing effort in the United States to reduce the effects of sulfur dioxide in the atmosphere has already resulted in more than 20% reduction in SO_2 emission during the period 1977-1982 (1). The source-receptor relationship of such reductions depends critically on the background concentrations of natural sulfur. Several reports published in recent years have suggested that natural sulfur compounds may contribute significantly to the global atmospheric load of sulfate aerosols. Charlson and Rodhe (2) have pointed out that precipitation pH could be reduced from 5.6 (the calculated atmospheric CO_2 equilibrium pH) as a result of the influence of sulfuric acid produced from natural sulfur emission.

The global biogenic sulfur emission into the atmosphere can be approximated at 103 Tg (S) year⁻¹, on the basis of findings of Adams et al. (3), who estimated that the contribution of continental sources is 64 Tg (S) year⁻¹, and of Andreae and Raemdonck (4), who estimated a marine flux of 39 Tg (S) year⁻¹. Natural sulfur emission also includes volcanic activity, which may be assumed to contribute as much as 30 Tg (S) year⁻¹ (5). When these values are compared with the global anthropogenic emissions, estimated by Möller (6) at 62 Tg (S) year⁻¹, one can appreciate the importance of the uncontrollable natural sources to the overall sulfur budget.

A potential contribution of natural sulfur compounds to the overall North America sulfur budget was originally proposed by Reisinger and Crawford (7), who showed that the mass transport of sulfate through the Tennessee Valley region was higher when airflow was from the southwest than during northerly flows, despite an anthropogenic SO_2 emission rate that was eightfold higher north of the valley than to the south. They interpreted these findings to mean that precursors other than SO_2 , possibly of biogenic origin,

contribute to sulfate formation south of the Tennessee Valley.

To assess the sulfur contribution of the Gulf of Mexico, possibly one of the major natural sources, to the North American sulfur budget, the Air Quality Division (AQD) of NOAA's Air Resources Laboratory (ARL) conducted a series of air sampling flights over the gulf. Findings on dimethyl sulfide (DMS) and carbonyl sulfide (COS) were published in the first report from this program (8). The data, collected during later summer of 1984, revealed that within the experimental uncertainty the COS concentration was nearly constant at 440 ± 35 pptv [parts per trillion (volume)] whereas the DMS level varied significantly. DMS was not detected above the boundary layer, and its average concentration changed from 27 ± 30 pptv during southerly flow to 7 ± 3 pptv when airflow was offshore. A strong negative correlation between the DMS level and trace atmospheric pollutants (such as CO) was demonstrated. There was no demonstrable difference between daytime and nighttime measurements of DMS.

In this paper we discuss the aerosol data obtained during the air sampling flights and the correlation between these data and the gas-phase measurements. The experimental observations are further used to estimate the contribution of the gulf's natural sulfur emission to the total North American sulfur budget and the potential influence of this flux on precipitation acidification.

Experimental Methods

Two series of atmospheric sampling flights were performed during the summer of 1984. The first took place during Aug 10-15 and the second from Aug 29 to Sept 3. All flights were performed 30-80 km south of the gulf coastline at elevations of 30-3500 m during the day and 300-3300 m at night. Flight duration was 3-4 h during which several "tracks" were made at constant altitude. The geographical location of the study area is shown in Figure 1.

A twin-engine Beechcraft King Air C-90 was used for the air sampling. Detailed information on the instrumentation aboard the aircraft has been published previously (8). The aerosols were measured by using PMS, Inc., Model ASASP-100X and FSSP aerosol size distribution monitors, covering the aerosol size range of 0.1-3.0 and 1.25-42.5 μm , respectively. The aerosol monitors were mounted beneath the wings of the aircraft in the free airstream. A 47-mm tandem filter pack was used for the collection of aerosol samples (9). Flask air samples were collected and analyzed later for hydrocarbons, DMS, COS, and CO (8).

The aerosol samples were analyzed for SO_4^{2-} , Cl^- , NO_3^- , and gaseous SO_2 by ion chromatography at the Air Quality Branch, Tennessee Valley Authority. The air samples were analyzed at the Oregon Graduate Center by using a gas chromatograph equipped with flame photometric and flame ionization detectors. Meteorological data for the duration of the flights was provided by the regional facility of the National Weather Service (NWS) located at Slidell, LA. The details of the weather conditions prevailing

*Permanent address: Environmental Sciences Division, School of Applied Science, The Hebrew University, Jerusalem, Israel.



Figure 1. Area over which air sampling flights for this study were performed (shaded), presented on a map of the northern Gulf of Mexico area.

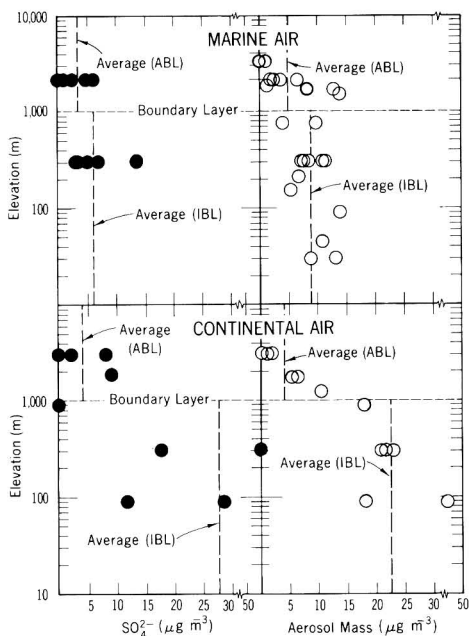


Figure 2. Sulfate (left side) and total mass (right side) as a function of altitude. The upper part of this figure presents data collected during the onshore airflow (marine air), and the lower part presents data collected during offshore airflow (continental air). ABL is above the boundary layer; IBL is in the boundary layer. The bold open circles represent more than one observation.

during the study were presented in our previous publication (8).

Results

As mentioned earlier, the DMS data collected during this study can be divided into two subsets. One set was collected during southerly airflow in marine air (all the data collected until and including August 31), and the other was collected during offshore flows in continental air (first 3 days in September). The aerosol data, presented in Figure 2, reflect the different characteristics. The left-hand side of this figure shows SO_4^{2-} concentrations; these were corrected for sea salt aerosols by using Cl⁻ concentrations as an indicator for the amount of ocean-

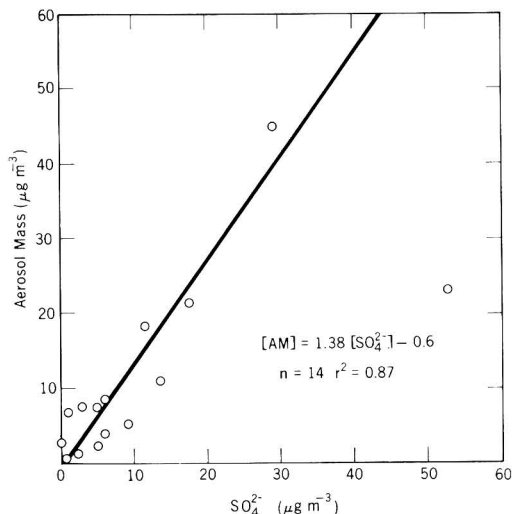


Figure 3. Linear correlation between total aerosol mass (AM) and SO_4^{2-} concentrations (the data point on the extreme right was excluded from the statistical analysis).

released SO_4^{2-} and assuming that the $[\text{Cl}^-]/[\text{SO}_4^{2-}]$ ratio in the aerosols equals 7.1, as it is in the open ocean water (10). Under all circumstances the correction that was applied was less than 10% of the measured value; thus, deviations from this ratio would have a negligible effect. The right-hand side of Figure 2 shows the accumulation mode aerosol mass, calculated from the optical aerosol size analyzer. The reported aerosol volume is the sum of the products of the number density at each size group with the corresponding average volume. Aerosol volume was converted into aerosol mass, assuming 2.0 g cm^{-3} for the aerosol density, which is approximately the average of maritime aerosol (11).

The similarity between aerosol mass (measured during all flights) and SO_4^{2-} content of the aerosols (measured only during the second series), as shown in Figure 2, is further emphasized in Figure 3, which shows the correlation between these two parameters. With the exclusion of one data point, which was either too high in SO_4^{2-} or too low in total aerosol mass, the linear regression analysis between the two data sets shows a near zero intercept and a high correlation coefficient ($r^2 = 0.87$). It further suggests that approximately 72% of the aerosol load consists of non sea salt SO_4^{2-} . This finding is in agreement with our previous data from Whiteface Mountain (12), suggesting that 63% of the dry aerosol mass consisted of sulfate, and data from aerosol sampled in Colorado (13), which contained 76% sulfate.

As was the case with the previously reported gas analyses, the particle number and volume distributions can be divided into two subsets. Figure 4 shows particle number and volume distributions observed during the two parts of the study, inside the boundary layer (IBL) and above the boundary layer (ABL). Boundary layer depth was evaluated from the CO data (8). The ABL data for both parts of the study (curves 2 and 3) are similar. Curves 1 and 4 on the number distribution plots were taken IBL during the clean and polluted episodes, respectively. The distribution taken during the clean air episode shows a higher number density for large particles whereas the one taken during the polluted episode is enriched by more than an order of magnitude in small particles.

Table I. Average Gas-Phase and Aerosol Concentrations Obtained during Air Sampling Flights over the Gulf of Mexico

parameter	marine air		continental air	
	IBL ^a	ABL ^b	IBL	ABL
DMS, pptv	27 ± 30 (23) ^c	<3 (23)	7 ± 3 (14)	<3 (14)
COS, pptv	459 ± 31 (23)	434 ± 30 (23)	443 ± 21 (14)	416 ± 12 (14)
CO, ppbv	69 ± 8 (23)	64 ± 7 (23)	127 ± 18 (14)	94 ± 26 (14)
total aerosol mass, μg m ⁻³	9.1 ± 2.8 (13)	5.0 ± 5.1 (9)	24.6 ± 10.2 (6)	4.3 ± 3.9 (6)
SO ₄ ²⁻ , μg m ⁻³	6.1 ± 4.3 (5)	2.9 ± 2.6 (5)	28 ± 18 (4)	4.0 ± 4.3 (5)

^a Inside boundary layer. ^b Above boundary layer. ^c Number of samples used for averaging.

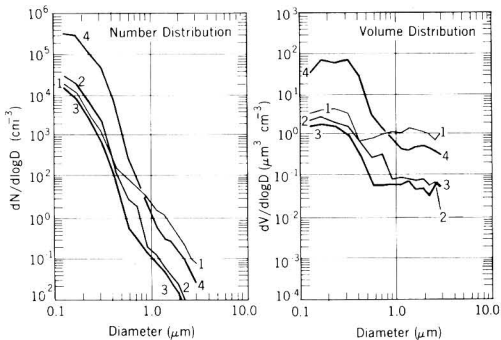


Figure 4. Particle number and volume distributions obtained from the PMS ASASP-100X optical sensor. Curve 1, data taken on Aug 15 at an elevation of 210 m above sea level; curve 2, data taken on Aug 30 at 2100 m; curve 3, data taken on Sept 2 at 3000 m; curve 4, data taken on Sept 2 at 90 m.

When the number distribution is converted into volume distribution, a bimodal curve is obtained for all four cases. The volume maximum in the 0.2–0.4-μm interval is consistent with the peak associated with a fully developed sulfate aerosol (14). The peak at around 2 μm is similar to the one observed from oceanic haze (15). Despite the fact that the integrated aerosol volume obtained from the data presented on curve 4 (45.0 μm³ cm⁻³) is over 6 times larger than the aerosol volume obtained from curve 1 data (7.2 μm³ cm⁻³), the relative and absolute contribution of the coarse mode to the integrated aerosol volume is greater in the latter case. This observation is consistent with the expectation of a greater number of coarse-mode particles in the air mass with a long over-water history, as compared with the polluted air mass that is much richer in small, anthropogenic aerosols.

The results obtained from marine air (Figure 2, upper part) show only a small difference in total aerosol mass (and in sulfate concentration) between the boundary layer and the free troposphere. In continental air (Figure 2, lower part), the IBL aerosol load was much greater than the ABL, but the ABL aerosol load showed little difference between polluted and clean conditions. This observation is consistent with the gas-phase measurements reported earlier (8). A summary of the average aerosol and gas-phase concentrations is presented in Table I.

Linear regression analysis between the aerosol mass and carbon monoxide concentrations, shown in Figure 5, also demonstrates a high level of correlation ($r^2 = 0.83$). The intercept of the linear-fit line suggests that the "aerosol-free atmosphere" may contain 48 ppbv of CO, which is slightly below the range of background CO measurements (16).

Discussion

As a result of its large atmospheric emission rate and its short atmospheric life time, DMS is one of the major sources for atmospheric sulfate aerosols and, therefore, for

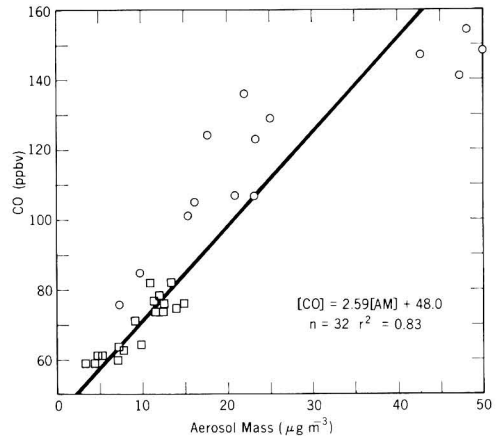
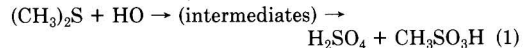
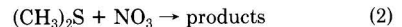


Figure 5. Best linear fit between aerosol mass and CO concentrations for the measurements performed inside the boundary layer. Square symbols represent data obtained during the first series; circles represent data from the second series of flights.

natural acidification of precipitation. We assume that the following two reactions remove the bulk of DMS from the atmosphere. During the sunlight hours DMS reacts very efficiently with the hydroxyl radical (HO):



at a rate constant k_1 of nearly $1.0 \times 10^{-11} \text{ cm}^3 \text{ s}^{-1}$ (17, 18). DMS was also found to be removed during dark hours (8). According to Winer et al. (19), it reacts with NO_3



with a rate coefficient $k_2 = 5 \times 10^{-13} \text{ cm}^3 \text{ s}^{-1}$, and can provide a very efficient nighttime sink. Hence, the rate law for DMS can be written as

$$d[\text{DMS}]/dt = R(\text{DMS}) - k_1[\text{HO}][\text{DMS}] - k_2[\text{NO}_3][\text{DMS}] \quad (3)$$

where $R(\text{DMS})$ is the rate of DMS release from the ocean.

Since DMS levels, as measured during the first part of this study, showed no pronounced diurnal cycle, the steady-state approximation can be used. If we further assume that the average HO level during the daytime is $3 \times 10^6 \text{ molecules cm}^{-3}$ (20) and the nighttime average NO_3 is $6 \times 10^7 \text{ molecules cm}^{-3}$ (21), then the DMS lifetime can be estimated to be approximately 9.3 h throughout the 24-h day. This is in agreement with the boundary layer mixing time. The average DMS concentration during the first part of this study was 27 pptv ($6.6 \times 10^8 \text{ molecules cm}^{-3}$) throughout the boundary layer. If we further assume an average mixing depth of 1000 m, in agreement with our observations (8), we can calculate $R(\text{DMS})$ to be $2 \times 10^9 \text{ molecules cm}^{-2} \text{ s}^{-1}$. An extrapolation to the global ocean,

which may not be justifiable, would result in an estimated emission flux of 12.1 Tg (S) year⁻¹. This value is approximately one-third of the estimate made by Andreae and Raemdonck (4) for the remote oceans. The threefold factor between the two estimates should not be any surprise, since the Andreae and Raemdonck estimates are based on measurements performed over the remote oceans and therefore better represent the global emission.

On the basis of our data, the biogenic annual emission from the gulf can be estimated to be about 0.1 Tg (S) year⁻¹. The actual amount of sulfur from the gulf area transported into North America is a function of two major parameters, the atmospheric lifetime of the sulfur compounds and the volume of the air mass entering through the corridor between Texas and Florida. The only removal mechanisms for SO₄²⁻ in the troposphere are wet and dry deposition. The rates of these processes can vary significantly according to the prevailing meteorological conditions, and therefore, only upper and lower limit estimates for these variables can be made.

Galloway (22), who studied the sulfur budget for the western Atlantic Ocean, estimated that 4.5 Tg (S) year⁻¹ is transported eastward to the Atlantic Ocean from the continent, and only 2.6 Tg (S) year⁻¹ remains in the atmosphere after 1100 km of travel over the Atlantic. During this travel, 0.3 Tg (S) year⁻¹ is added from natural sources, and 1.0 and 1.2 Tg (S) year⁻¹ are removed by wet and dry deposition, respectively. If a wind speed of 5 m s⁻¹ is assumed, the average travel time can be estimated at 60 h. If we further assume that SO₄²⁻ removal can be approximated by a first-order process, then

$$[\text{SO}_4^{2-}]_t = [\text{SO}_4^{2-}]_0 e^{-(k_w + k_d)t} \quad (4)$$

where [SO₄²⁻]₀ and [SO₄²⁻]_t represent initial and final concentrations of SO₄²⁻, and *k_w* and *k_d* represent pseudo-first-order rate constants for total wet and dry deposition, respectively. The solution of eq 4 for the western Atlantic case suggests that *k_w* + *k_d* = 1.1 × 10⁻² h⁻¹, which translates to a SO₄²⁻ atmospheric lifetime of approximately 90 h.

An alternative approach for calculating the SO₄²⁻ lifetime is based on the chemistry of DMS. If we assume that the only significant source of maritime sulfate is DMS oxidation, that most (>95%) of the atmospheric sulfur is in the form of SO₄²⁻, and that reaction 2 is stoichiometric, then the rate law for SO₄²⁻ can be written as

$$d[\text{SO}_4^{2-}]/dt = (k_1[\text{HO}] + k_2[\text{NO}_3])[\text{DMS}] - (k_w + k_d)[\text{SO}_4^{2-}] \quad (5)$$

To solve this equation for *k_w* + *k_d*, we have to assume that the rate of DMS oxidation is constant throughout the day (or that the fluctuations are small and it can be averaged throughout the day) and that the steady-state assumption is valid (i.e., the SO₄²⁻ concentration is constant over long time periods).

On the basis of our previous results, showing that DMS could not be detected above the boundary layer, we can further assume that practically all of the DMS oxidation takes place inside the boundary layer. Therefore, if we use the average SO₄²⁻ concentration measured during the clean atmospheric conditions inside the boundary layer (Table I), *k_w* + *k_d* can be estimated. In this case the average value of *k₁*[HO] + *k₂*[NO₃] = 3 × 10⁻⁵ s⁻¹, [DMS] = 6.6 × 10⁸ molecules cm⁻³, and [SO₄²⁻] = 3.8 × 10¹⁰ molecules cm⁻³ (6.1 μg m⁻³). The solution of eq 5 under steady-state conditions provides *k_w* + *k_d* = 5.2 × 10⁻⁷ s⁻¹ which means that the SO₄²⁻ atmospheric lifetime equals 530 h.

The sixfold difference between the two estimates of *k_w* + *k_d* may suggest that SO₄²⁻ levels used in the latter cal-

Table II. Upper and Lower Limit Estimates of Natural Sulfur Entering North America through the Texas-Florida Corridor

parameter	upper limit estimate	lower limit estimate
boundary layer depth, m	1000	1000
Texas-Florida corridor width, m	1.57 × 10 ⁶	1.57 × 10 ⁶
wind speed (IBL), m s ⁻¹	5	5
southerly airflow (IBL), % year ⁻¹	50	50
annual volume of air mass, m ³ /year ⁻¹	1.24 × 10 ¹⁷	1.24 × 10 ¹⁷
SO ₄ ²⁻ atmospheric lifetime (<i>k_w</i> + <i>k_d</i>) ⁻¹ , h ^a	530	90
average [SO ₄ ²⁻], μg m ⁻³	6.1	1.0
average SO ₄ ²⁻ flux, μg m ⁻² s ⁻¹	30.5	5.0
annual sulfur flux, Tg (S) year ⁻¹	0.251	0.041

^a *k_w* and *k_d* represent wet and dry deposition in terms of first-order rate coefficients.

Table III. Potential pH of Cloud Water Resulting from Natural Sulfur Compounds, for Clouds Containing Three Different Amounts of Water

	0.1 g m ⁻³	0.5 g m ⁻³	2.5 g m ⁻³
lower limit (SO ₄ ²⁻ = 1.0 μg m ⁻³)	3.7	4.4	5.1
upper limit (SO ₄ ²⁻ = 6.1 μg m ⁻³)	2.9	3.6	4.3

culations were unrealistically high. In fact, measurements inside the marine boundary layer (23, 24) have indicated SO₄²⁻ concentrations on the order of 1.0 μg m⁻³. Using this value and solving eq 5, one would get the SO₄²⁻ lifetime equal to 87 h, which is very close to the value derived from Galloway's data (22). It is possible that some of the sulfate measured during the clean atmospheric days resulted from nonbiogenic sources, despite the fact that during these days the area was affected by southerly flow. However, the fact that CO levels measured during the clean days were extremely low (see Table I) does not provide any support for this hypothesis. Hence, the two lifetime estimates derived earlier will be used as upper and lower limits for the SO₄²⁻ atmospheric lifetime.

Using the extreme values of *k_d* + *k_w*, we have estimated upper and lower limits for the sulfur flux that may be entering the continent through the Texas-Florida corridor. A summary of the parameters used for the two estimates is presented in Table II. A comparison between these data and the anthropogenic emission (1) shows that the upper limit estimate may contribute less than 1.5% to the total sulfur emission of the United States. As expected, the lower limit estimate suggests an insignificant contribution of the natural sulfur to the total North American budget (<0.25%). On the other hand, although it might seem that the upper limit reported in Table II may overestimate the contribution from natural sources, the derived sulfur flux is still too small to explain the high sulfur flux drifting through the Tennessee Valley under southwesterly flows (7).

Finally, on the basis of our data we can estimate the effect of the natural emission on acidification of cloud water. In parallel to the study of Charlson and Rodhe (2), we have calculated the pH for three types of clouds containing 0.1, 0.5, 2.5 g m⁻³ water, respectively. In these calculations we assumed that all the natural sulfate is converted to H₂SO₄, that all the H₂SO₄ is dissolved in water droplets, and that the effect of all other trace atmospheric gases (CO₂, NH₃, SO₂, etc.) and cations can be neglected. Obviously, such calculated pHs do not represent the real atmosphere but rather establish outer boundaries. A summary of this estimate is given in Table III. It is worth mentioning that for the lower flux estimates our

calculations are in total agreement with Charlson and Rodhe (2).

Conclusion

The results of this study indicate that the potential contribution of biogenic sulfur to the overall North American sulfur budget is minimal (between 1.5% and 0.25%). Cloud water pHs evaluated from the lower limit estimate are identical with those calculated by Charlson and Rodhe (2) from theoretical considerations. The upper limit estimate of natural sulfur transport into the continent may cause acidification of rainwater. Nevertheless, even the higher sulfur flux estimate is still substantially lower than the value postulated by Reisinger and Crawford (7).

A more accurate evaluation of the exact contribution of natural sulfur would require additional SO_4^{2-} /DMS simultaneous measurements to be carried out during strong southerly airflows. Under these conditions, the potential effects of any anthropogenic sources are expected to be minimal.

Acknowledgments

We acknowledge J. F. Meagher and R. Garber from the Tennessee Valley Authority for providing us with the aerosol sampling system and for the analysis of the filter samples and J. Boatman from Air Resources Laboratory, Air Quality Division, NOAA, for performing particle size analysis.

Registry No. Sulfur, 7704-34-9.

Literature Cited

- (1) Pechan, E. H.; Wilson, J. H., Jr. *J. Air Pollut. Control Assoc.* **1984**, *34*, 1075-1078.
- (2) Charlson, R. J.; Rodhe, H. *Nature (London)* **1982**, *295*, 683-685.
- (3) Adams, D. F.; Farwell, S. O.; Robinson, E.; Pack, M. R.; Bamesberger, W. L. *Environ. Sci. Technol.* **1981**, *15*, 1493-1498.
- (4) Andreae, M. O.; Raemdonck, H. *Science (Washington D.C.)* **1983**, *221*, 744-747.
- (5) Cadle, R. D. *Rev. Geophys. Space Phys.* **1980**, *18*, 746-752.

- (6) Möller, D. *Atmos. Environ.* **1984**, *18*, 19-27.
- (7) Reisinger, L. M.; Crawford, T. L. *J. Air Pollut. Control Assoc.* **1980**, *30*, 1230-1231.
- (8) Van Valin, C. C.; Luria, M.; Wellman, D. L.; Gunter, R. L.; Pueschel, R. F. submitted for publication in *Atmos. Environ.*
- (9) Forrest, J.; Garber, R.; Newman, L. *Atmos Environ.* **1979**, *13*, 1287-1297.
- (10) Chemical Rubber Co. "Handbook of Physics and Chemistry," 47th ed.; CRC Press: Cleveland, OH, 1966-1976; p F-117.
- (11) Pruppacher, H. R.; Klett, J. D. "Microphysics of Clouds and Precipitation"; D. Reidel: Dordrecht, Holland, 1978; p 195.
- (12) Van Valin, C. C.; Wellman, D. L.; Stearns, L. P. Submitted for publication in *J. Geophys. Res.*
- (13) Sievering H.; Van Valin, C. C.; Barrett, E. W.; Pueschel, R. F. *Atmos. Environ.* **1984**, *18*, 2685-2690.
- (14) Luria, M.; Stockburger, L.; Olszyna, K. J.; Meagher, J. F. *Atmos. Environ.* **1982**, *16*, 697-708.
- (15) Schnell, R. C.; Raatz, W. E. *Geophys. Res. Lett.* **1984**, *11*, 369-372.
- (16) Seiler, W.; Fishman, J. *J. Geophys. Res.* **1981**, *86*, 7255-7265.
- (17) Kurylo, M. *J. Chem. Phys. Lett.* **1978**, *58*, 233-236.
- (18) Atkinson, R.; Perry, R. A.; Pitts, J. N., Jr. *Chem. Phys. Lett.* **1978**, *54*, 14-16.
- (19) Winer, A. M.; Atkinson, R.; Pitts, J. N., Jr. *Science (Washington, D.C.)* **1984**, *224*, 156-159.
- (20) Chatfield, R. B.; Crutzen, P. J. *J. Geophys. Res.* **1984**, *89*, 7111-7132.
- (21) Platt, U.; Perner, D.; Winer, A. M.; Harris, G. W.; Pitts, J. N., Jr. *Geophys. Res. Lett.* **1980**, *7*, 89-92.
- (22) Galloway, J. N. "Briefing to NSF on WATOX"; University of Virginia, Charlottesville, VA, Nov 30, 1983, University of Virginia document.
- (23) Huebert, B. J.; Lazarus, A. L. *J. Geophys. Res.* **1980**, *85*, 7337-7344.
- (24) Bonsang, B.; Nguyen, B. C.; Gaudry, A.; Lambert, G. *J. Geophys. Res.* **1980**, *85*, 7410-7416.

Received for review April 3, 1985. Accepted July 5, 1985. This research has been funded as part of the National Acid Precipitation Assessment Program by the National Oceanic and Atmospheric Administration. M.L. acknowledges the National Research Council for providing a research fellowship award.

Sequential Dehalogenation of Chlorinated Ethenes

Gladys Barrio-Lage,* Frances Z. Parsons, Raja S. Nassar, and Pedro A. Lorenzo

Drinking Water Research Center, Florida International University, Miami, Florida 33199

■ Reductive dehalogenation of tetra- and trichloroethene to *cis*- and *trans*-1,2-dichloroethene in microcosms simulating groundwater environment has previously been demonstrated. In this study, anoxic microcosms containing organic sediment and water were spiked to contain 5 mg/L of one of the following compounds: 1,1-dichloroethene (1,1-DCE), *cis*-1,2-dichloroethene (CIS), or *trans*-1,2-dichloroethene (TRANS). After incubation in the dark at 25 °C for up to 6 months, contents were analyzed by gas chromatography and verified by gas chromatography/mass spectrometry in an attempt to identify sequential steps in the transformation process. Vinyl chloride (VC) was produced after 1-2 weeks of incubation in all spiked microcosms, but none was observed in sterile and unspiked controls. Chloroethane (CE) was produced only in microcosms spiked with CIS, indicating isomer specificity and the occurrence of mechanisms other than reductive dechlorination. Kinetic parameters associated with the microbial dehalogenation of 1,1-DCE, CIS, and TRANS were calculated.

Introduction

Previous studies of transformations of chlorinated alkenes in microcosms simulating underground environments (1, 2) indicated that tetrachloroethene (PCE) and trichloroethene (TCE) undergo reductive dehalogenation to form *cis*- and *trans*-1,2-dichloroethene (CIS and TRANS, respectively). This was recently verified with TCE isotopically labeled with one ¹³C atom (3). Further transformation to vinyl chloride was indicated (4) but not proven. It was reported (2, 4) that microcosms spiked to contain 5 mg/L of a chlorinated alkene produced compounds with one less chlorine than the parent substrate in quantities less than 10% of the original compound, in 8 weeks of incubation. This means that if *cis*- and *trans*-1,2-dichloroethene were transformed to vinyl chloride, the resulting concentration of vinyl chloride was too small for detection by the methods used (1, 4).

Horowitz et al. (5) and Suflita et al. (6) reported sequential reductive dehalogenation of halogenated benzoates with 100% of the dichlorinated benzoates transformed to monochlorinated benzoates in approximately 1 month.

Bouwer and McCarty (7, 8) studied the biotransformation of several 1- and 2-carbon halogenated aliphatic compounds under methanogenic and denitrification conditions. They observed that removal of chlorine by biooxidation or hydrolysis can occur simultaneously with reductive dehalogenation, thus causing a greater confusion in determining the mechanistic steps involved in the complete removal of halogenated compounds.

Chlorinated ethenes transform very slowly, and apparently with several simultaneous removal reactions. All of the intermediate products of biotransformation between PCE and vinyl chloride, including vinyl chloride itself, that were observed in laboratory studies have been found in groundwater. The processes involved and rates at which these changes occur are important in assessing risk from use of affected waters. This study was made to further elucidate the behavior and fate of these toxic environmental contaminants by examining each intermediate step of the transformation of PCE to VC.

The specific objective of this research was to study the biotransformation of CIS, TRANS, and 1,1-DCE to vinyl chloride and to measure the rate of depletion of these substrates in microcosms simulating groundwater environments.

Experimental Procedures

Chemicals. 1,1-Dichloroethene (99%) (1,1-DCE), *cis*-1,2-dichloroethene (97%) (CIS), and *trans*-1,2-dichloroethene (98%) (TRANS) were purchased from Aldrich Chemical Co., Milwaukee, WI. Vinyl chloride (0.2 mg/mL methanol) (VC) was obtained from Supelco, Inc., Bellefonte, PA. Chloroethane (CE) was purchased from Eastman Chemical Co., Rochester, NY.

Preparation of Microcosms. Natural organic sediment collected from the Everglades, a graminoid wetland that is the recharge basin for the Biscayne Aquifer in southern Florida, was used to construct microcosms. Muck samples from two sites in the same area were obtained: site "A", which was the bottom of a shallow canal, and site "B", which was near the surface. Sites previously uncontaminated by chlorinated organic compounds were chosen for sediment sources to prevent selection of adapted microorganisms, which may yield different and variable results depending on quantity, nature, and age of contaminant.

Each sediment sample was thoroughly mixed and passed through a 6.34-mm sieve and then weighed (wet) into 50-mL septum bottles. Care was taken to prepare microcosms as uniformly as possible. The sediments were used in their natural state. Average dry weight was determined for purposes of comparison and to determine uniformity on a separate set of subsamples and amounted to 4 g dry weight per 50-mL bottle. After addition of sediment, the bottles were completely filled with water taken from the sample site. The water was purged with nitrogen prior to use to eliminate any highly volatile contaminants and to purge oxygen entrapped by sampling. Microcosms were prepared in sets that included the following controls: sterile, no-spike, and distilled water. Distilled water controls contained the organic sediment, but nitrogen-purged distilled water was substituted for site water. Sterile controls were prepared by autoclaving the organic sediments and the site water for 20 min on two consecutive days. After the materials were cooled, microcosms were constructed under aseptic conditions and sealed with sterile Teflon-lined septa, preventing headspace formation.

Spiking solutions were prepared in 50-mL serum bottles that were autoclaved along with the distilled water, magnetic stirrers, pipets, and the microsyringe used to prepare solutions. Accurately measured amounts of the three compounds, CIS, TRANS, and 1,1-DCE, were injected into separate, sterile bottles containing 50 mL of sterile, nitrogen-purged water and allowed to stir overnight. The final concentration of each compound in the spiking solutions was 500 mg/L. Half milliliter of each solution was spiked into each 50-mL microcosm to yield a final concentration of 5 mg/L in the microcosms. The microcosms were spiked 2 weeks after construction to allow equilibration and oxygen depletion to occur inside the test and control bottles and thus simulate the original conditions of the sample site. All microcosms and controls were al-

lowed to incubate in the dark at 25 °C for measured time periods of up to 6 months. Repeated sampling of a single microcosm in preliminary studies caused contamination and a change in the volume of the contents and introduced a gas phase (headspace). For this reason, duplicate microcosms were constructed as described above, for each scheduled test period, so that each microcosm was used only once in an analysis. Replicate microcosms were provided for concurrently measuring pH and redox potential (Eh). Although the microcosms were prepared homogeneously, variability of activity was accounted for by calculating the mean of replicate runs.

Sterility of sterile controls and spiking solutions was determined by streaking these materials on plates of R₂A medium (2, 9), incubating the plates, and observing them for growth.

Instrumentation. A Tracor Model 222 gas chromatograph with a 244 cm × 2.5 mm i.d. stainless-steel column, packed with 60/80 mesh Tenax GC, and a Hall electrolytic conductivity detector, Model 700, were employed for analysis. Nitrogen carrier gas at 40 mL/min and hydrogen reaction gas at 50 mL/min were supplied. The column oven was programmed to hold isothermal for 6 min at 40 °C while 5 mL of microcosm contents or standards were purged with N₂ directly on the head of the column (10). The column temperature was then increased from 40 to 220 °C at 8 °C/min. The temperature of the detector was kept at 850 ± 20 °C. The three isomers were successfully separated under the stated working conditions as follows: 1,1-DCE at 15.03 min of retention time and TRANS and CIS at 16.21 and 17.53 min, respectively.

Gas chromatography/mass spectrometry (GC/MS) data were obtained on a Finnigan 4500 GC/MS system interfaced to a Tekman LSC-2 purge-and-trap system. The gas chromatographic column was a 6 ft × 2 mm i.d. 0.2% Carbowax 1500 on 80/100 Carbowax B. The data system was standardized for the dichloroethenes and the purgeable gases (vinyl chloride, bromoethane, chloromethane, and chloroethane). An internal standard mix of fluorobenzene and *p*-bromofluorobenzene at the 25 µg/L level was added to each sample on the basis of volume of extractant water available.

Redox potentials (Eh) and pH were measured with a Corning Model 7 meter by using a Corning glass electrode for pH measurements and a Fisher platinum combination electrode for redox measurements. For pH measurements the instrument was calibrated at pH 4 and 7 with Scientific Products reference buffer solutions. For Eh measurements the instrument was calibrated at 180 and 0.0 mV by using pH 4 and 7 buffer solutions supersaturated with hydroquinone crystals.

Standard Solutions. Stock aqueous solutions of 1,1-DCE, CIS, and TRANS were prepared at 500 mg/L (ppm), by volumetric dilution, similar to the spiking solutions. Working standard of the five chlorinated compounds, 1,1-DCE, CIS, TRANS, VC, and CE, were prepared by diluting aliquots of the stock solutions with water and stirring overnight to achieve solutions of the desired concentrations. All bottles were wrapped in aluminum foil to avoid photodecomposition and kept at 4 °C. The system was checked daily against standard solutions and was recalibrated when the deviation was greater than 3%.

Results and Discussion

Evidence for Dehalogenation. The organic compounds produced when 1,1-DCE, CIS, and TRANS were incubated with oxygen-depleted sediment were identified by gas chromatography/mass spectrometry. Vinyl chloride was detected in all microcosms (Figures 1–3). VC was not

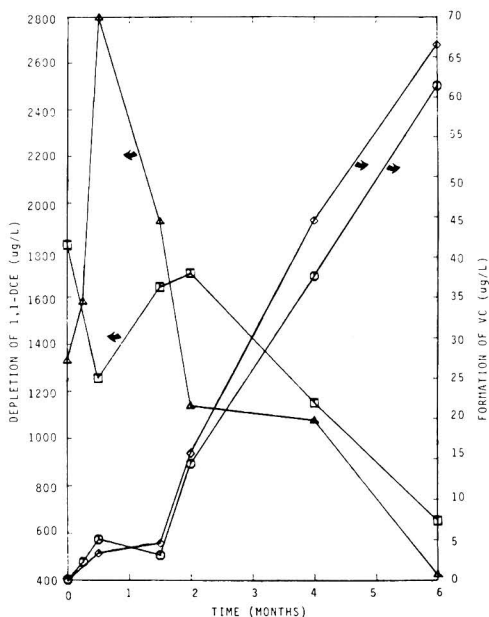


Figure 1. Patterns of anaerobic degradation of 1,1-DCE by sediment and water microcosms. (Δ) Depletion of 1,1-DCE in sediment and water from site B. (□) Depletion of 1,1-DCE in sediment and water from site A. (◇) Formation of VC in sediment and water from site B. (○) Formation of VC in sediment and water from site A.

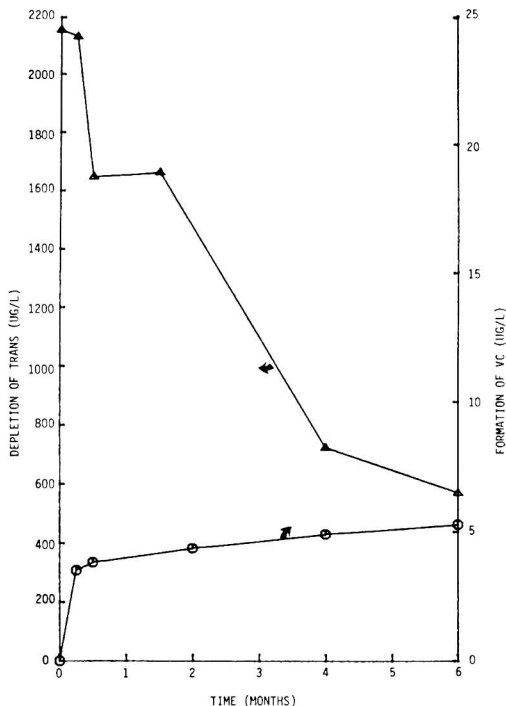


Figure 2. Pattern of anaerobic degradation of TRANS in sediment and water microcosms. Site A muck sample. (Δ) Depletion of TRANS. (○) Formation of VC.

detected in the no-spiked and sterile controls. A peak identified as chloroethane was observed to increase with

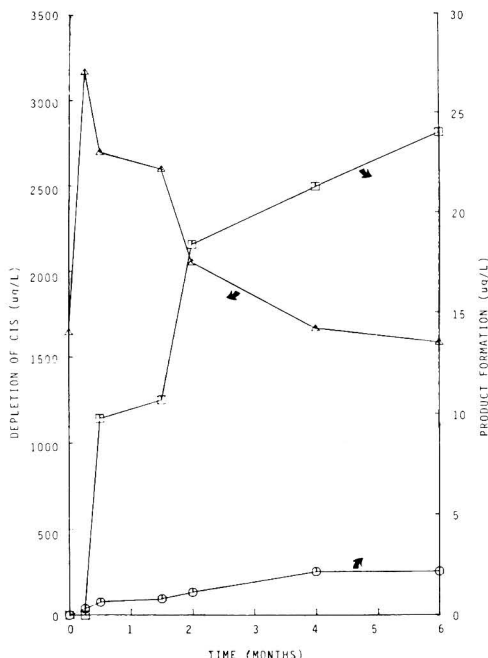


Figure 3. Pattern of anaerobic degradation of CIS in sediment and water microcosms. Site A muck sample. (Δ) Depletion of CIS. (□) Formation of CE. (○) Formation of VC.

time in all microcosms spiked with CIS (Figure 3). Samples spiked with 1,1-DCE and TRANS did not produce CE, nor did the sterile microcosms spiked with CIS. Analyses were made only for the intermediate compounds VC and CE and not for the complete mineralization of the spike. Only the intermediate steps were sought to demonstrate the stepwise nature of the transformation process.

Dechlorination of the three compounds under study did not occur in sterilized microcosms. In microcosms spiked with 1,1-DCE and TRANS (Figures 1 and 2), only the formation of vinyl chloride was observed. When CIS was the parent substrate (Figure 3), however, CE also was produced. In microcosms spiked with CIS (Figure 3), the concentration of VC remained low and nearly constant after 2 weeks of incubation, while chloroethane increased slowly. Microcosms spiked with TRANS (Figure 2) showed production of VC similar to the transformation of CIS; i.e., low and nearly constant concentration after 2 weeks, but CE was not produced in this case.

Figures 1 and 3 show that the depletion of the parent substrate was frequently preceded by an apparent initial increase in concentration. This was caused by an initial physical equilibration time and adaptation of the microbiota to the microcosm and assimilation of the introduced substrate. The microcosms were shaken vigorously upon spiking to distribute the chlorinated substrate. As the microcosm contents were allowed to settle in the dark at room temperature, most of the added organic compound was trapped, and some was adsorbed in the interstices of the solid phase, i.e., muck. Equilibrium between solid and liquid phases was established in about 2-weeks incubation time. Other authors have reported lag periods of up to 6 months (5), caused by the adaptation of the microbiota to utilize one specific substrate.

The inconsistency of this initial equilibration time made it impossible to measure the initial velocities that are

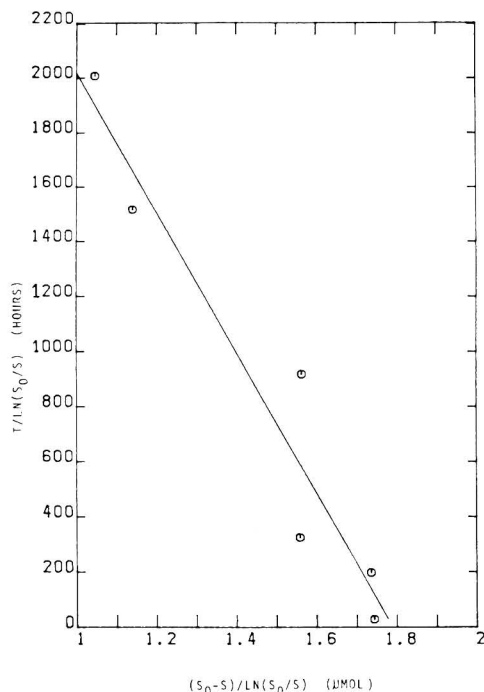


Figure 4. Michaelis-Menten fit of the data (eq 1) from the depletion of TRANS in sediment and water from site B.

valuable in calculating the true order of reactions.

Figure 3 is a typical plot of a consecutive reaction where the concentration of the intermediate (VC) rose to a maximum and then decreased or stayed constant, and the concentration of the last product (CE) rose to a maximum. However, VC is not believed to be an intermediate species between CIS and CE because chloroethane was not observed in samples spiked with 1,1-DCE and TRANS where VC was detected.

First-order kinetic models were attempted to depict the decay of 1,1-DCE, CIS, and TRANS. In every case, however, we found that semilogarithmic plots of the data deviated from linearity usually after 3-4 months of incubation.

Horowitz et al. (5) observed that when 3-chlorobenzoate was the initial substrate, the data followed first-order depletion kinetics. If the parent substrate was 3,5-dichlorobenzoate (6), the dichlorinated substrate competitively inhibited the dehalogenation of the monochlorinated substrate, causing a deviation from first-order kinetics. These authors (6) found that dehalogenation of mono- and dichlorinated benzoates exhibited Michaelis-Menten kinetics. Good linearity was obtained when our data was fitted to the linearized form of the Michaelis-Menten equation which was also used by Suflita et al. (6)

$$t / [\ln(S_0/S)] = (1/V) [(S_0 - S) / \ln(S_0/S)] + K_m/V \quad (1)$$

where t is time, S_0 is the initial substrate concentration, S is the substrate concentration at time t , V is the maximum rate of substrate depletion, and K_m is the half-saturation constant. Michaelis-Menten kinetics only describes bacterial substrate when this process is unlinked to growth of microbial biomass.

Figure 4 shows the Michaelis-Menten fit of the data for the depletion of TRANS in microcosms with sediment

Table I. Kinetic Parameters Describing the Dehalogenation of the Isomers of Dichloroethene by Anoxic Sediment

substrate	dehalogenation muck	$K_m, \mu\text{M}$	$V_{\text{max}}, \mu\text{mol L}^{-1} \text{h}^{-1}$	k_1, h^{-1} ^a
1,1-DCE	site B	43.4	0.0155	3.57×10^{-4}
	site A	36.7	0.0061	1.67×10^{-4}
CIS	site B	65.3	0.0214	3.28×10^{-4}
	site A	41.8	0.0036	0.853×10^{-4}
TRANS	site B	35.8	0.0078	2.19×10^{-4}
	site A	29.6	0.0058	1.97×10^{-4}

^aFirst-order rate constant obtained by V_{max}/K_m .

from site B. 1,1-DCE showed the largest deviation from the Michaelis–Menten model with correlation coefficients between 0.75 to 0.91. This may be due to 1,1-DCE producing the largest amounts of VC, and an inhibition factor from the consecutive depletion of VC may be important in this case.

Table I summarizes the kinetic parameters associated with dehalogenation by the sediment microflora. K_m and V_{max} values reported in Table I were attained from a linear regression analysis of the Michaelis–Menten fit of the data and subsequently divided by the microcosm volume to obtain the reported values. As it can be seen, the K_m values for the dehalogenation of the three isomers in the tested environment varied by a factor of about 2 (30–65 μM), whereas the V_{max} values varied by a factor of 6 (0.0036–0.0214 $\mu\text{mol L}^{-1} \text{h}^{-1}$). The first-order rate constant of dehalogenation ranged from $0.853 \times 10^{-4} \text{h}^{-1}$ for CIS in sediment to $3.57 \times 10^{-4} \text{h}^{-1}$ for 1,1-DCE in site “B” sediment, indicating a very slow rate of dehalogenation.

pH of all microcosms was measured and found to remain constant at 7.0 ± 0.5 . Redox potential data (Eh) changed drastically in the first 2 weeks of incubation while equilibrium was attained, after which time it remained almost constant between –20 and –130 mV.

Not all the substrate that was depleted was transformed to VC (Figures 1–3), indicating that mechanisms of transformation other than reductive dechlorination were taking place. Transformation of substrate by biooxidation (7) or hydrolysis (8) are possible removal mechanisms. The appearance of CE (Figure 3) in microcosms spiked with CIS indicates isomer specificity and a different pathway of transformation in the sequential dechlorination.

Figure 5 shows a summary of transformations that may occur to tetra- and trichloroethene in oxygen-depleted sediment. Steps a–c were reported previously (2). Step d was suspected to occur but never reported because of possible interference from contaminants (2). Recently it was reported (3) that this isomer did not result from the biotransformation of isotopically labeled trichloroethene. Steps e–h are reported in this paper. It is not known whether steps e and f occur independently or are inter-related.

Depletion of these substrates, similar to that reported for trichloroethylene (2), required longer periods of time than other chlorinated alkanes reported by different authors (5–8). Most probably the slow biotransformation of such compounds caused Bouwer et al. (11) to report observing no appreciable anaerobic degradation of tetra- and trichloroethylene. Figures 1–3 show that only 50–80% of 1,1-DCE, CIS, and TRANS was depleted in 6 months of incubation.

Conclusions

This study has shown that 1,1-DCE, CIS, and TRANS, subjected to the indigenous microbiota of uncontaminated

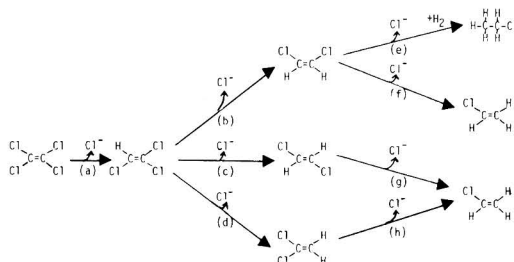


Figure 5. Summary pathways for dechlorination of tetra- and trichloroethene in anaerobic environments. Steps a–c from Parsons and Lage (2).

environmental organic sediments, under anoxic conditions, undergo reductive dechlorination leading to the formation of vinyl chloride. Mechanisms of transformation other than reductive dechlorination also occur because the sum of the products observed does not account for all of the substrate that is removed. Isomers undergo different transformations; CIS led to the formation of CE and only traces of VC; 1,1-DCE yielded greater concentrations of VC and no CE; TRANS produced VC only.

Kinetic parameters associated with the microbial dehalogenation of 1,1-DCE, CIS, and TRANS were calculated. The first-order rate constant k_1 , for the depletion of the parent substrate ranged from 0.853×10^{-4} to $3.57 \times 10^{-4} \text{h}^{-1}$.

Acknowledgments

The mass spectrometry analysis of Garmon B. Smith, Jr., and the help of John Wilson, both of the U.S. EPA, Ada, OK, are gratefully acknowledged.

Registry No. 1,1-DCE, 75-35-4; CIS, 156-59-2; TRANS, 156-60-5; VC, 75-01-4; CE, 75-00-3; PCE, 127-18-4; TCE, 79-01-6.

Literature Cited

- Parsons, F. Z.; Wood, P. R.; DeMarco, J. J.—*Am. Water Works Assoc.* **1984**, *76*, 56–59.
- Parsons, F. Z.; Lage, G. B. J.—*Am. Water Works Assoc.* **1985**, *77*, 52–59.
- Kleopfer, R. D.; Easley, D. M.; Haas, B. B., Jr.; Deihl, T. G.; Jackson, D. E.; Wurrey, C. J. *Environ. Sci. Technol.* **1985**, *19*, 277–280.
- Parsons, F. Z.; Lage, G. B.; Rice, R. *Environ. Toxicol. Chem.*, in press.
- Horowitz, A.; Sufliya, J. M.; Tiedje, J. M. *Appl. Environ. Microbiol.* **1983**, *45*, 1459–1465.
- Sufliya, J. M.; Robinson, J. A.; Tiedje, J. M. *Appl. Environ. Microbiol.* **1983**, *45*, 1466–1473.
- Bouwer, E. J.; McCarty, P. L. *Appl. Environ. Microbiol.* **1983**, *45*, 1286–1294.
- Bouwer, E. J.; McCarty, P. L. *Appl. Environ. Microbiol.* **1983**, *45*, 1295–1299.
- Reasoner, D. J.; Geldreich, E. E. *Appl. Environ. Microbiol.* **1985**, *49*, 1–7.
- Mehran, M. “Abstracts of Papers”, 189th National Meeting of the American Chemical Society, Miami, FL, 1985; American Chemical Society: Washington, DC, 1985; ENVR 22.
- Bouwer, E. J.; Rittman, B. E.; McCarty, P. L. *Environ. Sci. Technol.* **1981**, *15*, 596–599.

Received for review March 29, 1985. Accepted August 5, 1985. This work was supported by the U.S. Environmental Protection Agency, Ground Water Research Branch, under Contract CR809994-02 to Florida State University and Subcontract 281308-500 to Florida International University. The contents do not necessarily reflect the views or policies of the Agency nor does mention of trade names constitute endorsement.

Perfluorocarbon Measurement Using an Automated Dual-Trap Analyzer

Ted W. D'Ottavio,* Robert W. Goodrich, and Russell N. Dietz

Environmental Chemistry Division, Department of Applied Science, Brookhaven National Laboratory, Upton, New York 11973

■ A new instrument designed to measure perfluorocarbon concentrations in air has been developed at Brookhaven National Laboratory (BNL). This instrument, called the dual-trap analyzer, is described in this paper along with some current applications. Perfluorocarbons are collected on a solid adsorbent and then thermally desorbed, separated by gas chromatography, and detected by electron capture. A new measurement is obtained every 2-10 min depending on the number of perfluorocarbons present in the collected air sample. The limit of detection for a collection time of 2 min is 0.005 parts per trillion for any one of the four perfluorocarbons that have been studied.

Introduction

The use of perfluorocarbons as tracers has become increasingly popular due to their unique characteristics. Most are very stable, even at high temperatures, highly unreactive to most materials and surfaces, insoluble in H₂O, and totally nontoxic to human life (1). In addition, although they have appreciable vapor pressures, their atmospheric background concentration is low and stable due to few, if any, global sources (2).

This combination of properties has led to their recent use in several applications. Probably the most well-known is the use of perfluorocarbons as atmospheric tracers (2, 3). In this application a perfluorocarbon is released into the atmosphere and one or more measurements are made of its downwind concentration at distances of 100-1000 km from the release point. These results, which are then used to assess the transport and dispersion of pollutants from a point source, represent a good test of predictions made from meteorological models.

Fluid tagging is becoming another important application of perfluorocarbons. Underground leaks of natural gas and of oil insulating high-voltage electric cables are becoming increasingly common due to deterioration and old age. Repairs to these underground systems can be costly, in part, because of the difficulty of precisely locating the leaks. The expense of determining leak locations can be significantly reduced by tagging the underground fluids with a volatile perfluorocarbon that can then be detected above ground to pinpoint the leak location.

Perfluorocarbons are also being used to assess the degree of air infiltration into homes (4). This is done by releasing a perfluorocarbon into a home at a constant rate and measuring the resulting steady-state concentration that is generated within the home. This measurement is then used to calculate the air exchange rate, or the rate at which air in the home is exchanged with outside air, a very useful piece of information for energy conservation and indoor air pollution studies.

Finally, a viable technique was developed to tag electric blasting caps with a perfluorocarbon tracer to facilitate the detection of clandestine bombs in luggage at airport environments (5).

Two types of samplers have been used in the past for the collection of perfluorocarbons in air. One is a passive sampler called a CATS (capillary adsorption tube sampler) and is typically used for air infiltration studies. The CATS is a cylindrical tube about 5 cm long containing a carbonaceous material called Ambersorb (Rohm and Haas, Philadelphia, PA) and samples by diffusion of the per-

fluorocarbon down the tube and onto the Ambersorb (4).

A second type of sampler, dubbed the Brookhaven atmospheric tracer sampler (BATS), is a programmable cassette-type sampler containing 23 adsorbent tubes and was originally developed for large-scale atmospheric tracer experiments (2). This unit samples air through the use of a pump instead of by diffusion for better sensitivity and time resolution than is achievable with the CATS.

With both types of samplers the tubes are analyzed in the lab by heating the Ambersorb to thermally desorb the perfluorocarbons, separating them via gas chromatography, and detecting them by electron capture.

In recent years, with the advent of atmospheric tracer sampling by aircraft and the uncertainties involved in stationing aircraft based on meteorological predictions of plume trajectories, a need has developed for a transportable system capable of both sampling and on-the-spot analysis of perfluorocarbons.

In this paper we report on a new instrument for the detection and analysis of perfluorocarbons called the dual-trap analyzer. It combines high sensitivity, semi-real-time resolution, and in situ analysis all in a single, portable, and fully automatic instrument.

The original prototype was designed in 1976 by Lovelock under contract from NOAA. That unit contained two adsorbing traps that automatically cycled every 5 minutes so that while one trap was sampling, the other was being analyzed. The instrument was designed to measure one perfluorocarbon tracer (PFT) called perfluorodimethylcyclohexane, or PDCH, and had a limit of detection of approximately 0.8 parts per trillion (ppt). The Lovelock instrument was used in a field experiment in 1977 at the Idaho National Engineering Laboratory sampling 50 km downwind of a PDCH release (6). Comparison to measurements made by a cassette sampler followed by laboratory analysis indicated good agreement between the two techniques.

In 1980, the original prototype was modified by Brookhaven to collect and measure PDCH and PMCH (perfluoromethylcyclohexane) simultaneously and also to improve the limit of detection to 0.01 ppt. The modified dual-trap analyzer was successfully used in two field experiments in 1980: a feasibility study at Oklahoma State University where both PDCH and PMCH were released (2) and the ASCOT (atmospheric studies in complex terrain) experiment in the geyser area of northern California. The dual-trap analyzer was again used in ASCOT in 1981.

Further refinement of the dual-trap analyzer occurred in 1983 when a new instrument was built at Brookhaven. This new instrument can resolve four different perfluorocarbons and has a minimum cycling time of 2 minutes with a limit of detection of 0.005 ppt at a signal-to-noise ratio of 2. A detailed description of this instrument, along with its abilities and specifications, will now be discussed, and a second paper describing the use of the dual-trap analyzer in the recently completed CAPTEX (cross appalachian tracer experiments) aircraft flights will be presented at a later date.

Experimental Section

The operation of the dual-trap analyzer can be represented by a series of schematic diagrams (parts a-c of

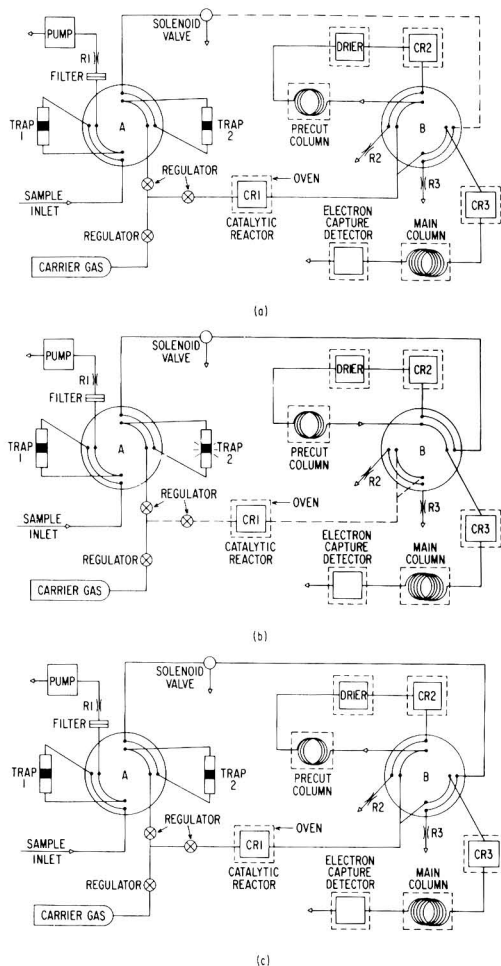


Figure 1. Schematic diagram of the dual-trap analyzer: (a) vent mode; (b) foreflush mode; (c) backflush mode.

Figure 1), each describing a different stage of the analysis cycle.

Figure 1a. Valves A and B are eight-port rotary valves (Valco Instruments Co., Houston, TX) that rotate 90° in one direction or the other making two different sets of connections. Valve A is used to switch trap 1 and 2 between sample collection and analysis resulting in continuous sampling and integrated semicontinuous concentration measurements. Valve B is involved in the chromatographic analysis and will be discussed later.

As a convenient starting point for the cycle we assume that trap 2 has just finished collecting a sample, trap 1 has been analyzed, and valve A has rotated clockwise 90°. Sample air is now drawn through trap 1 with a pump, the flow being controlled by a restrictor. The restrictor is operated critically so that small fluctuations in downstream pressure do not affect the flow rate. In the actual instrument a three-way valve selects one of two restrictors (1000 or 50 cm³/min) allowing the user to control the sample volume and, thereby, increase the effective dynamic range of the instrument. Each of the two adsorbing traps is a 7 cm long, 4 mm i.d. glass tube containing 75 mg of Amborsorb 347, a carbonaceous material formerly made

by Rohm and Haas (Philadelphia, PA), but no longer in production. It has been shown that coconut charcoal works equally well as an adsorbent material. Resistance heating from nichrome wire wrapped around each trap is used for thermal desorption.

Because of the moderately high electron capture cross section of oxygen and its reactivity with PFTs at elevated temperatures in the adsorbed state, the analysis of trap 2 begins by first purging the system of any air remaining in the trap and its connecting lines. This is accomplished by opening a three-way solenoid valve to vent and flushing the system with carrier gas at a flow rate controlled by R2 of 300 cm³/min. This operation takes about 3 s.

The carrier gas is 5% ultra high purity (UHP) H₂ in UHP N₂ (Scientific Gas Products, So. Plainfield, NJ) and is metered into the system by two-stage pressure regulation from an internal gas supply. Normal flow rates are in the range of 20–50 cm³/min. In addition, the carrier gas supply is also used to turn the gas-actuated rotary valves.

Figure 1b. Valve B rotates clockwise 90°, and the solenoid valve is deactivated directing carrier gas from trap 2 to the chromatographic detection system. Simultaneously an electric current is passed through the nichrome wire wrapped around trap 2. This heats the Amborsorb to about 400 °C, driving off the perfluorocarbons and any other adsorbed constituents.

The material then enters catalytic reactor CR2. This reactor and the other two contained in the system consist of a 1 in. long bed of 3% palladium supported on 30–35 mesh molecular sieve 5A lodged in a 3/16 in. i.d. stainless-steel tube held at 250 °C. At this temperature, interfering chlorofluorocarbons are destroyed, and any remaining oxygen is converted to water vapor, which is then removed from the gas stream by a permeation drier utilizing Nafion tubing (Du Pont, Wilmington, DE) (7).

Preliminary separation of the perfluorocarbons occurs in the precut column. This column is an 18 in. long, 1/8 in. o.d. stainless-steel tube packed with 0.1% SP-1000 on 80–100 mesh Carboxpack C (Supelco, Inc., Bellefonte, PA). This packing has been shown in the past to separate a variety of different halocarbon materials (3). The partially separated perfluorocarbons of interest then pass again through valve B and into catalytic reactor CR3 for a final cleanup.

Figure 1c. Valve B turns counterclockwise 90°. Carrier gas continues to pass through trap 2 but is now vented to the atmosphere through restrictor R3. In addition, carrier gas also passes through CR1 and splits. One path back-flushes the precut column, drier, and CR2 circuit. This operation keeps the system clean and can be timed to prevent unwanted heavier components from entering the detection system.

The other carrier gas path continues the analysis of the perfluorocarbons, which now enter the main chromatographic column. This column is 3 ft in length and is packed with the same material as the precut column. The columns have been wound into concentric coils and are kept at 130–150 °C by placing them in a temperature-controlled dewar (Kontes Glass, Vineland, NJ).

Detection of the perfluorocarbons is by electron capture. The detector, based on a Varian design (8), is made at BNL and has been used in the past for detection of SF₆ (9). A 250-mCi titanium tritide foil (Safety Lite Corp., Bloomsburg, PA) is used as a beta source, and the detector is temperature controlled at 50 °C in a dewar.

Once the perfluorocarbon detection is completed, valve A rotates 90° and the analysis cycle begins again except that now trap 1 is being analyzed while trap 2 is sampling.

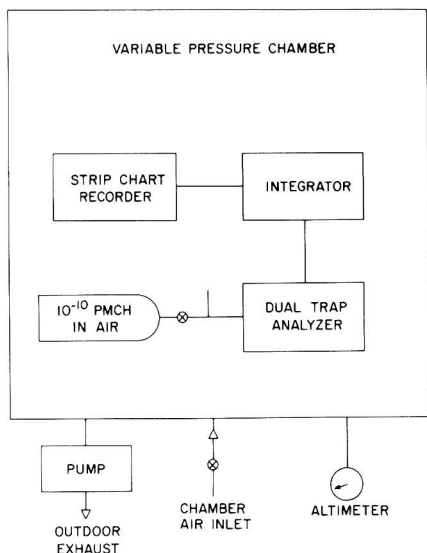


Figure 2. Calibration system.

All of the valve switching and heating operations are performed automatically by an electronic circuit built at BNL. In addition, the instrument incorporates microprocessor-controlled circuitry capable of direct concentration readouts based on peak height.

Calibration of the dual-trap analyzer for PMCH concentration at several different inlet pressures was done in an altitude chamber using the system shown in Figure 2. Various concentrations of PMCH were produced by diluting a standard of 10^{-10} PMCH in air. Peak areas were measured with an integrator (Laboratory Data Control, Riviera Beach, FL), and the pressure in the chamber was monitored with an altimeter (Garwin, Inc., Wichita, KS).

Results and Discussion

The Ambersorb trap can be viewed as a chromatographic column slowing the movement of the perfluorocarbon material.

It is reasonable to expect, therefore, that as sampling continues through the trap, more and more of each perfluorocarbon will "break through" the Ambersorb and be lost, thus reducing the collection efficiency. Measured as a percentage of the inlet concentration, this perfluorocarbon breakthrough is plotted in Figure 3. As with any chromatographic separation, this breakthrough depends on the temperature and geometry of the packing, the flow rate of the gas passing through it, and the volatility of the adsorbed constituents.

Figure 3 indicates that under conditions of relatively high temperature (45°C) and flow rate (1.5 L/min), breakthrough is small for PMCH and PDCH and significant for the more volatile PDCB (perfluorodimethylcyclobutane). In normal operation of the dual-trap analyzer (traps held at ambient temperature, sample flow rate ~ 1 L/min, sampling time ~ 4 min), breakthrough should be reduced by a factor of 2 or more.

The efficiency of the catalytic reactor has also been looked at in some detail. Figure 4 shows the scrubbing performance of the catalytic reactor as a function of temperature for a variety of electron capturing materials. For perfluorocarbon measurements, we operate the reactor at $225\text{--}250^{\circ}\text{C}$ permitting efficient removal of freons and

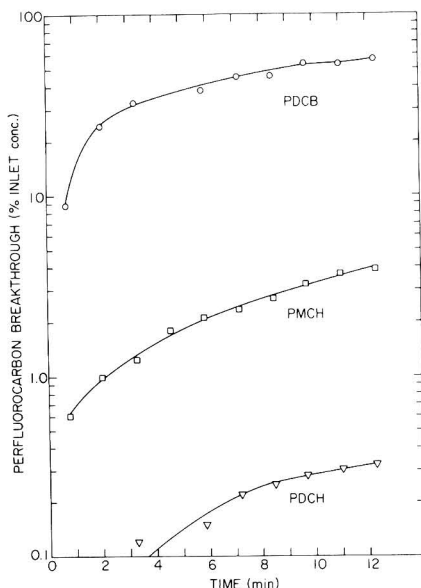


Figure 3. Collection efficiency of Ambersorb 347 to three perfluorocarbons.

Effect of Catalyst Bed (Reactor) Temperature on Destruction of Perfluorocarbons and Interferents

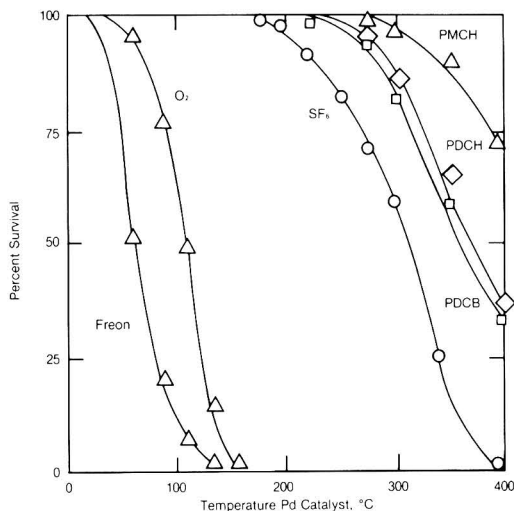


Figure 4. Destruction efficiency of a palladium catalytic reactor to various electron capturing materials.

small amounts of oxygen in the gas stream. SF_6 , although not removed at this temperature, is not retained by the Ambersorb and, therefore, does not present an interference problem.

The sensitivity of the dual-trap analyzer to PMCH is shown in Figure 5. In addition to the near sea level calibration, results obtained by simulating two other altitudes (5000 and 9000 ft) are also shown. Instrumental parameters were set as follows: sample flow rate, 1 L/min at 1-atm inlet pressure; sample time, 4 min; carrier gas flow, $20\text{ cm}^3/\text{min}$; and column temperature, 130°C .

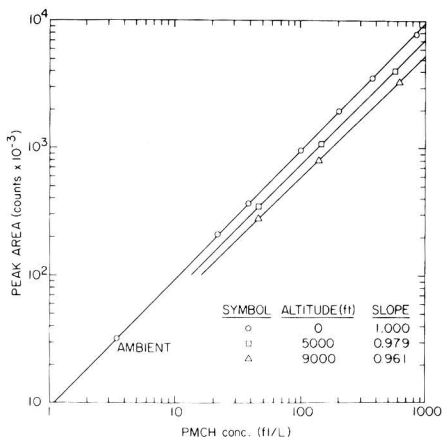


Figure 5. Calibration curves for PMCH at three altitudes: cycle time, 4.1 min; carrier gas flow rate, 20 cm³/min.

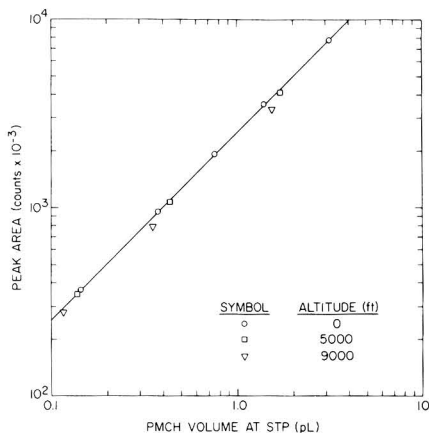


Figure 6. Calibration curve for PMCH with data corrected for inlet pressure and volumetric pump flow.

Concentrations are in units of fL/L or 10⁻¹⁵ parts PMCH/1 part air.

The calibration proved to be linear over the 3 orders of magnitude in concentration that were studied. Slopes for all three lines are very close to their theoretical value of 1 with a slight decrease at the higher altitudes. Although we have presented curves only for PMCH, similar curves are obtained for PDCH, PDCB, and PMCP (perfluorodimethylcyclopentane).

Using the data in Figure 5, we can calculate the total amount of material adsorbed onto a trap during one 4-min sampling period. After plotting these values against peak area we obtain Figure 6. As this plot indicates, the loss in sensitivity at reduced inlet pressures is due almost entirely to a reduction in the amount of collected sample. This results from a decrease in the density of the inlet airstream as simulated altitude increases and also from slight changes in the inlet volume flow rate.

Inlet pressure also affects the base-line standing current, which decreases as the inlet pressure decreases. This effect amounts to an effective PMCH concentration change of 6 fL/L per 100-ft change in altitude at ground level and 11 fL/L for every 100-ft change at 10 000 ft. Because this is a chromatographic instrument, peak heights or areas are measured relative to the base line, thus negating this al-

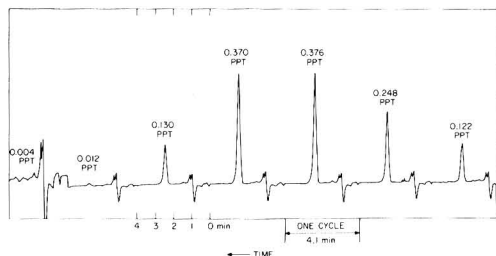


Figure 7. Strip chart recording from the dual-trap analyzer taken during the traverse of a PMCH plume: CAPTEX Mission 7, Oct 1983.

titude-dependent base-line drift under most conditions.

There are a variety of user-selectable instrument parameters that affect the overall operation of the dual-trap analyzer. These include the instrument cycle time, the carrier gas flow rate, the temperature of the columns and the backflush time, or the time at which the system switches into the backflush mode. In general, instrument sensitivity is directly proportional to the cycle time and inversely proportional to the carrier gas flow rate. Peak resolution is affected by the carrier gas flow rate and by the column temperature and, within limits, increases with a decrease in both of these parameters. This increase in peak resolution, however, will be accompanied by an increase in elution time, which may necessitate an increase in the cycle time over and above that which is necessary to measure the minimum observable concentration. The backflush time affects selectivity by eliminating those latter eluting peaks from the chromatogram that the user does not wish to see.

As an example of how these parameters are juggled to optimize the dual-trap analyzer for a given type of measurement, consider the data displayed in Figure 5. The instrument conditions that were used to obtain these results were picked because they were considered the optimum set for the measurement of PMCH during the CAPTEX experiments. An example of the dual-trap analyzer output from one of the experiments obtained during the traverse of a PMCH plume is shown in Figure 7.

During these experiments we were interested in measuring only PMCH at concentrations down to ambient levels (3.5 fL/L) with a minimum cycle time. Thus the carrier gas flow rate was set to a low 20 cm³/min for maximum sensitivity; the column temperature was kept low (130 °C) for better separation of the PMCH from earlier eluting peaks; and the precut column was set to backflush just after the PMCH had passed through keeping the elution time to a minimum. Allowing for all of the above, the minimum cycle time was about 4 min.

As the above example shows, the current limits of the dual-trap analyzer depend on how the instrument is set up. At a carrier gas flow rate of 20 cm³/min, the minimum volume of PMCH that can be detected is 10 fL (10⁻¹⁴ L) at STP. Thus, with the sample flow rate set to 1 L/min and the cycle time set to 5 min, the limit of detection for PMCH is 2 fL/L. These values do not differ by more than a factor of 3 for PDCH, PDCB, or PMCP. The minimum time necessary to separate all four perfluorocarbons simultaneously is 10 min, decreasing to 3–4 minutes for any one perfluorocarbon alone.

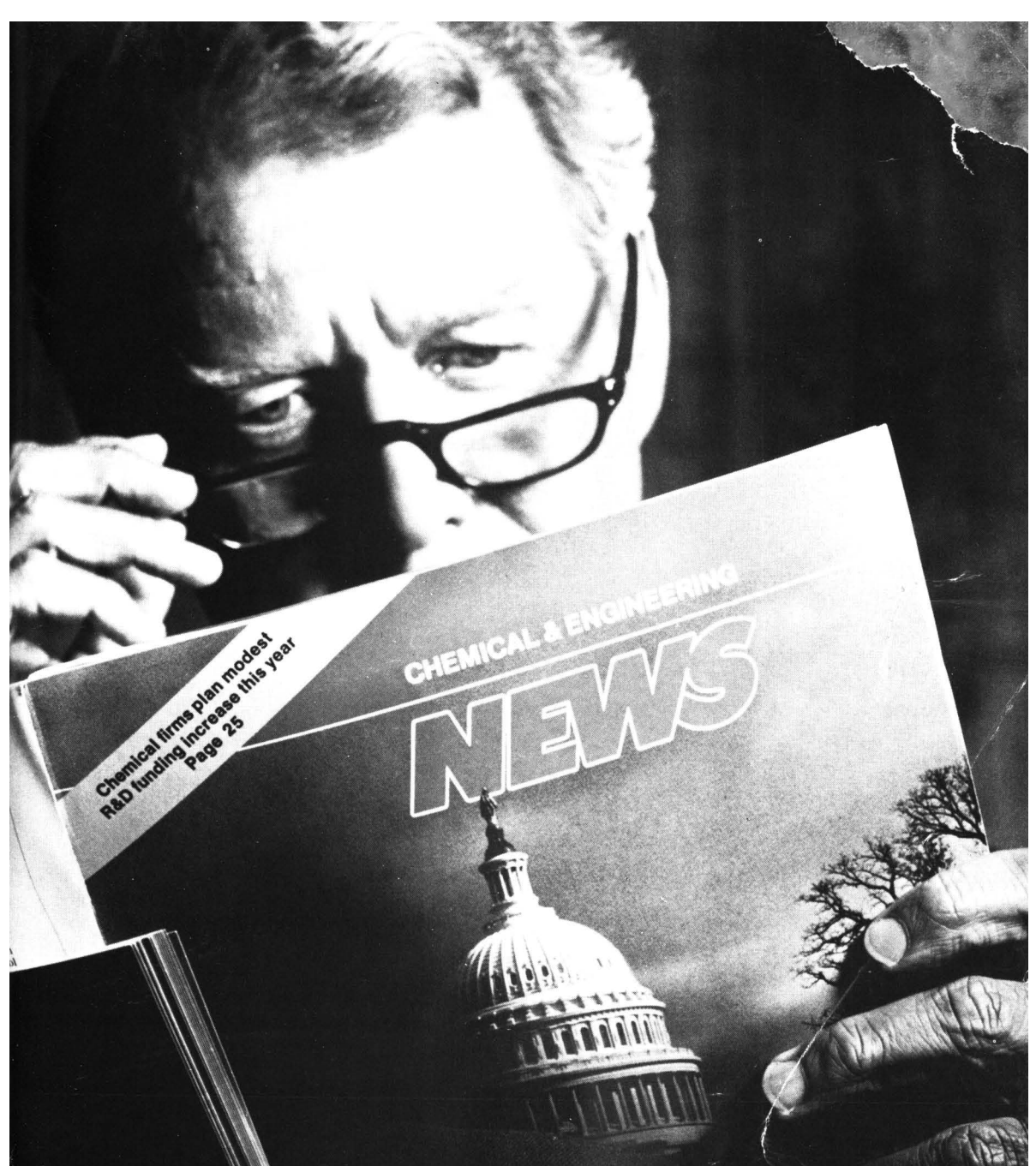
Work is now in progress to refine these limits further. The minute amount of material being chromatographed during each cycle makes this system ideal for micropacked or capillary chromatography. These columns, combined with better sample injection techniques, could increase

peak resolution by a factor of 5–10 and sensitivity by a factor of 3 or more.

Literature Cited

- (1) Lovelock, J. E.; Ferber, G. J. *Atmos. Environ.* **1982**, *16*, 1467–1471.
- (2) Ferber, G. J.; Telegadas, K.; Heffter, J. L.; Dickson, C. R.; Dietz, R. N.; Kreg, P. W. NOAA Technical Memorandum ERL ARL-101, 1981.
- (3) Zlatkis, A.; Poole, C. F. *J. Chromatog. Lib.* **1981**, *20*, 269–271.
- (4) Dietz, R. N.; Cote, E. A. *Environ. Int.* **1982**, *8*, 419–433.
- (5) Senum, G. I.; Gergeley, R. P.; Greene, M.; Dietz, R. N. Informal Report 25051; Brookhaven National Laboratory: Upton, NY, 1978.
- (6) Clements, W. E. Informal Report LA-7795-MS; Los Alamos Scientific Lab: Los Alamos, NM, 1978.
- (7) Cassidy, F. J. AID.8BA.74; Exxon Research and Energy Co.: Linden, NJ, 1974; pp 1–12.
- (8) Patterson, P. L. *J. Chromatogr.* **1977**, *134*, 25–37.
- (9) Dietz, R. N.; Cote, E. A.; Goodrich, R. W. International Atomic Energy Agency; Vienna, Austria, 1976; IAEA-SM-206/21, pp 277–299.

Received for review January 14, 1985. Accepted July 31, 1985. This research was performed under the auspices of the United States Department of Energy under Contract No. DE-AC02-76CH00016.



People who make the news, read the News.

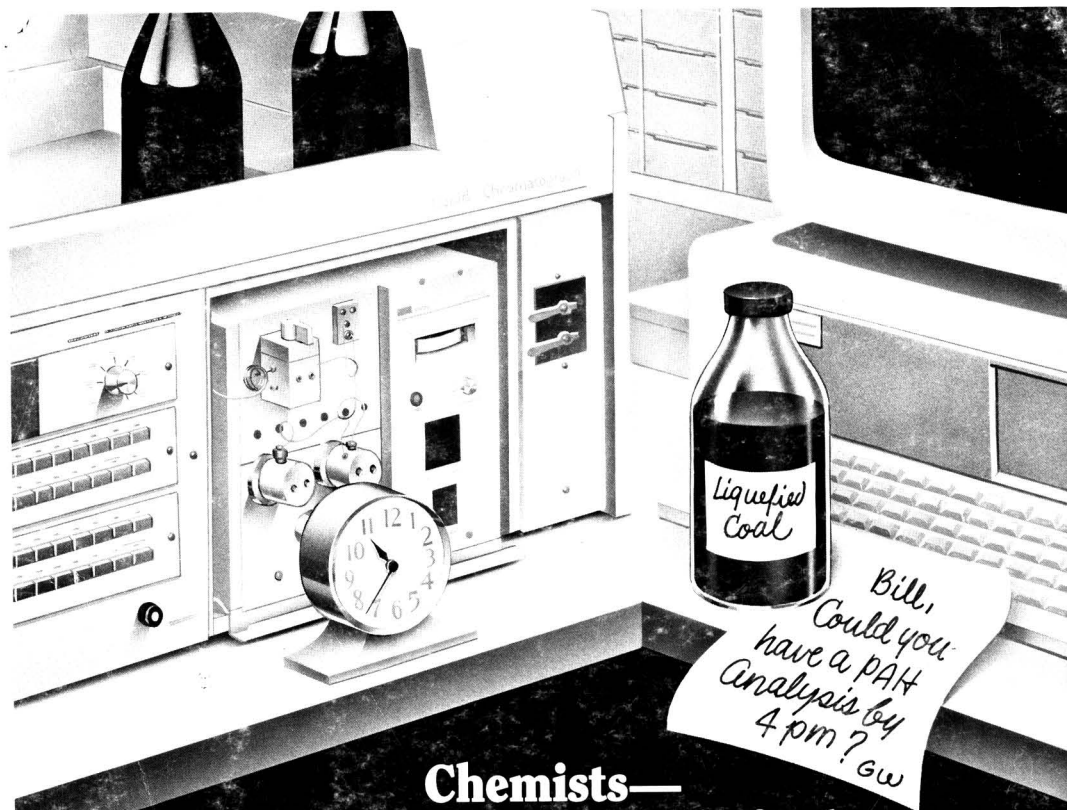
When you're sitting at the top, you need to get to the bottom of news that affects your business. That's why senior executives throughout industry read Chemical & Engineering News each week.

It's the only weekly chemical magazine that covers the news from three angles. Not just science. Not just technology. Not just business. But all three. So you not only know what's happening in chemistry, you know how it's going to affect your business.

Read the weekly the newsmakers read. Call 800-424-6747 and ask about our offer of six complimentary issues.



BUSINESS
SCIENCE
TECHNOLOGY



**Chemists—
How can you quickly find
an analytical procedure
to solve this problem?**

Search ACS JOURNALS ONLINE.

A high-efficiency chemical information search system that can save you hours of searching through chemical journals for an analytical procedure.

You can use it right in your laboratory. Just turn on your computer or terminal.

In minutes you'll be reading about the analytical procedure you need.

In this case, it's a high-performance liquid chromatography procedure for determining polycyclic aromatic hydrocarbons in liquid coal.

And with the touch of a key, you can even zero in on specific paragraphs that contain the data you need.

Find out how you can make this high-efficiency chemical information search system work for you. Call an American Chemical Society sales representative today at 800-424-6747. The call is free.

Or write, Sales Office, American Chemical Society, 1155 Sixteenth Street, N.W., Washington, D.C. 20036.

ACS JOURNALS ONLINE contains: Accounts of Chemical Research, Analytical Chemistry, Biochemistry, Chemical Reviews, Environmental Science & Technology, Industrial & Engineering Chemistry—Fundamentals—Process Design & Development—Product Research & Development, Inorganic Chemistry, Journal of Agricultural and Food Chemistry, Journal of Chemical and Engineering Data, Journal of the American Chemical Society, Journal of Chemical Information and Computer Sciences, Journal of Medicinal Chemistry, The Journal of Organic Chemistry, The Journal of Physical Chemistry, Langmuir, Macromolecules, and Organometallics.

The Computer-Powered
Full-Text Search System
From The American
Chemical Society

**ACS JOURNALS
ONLINE**



1155 Sixteenth Street, N.W., Washington, D.C. 20036